Planar Graphs and Face Areas
Area-Universality

vorgelegt von
M. Sc. Mathematik
Linda Kleist
geboren in Hamburg

Von der Fakultät II – Mathematik und Naturwissenschaften
der Technischen Universität Berlin
zur Erlangung des akademischen Grades
Doktor der Naturwissenschaften
– Dr. rer. nat. –

genehmigte Dissertation

Promotionsausschuss

Vorsitzender:	Prof. Dr. Boris Springborn
Gutachter:	Prof. Dr. Stefan Felsner
	Prof. Stephen Kobourov
	Prof. Dr. Ignaz Rutter

Tag der wissenschaftlichen Aussprache: 13. Juli 2018

Berlin 2018

Acknowledgements

This research was conducted in the *Arbeitsgruppe Diskrete Mathematik* at Technische Universität Berlin under the supervision of Stefan Felsner. I would like to thank all current and former members for the nice atmosphere, the interesting discussions and all kinds of valuable ideas. Specifically, I thank

- Stefan Felsner for the opportunity to join his group and for introducing me to area-universal graphs. In particular, I appreciate his concept of elegant proofs, the open door policy, the teaching approach and the freedom I enjoyed.
- my former colleagues Udo, Veit, Nieke, Irina, and Daniel for the smooth introduction and various perspectives and approaches to mathematics. Explicitly, I want to thank Udo for his assistance and our frequent discussions, and Veit for making me laugh; especially when we shared an office.
- my COGA-friends for the pleasant time, the coffee breaks, the coga-game-nights, and their support and encouragement.
- Ralf for creating cheerful and mindful atmosphere and especially for organizing the entertaining and relaxing sessions of *Recken und Strecken*.
- Tillmann for his enthusiasm for research, his mentoring advices and for his interest on the complexity of area-universality.
- Manfred for introducing me to Sage, winning the super cool mug by solving the prize question posed at EuroCG 2017 and his support during the last weeks of this thesis.
- Erhard Zorn for being a supportive mentor from the minute I came on campus.
- my friends and colleagues for proof-reading snippets or chapters of this thesis as well as for their mental support and encouragement: Laura, Daniel, Manfred, Sven, Frieder, Karl, Udo, Tillmann, Gerrit and Benjamin.
- Stephen Kobourov and Ignaz Rutter for their interest to read this thesis and being part of my committee.
- the program 'proMotion' for many valuable workshops.
- ... oder um es mit Worten eines bekannteren Namensvettern vom mir zu sagen: Ich danke ganz herzlich all denjenigen, die mir bei der 'allmähliche[n] Verfertigung der Gedanken beim Reden' zugehört haben. :)

Thank you!

Contents

1 Introduction

Many representations of planar graphs and their relatives are inspired by real-life situations. In this work, we study representations of planar graphs with prescribed face areas which are inspired by cartograms. A *cartogram* is a distorted map where the size of the regions (territories, countries, etc.) are proportional to some statistical parameter such as the population, the total birth, the gross national product, or some other special property. Figure 1.1 depicts a cartogram of Germany where the districts of the federal states are resized according to their population. In particular, cities such as Hamburg and Berlin are magnified compared to their geographic size, and territorial states such as Bavaria or Brandenburg diminish.

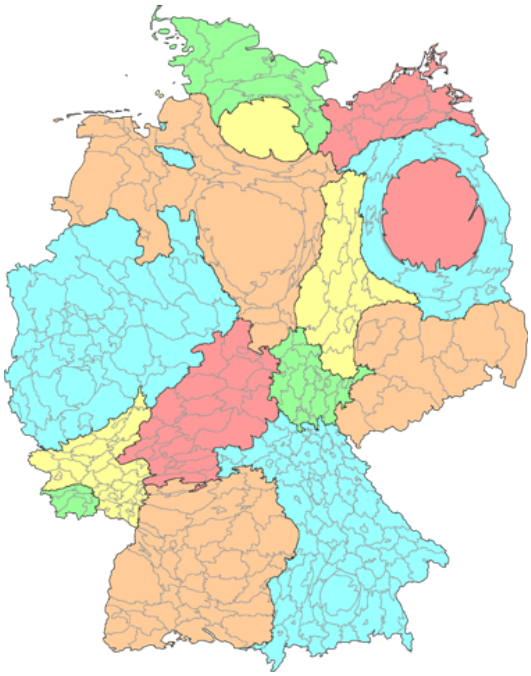

Figure 1.1: A population cartogram of Germany [Stoepel, 2010, CC BY-SA 3.0].

Cartograms have a fairly long history; there exist examples from the 19th century. According to Tobler [Tobler, 2004] the term *cartogram* appeared first in 1870. Moreover, he gives the reference of a cartogram that depicts the results of the German elections in 1903 [Haack and Wiechel, 1903]. Additionally, one can easily believe that in ancient maps little explored regions were represented disproportionally small, while religious or cultural centers were magnified.

Cartograms have several natural abstractions. Most commonly, *proportional contact representations* have been studied: The geography defines a plane contact graph where vertices correspond to the regions and the edges represent the neighborhood relations.

Given a graph and an assignment of areas, a proportional contact representation is a set of interiorly disjoint polygons whose contact graph is the given graph and additionally the areas of the polygons are equal to the assigned numbers. Figure 1.2 illustrates two examples of proportional contact representations with orthogonal polygons; one with orthogonal polygons of different complexity and one with rectangles.

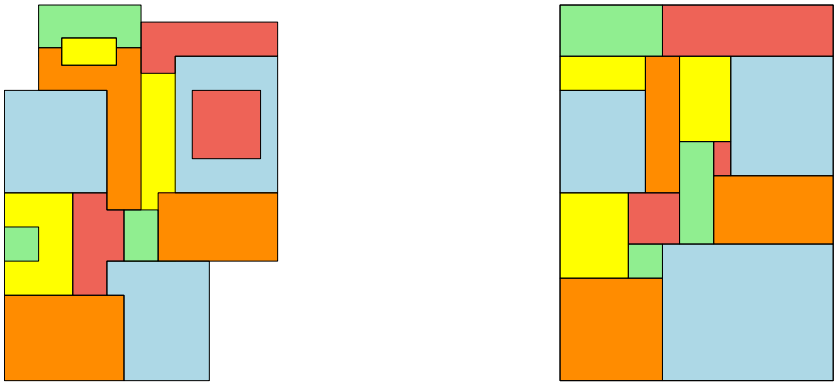

Figure 1.2: Proportional contact representations.

For proportional contact representations of triangulations, the polygonal complexity sufficient to represent all area assignments was studied intensively. In a series of papers [Kawaguchi and Nagamochi, 2007, de Berg et al., 2009, Biedl and Velázquez, 2011], the polygonal complexity has been improved from 40 sides, to 34 sides, and to 12 sides. Finally, Alam et al. [Alam et al., 2013] showed that 8-sided orthogonal polygons are always sufficient, which is known to be optimal.

For the special case of dissections of rectangles into rectangles, so called *rectangular layouts*, Eppstein et al. [Eppstein et al., 2012] characterized the area-universal rectangular layouts by an easily checkable property: A rectangular layout is area-universal if and only if it is one-sided.

For various other models of cartograms and their state of the art, we refer to the recent survey by Nusrat and Kobourov [Nusrat and Kobourov, 2016]. According to them, more than 70 papers have been published in the field of cartograms only within the last decade.

Instead of considering contact representations, we may also interpret the boundaries of the regions in a cartogram as a plane graph. The values of the statistical data are then associated with the faces and we look for a drawing in which the face areas equal the prescribed values. It is well known that every plane graph has a straight-line drawing [Wagner, 1936, Fáry, 1948, Stein, 1951]. Consequently, we may even seek for a realizing straight-line drawing. This concept of straight-line drawings with prescribed face areas was first introduced by Ringel [Ringel, 1990].

It is worth to note that proportional contact representations and realizing drawings are *dual* models in the following sense: In the first setting, areas are assigned to vertices whereas in the second setting, areas are assigned to faces of a given plane graph. In both settings, however, the graph captures the geometry or other neighborhood relations.

1.1 The Concept and the State of the Art

The thesis focuses on the following problem: Given a plane graph G and a positive real number for each inner face of G, we ask for an equivalent straight-line drawing of G where the area of each face equals the assigned number; such a drawing is called *realizing*. We are mainly dealing with an even more demanding property: A plane graph is *area-universal* if every area assignment to the inner faces has a realizing straight-line drawing.

To introduce the reader to the concept of area-universal graphs, we consider the class of *stacked triangulations*, which are also known as *Apollonian networks* or *plane 3-trees*. A stacked triangulation can be constructed from a triangle by repeatedly choosing an inner face and subdividing it into three triangles by inserting a new vertex of degree 3, for examples consider Figures 1.3 and 1.4(a). For the complete graph K_4 on four vertices, which is also a stacked triangulation, area-universality is easy to see: Recall that the area of a triangle is proportional to the product of the lengths of a base segment and its respective height. Thus, for a fixed outer face of correct total area, each inner triangle is realized when the inner vertex is placed on a particular line parallel to its outer edge. Placing the inner vertex on the intersection point of two lines, the area of the third triangle is also realized due to the correct sum. For an illustration consider Figure 1.3. By repeatedly using the area-universality of K_4, we obtain the following result:

Observation 1.1 ([Biedl and Velázquez, 2013])**.** *Stacked triangulations are area-universal.*

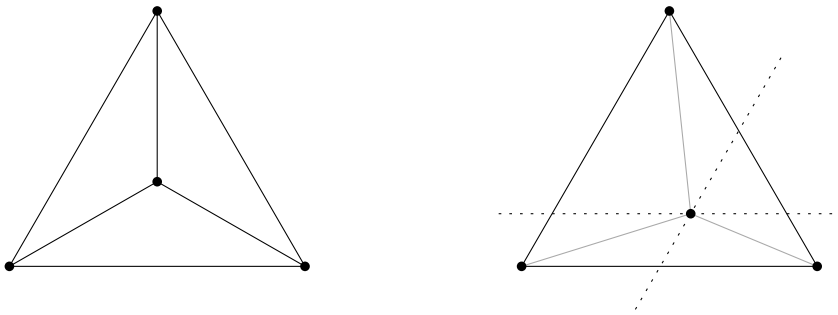

Figure 1.3: The complete graph K_4 and an illustration of a realizing drawing.

Besides the area-universality of stacked triangulations, two further interesting facts were known in the beginning of this thesis. As mentioned before, Ringel [Ringel, 1990] initiated the study of realizing drawings. He was interested in drawings where all face areas are of the same size. He called this property *equiareal* and showed that not all plane graphs are equiareal. His result implies that the plane octahedron graph, depicted in Figure 1.4(c), is not area-universal. Moreover, Ringel conjectured that plane cubic graphs are equiareal. This was proved by Thomassen [Thomassen, 1992]. Indeed, Thomassen showed an even stronger statement, namely that every plane cubic graph is area-universal. To the best of our knowledge, this was the state of the art of published results in 2013.

Furthermore, there have been some student projects on questions of realizing drawings. In a Predoc-Course in Berlin on 'Optimization Methods in Discrete Geometry' under the supervision of Günther Ziegler, Sabariego and Stump [Sabariego and Stump, 2006] investigated equiareal triangulations. Unaware of Ringel's work, they reproved the fact that the stacked octahedron is not equiareal with the same method and studied the question

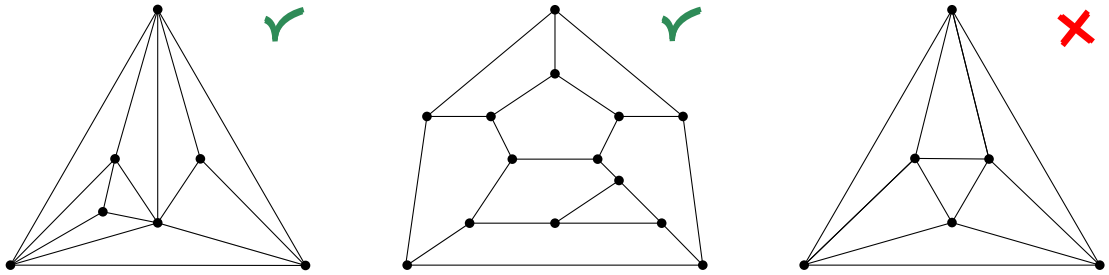

(a) A stacked triangulation. (b) A plane cubic graph. (c) The octahedron graph.

Figure 1.4: Illustration of the state of the art. A checkmark indicates that the depicted graph is area-universal whereas a cross indicates that it is not.

whether all 4-connected triangulations are equiareal. However, they also encountered the problem that computer tools and, in particular, computer algebra systems fail already for fairly small instances.

In her bachelor thesis, Anna Bernáthová [Bernáthová, 2009] disproved the unpublished conjecture of Jan Kratochvíl that every triangulation with minimum degree exceeding 3 is not area-universal. She showed that the triangulation on seven vertices is area-universal. Additionally, she wrote a program in order to find realizing drawings and presented some triangulations with area assignments for which her program did not find solutions.

In conclusion, even though studying plane graphs and face areas seems to be a very natural and interesting problem, area-universal graphs are not yet well understood. The aim of this thesis is to shed some more light onto the world of area-universal graphs. From the various open problems, we approach the following selected set of research questions.

Non-area-universal graph classes As every known non-area-universal graph contains the octahedron graph as a subgraph, we wonder if the octahedron graph is the only obstruction for area-universality. In particular, whether a graph is area-universal if and only if it contains the octahedron graph as a subgraph?

Area-universal graph classes Besides the plane cubic graphs, what other graph classes are area-universal? Are plane bipartite graphs area-universal? Are there other sufficient criteria for area-universality? Are graphs with high vertex connectivity area-universal? Can area-universality be characterized by local properties? Does area-universality depend on the embedding of a planar graph or is it independent? In other words, is area-universality a property of a plane or the planar graph?

Further properties of realizing drawings Can we ask for even more properties of realizing drawings? For instance, can we prescribe the outer face or ask for convex faces? More specifically, do plane 3-connected cubic graphs also have convex realizing drawings? What about plane bipartite graphs?

Relaxing the straight-line property Given the fact that not all plane graphs are area-universal, how much do we have to relax the straight-line property in order to guarantee the existence of realizing drawings for each area assignment of every plane graph?

Computational complexity What is the computational complexity of deciding the realizability of a given area assignment? What is the computational complexity of

deciding the area-universality of a plane graph? Is a graph area-universal if all area assignments consisting of 0 and 1 are realizable?

Equiareality Are there interesting equiareal graph classes? For instance, are 4-connected triangulations equiareal? Is equiareality a property of plane or planar graphs?

In the remainder of this introduction, we want to reveal some results which we encountered in the framework of this thesis. Among them, we present some surprising properties of area-universal graphs.

1.2 Selected Results

We develop techniques to prove and disprove area-universality: By a compactness argument, a triangulation is area-universal if and only if all non-negative area assignments are realizable. This streamlines many arguments for disproving area-universality. In particular, we present a new proof to show that the octahedron graph is not area-universal. Our proof relies on a simple counting argument that can also be used to show that no **Eulerian triangulation** is area-universal. A triangulation is *Eulerian* if and only if all vertex degrees are even. Figure 1.5(a) depicts an Eulerian triangulation together with a coloring of its faces. Assigning a value of 0 to the white faces and a value of 1 to the gray faces, the resulting area assignment of the Eulerian triangulation has no realizing drawing. This result already answers our first question in the negative: There exist non-area-universal graphs which do not contain the octahedron as a subgraph. Moreover, the result has several interesting consequences. For instance, there is no hope for constant factor approximations of realizing drawings even in the set of 4-connected triangulations.

Adding some geometric arguments, a similar reasoning can be applied to show that the 5-connected **icosahedron** graph, depicted in Figure 1.5(c), is not area-universal. Consequently, there exist highly connected graphs which are not area-universal.

Relaxing the straight-line property, we show that the **1-subdivision** of every plane graph is area-universal. In other words, for each area assignment of a plane graph there exists a realizing drawing where each edge has at most one bend. For the subclass of plane bipartite graphs, even half of the bends are sufficient. For an example of a 1-subdivision of the octahedron graph with a non-realizable area assignment consider Figure 1.5(b).

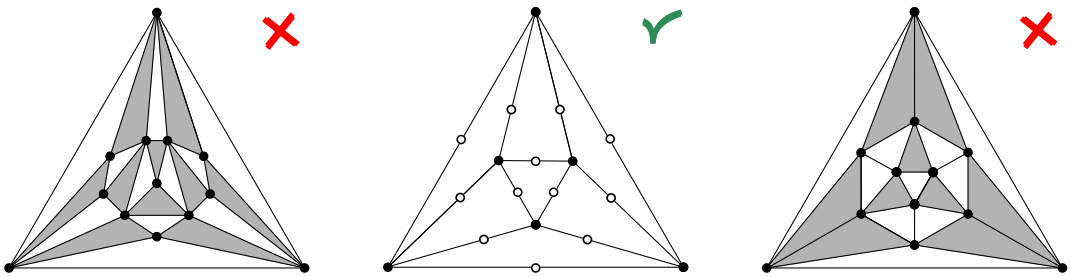

(a) An Eulerian triangulation. (b) The 1-subdivision of the octahedron. (c) The icosahedron graph.

Figure 1.5: Illustration of some considered graph classes.

As it turns out, the area-universality of a **triangulation** can be characterized by a polynomial equation system which encodes the area of each face. Based on this fact, we develop a sufficient criterion to prove area-universality for triangulations with special vertex orders. Combining our knowledge of Eulerian triangulations with this method, we can fully characterize the area-universality of accordion graphs: An *accordion* graph can be obtained from the plane octahedron graph by an operation which we call *diamond addition*. By this operation, an edge of the central triangle of the octahedron is subdivided by several vertices and additional edges are introduced such that the new vertices have vertex degree 4. Figure 1.6 shows the octahedron graph and three further accordion graphs obtained by the diamond addition operation. We say an accordion is *even* if it has an even number

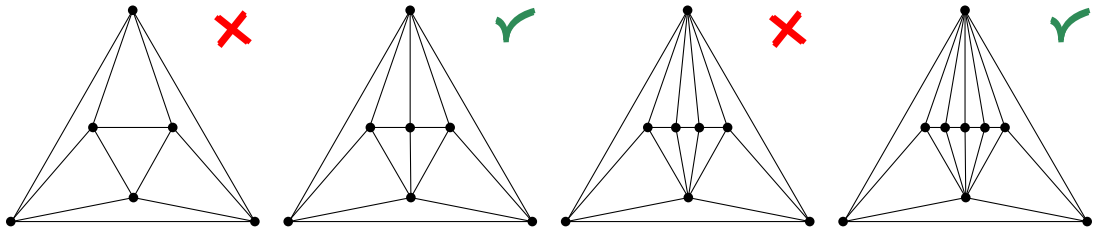

Figure 1.6: The accordion graphs on six, seven, eight, and nine vertices.

of vertices; otherwise it is *odd*. Obviously, even and odd accordion graphs are structural very similar. However, they have some surprising distinction. As a matter of fact, even accordion graphs are Eulerian and hence not area-universal whereas we prove that odd accordion graphs are area-universal. This shows how sensitive area-universality is to small local changes. In this sense, area-universality might be a *global* property.

Interestingly, if our method shows the area-universality for one embedding of a planar graph T, then all embeddings of T are area-universal as well. Combining these two methods of proving and disproving area-universality, we study small 4-connected triangulations. Up to this date, we do not know an example of a planar graph where the area-universality depends on the embedding, i.e., where one embedding is area-universal while another embedding is not. In other words, in our list of graphs all plane graphs belonging to the same planar graph are either all area-universal or not – or have unknown status.

An interesting example is the planar triangulation on nine vertices depicted in Figure 1.7; it has three different plane graphs. One of them, namely the plane graph in Figure 1.7(a),

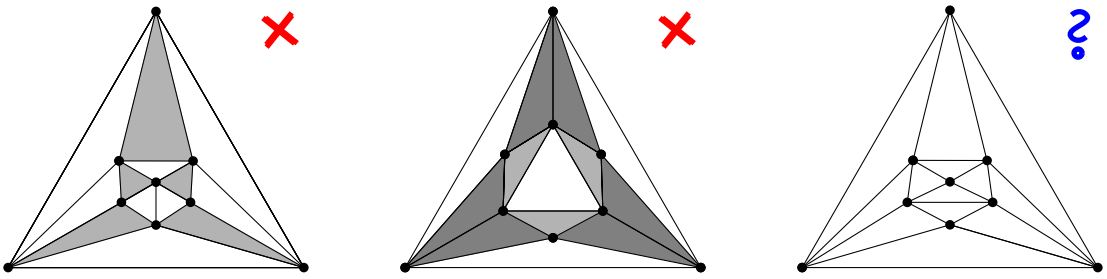

(a) (b) (c)

Figure 1.7: Three plane triangulations on nine vertices belonging to the same planar graph. While the plane graphs in (a) and (b) are not area-universal, it is unknown whether the plane graph in (c) is area-universal.

has an area assignment consisting of 0's and 1's which is not realizable; for simplicity we call such an area assignment a 01-*assignment*. Interestingly, computer search asserts that all 01-assignments of the other two plane graphs are realizable. However, the graph in Figure 1.7(b) is not area-universal since it has a non-realizable 012-assignment, whereas we do not know whether or not the last plane graph in Figure 1.7(c) is area-universal. Note that the plane graph in Figure 1.7(b) asserts that it is not enough to test 01-assignments in order to check for area-universality.

As we have just discussed, even for a small graph it may be tricky to decide its area-universality. This suggests that the **computational complexity** of area-universality is hard. While many geometric problems are complete for the $\exists\mathbb{R}$ [Matoušek, 2014, Mnëv, 1988], i.e., as hard as deciding if a polynomial equation system has a real solution, the nature of area-universality seems to be different. The definition of area-universality suggests that the computational complexity of deciding whether a plane graph is area-universal is complete for the complexity class $\forall\exists\mathbb{R}$. This complexity class naturally generalizes $\exists\mathbb{R}$, analogous to the polynomial time hierarchy. Area-universality may turn out to be the first natural geometric problem which is complete for this class. While we do not provide a complete answer to the computational complexity of area-universality, we introduce first tools to prove $\forall\exists\mathbb{R}$-hardness and show that problems related to area-universality are $\exists\mathbb{R}$- and $\forall\exists\mathbb{R}$-hard; among them the analogous questions in three dimensions. These results on the computational complexity are joint work with Michael Dobbins, Tillmann Miltzow, and Paweł Rzążewski.

Additionally, we investigate several options to impose further restrictions on realizing drawings. Firstly, we study **convex** realizing drawings. Our interest in convexity is motivated by two facts. On the one hand, convexity is a very visually appealing property. On the other hand, realizing drawings of cubic graphs (and also bipartite graphs seem to) have a high degree of freedom. Therefore, one has little starting points to construct realizing drawings. Thus, further properties may reduce the degrees of freedom and be useful in order to find alternative proofs. However, convexity does not seem to be the right direction as we show that realizing drawings of 3-connected bipartite and cubic graphs do not always exist. Nevertheless, we present some graphs which are *convex area-universal*, i.e., they have a convex realizing straight-line drawing for every area assignment. As an example, we present four proofs of this fact for the cube graph depicted in Figure 1.8(a).

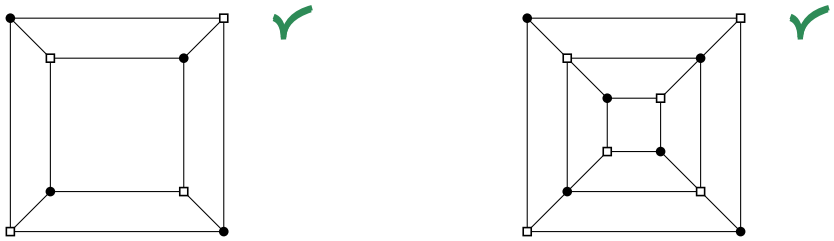

(a) The cube graph. (b) A stacked cube graph.

Figure 1.8: Illustration of the cube graph and a stacked cube graph.

Indeed, the cube graph allows for even more shape restrictions of its realizing drawings, namely, it is also **strongly area-universal**. We say a plane graph is strongly area-universal, if for every area assignment and fixed outer face of correct total area, there exists a realizing drawing. Note that an area-universal graph with an triangular outer face is also strongly area-universal due to affine linear transformations. We have already used this idea for

Observation 1.1. Therefore, the property of strong area-universality can be very useful in order to recursively construct new area-universal graphs from graphs that are already known to be area-universal. In particular, consider a stacked cube graph which is obtained from two cube graphs by identifying an inner 4-face on one copy with the outer 4-face of the other copy as depicted in Figure 1.8(b). Since the cube graph is strongly area-universal, the stacked cube graph is area-universal as well.

Among other things, we use the concept of strong area-universality to tackle the conjecture that **plane bipartite graphs** are area-universal. By reductions to area-universal triangulations, we establish area-universality for large classes of plane quadrangulations. In particular, we prove the area-universality of all plane quadrangulations with up to 13 vertices. The research on quadrangulations is joint work with William Evans, Stefan Felsner, and Stephen Kobourov.

As the last selected result, we announce the *butterfly graph*, depicted in Figure 1.9, as the first non-area-universal graph that does not contain a non-area-universal triangulation as a subgraph. Consequently, we found a further type of obstruction. In several respects, the butterfly graph enables us to show that 4-connected triangulations behave similar to 3-connected triangulations in field of area-universal graphs.

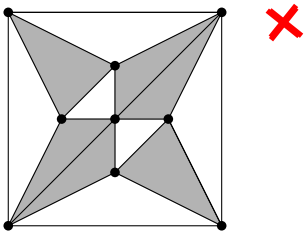

Figure 1.9: The butterfly graph.

1.3 Outline

This thesis is structured as follows: In Chapter 2, we introduce the basic notions and discuss properties of area-universal graphs. In particular, we introduce area-universality preserving operations and several characterizations of area-universality. These tools will be used repeatedly throughout this thesis.

In Chapter 3, we study area-universality of maximal planar graphs, i.e., triangulations. We present both, methods to prove and disprove area-universality. Firstly, we show that no Eulerian triangulation is area-universal. Secondly, prove area-universality for some triangulations with a special vertex order called a p-order. Combining these two techniques, we are then able to fully understand the area-universality of accordion graphs. Additionally, we use these tools to determine whether small triangulations are area-universal or not; in particular, we characterize all triangulations on up to ten vertices with a p-order.

We then proceed to study quadrangulations in Chapter 4. Even though we do not provide a full answer to the very promising conjecture that all quadrangulations are area-universal, we establish the area-universality of large classes of quadrangulations. From our results it follows that a minimal counter example to the conjecture has at least 14 vertices.

Given that not all plane graphs are area-universal, we investigate how many bends are sufficient to realize each area assignment of every plane graph. In Chapter 5, we show that

the 1-subdivision of every planar graph is area-universal. This result can be strengthened for plane bipartite graphs in the following sense: For every plane bipartite graph, there exists an area-universal subdivision where at most half of the edges have exactly one bend and all other edges have no bend.

In Chapter 6, we study more restricted concepts of area-universality. We start with convex realizing drawings in Section 6.1, and present a 3-connected quadrangulation and a 3-connected cubic graph which are not convex area-universal. Consequently, convex realizing drawings seem to be to much to ask for. In Section 6.2, we discuss some interesting facts of equiareality. In particular, we show that equiareality is a property of plane graphs rather than planar graphs and that all plane 4-connected triangulations on up to ten vertices are equiareal.

Chapter 7 deals with the computational complexity of area-universality. We present hardness proofs of several variants of area-universality. Among them, we consider the analogous questions in three dimensions, a partial extension problem and a variant where we relax the planarity condition. The introduced tools might be of independent interest to show hardness of other geometric problems.

In Chapter 8, we present the air pressure method which has previously been used in the context of area-universal rectangular layouts and seems promising to show area-universality of cubic graphs or other graph classes. We show how the ideas can be transferred to our setting. We conclude this thesis with our favorite set of open questions and ideas for further projects related to the study of plane graphs and faces areas in Chapter 9.

2 | The Toolbox

The aim of this chapter is to reveal basic properties of area-universal plane graphs in general and triangulations in particular. We introduce several characterizations of area-universality and present graph operations that preserve area-universality. Many of the presented tools are repeatedly used throughout this thesis. We start with general statements for plane graphs in Section 2.1 and proceed with particular properties of triangulations in Section 2.2.

2.1 Plane Graphs

All graphs considered in this thesis are finite and simple, i.e., they contain neither loops nor parallel edges. Our notation and terminology is mostly standard. For instance, we denote the vertex set of a graph by V, its edge set by E and the number of vertices by n. Any graph-theoretic term not defined here is explained in [West, 2001].

Since we are interested in drawings of plane graphs, we first clarify the considered types of drawings. In a *straight-line drawing* of a graph, vertices are represented by points in the plane and edges by segments. Such a drawing can be encoded by the vertex coordinates in the plane, i.e., for a plane graph on n vertices, the $2n$ coordinates can be represented by a point in the Euclidean space $\mathbb{R}^{2n}$. We call this vector of vertex coordinates a *vertex placement*. From a vertex placement, we easily recover the straight-line drawing by connecting the two endpoints of every edge by a segment.

In a *planar* drawing, no two edges intersect except in common vertices. Figure 2.1(a) depicts a planar straight-line drawing of the octahedron graph. Note that in a planar drawing all face areas are positive. As it turns out, it is worthwhile to be slightly more

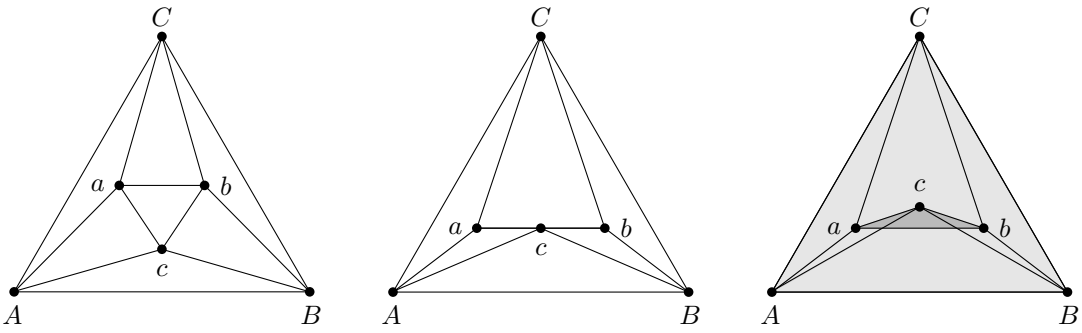

(a) crossing-free, planar (b) crossing-free, degenerate (c) not crossing-free

Figure 2.1: Straight-line drawings of the octahedron graph with different properties. In (b), the area of face abc vanishes. In (c), the edges ab and Ac have a proper crossing.

generous and consider crossing-free drawings which also account for vanishing face areas. Therefore, we extend the set of drawings by the *degenerate drawings*, i.e., all drawings which can be obtained as the limit of a sequence of planar drawings. More specifically for straight-line drawings, we allow degeneracies which are usually forbidden: edges may have zero length, i.e., adjacent vertices may be mapped to the same point, vertices may lie in a non-incident edge if they belong to the boundary of a common face and the union of two edges are allowed to form a segment. Two intersecting segments whose union is not a segment form a *proper crossing*. We call the resulting set of straight-line drawing *crossing-free* since no two edges properly cross. Figure 2.1(b) displays a *crossing-free* drawing of the octahedron which is not planar since the edges ab and ac are intersecting in interior points; however their union forms a segment. Note that for triangulations, a crossing-free drawing is degenerate if and only if the area of at least one face vanishes.

As usual, we say a graph is *planar* if it has a planar drawing. By a *plane graph*, we refer to a graph with a fixed planar drawing. A planar drawing partitions the plane into path-connected regions, which we call *faces*. By F, we denote the set of faces of G. In a plane graph G, there exists a unique unbounded face, which we call the *outer face* of G. All other faces are *inner* faces of G. We denote the set of inner faces by F'. Likewise, we call a vertex or edge *outer* if it is incident to the outer face and *inner* otherwise.

A planar drawing also determines the *rotation system*, i.e., a cyclic ordering of incident edges around each vertex. We consider two crossing-free drawings of a planar graph as *equivalent* if the outer faces and the rotation systems coincide in both drawings. Thus, the above definitions of *inner* and *outer* do not depend on a specific drawing of a plane graph but remain the same for all equivalent drawings.

For a plane graph G, we denote the set of vertex placements, corresponding to straight-line crossing-free drawings equivalent to G, by $\mathcal{D}(G)$; we also write $\mathcal{D}$ if G is clear from the context. From now on and for the sake of simplicity, we usually omit the terms *crossing-free* and *straight-line*; however, we ask the reader to think about such drawings unless stated otherwise.

An *area assignment* of G is a function $\mathcal{A}\colon F' \to \mathbb{R}_{>0}$, where $\mathbb{R}_{>0}$ denotes the set of positive real numbers. The *total area* of $\mathcal{A}$, denoted by $\Sigma\mathcal{A}$, is the sum of all assigned areas, i.e., $\Sigma\mathcal{A} := \sum_{f\in F'} \mathcal{A}(f)$. The function $\textsc{area} : F' \times \mathcal{D} \to \mathbb{R}_{>0}$ measures the area of a face f in a specific drawing D of G. A drawing $D \in \mathcal{D}(G)$ *realizes* an area assignment $\mathcal{A}$ of G if for all inner face $f \in F'$ it holds that $\textsc{area}(f, D) = \mathcal{A}(f)$. We also say D is $\mathcal{A}$*-realizing*. Furthermore, we call an area assignment $\mathcal{A}$ *realizable* if there exists an $\mathcal{A}$-realizing drawing in $\mathcal{D}(G)$. We are now ready for the crucial definition of area-universality:

Definition. *A plane graph G is* area-universal *if every area assignment is realizable.*

We now start to examine interesting properties. For any positive real number $\alpha > 0$ and every area assignment $\mathcal{A}$, let $\alpha\mathcal{A}$ denote the α*-scaled area assignment* of $\mathcal{A}$ where for all inner faces $f \in F'$ it holds that $\alpha\mathcal{A}(f) := \alpha \cdot \mathcal{A}(f)$.

▶ **Lemma 2.1.** *Let G be a plane graph with an area assignment $\mathcal{A}$. For every $\alpha \in \mathbb{R}_{>0}$, G has an $\alpha\mathcal{A}$-realizing drawing if and only if it has an $\mathcal{A}$-realizing drawing.*

Proof. Let $\alpha_1, \alpha_2 \in \mathbb{R}_{>0}$. We show how to transform an $\alpha_1\mathcal{A}$-realizing drawing D_1 into an $\alpha_2\mathcal{A}$-realizing drawing D_2 of G. To obtain D_2 from D_1, scale one axis of the plane by α_2/α_1. This is a linear transformation where the determinant of the associated matrix is α_2/α_1. Consequently, all face areas are scaled by this factor and D_2 is an $\alpha_2\mathcal{A}$-realizing drawing. ◀

The following corollary is an immediate consequence.

■ **Corollary 1.** *Let $c \in \mathbb{R}_{>0}$. A plane graph is area-universal if and only if all area assignments with a total area of c are realizable.*

Our next lemma concerns the fact that we may delete edges and vertices from an area-universal graph while maintaining area-universality. This has also already been observed in [Biedl and Velázquez, 2013].

▶ **Lemma 2.2.** *Every plane subgraph G' of a plane area-universal graph G is area-universal.*

Proof. Let $\mathcal{A}'$ be an area assignment of G'. We construct an area assignment $\mathcal{A}$ of G. Each face f of G' corresponds to a collection of faces $\mathcal{C}_f$ in G. We define $\mathcal{A}$ such that for each face f in G', the area assigned to the faces in $\mathcal{C}_f$ sums to $\mathcal{A}'(f)$. Since G is area-universal, we may consider an $\mathcal{A}$-realizing drawing D of G. Restricting D to G' yields an $\mathcal{A}'$-realizing drawing of G'. ◀

Combining Lemma 2.2 with the area-universality of stacked triangulations, which we established in Observation 1.1, yields the area-universality of several graph classes. Therefore, we introduce subclasses of stacked triangulations.

An *outerplane graph* is a plane graph where all vertices are incident to the outer face. For an example, consider Figure 2.2(a). A graph is *series-parallel* if it can be reduced to K_2, the complete graph on two vertices, by the following two operations: replacing a vertex of degree 2 and its two incident edges by a single edge between its neighbors (series reduction rule) and replacing a double edge by a single edge (parallel reduction rule). Figure 2.2(b) displays an example of a series-parallel graph. A plane *Halin graph* can be constructed by connecting the leaves of a plane tree with a cycle. In order to obtain a simple graph, the plane tree must have at least one vertex of degree (at least) three, see also Figure 2.2(c).

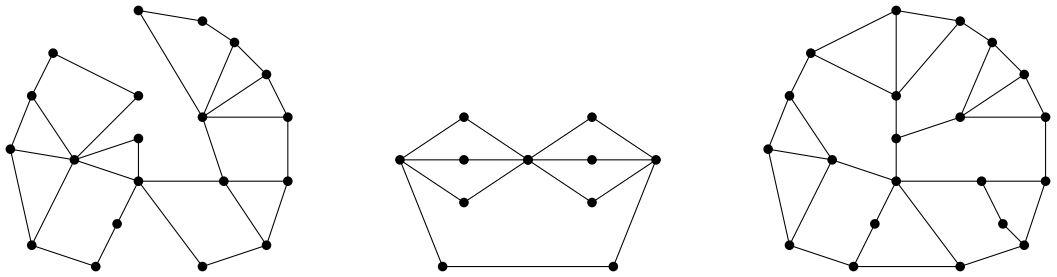

(a) An outerplane graph. (b) A series-parallel graph. (c) A Halin graph.

Figure 2.2: Examples of subgraphs of stacked triangulations.

In fact, these three graph classes are subgraphs of stacked triangulations. For this reason, Lemma 2.2 and Observation 1.1 imply their area-universality.

■ **Corollary 2.** *Subgraphs of stacked triangulations are area-universal. In particular, outerplane graphs, series-parallel graphs, and Halin graphs are area-universal.*

Proof. Since stacked triangulations are area-universal by Observation 1.1, Lemma 2.2 implies the area-universality of all subgraphs of stacked triangulations. It remains to show that the stated graph classes are subgraphs of stacked triangulations. Planar graphs with treewidth at most k are exactly subgraphs of planar k-trees [Arnborg et al., 1987]. Since series-parallel graphs have treewidth at most 2 [Wald and Colbourn, 1983] and Halin graphs have treewidth 3 [Bodlaender, 1988], the claim follows. ■

Figure 2.3 illustrates the containment relations of plane partial 3-trees. Note that Halin graphs and outerplanar graphs are incomparable with respect to set inclusion: While Halin graphs contain K_4-minors, e.g. contract all inner vertices to a single vertex and all outer vertices to three vertices, series-parallel graphs can be characterized as K_4-minor-free graphs [Dirac, 1952].

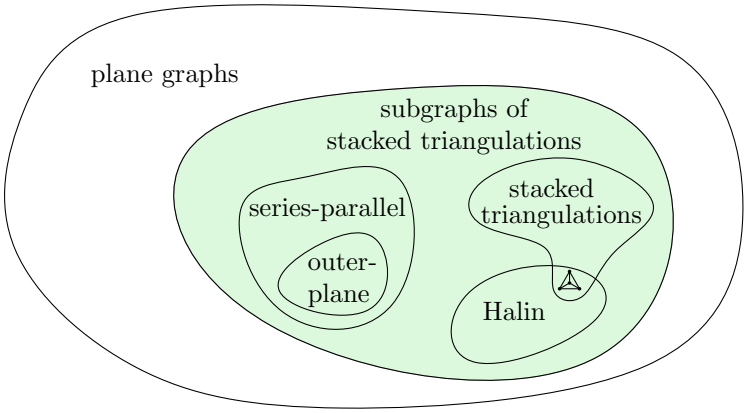

Figure 2.3: Containment relations of subgraphs of stacked triangulations; since this is not a cartogram, the areas do not indicate the relative sizes of these classes.

Moreover, note that Halin graphs are 2-outerplane, i.e., after removal of the outer vertices, all remaining vertices lie on the outer face. One could think that k-outerplanarity and area-universality are linked. However, we will see that some 2-outerplane graphs, for instance the octahedron graph, are not area-universal.

The following lemma generalizes Lemma 2.2. Besides inserting edges and vertices, we can also perform face-maintaining edge contractions to obtain an area-universal graph. An edge contraction is *face-maintaining* if the number of faces remains, i.e., for a face of degree d at most $d-3$ edges are contracted. In other words, every face must remain at least a triangle as otherwise its area vanishes in a straight-line drawing.

▶ **Lemma 2.3.** *Let G be a plane graph which can be transformed into an area-universal plane graph G' by inserting vertices, inserting edges, and performing face-maintaining edge contractions. Then G is area-universal.*

Proof. Let $\mathcal{A}$ be a fixed but arbitrary area assignment of G. A face f of G corresponds to a non-empty collection of faces C_f in G'. We define $\mathcal{A}'$ such that for each face f of G it holds that

$$\mathcal{A}(f) = \sum_{f' \in C_f} \mathcal{A}'(f').$$

Since G' is area-universal, there exists an $\mathcal{A}'$-realizing drawing D' of G'. Deleting all vertices and edges of G' which are not in G yields a (degenerate) drawing D of G. By definition of $\mathcal{A}'$, D is $\mathcal{A}$-realizing. ◀

We provide a further operation preserving area-universality. It is based on graph decomposition. To do so, we need a stronger concept of area-universality.

Definition. *A plane graph G is* strongly area-universal *if for every area assignment $\mathcal{A}$ of G and every fixed polygonal placement of the outer face with area $\Sigma\mathcal{A}$, there exists an $\mathcal{A}$-realizing drawing of G within the prescribed outer face.*

Informally, if a graph is strongly area-universal then we can choose our favorite outer face of correct total area and find a realizing drawing with this outer face. As an illustration of this concept, we consider the unique plane quadrangulation with five vertices depicted in Figure 2.4(a). For simplicity, we denote it by Q_5. It can be understood as a 4-face with a subdivided diagonal.

(a) The plane quadrangulation Q_5. (b) Illustration of the proof of Proposition 2.4.

Figure 2.4: The plane quadrangulation Q_5 is strongly area-universal.

▶ **Proposition 2.4.** *The plane quadrangulation Q_5 is strongly area-universal.*

Proof. Let $\mathcal{A}$ be an area assignment of Q_5 and q be a quadrangle of area $\Sigma\mathcal{A}$ whose corners are identified with the outer vertices of Q_5. Starting at a non-neighbor, move the inner vertex v on a curve connecting its two non-neighbors within q and observe the continuous change of the face areas incident to v. Since the area is 0 and $\Sigma\mathcal{A}$ at the extremes, the intermediate value theorem guarantees a position for v on the curve such that both inner faces have correct area. The gray curve in Figure 2.4(b) serves as an illustration. ◀

Strongly area-universality is beneficial if a graph decomposes into several strongly area-universal graphs, see also Figure 2.5. From a plane graph G with a simple cycle C, we obtain two plane graphs G_I and G_E by *decomposing along* C: G_I consists of the subgraph of G induced by C and its interior, while G_E consists of the subgraph of G induced by C and its exterior. Reversely, we obtain G from G_I and G_E by identifying the outer face of G_I with an inner face of G_E of same degree.

▶ **Lemma 2.5.** *Let G be a plane graph, and let G_I and G_E be obtained by decomposing G along a simple cycle C of G. If G_E is area-universal and G_I strongly area-universal, then G is area-universal. Moreover, if G_E is strongly area-universal, then G is also strongly area-universal.*

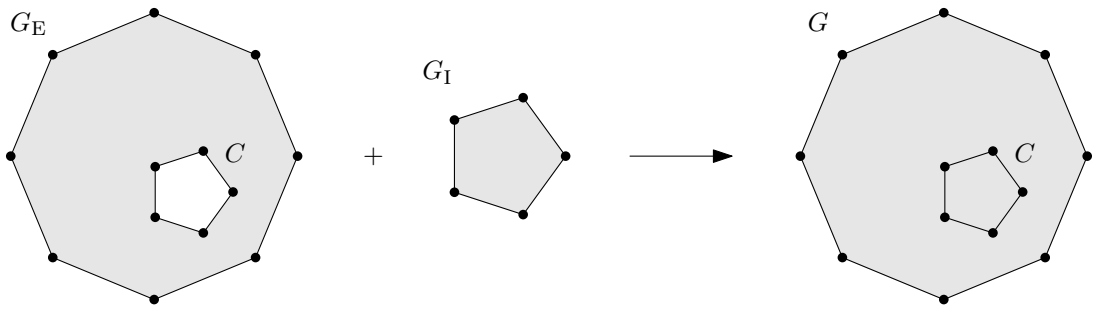

Figure 2.5: Decomposing G along C yields two plane graphs G_E and G_I. If G_E is area-universal and G_I strongly area-universal, then G is area-universal.

Proof. Let $\mathcal{A}$ be an area assignment of G. For $i \in \{\text{I},\text{E}\}$, $\mathcal{A}_i$ denotes the induced area assignment of G_i. Note that the interior of C is a face f of G_E. In particular, it holds that $\mathcal{A}_\text{E}(f) = \Sigma A_\text{I}$. Since G_E is area-universal, there exists an $\mathcal{A}_\text{E}$-realizing drawing D_E of G_E. Since G_I is strongly area-universal, we find an $\mathcal{A}_\text{I}$-realizing drawing D_I of G_I whose outer face coincides with the polygon representing f in D_E. Thus, identifying D_E and D_I along f yields an $\mathcal{A}$-realizing drawing of G. If G_E is strongly area-universal, then this property immediately passes over to G. ◀

Combining Proposition 2.4 with Lemma 2.5, we obtain area-universality for 2-degenerate quadrangulations. A graph is *k-degenerate* if every subgraph has a vertex of degree at most k.

▶ **Proposition 2.6.** *Every 2-degenerate quadrangulation is strongly area-universal.*

Proof. A 2-degenerate quadrangulations can be constructed from a plane 4-cycle by iterative insertion of a degree 2-vertex, acting as a subdivided diagonal, into a 4-face. Therefore, in every step we insert the inner vertex of Q_5 in a 4-face of correct area. Thus, Proposition 2.4 and Lemma 2.5 imply the claim. ◀

2.2 Triangulations

Not surprisingly area-universality of maximal planar graphs, namely triangulations, is slightly easier to grasp than for general plane graphs. Here we present three characterizations of their area-universality which we exploit in our further analysis. For some of the properties, we only need that some face, for instance the outer face, is a triangle. In these cases, we state the observations as general as possible. Clearly, these properties particularly hold for triangulations.

The first observation follows directly from the fact that triangles are affine equivalent. It enables us to prescribe the outer face of a triangulation without loss of generality.

▶ **Lemma 2.7.** *Let G be a plane graph with a triangular outer face and let $\mathcal{A}$ be a realizable area assignment. Then there exists an $\mathcal{A}$-realizing drawing for every outer face of area $\Sigma\mathcal{A}$.*

Proof. Any $\mathcal{A}$-realizing drawing of G can be transformed by an affine linear transformation into a drawing with a given outer face. If the area of the two triangles are equal, the determinant of the associated matrix is 1, and the areas are maintained. ◀

For later reference, we note that combining Lemma 2.7, Observation 1.1 and Lemma 2.2 yields the following result.

▶ **Lemma 2.8.** *Let G be a plane graph and G^+ the plane graph where a vertex of degree 3 is inserted in a triangle of G. Then G is area-universal if and only if G^+ is area-universal.*

Moreover, it follows immediately from Lemma 2.7 that

▶ **Proposition 2.9.** *A plane graph G with a triangular outer face is area-universal if and only if G is strongly area-universal.*

This fact enables us to restrict our attention to 4-connected triangulations when studying area-universality. A 4-*connected component* of a graph is a maximal 4-connected subgraph. We say a triangle t of a plane graph G is *separating* if at least one vertex of G lies inside t and at least one vertex lies outside t. In other words, t is not facial and therefore, when decomposing G along t, neither G_E nor G_I is isomorphic to t.

▶ **Lemma 2.10.** *A plane graph G with a separating triangle t is area-universal if and only if the plane graphs G_E and G_I, obtained by decomposing G along t, are area-universal.*

Proof. If G is area-universal, then by Lemma 2.2, every subgraph is area-universal. Thus, in particular G_E and G_I are area-universal.

Suppose now that G_E and G_I are area-universal. Since G_I has a triangular outer face, it is even strongly area-universal by Proposition 2.9. Clearly, identifying G_E and G_I along t yields G. Therefore, by Lemma 2.5, G is area-universal. ◀

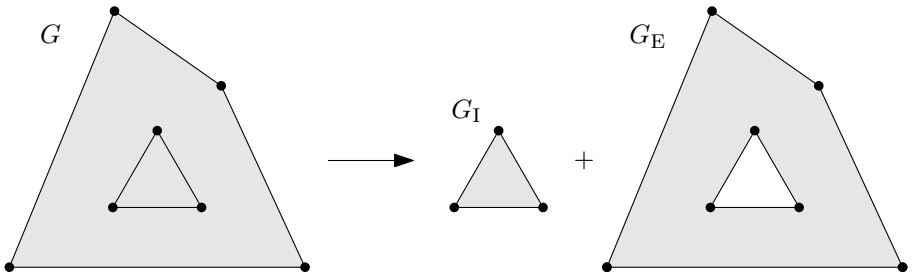

Figure 2.6: Decomposing a graph along a separating triangle.

It is well-known and easy to see that a triangulation is 4-connected if and only if it has no separating triangle. With this fact at hand, we obtain the following characterization.

▶ **Proposition 2.11.** *A plane triangulation T is area-universal if and only if every 4-connected component of T is area-universal.*

Proof. By Lemma 2.2, it is only interesting to consider the reverse direction which we show by induction. Note that the small triangulations on three and four vertices are area-universal and have no 4-connected components. Suppose that T is not area-universal. If T is 4-connected, then it certifies a 4-connected component which is not area-universal. Thus, we suppose that T has a separating triangle t. Let T_E and T_I denote the triangulations obtained by decomposing along t. By Lemma 2.10, at least one of T_E and T_I is not area-universal. Clearly, T_E and T_I are triangulations and have less vertices than T. Thus, by induction, there exists a 4-connected component C of T_E or T_I which is not area-universal. The separating triangle guarantees that C is also a component of T. ◀

Remark. Note that a stacked triangulation has no 4-connected component. Thus, Proposition 2.11 offers an alternative proof for the area-universality of stacked triangulations.

The fact that we may choose the outer face of a triangulation, namely Lemma 2.7, has further nice consequences. Recall that $\mathcal{D}$ denotes the vertex placements of all equivalent straight-line drawings of a plane graph G. Now, we restrict the set of drawings a little further. Let f be a triangular face of G and $\triangle$ be a triangle whose corners are identified with the vertices of f. Then $\mathcal{D}|_{f\to\triangle}$ denotes the subset of vertex placements where face f coincides with $\triangle$. By Lemma 2.7, we may fix the outer face f_o without loss of generality. This has fruitful consequences.

▶ **Lemma 2.12.** *For a plane graph G with a triangular outer face f_o and a triangle $\triangle$, the set of vertex placements $\mathcal{D}|_{f_o\to\triangle}$ is compact.*

Proof. Since $\mathcal{D}$ contains the degenerate drawings, which are by definition the limit of plane drawings, $\mathcal{D}$ is a closed subset of the Euclidean space $\mathbb{R}^{2n}$. Due to the fixed outer face, all vertex coordinates are bounded. Therefore, $\mathcal{D}|_{f_o\to\triangle}$ is compact. ◀

With the help of this fact, we obtain a very handy lemma which characterizes area-universality for plane graphs with a triangular outer face, e.g., for triangulations. To do so, we understand an area assignment as a vector in $\mathbb{R}^{|F'|}$. Recall that an area assignment assigns positive real numbers to the inner faces. A *non-negative area assignment* is a function $\mathcal{A}\colon F' \to \mathbb{R}_{\geq 0}$, i.e., every inner face is assigned to a non-negative real number. For a fixed graph, let $\mathbb{A}$ denote the set of non-negative area assignments with a total area of c, for any fixed $c \in \mathbb{R}_{>0}$. We consider $\mathbb{A}$ as a subset of $\mathbb{R}^{|F'|}$.

▶ **Proposition 2.13.** *Let G be a plane graph with triangular outer face. Then $\mathcal{A} \in \mathbb{A}$ is realizable if and only if every open neighborhood of $\mathcal{A}$ in $\mathbb{A}$ contains a realizable area assignment.*

Proof. Suppose $\mathcal{A} \in \mathbb{A}$ is realizable, then clearly $\mathcal{A}$ itself is in every of its open neighborhoods and serves as a certificate of a realizable area assignment.

Suppose in every open neighborhood of $\mathcal{A}$, there exists a realizable area assignment. Hence, we may construct a sequence of realizable assignments $(\mathcal{A}_i)_{i\in\mathbb{N}}$ converging to $\mathcal{A}$. For each $\mathcal{A}_i$, we pick a realizing drawing D_i. By Lemma 2.7, we may assume that the outer face f_o coincides in all drawings D_i and is a fixed triangle $\triangle$ of area $\Sigma\mathcal{A}$. Consequently, the sequence $(D_i)_{i\in\mathbb{N}}$ is contained in $\mathcal{D}|_{f_o\to\triangle}$ and, thus, bounded by Lemma 2.12. Therefore, by the Bolzano-Weierstrass theorem, the sequence $(D_i)_{i\in\mathbb{N}}$ contains a converging subsequence with limit D. By the compactness, D is contained in $\mathcal{D}|_{f_o\to\triangle}$ and thus yields a crossing-free drawing of G. By definition of D, for every inner face f it holds that

$$\textsc{area}(f, D) = \lim_{i\to\infty} \textsc{area}(f, D_i) = \lim_{i\to\infty} \mathcal{A}_i(f) = \mathcal{A}(f).$$

Consequently, D is $\mathcal{A}$-realizing. ◀

Proposition 2.13 implies immediately that every non-realizable area assignment has a neighborhood of non-realizable area assignments. This gives the following fact.

■ **Corollary 3.** *If a plane graph with triangular outer face has a non-negative area assignment that is not realizable, then it also has a (positive) non-realizable area assignment.*

Intuitively speaking, Proposition 2.13 is particularly useful when we want to show the realizability of an area assignment $\mathcal{A}$ with some unlikely but bad properties. Then, instead of considering $\mathcal{A}$, it is sufficient to show the existence of a realizable area assignment in every neighborhood of $\mathcal{A}$. In particular, area-universality is guaranteed by the realizability of a dense subset of $\mathbb{A}$. We will exploit this fact in the next chapter.

Restricting to triangulations, we may strengthen some of the above observations. Let T be a plane triangulation and f some triangle of T. As discussed in Lemma 2.12, if f is the outer face and $\triangle$ a triangle, then $\mathcal{D}|_{f\to\triangle}$ is compact. For our purposes in Chapter 3, we need a slightly more general statement. For a positive real value $c \in \mathbb{R}_{>0}$, let $\mathcal{D}^c|_{f\to\triangle}$ denote the subset of $\mathcal{D}|_{f\to\triangle}$ where additionally the total area in each drawing does not exceed c.

▶ **Lemma 2.14.** *Let T be a plane triangulation, f a face of T, $\triangle$ a triangle of positive area, and $c \in \mathbb{R}_{>0}$. Then the set of vertex placements $\mathcal{D}^c|_{f\to\triangle}$ of T is compact.*

Proof. First note that closedness follows from the fact that we allow for degenerate drawings. Second, we show that $\mathcal{D}^c|_{f\to\triangle}$ is bounded. By assumption f coincides with a triangle $\triangle$. Since $\triangle$ has positive area, its three sides are pairwise not parallel. If f is the outer face, then clearly all inner vertex coordinates are bounded by $\triangle$. Hence, it remains to consider the case that f is an inner face.

We show that all vertices lie inside a bounded region which consists of the intersection of three half spaces. Consider Figure 2.7. For each side s of $\triangle$, let ℓ_s denote the line such

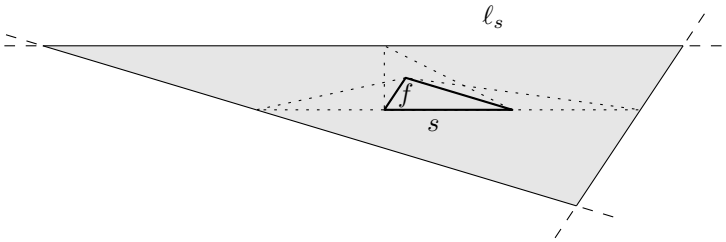

Figure 2.7: Illustration of Lemma 2.14 and its proof.

that the segment s and any point of ℓ_s form a triangle of area c that intersects $\triangle$. Moreover, let H_s denote the half space defined by ℓ_s that contains $\triangle$. We claim that any drawing D in $\mathcal{D}^c|_{f\to\triangle}$ lies in H_s. Suppose a vertex v of T lies outside H_s, then the triangle t' formed by s and v is contained in D since the outer face is triangular and thus convex. However, the area of t' exceeds c. Therefore all vertices lie within the intersection of the three half spaces H_s. ◀

Following the same argument, Lemma 2.14 enables us to prove the following stronger version of Proposition 2.13 for triangulations. Let T be a triangulation and $\mathbb{A}^c$ denote the set of all area assignments of T with total area at most c. For a fixed face f of T, the subset of area assignments of $\mathbb{A}^c$ where f is assigned to the area a is denoted by $\mathbb{A}^c|_{f\to a}$.

▶ **Proposition 2.15.** *Let T be a plane triangulation with an area assignment $\mathcal{A}$, f a face of T with $a := \mathcal{A}(f) > 0$, and $c \geq \Sigma\mathcal{A}$. Then $\mathcal{A}$ is realizable if and only if every open neighborhood of $\mathcal{A}$ in $\mathbb{A}^c|_{f\to a}$ contains a realizable area assignment.*

The proof of Proposition 2.15 goes along the same line as Proposition 2.13. At the appropriate place, we use the fact that for a realizable area assignment $\mathcal{A}' \in \mathbb{A}^c|_{f\to a}$, there exists an $\mathcal{A}'$-realizing drawing in $\mathcal{D}^c|_{f\to\triangle}$ where f is fixed to a triangle $\triangle$ of area $a = \mathcal{A}(f)$.

Note the sequence argument used in Propositions 2.13 and 2.15 does not work for all plane graphs. The boundedness of the drawings is crucial as the example in Figure 2.8 illustrates: For a sequence of $\varepsilon > 0$ with $\varepsilon \to 0$, consider a sequence of realizing drawings where the face of area ε is a regular triangle. Then the edge length of the regular triangle goes to 0 as $\varepsilon \to 0$ and the left vertex tends to $-\infty$. Thus, the limit does not exist.

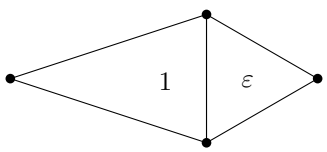

Figure 2.8: A sequence of realizing drawings with $\varepsilon \to 0$ where the right triangle is regular does not yield a realizing drawing for $\epsilon = 0$.

2.3 Characterization by Polynomial Equations

In this section, we show that the realizability of an area assignment for a plane graph can be characterized by a polynomial equation system. As we will later see, this implies that area-universality can be decided with the help of a boolean formula over the reals.

A plane graph G induces an orientation of the vertices of each face. For a face f with vertices $v_1, \dots, v_k$ we say $v_1, \dots, v_k$ are in *counter clockwise* order on f if they appear in this order on a walk on the boundary of f in counter clockwise direction. Otherwise $v_1, \dots, v_k$ are in *clockwise* order on f. Figure 2.9 illustrates both, a clockwise and a counter clockwise triangle.

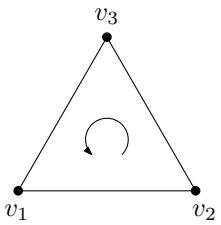

(a) $v_1v_2v_3$ is a counter clockwise face.

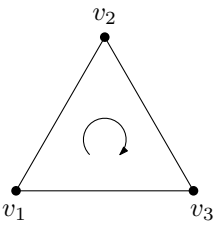

(b) $v_1v_2v_3$ is a clockwise face.

Figure 2.9: Orientation of faces.

Let D be a straight-line drawing of G. We denote the coordinates of a vertex v_i in D by (x_i, y_i). Given a counter clockwise triangle t with vertices v_1, v_2, v_3, we can compute its area in D by the following determinant:

$$2 \cdot \text{AREA}(t, D) = \det \begin{pmatrix} x_1 & x_2 & x_3 \\ y_1 & y_2 & y_3 \\ 1 & 1 & 1 \end{pmatrix} =: \text{Det}(v_1, v_2, v_3). \tag{2.1}$$

Note that using the clockwise order of v_1, v_2, v_3 instead of the counter clockwise order has the effect of switching the sign, i.e., $\text{Det}(v_1, v_2, v_3) = -\text{Det}(v_3, v_2, v_1)$. This formula can be generalized for simple polygons.

▶ **Proposition 2.16** ([Meister, 1769])**.** *Let $v_1, \dots, v_n$ be the vertices of a simple polygon P in counter clockwise order, then the area A of P can be computed by*

$$2 \cdot A(P) = \sum_{i=2}^{n-1} \mathit{Det}(v_1, v_i, v_{i+1}). \tag{2.2}$$

The formula in (2.2) is called the *shoelace formula* and was first described by Meister [Meister, 1769]. It is also referred to as the *Gauss's area formula*. The formula is obvious for a convex polygon, see also Figure 2.10: Consider the star triangulation of the polygon with center v_1. Then, the formula states that the area of the triangles sum up to the area of the polygon. The interesting part is that v_1 must not be the center of a crossing-free triangulation. For completeness, we present a proof of Proposition 2.16.

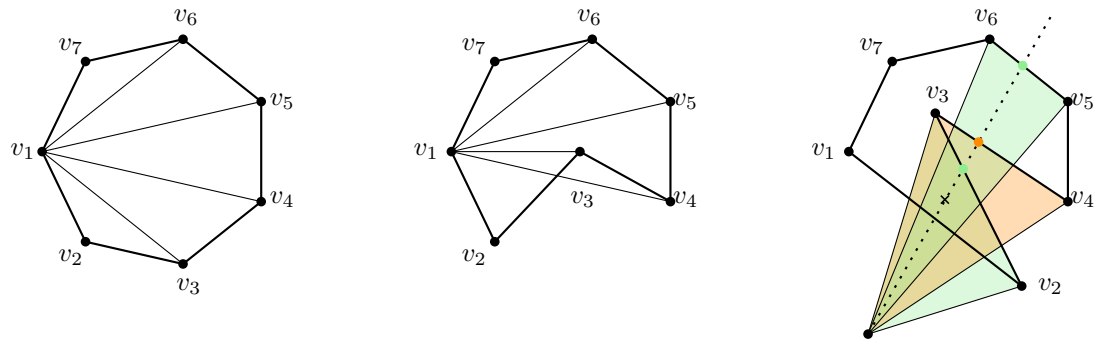

Figure 2.10: Visualization of the shoelace formula and its proof.

Proof of Proposition 2.16. We show a slightly more general statement. Namely that v_1 can be replaced by any point in the plane, without loss of generality the origin 0. Then the formula reads as follows:

$$2 \cdot A(\mathcal{P}) = \sum_{i=1}^{n} \mathrm{Det}(0, v_i, v_{i+1})$$

Consider a point p inside P and the ray $0p$. For an illustration consult Figure 2.10. The ray intersects the boundary several times; each time it either enters or leaves P in an alternating fashion. In fact, every intersection point of the ray with the boundary of P that lies after p certifies a triangle $0v_iv_{i+1}$ containing p. This triangle contributes one summand in the formula. The determinants of these triangles alternate in sign. Since the ray ends outside P and p is inside, the first and last intersection point have positive sign. Thus p is contained in an odd number of triangles; in particular the number of even triangles exceed the number of odd triangles by one.

Likewise, a point p outside P is contained in even number of triangles with alternating sign. Introducing all segments $0v_i$, the plane is split into several cells by the segments and P; all points of one cell behave alike and can be considered as equivalent. Thus by the above argument, the formula accounts exactly for the area of a cell contained in P. ◀

In a realizing drawing of an area assignment $\mathcal{A}$ of a plane graph G, each inner face fulfills a prescribed area, i.e., an equation as in (2.2). Clearly, the existence of a realizing drawing implies a real solution for these equations. We now show that such a real solution corresponds to a vertex placement that yields a realizing drawing.

▶ **Proposition 2.17.** *Let G be a plane graph with a non-negative area assignment $\mathcal{A}$. Then there exists a system $\mathcal{E}$ of polynomial equations of polynomial size which has a real solution if and only if $\mathcal{A}$ is realizable.*

Proof. In a fixed drawing D of G, the variables (x_i, y_i) represent the coordinates of v_i and $N(v_i)$ denotes the set of adjacent vertices. The outer face is denoted as f_o. Recall that $\mathcal{A}$ is realizable if there exists a vertex placement $(x_1, y_1, \ldots, x_n, y_n)$ encoding a crossing-free, straight-line, and equivalent drawing of G where the area of face each inner face f is $\mathcal{A}(f)$. By definition, two drawings of G are equivalent if they have the same outer face and rotation system. Hence, we ensure these properties by the following three conditions:

(i) The face areas are realized (Area).
(ii) All pairs of independent edges are crossing-free (CrossFree).
(iii) The rotation system remains the same (RotSys).

By Area, CrossFree, and RotSys, we denote the predicates ensuring the three properties. Note that these properties imply that the outer face is preserved: Consider the region of the plane in a crossing-free straight-line drawing which is covered by the polygonal region belonging to the inner faces of G. Note that each inner edge cannot bound this region as it is covered from both sides by its two incident faces. Thus the region must be bounded by the edges of the outer face.

We define a quantifier-free boolean formula $\mathcal{E}'$, consisting of polynomial equations and inequalities which are linked by disjunctions or conjunctions. (With the usual tricks, we may afterwards turn $\mathcal{E}'$ into an equation system $\mathcal{E}$.) We define $\mathcal{E}'$ as follows:

$$\mathcal{E}'(G,\mathcal{A}) := \Big(\bigwedge_{f\in F'} \textsc{Area}(\mathcal{A}(f),f)\Big) \wedge \Big(\bigwedge_{e,e'\in E} \textsc{CrossFree}(e,e')\Big) \wedge \Big(\bigwedge_{v\in V} \textsc{RotSys}(v)\Big).$$

The predicate Area is already defined by the Equation (2.2). It remains to describe CrossFree and RotSys. Let us start with the CrossFree predicate. For notational convenience, we denote the edges by $e = uv$ and $e' = rs$ and the coordinates of a vertex v by (v_x, v_y). Recall that a point p is strictly *left* of an oriented line through the points a and b if and only if $\mathrm{Det}(p,a,b) > 0$. We denote the oriented line through the points x and y by $\ell(x,y)$. It is easy to see that the two segments $e = uv$ and $e' = rs$ have no proper crossing if and only if at least one of the following conditions hold:

(i) Points r and s are on the same side of $\ell(u,v) \iff \mathrm{Det}(r,u,v)\cdot\mathrm{Det}(s,u,v) \geq 0$.

(ii) Points u and v are on the same side of $\ell(r,s) \iff \mathrm{Det}(u,r,s)\cdot\mathrm{Det}(v,r,s) \geq 0$.

Figure 2.11(a) illustrates property (i); since r and s are on the same side of $\ell(u,v)$, the two segments have no proper crossing. As indicated, each of the conditions (i) and (ii) can easily be described as a product of determinants and thus each CrossFree condition is a disjunction of these two products.

Next, we describe the RotSys predicate. For this it is important to distinguish whether or not v is a reflex vertex of one of its incident faces. First assume v is not a reflex vertex as illustrated in Figure 2.11(b). Let $(v_1,\ldots,v_d)$ denote the vertices around v in counter clockwise order. We enforce the condition that v_{i+1} is left of the line $\ell(v,v_i)$, for $i = 1,\ldots,(d-1)$ and v_1 left of $\ell(v,v_d)$.

In case that v is a reflex vertex of one of its faces, exactly one of the conditions is negated, namely the one corresponding to the reflex angle at v. Figure 2.11(c) illustrates this case. We make a disjunction of all d variants. We also need to force the winding

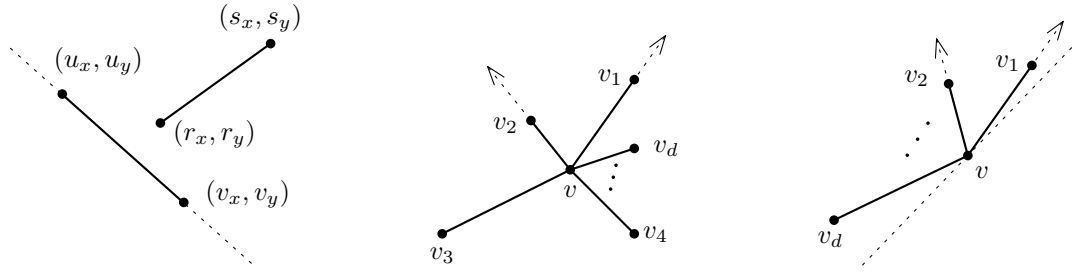

(a) Two non-crossing segments. (b) For every face, v is convex. (c) For one face, v is reflex.

Figure 2.11: Illustration of the predicates CrossFree and RotSys.

number around v to be 1, i.e., the cyclic sequence of angles between consecutive neighbors of v sums to 2π. For this, we use the disjunction over each $s, t \in \{1, \dots, d\}$ not necessarily distinct such that $s \neq t + 1 \pmod{d}$ of the following conditions. The first coordinate of each of the vectors $(v_s - v), (v_{s+1} - v), \dots, (v_t - v)$ is strictly positive, and that the first coordinate of each of the vectors $(v_{t+1} - v), \dots, (v_{s-1} - v)$ is non-positive, where all indices are in the integers mod d. This divides the neighbors of v into two contiguous intervals, one that is strictly to the right of v and another that is to the left or vertically aligned with v.

In this way, we have described the formula $\mathcal{E}'$ completely. Due to the predicates Area, CrossFree, and RotSys a real solution of $\mathcal{E}'$ yields a realizing drawing. Note that the size of $\mathcal{E}'$ is polynomial in n. We transform $\mathcal{E}'$ into an equation system $\mathcal{E}$ with the following set of tricks: Let $p(x)$ and $q(x)$ denote two real polynomials.

$$\begin{aligned} p(x) \geq 0 &\iff (p(x) = 0 \vee p(x) > 0) \\ p(x) > 0 &\iff \exists z \in \mathbb{R} \colon p(x) \cdot z^2 = 1 \\ (p(x) = 0 \vee q(x) = 0) &\iff p(x) \cdot q(x) = 0 \\ (p(x) = 0 \wedge q(x) = 0) &\iff (p(x))^2 + (q(x))^2 = 0) \end{aligned}$$

This finishes our proof. ◀

Remark. Later, we use this fact to show that the computational problem of deciding whether a given plane graph is area-universal lies in $\forall\exists\mathbb{R}$; see Proposition 7.1 in Chapter 7.

We will now discuss the fact that for inner triangulations, the polynomial equation system of Proposition 2.17 can be simplified. In particular, the predicate Area is sufficient.

2.3.1 Triangulations

As seen in Proposition 2.17, there is a close connection of area-universality and polynomial equation systems: For every plane graph G with area assignment $\mathcal{A}$ there exists a polynomial equation system $\mathcal{E}$ such that $\mathcal{A}$ is realizable if and only if $\mathcal{E}$ has a real solution. Recall that an essential part of the equation system is given by the determinant equations, defined in Equation (2.1), which describe the areas of the faces. We now show that for inner triangulations these equations suffice.

An *inner triangulation* is a 2-connected plane graph where every inner face is a triangle. Given a face area assignment $\mathcal{A}$ for an inner triangulation T, we seek for a drawing where every inner face has a prescribed area. By Lemma 2.1, we may scale the area assignment as wished and consider for a counter clockwise face f with vertices v_1, v_2, v_3 the *area equation*

$$\mathrm{Det}(v_1, v_2, v_3) = \mathcal{A}(f). \tag{2.3}$$

Every area assignment has a natural extension from the set of inner faces F' to the set of all faces F. In a realizing drawing the area of the (complement of the) outer face equals the total area. Therefore, we define $\mathcal{A}(f_o) := \Sigma\mathcal{A}$. For a set of faces $\tilde{F} \subset F$, we define the *area equation system of* $\tilde{F}$

$$\textsc{aeq}(T, \mathcal{A}, \tilde{F})$$

consisting of one area equation as defined in Equation (2.3) for each face $f \in \tilde{F}$.

Clearly, the vertex placement of an $\mathcal{A}$-realizing drawing of T yields a real solution of $\text{AEQ}(T, \mathcal{A}, \tilde{F})$. We will show that for inner triangulations the converse also holds true for any set $\tilde{F} \subset F$ with $|\tilde{F}| = |F| - 1$. For general graphs, this is not always true; however, as seen in Section 2.3, a correct crossing-free embedding can be guaranteed by additional equations. The main tool to prove Theorem 4 is the following very neat and useful lemma.[1] Here we present two proofs, one of which is due to [Angelini et al., 2016].

▶ **Lemma 2.18.** *Let D be a vertex placement of an inner triangulation T where the orientation of each inner face in D coincides with the orientation in T. Then D represents a straight-line drawing of T.*

Proof 1. Given a vertex placement D of a triangulation T, every inner face is represented by a triangle in the plane. We want to argue that these triangles are interiorly disjoint. We are interested in the region $\mathcal{T}$ covered by the triangles corresponding to a set of inner faces in F'. Let $\partial\mathcal{T}$ denote the boundary of $\mathcal{T}$ and observe that every inner edge of T is covered by its two triangles from both sides, see also Figure 2.12. Hence the boundary $\partial\mathcal{T}$ must be formed by the outer edges and vertices of T. Let $v_1, v_2, \ldots, v_k$ denote the vertices of the outer face f_o in counter clockwise orientation. Now, we show that the covered area of $\mathcal{T}$ corresponds to the area of the sum of the triangles: Recall that $\text{Det}(u, v, w)$ denotes the determinant of the homogeneous coordinates of u, v, w as defined in Equation (2.1). Moreover, $\det(u, v)$ denotes the determinant of the 2-dimensional coordinates of u and v.

$$\begin{aligned} 2 \cdot \text{AREA}(f_o, D) &= \sum_{i=2}^{k-1} \text{Det}(v_1, v_i, v_{i+1}) = \sum_{i=1}^{k-1} \det(v_i, v_{i+1}) \\ &= \sum_{i=1}^{k-1} \det(v_i, v_{i+1}) + \sum_{e=(u,v) \text{ inner}} \big(\det(u, v) + \det(u, v)\big) \\ &= \sum_{(u,v,w)\in F'} \text{Det}(u, v, w) = 2 \cdot \sum_{f \in F'} \text{AREA}(f, D) \end{aligned}$$

In the second line, we add the terms $(\det(u, v) + \det(u, v))$ which are canceling each other since $(\det(u, v) = -\det(u, v))$. Figure 2.12 illustrates that every inner edge appears twice - once in each direction - and every outer edge appears once in counter clockwise orientation. Therefore, we may group the edges such that they appear once for each face in counter clockwise orientation. This shows that the covered area of $\mathcal{T}$ corresponds to the area of the sum of the triangles. Consequently, the triangles cannot overlap and the vertex placement yields a crossing-free straight-line drawing. ◀

Proof 2. This proof is due to [Angelini et al., 2016]. We consider a function $\phi : \mathbb{R}^2 \to \mathbb{N}$, where $\phi(x)$ counts the number of triangles of G in which a point x is contained. As argued above, the region covered by the inner triangles must be bounded by outer edges of T, i.e., we have $\phi(x) = 0$ at infinity. Furthermore, due to the correct orientation of all triangles, $\phi(x)$ does not change when x crosses an inner edge. Thus, the function $\phi(x)$ changes only by 1 when it crosses an outer edge. Since it holds that $\phi(x) = 0$ at infinity, it follows that $\phi(x) = 1$ inside the covered region (except on edges and vertices). It follows that D is a straight-line drawing of T. ◀

[1] Various graph theorist consider this fact to be folklore. Nevertheless it turned out to be quite difficult to find an appropriate reference. In particular, the presented proof in [Angelini et al., 2016] is hidden in continuous text. I would be happy to be pointed to further references.

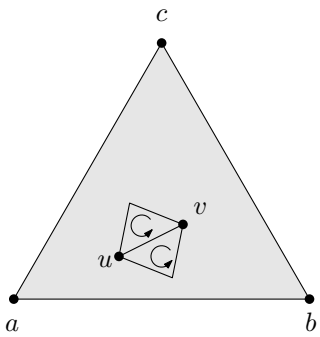

Figure 2.12: Illustration of proof 1 of Lemma 2.18.

We are now ready to prove the theorem.

■ **Theorem 4.** *Let T be an inner triangulation with a non-negative area assignment $\mathcal{A}$ and some face f. Then $\mathcal{A}$ is realizable if and only if the equation system* $\textsc{aeq}(T, \mathcal{A}, F - f)$ *has a real solution.*

Proof of Theorem 4. The proof consists of two directions. If $\mathcal{A}$ is realizable, then the vertex placement of an $1/2\mathcal{A}$-realizing drawing is a real solution of the equation system $\textsc{aeq}(T, \mathcal{A}, F - f)$.

So suppose the equation system $\textsc{aeq}(T, \mathcal{A}, F - f)$ has a real solution. This solution yields a vertex placement D satisfying the (scaled) area assignment and preserving the orientation of all but one face f. It remains to show that the drawing is crossing-free.

If f is the outer face, then all inner faces have the correct orientation and Lemma 2.18 implies that D is an equivalent straight-line drawing of T. Thus, we suppose that f is an inner face. In the proof of Lemma 2.18, we have seen that for the outer face f_o it holds that

$$\textsc{area}(f_o, D) = \sum_{f \in F'} \textsc{area}(f, D).$$

Moreover, by definition and since $f_o \neq f$, it holds in D that $\textsc{area}(f_o, D) = \mathcal{A}(f_o) := \Sigma\mathcal{A}$. Therefore, by basic algebra $\textsc{area}(f, D)$ evaluates to $\mathcal{A}(f)$. Consequently, D is a real solution for $\textsc{aeq}(T, \mathcal{A}, F)$ and Lemma 2.18 guarantees that D induces a crossing-free straight-line drawing. ■

3 | Triangulations

In this chapter, we establish several interesting facts on area-universality of triangulations. We introduce tools to prove and disprove area-universality. In Section 3.1, we show that all Eulerian triangulations and the icosahedron graph are not area-universal. In Section 3.2, we develop a method to prove area-universality for certain triangulations. In particular, we use these tools to characterize the area-universality of some graph classes, including the accordion graphs mentioned in the introduction, as well as to classify small triangulations.

3.1 On Non-Area-Universal Triangulations

As maximal plane graphs, triangulations are natural candidates for non-area-universal graphs. In the beginning of our studies, the only known non-area-universal graphs were the octahedron graph and all graphs containing it as a subgraph. In this section, we present further non-area-universal triangulations. In response to our question in the introduction, this shows that the octahedron is not the only obstruction to area-universality. Additionally, among the presented triangulations, there are 4- and 5-connected graphs. Thus, high vertex connectivity does not imply area-universality. The results of this section also appear as an extended abstract in [Kleist, 2016] and as a full version in [Kleist, 2018a].

3.1.1 Eulerian Triangulations

We mentioned already that the octahedron graph, which is an Eulerian triangulation, is not area-universal [Ringel, 1990]. Two proofs for this fact are known; both of which use similar non-realizable area assignments illustrated in Figure 3.1. Before we present a new proof, we review the two known proofs. Ringel [Ringel, 1990] considered the octahedron

(a) Ringel's stacked octahedron is not equiareal.

(b) This area assignment is not realizable.

Figure 3.1: Illustration of the two known proofs that the octahedron is not area-universal.

graph with two additional vertices of degree 3. This graph is depicted in Figure 3.1(a) and we refer to it as *Ringel's stacked octahedron*. Ringel shows that the area equation system of the inner faces, as defined in Equation (2.3), has no real solution when all face areas are asked to have the same size. Since a real solution is a necessary condition for each realizing drawing, its non-existence proves that Ringel's stacked octahedron is not equiareal. Hence, Lemma 2.8 implies that the octahedron graph is not area-universal.

A different proof relies on a classical geometric result concerning the area of a triangle inscribed into a triangle: We say a triangle $x_1x_2x_3$ is inscribed into a triangle $v_1v_2v_3$, when vertex x_i is placed on the side v_iv_{i+1}, respectively, where $v_{i+3} := v_i$. The inscription partitions the triangle into four smaller triangles, namely in the central triangle $x_1x_2x_3$ and three triangles of type $v_ix_ix_{i+2}$, $i \in [3]$. We denote their areas by a, b, c, d as depicted in Figure 3.2(a). Studying the relations of these areas, Debrunner [Debrunner, 1956] observed the following relation, which was first proved by Bager [Bager, 1957].

▶ **Proposition 3.1.** *Inscribing a triangle $x_1x_2x_3$ in the triangle $v_1v_2v_3$ partitions it into four triangles of areas a, b, c, d. For the area d of the central triangle it holds that $d \geq \min\{a, b, c\}$.*

Proposition 3.1 implies the non-area-universality of the octahedron graph as follows: When the area of the three triangles incident to the outer segments is supposed to vanish, each inner vertex is forced to lie on an outer segment. In this way, we obtain a triangle inscribed into a triangle. Then, any area assignment with $d < \min\{a, b, c\}$ is not realizable by Proposition 3.1. Figure 3.1(b) illustrates such an area assignment of the octahedron. The idea of this proof originates from Alam et al. [Alam et al., 2012]; they have used Proposition 3.1 to show that proportional contact representations may require non-convex shapes. For completeness, we present a nice geometric proof from Esther Szekeres [Szekeres, 1967].

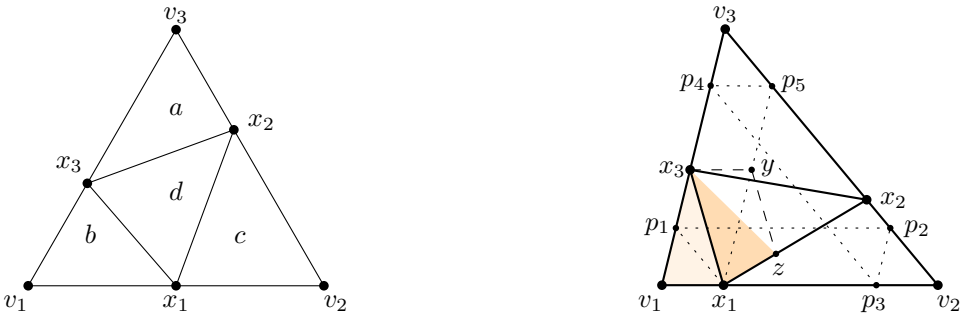

(a) The triangle $x_1x_2x_3$ inscribed into $v_1v_2v_3$.

(b) Depiction of the construction.

Figure 3.2: Illustration of Proposition 3.1 and its proof.

Proof of Proposition 3.1. Consider the six ratios of type $v_ix_i : v_iv_{i+1}$ and $x_iv_{i+1} : v_iv_{i+1}$ for $i \in [3]$. Without loss of generality we may assume that $v_1x_1 : v_1v_2$ is a smallest ratio among these six ratios. We construct five helper points $p_1, \ldots, p_5$ as follows: Let p_1 be a point on v_1v_3 such that x_1p_1 and v_2v_3 are parallel. Furthermore, we construct p_{i+1} after p_i such that p_ip_{i+1} is parallel to v_1v_2 if $i \in \{1, 4\}$, v_1v_3 if $i = 2$, and v_2v_3 if $i = 3$. The construction is depicted in Figure 3.2(b). Since $v_1x_1 : v_1v_2$ is a smallest ratio, x_2 and x_3 lie on the segments p_2p_5 and p_1p_4, respectively. Choose y such that $v_1x_1yx_3$ is a parallelogram. Then, the triangles $v_1x_1x_3$ and x_1yx_3 have the same area. Moreover, there exists a point z on x_1x_2 such that yz is parallel to x_1x_3. The triangle x_1zx_3 has the same area as the triangle $v_1x_1x_3$ and is contained in the triangle $x_1x_2x_3$. This shows the claim. ◀

In contrast to both proofs, we use a simple counting argument to show that the octahedron graph is not area-universal. Interestingly, this argument can be extended to prove that no plane Eulerian triangulation is area-universal. A graph is *Eulerian* if it has an Euler cycle, i.e., a cycle using each edge exactly once. As Euler showed, all vertices in an Eulerian graph have an even degree. For connected graphs even degree is indeed necessary and sufficient. Consequently, a triangulation is *Eulerian* if and only if all vertex degrees are even. We will use the fact that the dual graph of a plane Eulerian triangulation is bipartite, and hence has an inner face 2-coloring. An *inner face 2-coloring* of a plane triangulation is a coloring of the inner faces with white and black such that every inner edge is incident to a white and a black face; Figure 3.3 depicts such a coloring for the octahedron. In fact, Eulerian triangulations are characterized by the existence of an inner face 2-coloring.

▶ **Proposition 3.2.** *A plane triangulation has an inner face 2-coloring if and only if it is Eulerian.*

Proof. If T is Eulerian, its dual graph is bipartite and thus it has an inner 2-face coloring. Suppose, for a contradiction, that there exists a triangulation T with an inner face 2-coloring that is not Eulerian. Then T has exactly two outer vertices u and v of odd degree, since all inner vertices have even degree and the number of vertices with odd degree must be even. Deleting the edge (u, v) results in an Eulerian inner triangulation with $3n - 7$ edges. However, as shown by Tsai and West [Tsai and West, 2011, Lemma 3.2], the number of edges of an Eulerian inner triangulation is divisible by three. This yields a contradiction and thus, shows the claim. ◀

■ **Theorem 5.** *No plane Eulerian triangulation on $n \geq 4$ vertices is area-universal.*

Proof. Let T be an Eulerian triangulation on $n \geq 4$ vertices with an inner face 2-coloring. We denote the set of white faces by W and the set of black faces by B. A triangulation with n vertices has $2n-5$ inner faces. Without loss of generality, we assume that $|W| > |B|$ and therefore, $|W| \geq n - 2$. Figure 3.3 illustrates the proof for the octahedron graph. We show that the following non-negative area assignment $\mathcal{A}$ of T is not realizable:

$$\mathcal{A}(f) := \begin{cases} 0 & \text{if } f \in W, \\ 1 & \text{if } f \in B. \end{cases}$$

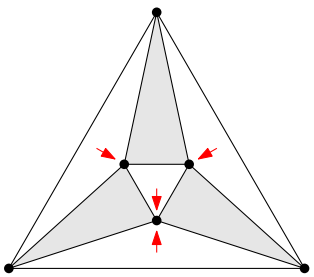

Figure 3.3: An inner face coloring of the octahedron graph depicting a non-realizable area assignment; white faces are assigned to 0 and black faces to 1. In every flat angle assignment, two white faces are assigned to the same inner vertex.

For the purpose of contradiction, suppose that T has an $\mathcal{A}$-realizing drawing D. We show that D has two contradicting properties.

Firstly, every white face has an angle of size π; we call such an angle a *flat angle:* Note that every inner edge is incident to a black face and thus has positive length in D; otherwise, the area of the black face is not realized. Additionally, the area of a white face vanishes only if one of its vertices lies on the opposite, non-incident edge. Due to the positive edge lengths, the vertex lies in the interior of the non-incident edge. Consequently, one angle of every white face in D is *flat*.

Secondly, the number of white flat angles is bounded by the number of inner vertices: In D, we *assign* (the flat angle of) every white face to the vertex with the flat angle and obtain a *flat angle assignment*. In Figure 3.3, a flat angle assignment for the octahedron graph is indicated by the red arrows. Since the boundary of the outer face is a triangle with positive area, only inner vertices may have flat angles. Moreover, every vertex is incident to a black face by the inner face 2-coloring. Suppose there exists an inner vertex v in D which has two flat angles. Then, no space remains to realize the area of any black face incident to v. Therefore, in D every inner vertex has at most one flat angle and the number of white flat angles is bounded by the number of inner vertices.

Since T has at least $n-2$ white faces and $n-3$ inner vertices, the number of white faces exceeds the number of inner vertices and we obtain a contradiction. Therefore, $\mathcal{A}$ is not realizable and Corollary 3 guarantees the existence of a non-realizable (positive) area assignment. Thus T is not area-universal. ■

Theorem 5 and its proof have several nice implications. First of all, note that in the proof of Theorem 5, we only use the fact that the black faces are assigned to positive real numbers. Therefore, the following stronger statement holds true:

▶ **Proposition 3.3.** *Any non-negative area assignment of an Eulerian triangulation with an inner face 2-coloring where each white face is assigned to 0 and each black face to some positive real number is not realizable.*

Moreover, the proof of Theorem 5 implies that we cannot hope for drawings realizing the areas up to a constant factor. For a real $c > 1$, we say a straight-line drawing D of G is *c-approximating* of an area assignment $\mathcal{A}$ if for each inner face f it holds that

$$1/c \cdot \mathcal{A}(f) \leq \text{AREA}(f, D) \leq c \cdot \mathcal{A}(f).$$

In fact, no Eulerian triangulation has a c-approximating drawing for every area assignment.

■ **Corollary 6.** *For every $c > 1$, every Eulerian triangulation T on at least $n \geq 4$ vertices has an area assignment $\mathcal{A}$ such that no drawing of T is c-approximating $\mathcal{A}$.*

Proof. We consider an inner face 2-coloring of T. For every $k \in \mathbb{N}$, let $\mathcal{A}_k$ denote the area assignment of T where each white face is assigned to $1/k$ and each black face to 1. Suppose every $\mathcal{A}_k$ has a drawing D_k which is c-approximating $\mathcal{A}_k$. We may assume that the outer face of T in D_k is a right triangle where two outer vertices coincide for all D_k. Then the sequence $(D_k)_{k\in\mathbb{N}}$ is bounded and by the Bolzano-Weierstrass theorem, it has a converging subsequence with limit D. In D_k, the area of a white face is at most c/k and of a black face at least $1/c$. Consequently, in D, the area of each white face is 0 and of each black face positive. However, such a drawing of T does not exists as discussed in Proposition 3.3. ■

Remark. As a consequence of Corollary 6, c-approximations of equiareal drawings do also not exist for triangulations: For every c, there exists a rational area assignment of the octahedron graph without a c-approximating drawing. By scaling, we obtain a non-realizable integer area assignment $\mathcal{A}$. Then, in every face f we insert a stacked triangulation with $\mathcal{A}(f)$ vertices; this subdivides f into $3 \cdot \mathcal{A}(f)$ faces. The resulting triangulation T that has no c-approximating equiareal drawing.

3.1.2 Icosahedron Graph

Since every Eulerian triangulation (with at least four vertices) has a vertex of degree four, the graphs of Theorem 5 are at most 4-connected. Adding some geometric arguments, we can use similar ideas to show that the 5-connected icosahedron graph is not area-universal. We start with the geometric argument.

Let $ABCD$ be a quadrangle and let E be a point on the segment CD. Together with the segments AE and BE we call this configuration a *seesaw* with *base* AB. A seesaw is *base-bounded* if there exists a pair of parallel lines ℓ_A and ℓ_B through A and B, respectively, such that the seesaw lies (not necessarily strictly) between the lines ℓ_A and ℓ_B. Figure 3.4(a) depicts a base-bounded seesaw in which the base is horizontal and the two lines are vertical; thus, the x-coordinates of C and D are bounded by the x-coordinates of A and B. We call a seesaw *equiareal* if the triangles AED, ABE, and BCE have the same positive area.

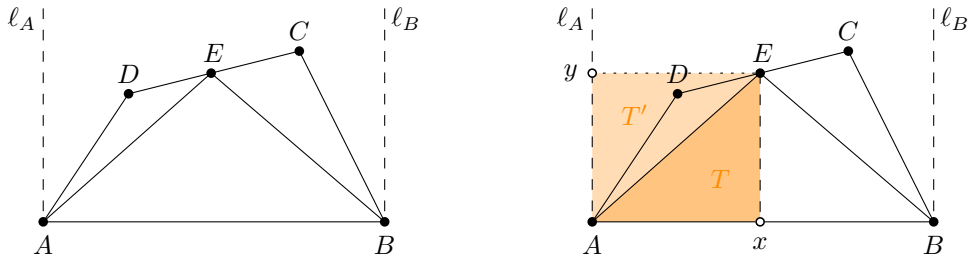

(a) A base-bounded seesaw.

(b) AED is smaller than AxE.

Figure 3.4: Illustration of Lemma 3.4 and its proof.

▶ **Lemma 3.4.** *No base-bounded seesaw is equiareal.*

Proof. For a contradiction, suppose that there exists a base-bounded equiareal seesaw. Without loss of generality, we assume that AB is horizontal and that E lies above AB.

Note that E lies strictly between ℓ_A and ℓ_B; otherwise the triangle AED or BCE has area 0. Due to the symmetry, we may assume that D does not lie above C as depicted in Figure 3.4(b). Let x denote the intersection point of the segment AB and the line parallel to ℓ_A through E; let y be the intersection point of ℓ_A and the horizontal line through E. Since E lies strictly between ℓ_A and ℓ_B, x lies strictly between A and B. Therefore, the triangle $T := AxE$ is strictly contained in ABE and has the same area as $T' := AEy$. By assumption D is not to the left of ℓ_A and not above E and therefore D is contained in T'. Consequently, it holds that

$$\text{AREA}(ABE) > \text{AREA}(T) = \text{AREA}(T') \geq \text{AREA}(AED).$$

This is a contradiction to the equiareality of the seesaw and therefore proves the claim. ◀

As a side remark, we mention that Lemma 3.4 yields an alternative proof for the fact that the octahedron is not area-universal. Combining the argument of the proof of Theorem 5 and Lemma 3.4 yields the following result.

▶ **Proposition 3.5.** *The octahedron graph has no drawing where the gray faces have area 1, the central face has area 0, and the remaining faces either have area 0 or 1.*

Proof. In every flat angle assignment, the flat angle of the central face is assigned to some inner vertex v. If v is incident to two white faces, then both flat angles are assigned to v. This yields a contradiction as already seen in Theorem 5. Otherwise v is incident to three white faces of area 1. This yields a base-bounded seesaw which is not equiareal by Lemma 3.4. ◀

We have already seen in Theorem 5 that the area assignment where the three white faces have area 0 is not realizable. Figure 3.5 illustrates the other three types of area assignments.In fact, these area assignments are exactly all non-realizable 01-assignments of the octahedron, i.e., an 01-assignments of the octahedron is realizable if it is not one of the area assignments in Proposition 3.5. In particular, every area assignment with two adjacent faces of area 0 is realizable since the contraction of the common edge results in a (stacked) triangulation with 5 vertices, and thus in an area-universal graph.

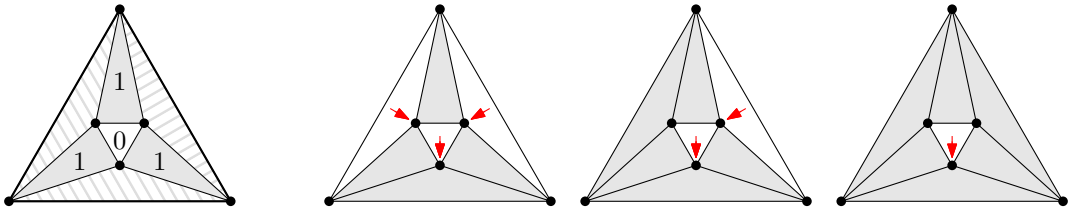

Figure 3.5: Non-realizable area assignments of the octahedron based on Lemma 3.4.

Now, we turn our attention to the icosahedron.

■ **Theorem 7.** *The icosahedron graph is not area-universal.*

Proof. We will show that there is no straight-line drawing of the icosahedron in which the white faces in Figure 3.6 vanish and the total area is distributed evenly among all black faces. Then Corollary 3 guarantees the existence of a positive area assignment that is not realizable. Note that there are three edges which are adjacent to two white faces; namely the red edges in Figure 3.6.

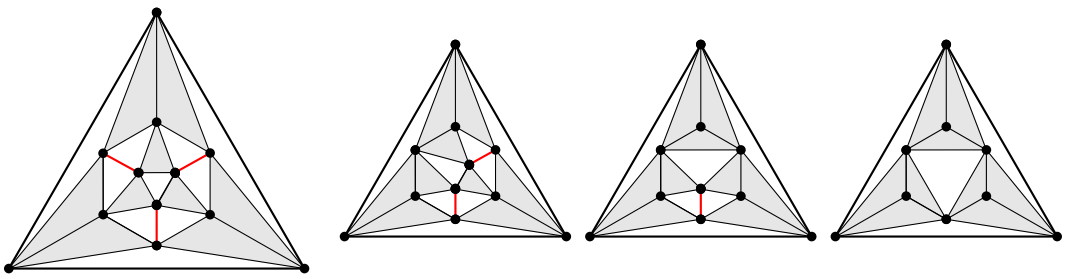

Figure 3.6: The icosahedron with a face coloring depicting a non-realizable area assignment; from left to right, no, one, two and three edges are contracted.

For a contradiction, we suppose that there exists a realizing drawing D. For a white face incident to a red edge, there exists two possibilities in D: either the red edge is contracted or one of its angles is flat. Thus, we distinguish four cases according to how many of the red edges are contracted: In case i, we contract exactly i edges with $i \in \{0, 1, 2, 3\}$. Then, the remaining white faces must have a flat angle. Moreover, note that every inner vertex is incident to a black face and thus may only be incident to at most one flat angle. Therefore, we say a flat angle assignment is *valid* if no two faces are assigned to the same vertex. In each case, we either find a base-bounded seesaw or no valid flat angle assignment.

Case 0: If no edge is contracted, then there are ten white faces and nine inner vertices. By the pigeonhole principle, there exists no valid flat angle assignment.

Case 1: The contraction of one edge results in a graph with eight white faces and eight inner vertices. Hence, in any valid flat angle assignment each inner vertex has exactly one flat angle. We label the vertices as depicted in Figure 3.7. In particular, v_1, v_3, v_4, v_5, v_6 are assigned by a unique white face. In total, there are two different flat angle assignments, where the vertices v_2, v_7, v_8 are either assigned in clockwise or counter clockwise direction. Since these two flat angle assignments are mirror images of each other, we consider without loss of generality the one illustrated in Figure 3.7(a).

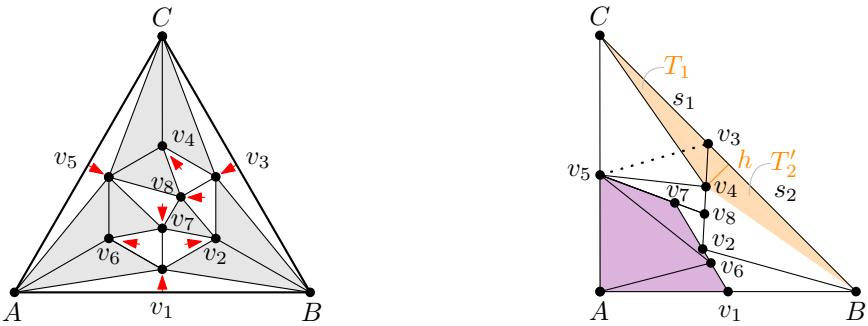

(a) The up to symmetry unique flat angle assignment in Case 1.

(b) A drawing respecting the flat angle assignment; it contains a seesaw with base v_5A.

Figure 3.7: Illustration of Case 1 of the proof of Theorem 7.

To obtain a contradiction, we consider a realizing drawing D within the triangle ABC with vertices (0,0), (1,0), (0,1) where the collinearities from the flat angle assignment are respected and all remaining faces have the same area. For a vertex v_i, we denote its coordinates in D by (x_i, y_i). We will show that D contains a base-bounded seesaw. Specifically, a straight-line drawing of the subgraph induced by the vertices A, v_1, v_6, v_7, v_5 yields a seesaw with base v_5A, as highlighted in violet in Figure 3.7(b). If $y_5 \geq y_7$, then a pair of horizontal lines certifies that the seesaw is base-bounded and Lemma 3.4 yields a contradiction. Therefore, it remains to show that $y_5 \geq y_7$.

For a contradiction, we suppose that $y_5 < y_7$. First note that, since v_4 lies on the segment v_8v_3, the (artificial) segment v_5v_3 intersects segment Cv_4. Moreover, v_5 and v_3 lie on the outer segments AC and BC, respectively. Hence, all inner vertices are contained in the quadrangle $Q := ABv_3v_5$. Since $y_5 < y_7$ by assumption, it follows that $y_5 < y_3$.

Next, we show that $y_3 < 1/2$. Consider the two black faces incident to v_3, namely $T_1 := v_4v_3C$ and $T_2 := v_3v_2B$. Due to the flat angle assignment, v_4 lies on the segment v_2v_3 and the triangle $T_2' := v_3v_4B$ is strictly contained in the triangle T_2. Consequently, it holds that $\text{AREA}(T_1, D) = \text{AREA}(T_2, D) > \text{AREA}(T_2', D)$. When we consider the segments s_1

and s_2 on BC as the base segments of T_1 and T_2', respectively, then their heights coincide. Therefore, $\text{AREA}(T_1, D) > \text{AREA}(T_2', D)$ implies directly that $s_1 > s_2$, and hence, $y_3 < 1/2$.

Since the quadrangle Q strictly contains seven facial triangles, it covers at least $7/9$ of the area in D. The area of Q can be expressed as the sum of the triangles Av_3v_5 with base length y_5 and height x_3 and ABv_3 with base length 1 and height y_3. With the facts that $y_5 < y_3 < 1/2$ and $x_3 = 1 - y_3$, we obtain the following chain of inequalities:

$$7/9 \leq 2 \cdot \text{AREA}(Q) = y_5 x_3 + y_3 < 1/2 \cdot (1 - y_3) + y_3 = 1/2 \cdot (1 + y_3) < 3/4.$$

Since this is a contradiction, we have that $y_5 \geq y_7$. This finishes Case 1.

Case 2: The contraction of two edges results in a graph with a unique flat angle assignment as shown in Figure 3.8(a). This flat angle assignment leads to a drawing as in Figure 3.8(b), which contains two seesaws. Due to its symmetry, we assume without loss of generality that $y_5 \geq y_3$. Hence, v_6 induces a seesaw with base Av_5 in the quadrangle $Av_1v_7v_5$; the base-boundedness is certified by a pair of horizontal lines. By Lemma 3.4, the base-bounded seesaw is not equiareal and we obtain a contradiction.

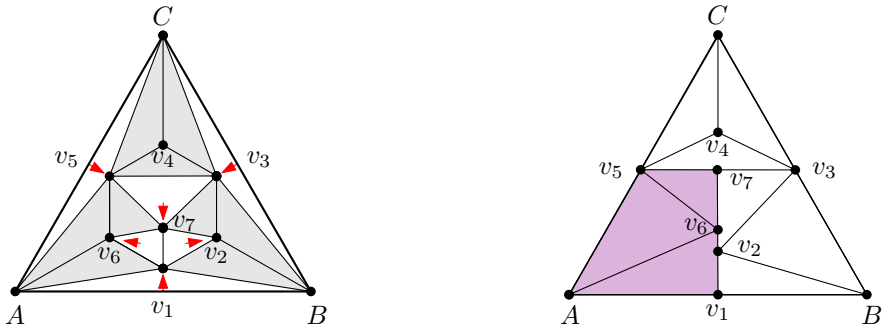

(a) The unique angle assignment when two edges are contracted.

(b) A drawing respecting the flat angle assignment; it contains two seesaws.

Figure 3.8: Illustration of Case 2 of the proof of Theorem 7.

Case 3: Contraction of three edges leads to a super graph of the octahedron graph as depicted in the rightmost image of Figure 3.6. This graph has four white faces and three inner vertices adjacent to white faces. Hence, there exists no valid flat angle assignment. ■

This finishes the section on non-area-universal graphs. We now turn our attention to realizing drawings. In particular, we learned that high connectivity does not imply area-universality. In the next section, we will see that it neither implies non-area-universality.

3.2 Proving Area-Universality of Triangulations

In this section, we prove area-universality of triangulations with special vertex orders. We present a sufficient criterion for area-universality that only requires the investigation of one area assignment. The method is based on Theorem 4, where a real solution of the area equation system characterizes the realizability of an area assignment of a triangulation. We use the developed machinery to present area-universal families of triangulations. In particular, we characterize the area-universality of accordion graphs, which we mentioned in the introduction. Additionally, we analyze the area-universality of small triangulations on up to ten vertices in Section 3.3. The results of this section also appear in [Kleist, 2018b].

The idea. We explain the general idea of our method by an example. Suppose we are interested in finding a realizing drawing of a given area assignment $\mathcal{A}$ for the depicted triangulation T in Figure 3.9(a). By Lemma 2.7, we may arbitrarily place the three outer vertices v_1, v_2, v_3 in a triangle of correct area. We set $v_1 = (0, 0)$, $v_2 = (1, 0)$, $v_3 = (1/2, \Sigma\mathcal{A})$. To realize the area of $v_1v_2v_4$, the vertex v_4 is placed on a horizontal line of correct distance to v_1v_2. Figure 3.9(b) illustrates the placement of the first four vertices. The x-coordinate x_4

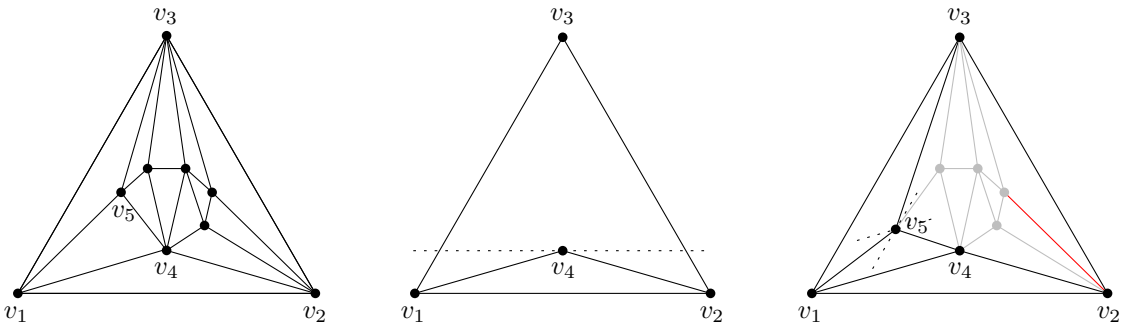

(a) A plane triangulation T. (b) Placement of v_1, v_2, v_3, v_4. (c) Placement of a next vertex.

Figure 3.9: Illustration of the idea.

of v_4 is the variable of our one-degree-of-freedom mechanism. The idea is to construct an (almost) realizing vertex placement for every choice of x_4. To do so, we insert one vertex after the other at a unique position in dependence of x_4. More specifically, choose an x_4 and consider v_5. The vertex v_5 has three neighbors, namely v_1, v_3, and v_4, all of which are already placed, see also Figure 3.9(c). There is a unique position for v_5 to realize the prescribed areas of the two incident triangles $v_1v_5v_3$ and $v_1v_4v_5$: For each of the two triangles, the vertex v_5 must lie on a specific line and thus, it is placed in their intersection point. Since the intersection point may lie outside of $v_1v_2v_3$, we do not ensure that the vertex placement yields a crossing-free drawing. Note that T has a vertex order $v_5, \dots, v_n$ such that every vertex has at least three neighbors with a smaller index. Thus, for v_i, we may follow the same procedure and place it such that two new face areas are realized. In particular, by placing each vertex v_i, we satisfy two equations of $\text{AEQ}(T, \mathcal{A}, F')$. In the end, all but two equations are satisfied and we obtain an *almost realizing vertex placement*. By Theorem 4, realizing one additional face area yields an $\mathcal{A}$-realizing drawing. Thus, finding an $\mathcal{A}$-realizing drawing reduces to the question whether there exists a value for x_4 such that, in the end, the remaining two face areas are as prescribed. For area-universality, we wonder: Is there a *good* position for x_4 for every area assignment?

To explore the described idea, we consider planar triangulations with the following property: We say an order of the vertices $(v_1, v_2, \ldots, v_n)$ together with a set of specified neighbors $\text{pred}(v_i) \subset N(v_i)$ for each vertex v_i, so called *predecessors*, is a *p-order* if the following conditions are satisfied:

- $\text{pred}(v_i) \subset \{v_1, v_2, \ldots, v_{i-1}\}$, i.e., the predecessors of v_i have an index $< i$,
- $\text{pred}(v_1) = \emptyset$, $\text{pred}(v_2) = \{v_1\}$, $\text{pred}(v_3) = \text{pred}(v_4) = \{v_1, v_2\}$, and
- for all $i > 4$: $|\text{pred}(v_i)| = 3$, i.e., v_i has exactly three predecessors.

Note that $\text{pred}(v_i)$ specifies a subset of preceding neighbors. Moreover, a p-order is defined for a planar graph independent of a drawing. We usually denote a p-order by $\mathcal{P}$ and state the order of the vertices. The predecessors are then implicitly given by $\text{pred}(v_i)$. Note that $v_1v_2v_3$ and $v_1v_2v_4$ form triangles by definition. Figure 3.10 illustrates a p-order of the triangulation in Figure 3.9(a).

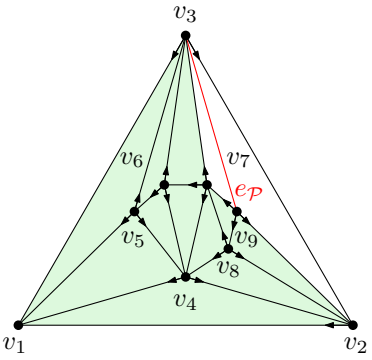

i	$\text{pred}(v_i)$
1	$\emptyset$
2	$\{v_1\}$
3	$\{v_1, v_2\}$
4	$\{v_1, v_2\}$
5	$\{v_1, v_3, v_4\}$
6	$\{v_3, v_4, v_5\}$
7	$\{v_3, v_4, v_6\}$
8	$\{v_2, v_4, v_7\}$
9	$\{v_2, v_7, v_8\}$

Figure 3.10: A plane 4-connected triangulation with a p-order $\mathcal{P}$. In the almost 3-orientation $\mathcal{O}_\mathcal{P}$ exactly one edge $e_\mathcal{P}$, highlighted in red, is not oriented (Lemma 3.6). In an almost realizing vertex placement constructed with $\mathcal{P}$, all face areas are realized except for the two faces incident to $e_\mathcal{P}$ (Lemma 3.13).

With this definition at hand, we state the outline of the proof idea as follows:

For a plane triangulation T with a p-order $(v_1, v_2, \ldots, v_n)$ and an area assignment $\mathcal{A}$, we pursue the following one-degree-of-freedom mechanism:

- Place the vertices v_1, v_2, v_3 at positions realizing the area equation of the face $v_1v_2v_3$. Without loss of generality, we set $v_1 = (0, 0)$ and $v_2 = (1, 0)$.
- Insert v_4 such that the area equation of the face $v_1v_2v_4$ is realized; this is fulfilled if y_4 equals $\mathcal{A}(v_1v_2v_4)$ while $x_4 \in \mathbb{R}$ is arbitrary. The value x_4 is our variable.
- Place each remaining vertex v_i with respect to its predecessors $\text{pred}(v_i)$ such that the area equations of the two incident face areas are respected; the coordinates of v_i are *nice* (*rational*) functions of x_4.
- Finally, all area equations are realized except for two special faces f_a and f_b. Moreover, the face area of f_a is a *nice* (*rational*) function $\mathfrak{f}$ of x_4.
- If $\mathfrak{f}$ is *super nice* (*almost surjective*), then there is a vertex placement D respecting all face areas and orientations, i.e., D is a real solution of $\text{AEQ}(T, \mathcal{A}, F)$.
- By Theorem 4, D guarantees the realizability of $\mathcal{A}$.
- If this holds for *enough* area assignments, then T is area-universal.

3.2.1 Properties of p-orders

A p-order $\mathcal{P}$ of a plane triangulation T induces an orientation $\mathcal{O}_\mathcal{P}$ of the edges: For a predecessor w of v_i, we orient the edge from v_i to w. We call $\mathcal{O}_\mathcal{P}$ the *almost 3-orientation* induced by $\mathcal{P}$ since most of the vertices have an outdegree of 3. Usually, we use almost 3-orientations to illustrate p-orders as in Figure 3.10. Note that not all edges are oriented.

Recall that by Proposition 2.11, a triangulation is area-universal if and only if all of its 4-connected components are area-universal. Hence, we may restrict our attention to 4-connected triangulations. Naturally, these triangulations have a minimum degree of 4. The 4-connectedness in not essential for our method; however, at several occasions, it is more convenient and gives a cleaner picture.

▶ **Lemma 3.6.** *Let T be a planar triangulation with a p-order $\mathcal{P}$ specified by $(v_1, v_2, \ldots, v_n)$. Then the almost 3-orientation $\mathcal{O}_\mathcal{P}$ is acyclic and has a unique unoriented edge $e_\mathcal{P}$. Moreover, if T has minimum degree 4, then $e_\mathcal{P}$ is incident to v_n.*

Proof. By definition of $\mathcal{O}_\mathcal{P}$ if an edge (v_i, v_j) is oriented from v_i to v_j, then $i > j$. Hence the orientation is acyclic. In particular, no edge is oriented in two directions.

The number of unoriented edges follows by double counting the edges of T. On the one hand, by Euler's formula, the number of edges in a triangulation is $|E| = 3n - 6$. On the other hand, the number of oriented edges $\vec{E}$ is given by the sum of the outdegrees.

$$|\vec{E}| = \sum_{i=1}^{n} \text{outdeg}(v_i) = 0 + 1 + 2 + 2 + 3(n-4) = 3n - 7.$$

Hence, $|E| - |\vec{E}| = 1$ and thus there is exactly one edge $e_\mathcal{P}$ without an orientation. Observe that the last vertex v_n in $\mathcal{P}$ has indegree 0. If T has minimum degree 4, then $e_\mathcal{P}$ is incident to v_n; otherwise v_n is a vertex of degree 3. ◀

Lemma 3.6 implies immediately that the p-order encodes all but one edge of the planar graph. If T is 4-connected, the missing edge is incident to v_n and we obtain the following:

Observation 3.7. *Any p-order of a 4-connected planar triangulation encodes the planar triangulation.*

For a plane triangulation T with a p-order $(v_1, v_2, \ldots, v_n)$, we denote the subgraph of T induced by the set of vertices $\{v_1, v_2, \ldots, v_i\}$ by T_i for $i \in [n]$.

▶ **Lemma 3.8.** *A planar triangulation T has a p-order if an only if there exists an edge e such that $T - e$ is 3-degenerate.*

Proof. If T has a p-order $\mathcal{P}$ given by $(v_1, v_2, \ldots, v_n)$, then $T - e_\mathcal{P}$ is 3-degenerate since, by the edge count of Lemma 3.6, every vertex v_i in $T_i - e_\mathcal{P}$, $i \in [n]$, has degree at most 3.

If e is an edge such that $T - e =: T'$ is 3-degenerate, we construct a p-order reversely. We set v_i, $i > 4$, as a vertex of degree at most 3 in $T' - \{v_{i+1}, \ldots, v_n\}$. If T is 4-connected, then by the edge count of Lemma 3.6 every vertex v_i, $i > 4$, has degree 3 in $T_i - e$; these three neighbors of v_i specify its predecessors. If T is 3-degenerate, T is a stacked triangulation. Then, the predecessors of v_i are its neighbors in T_i. ◀

Lemma 3.8 implies that not every triangulation has a p-order; specifically, a triangulation T with minimum degree 5, e.g. the icosahedron graph. After deletion of any edge e, $T - e$ has minimum degree 4 and is thus not 3-degenerate. Consequently, T has no p-order.

Now, we focus on triangulations with fixed drawings, i.e., plane triangulations. Recall that a drawing induces an orientation of each face.

Convention. We will follow the convention of stating inner faces counter clockwise and the outer face clockwise. This convention enables us to switch between different plane graphs of the same planar graph without changing the order of the vertices.

▶ **Lemma 3.9.** *Let T be a plane 4-connected triangulation with a p-order $\mathcal{P}$ specified by $(v_1, v_2, \ldots, v_n)$. For $i \geq 4$,*

- *T_i has one 4-face and otherwise only triangles,*
- *T_{i+1} can be constructed from T_i by inserting v_{i+1} in the 4-face of T_i, and*
- *the three predecessors of v_i can be named (p_F, p_M, p_L) such that $p_F p_M v_i$ and $p_M p_L v_i$ are (counter clockwise inner and clockwise outer) faces of T_i.*

Proof. We prove this statement by induction. For the induction base, note that T_4 has three faces: the triangle $v_3v_2v_1$, the triangle $v_1v_2v_4$, and the 4-face $v_1v_4v_2v_3$. Figure 3.11(a) depicts T_4 for the case that $v_3v_2v_1$ is the outer face. By 4-connectedness, v_3 and v_4 do not share an edge. With this notation, the inner faces are oriented counter clockwise and the outer face is oriented clockwise – independent of the choice of the outer face.

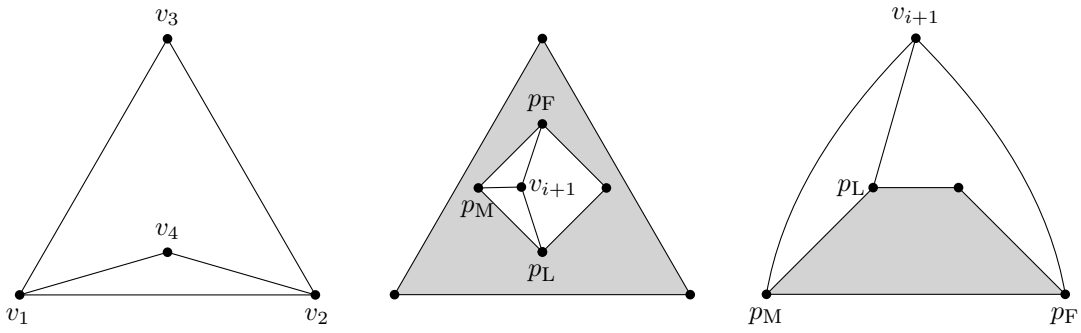

(a) Induction base: T_4

(b) Induction step where v_{i+1} is inserted in an inner 4-face.

(c) Induction step where v_{i+1} is inserted in an outer 4-face.

Figure 3.11: Illustration of Lemma 3.9 and its proof.

Now we consider the induction step and insert v_{i+1} in T_i. Since T is 4-connected, the vertex v_{i+1} can only be placed in the unique 4-face f of T_i. Clearly, any three vertices of f are consecutive on the boundary cycle of f. Hence, the predecessors of v_{i+1} form a path of length three along f. We define p_M as the middle vertex of this path. Naming the remaining predecessors by p_F and p_L, $p_F p_M v_{i+1}$ and $p_M p_L v_{i+1}$ are (not necessarily correctly oriented) triangles in T_{i+1}. Since T is 4-connected, these triangles of T_{i+1} are faces in T and thus also in T_{i+1}. Furthermore, $p_F v_{i+1} p_L w$ forms a 4-face of T_{i+1} where w is the vertex of f which is not in $\text{pred}(v_{i+1})$.

For the correct orientation we distinguish two cases: If f is an inner face, we define p_F as the counter clockwise first vertex (of the path of predecessors in f) and p_L as the counter clockwise last vertex. Figure 3.11(b) illustrates this definition for the case that f is an inner face. Otherwise, f is the outer face and we define p_F as the clockwise first vertex and p_L as the clockwise last vertex. This case is displayed in Figure 3.11(c). Then, $p_F p_M v_{i+1}$ and $p_M p_L v_{i+1}$ are counter clockwise faces in T_{i+1} if and only if they are inner faces of T. ◀

Remark. Note that for every (non-equivalent) plane graph T' of T, the three predecessors (p_F, p_M, p_L) of v_i in T' and T coincide.

The second property of Lemma 3.9 implies that there exist exponentially many distinct 4-connected planar triangulations with a p-order. Note that we prove the stronger statement of different planar triangulations; each of these may have up to linearly many plane triangulations.

▶ **Proposition 3.10.** *The number of 4-connected planar triangulations on n vertices with a p-order is $\Omega(1/n \cdot 2^n)$.*

Proof. First, we show that a 4-connected triangulation T on n vertices has at most $3n \cdot 2^{n-1}$ different p-orders. We consider every p-order in the reverse order $(v_n, ..., v_1)$. As a planar graph, T has at most $3n$ edges which may serve as the unique unoriented edge. Its deletion yields a 4-face. By Lemma 3.9, in every p-order the vertex v_i, $i \geq 5$, is incident to a 4-face in T_i. Removing v_i from T_i yields a graph T_{i-1} that has again a unique 4-face. By Lemma 3.8, v_i is a vertex of degree 3. Consequently, all neighbors of v_i in T_i are the predecessors of v_i. Let $f = x_1y_1y_2x_2$ be a 4-face of T_i. Consider Figure 3.12 and observe that two adjacent vertices of degree 3 on f certify a separating triangle, unless $n \leq 5$: Since all other faces of T_i are triangles, every pair of adjacent vertices has a common neighbor outside of f. If x_i has degree 3, the common neighbor of x_iy_i and x_1x_2 coincides; we call it z. Thus, zy_1y_2 is a separating triangle unless T_i contains only these five vertices. Therefore, by the 4-connectivity, the 4-face in T_i has at most two vertices of degree 3 and thus there are at most two choices for v_i when $i > 5$. For $i = 5$, the choices are upper bounded by the four vertices of the 4-face and for $i \leq 4$, by another four options; two for v_1, v_2 and two for v_3, v_4.

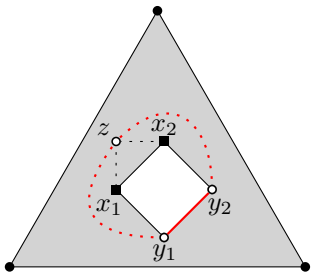

Figure 3.12: Two adjacent vertices of degree three in a 4-face certify a separating triangle.

Consequently, for a specific unoriented edge, the number of p-orders does not exceed $2^{n-5} \cdot 4 \cdot 4 = 2^{n-1}$. This makes a total of at most $3n \cdot 2^{n-1}$ different p-orders for a triangulation.

In order to build a 4-connected triangulation with a p-order $v_1, v_2, \ldots, v_n$, we specify the middle predecessor v_M of v_i for $5 \leq i \leq n$ from the 4-face of T_{i-1}. By Lemma 3.9, the remaining two predecessors of v_i are the two neighbors of v_M in the 4-face. Thus, we have four choices for v_M in each step $i > 5$. For $i = 5$, neither v_3 nor v_4 can serve as the middle predecessor since this results in a separating triangle. Thus, we obtain at least $2 \cdot 4^{n-5}$ different p-orders. By the above observation at most $3n \cdot 2^{n-1}$ belong to the same triangulation. Hence there are $\Omega(1/n \cdot 2^n)$ 4-connected planar triangulation with a p-order on n vertices. ◀

We are now ready to construct almost realizing vertex placement.

3.2.2 Construction of Almost Realizing Vertex Placements

Let T be a plane triangulation with an area assignment $\mathcal{A}$. We consider the extension of $\mathcal{A}$ to the set of all faces F. To account for our convention of stating the outer face in clockwise order, we define the area assignment of the outer face f_o as

$$\mathcal{A}(f_o) := -\Sigma\mathcal{A}.$$

Then $\det(f_o)$ evaluates to $\Sigma\mathcal{A}$. Moreover, without mentioning it any further, we consider usually $1/2\mathcal{A}$-realizing drawings in order to not deal with the factors. That is, if we say a triangle has area a, it will have area $1/2a$. However, as long as we scale all face areas consistently it has no further implications by Lemma 2.1.

We say a vertex placement D of T is *almost realizing* the area assignment $\mathcal{A}$ if there exist two faces f_a and f_b such that D satisfies the equation system $\text{AEQ}(T, \mathcal{A}, \tilde{F})$ of the set $\tilde{F} := F \setminus \{f_a, f_b\}$. In particular, we insist that the orientation and area of each face, except for f_a and f_b be correct, i.e., the corresponding determinant has the correct sign and value. Note that an almost realizing vertex placement may not correspond to a crossing-free straight-line drawing. Nevertheless, we want to obtain an $\mathcal{A}$-realizing drawing from an almost realizing vertex placement. Theorem 4 guarantees that the vertex placement is an $\mathcal{A}$-realizing drawing of T if additionally the area of f_a is respected since then, the equation system $\text{AEQ}(T, \mathcal{A}, F - f_b)$ is fulfilled. In other words, the following statement characterizes when an almost realizing vertex placement is also a realizing drawing.

Observation 3.11. *Let T be a plane triangulation with an area assignment $\mathcal{A}$ and let D be an almost realizing vertex placement where all faces except f_a and f_b are realized. Then D yields an $\mathcal{A}$-realizing drawing if and only if the face f_a has area $\mathcal{A}(f_a)$ in D.*

For triangulations with p-orders, we construct almost realizing vertex placements based on the following lemma.

▶ **Lemma 3.12.** *Let $a, b \geq 0$ and let $q_\text{F}, q_\text{M}, q_\text{L}$ be three vertices with a non-collinear placement in the plane. Then there exists a unique placement for vertex v such the counter clockwise triangles $q_\text{F}q_\text{M}v$ and $q_\text{M}q_\text{L}v$ fulfill the area equations for a and b, respectively.*

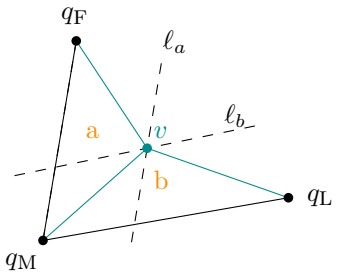

(a) If $q_\text{L}, q_\text{M}, q_\text{L}$ are not collinear, then the intersection point of ℓ_a and ℓ_b is the unique position of v realizing the face areas a and b.

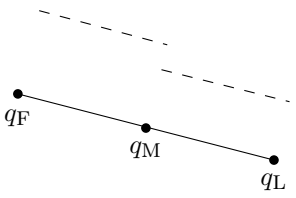

(b) If $q_\text{L}, q_\text{M}, q_\text{L}$ are collinear, then there may be either no or infinitely many positions for v realizing the face areas a and b.

Figure 3.13: Illustration of Lemma 3.12 and its proof.

Proof. To realize the areas, v must be placed on a specific line ℓ_a and ℓ_b, respectively, as depicted in Figure 3.13(a). Note that ℓ_a is parallel to the segment $q_\text{F}q_\text{M}$ and ℓ_b is parallel to the segment $q_\text{M}q_\text{L}$. Consequently, ℓ_a and ℓ_b are not parallel and their intersection point yields the unique position for vertex v. The coordinates (x, y) of v are specified by the two area equations

$$\text{Det}(q_\text{F}, q_\text{M}, v) \stackrel{!}{=} a$$
$$\text{Det}(q_\text{M}, q_\text{L}, v) \stackrel{!}{=} b.$$

Solving them for (x, y) yields the following expressions, where we denote the coordinates of q_i by (x_i, y_i):

$$x = x_{\text{M}} + \frac{a(x_{\text{L}} - x_{\text{M}}) - b(x_{\text{M}} - x_{\text{F}})}{x_{\text{F}}(y_{\text{M}} - y_{\text{L}}) + x_{\text{M}}(y_{\text{L}} - y_{\text{F}}) + x_{\text{L}}(y_{\text{F}} - y_{\text{M}})} \tag{3.1}$$

$$y = y_{\text{M}} + \frac{a(y_{\text{L}} - y_{\text{M}}) - b(y_{\text{M}} - y_{\text{F}})}{x_{\text{F}}(y_{\text{M}} - y_{\text{L}}) + x_{\text{M}}(y_{\text{L}} - y_{\text{F}}) + x_{\text{L}}(y_{\text{F}} - y_{\text{M}})} \tag{3.2}$$

This finishes the proof of the lemma. ◀

Note that if ℓ_a and ℓ_b are parallel and do not coincide, then there is no position for v realizing the face areas of the two triangles. If the lines are parallel and coincide, then all points on the line are realizing the two face areas, as depicted in Figure 3.13(b). Based on Lemma 3.12, we obtain our key lemma.

Before we are able to state it, we introduce the concept of algebraically independent area assignments. A set of real numbers $\{a_1, a_2, \ldots, a_k\}$ is *algebraically independent* over $\mathbb{Q}$ if for each polynomial $p(x_1, x_2, \ldots, x_k)$ with coefficients from $\mathbb{Q}$, different from the 0-polynomial, it holds that $p(a_1, a_2, \ldots, a_k) \neq 0$. We say an area assignment $\mathcal{A}$ of a plane graph G is *algebraically independent* if the set $\{\mathcal{A}(f) | f \in F'\}$ is algebraically independent over $\mathbb{Q}$. Note that then for all $f_0 \in F'$ it holds that $\{\mathcal{A}(f) | f \in F' \setminus f_0\} \cup \{\Sigma\mathcal{A}\}$ is algebraically independent. For a plane graph G, let $\mathbb{A}$ denote the set of area assignments with a fixed total area which is algebraically independent over $\mathbb{Q}$. We denote the subset of $\mathbb{A}$ consisting of all algebraically independent area assignments by $\mathbb{A}_I$.

▶ **Lemma 3.13.** *Let T be a plane 4-connected triangulation with a p-order $\mathcal{P}$ $(v_1, v_2, \ldots, v_n)$. Let f_a and f_b denote the two faces incident to the unoriented edge $e_{\mathcal{P}}$ in $\mathcal{O}_{\mathcal{P}}$, $\tilde{F} := F \setminus \{f_a, f_b\}$, and $f_0 := v_1v_2v_3$. Then, for area assignment $\mathcal{A} \in \mathbb{A}_I$ there exist a finite set $\mathcal{B}(\mathcal{A}) \subset \mathbb{R}$, rational functions $x_i(\cdot, \mathcal{A})$, $y_i(\cdot, \mathcal{A})$, and $\mathfrak{f}(\cdot, \mathcal{A})$, and a triangle $\triangle$ such that for all $x_4 \in \mathbb{R} \setminus \mathcal{B}(\mathcal{A})$, there exists a vertex placement $D(x_4)$ of T with the following properties:*

(i) f_0 coincides with the triangle $\triangle$,
(ii) the vertex placement $D(x_4)$ is almost realizing, i.e., it is a real solution of $\text{AEQ}(T, \mathcal{A}, \tilde{F})$,
(iii) every vertex v_i has the coordinates $\big(x_i(x_4, \mathcal{A}), y_i(x_4, \mathcal{A})\big)$, and
(iv) the area of face f_a in $D(x_4)$ is given by $\mathfrak{f}(x_4, \mathcal{A})$.

Proof. Consider a fixed but arbitrary algebraically independent area assignment $\mathcal{A} \in \mathbb{A}_I$. We think of $\mathcal{A}$ as an *abstract* area assignment, where the prescribed areas are still variables. The idea of the proof is simple. Given a placement of the vertices $v_1, \ldots, v_{i-1}$ we place v_i with the help of Lemma 3.12. To do so, we need to guarantee that the predecessors are not collinear.

Without loss of generality, we assume that the first two triangles read as $v_3v_2v_1$ and $v_1v_2v_4$ such that this order in counter clockwise for inner and clockwise for outer faces. For simplicity, we can think of f_0 as being the outer face. However, the construction works in all settings.

We place v_1 at $(0, 0)$, v_2 at $(1, 0)$ and set $y_3 := -\mathcal{A}(f_0)$; here it turns out to be convenient that we have defined the area of the outer face f_o as $\mathcal{A}(f_o) := -\Sigma\mathcal{A}$. We use the freedom to specify x_3 at a later state. This guarantees property (i). Furthermore, for $a := \mathcal{A}(v_1v_2v_4)$

we place v_4 at (x_4, a). Consequently, the face area of the triangle $v_1v_2v_4$ is realized for all choices of x_4.

For property (ii), we show that for all but finitely many values of x_4, we obtain an almost $\mathcal{A}$-realizing vertex placement $D(x_4)$. By Lemma 3.9, the three predecessors of v_i can be named (p_F, p_M, p_L) such that $p_F p_M v_i$ and $p_M p_L v_i$ are counter clockwise inner or clockwise outer faces of T. By Lemma 3.12, the vertex coordinates of v_i follow directly from its three predecessors p_F, p_M, p_L in the p-order – unless they are collinear. Note that the predecessors are collinear if and only if the denominators of Equations (3.1) and (3.2) vanish.

Assume for now, that we are considering an unproblematic position for x_4 such that no triple of predecessors becomes collinear. For $i = 5, \dots, n$, we place v_i according to Lemma 3.12 and realize two new faces. Together with the realized face area of the triangles $v_1v_2v_4$ and $v_1v_2v_3$, the total number of realized faces is $2(n-4)+2 = 2n-6$, i.e., all but two face areas are realized and $D(x_4)$ is an almost realizing vertex placement. Let $\mathcal{B}(\mathcal{A})$ denote the set of all x_4 where a triple of predecessors becomes collinear. We postpone to show that $\mathcal{B}(\mathcal{A})$ is finite. It is sufficient to show that the denominator of each vertex is not the 0-polynomial. We prove this simultaneously with property (iii).

Now, we show (iii). For each vertex v_i, we wish to represent its coordinates (x_i, y_i) in $D(x_4)$ by rational functions with a common denominator. Specifically, we aim for polynomials $\mathcal{N}_i^x, \mathcal{N}_i^y, \mathcal{D}_i$ in x_4, which are different from the 0-polynomial, such that

$$x_i = \frac{\mathcal{N}_i^x}{\mathcal{D}_i} \qquad \text{and} \qquad y_i = \frac{\mathcal{N}_i^y}{\mathcal{D}_i}.$$

We show the existence of such a representation by induction. Hence assume that we have such a representation of $v_1, \dots, v_{i-1}$. Note that by our placement of the first vertices we can define $\mathcal{D}_i := 1$ for all $i \in [4]$.

Consider a vertex v_i with $i > 4$. By Lemma 3.9, we denote the three predecessors of v_i by p_F, p_M, p_L such that the triangles $p_F p_M v_i$ and $p_M p_L v_i$ are counter clockwise inner or clockwise outer faces of T; we call the prescribed face areas of the two triangles a_i and b_i, respectively. Equations (3.1) and (3.2) of Lemma 3.12 yield the coordinates of vertex v_i in $D(x_4)$. As we will also aim for the fact that the representation is *crr-free*, we are already here a little more careful; two polynomials are *crr-free* if they have no common real roots.

For the later argument, it is convenient to consider v_5 explicitly. By 4-connectedness, neither v_3 nor v_4 are the middle predecessor of v_5. Thus, by symmetry, we may assume that the predecessors of v_5 are $\text{pred}(v_5) = \{v_1, v_4, v_3\}$. Equations (3.1) and (3.2) simplify to

$$x_5 = \frac{a_5 x_4 + b_5 x_3}{y_3 x_4 - a x_3} \qquad \text{and} \qquad y_5 = \frac{a a_5 + b_5 y_3}{y_3 x_4 - a x_3}. \tag{3.3}$$

Note that for $x_3 = 0$, the denominators of x_5 and y_5 would vary in a crr-free representation. Thus, for $x_3 \neq 0$, we define $\mathcal{N}_5^x := a_5 x_4 + b_5 x_3$, $\mathcal{N}_5^y := a a_5 + b_5 y_3$, $\mathcal{D}_5 := y_3 x_4 - a x_3$. Clearly, none of them is the 0-polynomial. Moreover, due to the 4-connectedness none of the following vertices have v_1 as a predecessor. Consequently, $\mathcal{N}_2^y$ is the only 0-polynomial which may belong to a predecessors of v_i for $i > 5$.

Next we consider the induction step for vertex v_i with $i > 5$. Equations (3.1) and (3.2) of Lemma 3.12 yield the coordinates of vertex v_i in the almost realizing vertex placement. By assumption, $\mathcal{D}_F \cdot \mathcal{D}_M \cdot \mathcal{D}_L$ is not the 0-polynomial, since none of its factors is the 0-polynomial. Therefore, we may expand the right term by $\mathcal{D}_F \cdot \mathcal{D}_M \cdot \mathcal{D}_L$. Using the

representations $x_j = \mathcal{N}_j^x/\mathcal{D}_j$ and $y_j = \mathcal{N}_j^y/\mathcal{D}_j$ for $j \in \{\text{F},\text{M},\text{L}\}$ yields the following identities:

$$x_i = \frac{\mathcal{N}_{\text{M}}^x}{\mathcal{D}_{\text{M}}} + \frac{\mathcal{D}_{\text{M}}(a_i\mathcal{N}_{\text{L}}^x\mathcal{D}_{\text{F}} + b_i\mathcal{N}_{\text{F}}^x\mathcal{D}_{\text{L}}) - (a_i+b_i)\mathcal{N}_{\text{M}}^x\mathcal{D}_{\text{F}}\mathcal{D}_{\text{L}}}{\tilde{\mathcal{D}}_i} \tag{3.4}$$

$$y_i = \frac{\mathcal{N}_{\text{M}}^y}{\mathcal{D}_{\text{M}}} + \frac{\mathcal{D}_{\text{M}}(a_i\mathcal{N}_{\text{L}}^y\mathcal{D}_{\text{F}} + b_i\mathcal{N}_{\text{F}}^y\mathcal{D}_{\text{L}}) - (a_i+b_i)\mathcal{N}_{\text{M}}^y\mathcal{D}_{\text{F}}\mathcal{D}_{\text{L}}}{\tilde{\mathcal{D}}_i} \tag{3.5}$$

$$\text{where } \tilde{\mathcal{D}}_i := \mathcal{N}_{\text{F}}^x(\mathcal{N}_{\text{M}}^y\mathcal{D}_{\text{L}} - \mathcal{N}_{\text{L}}^y\mathcal{D}_{\text{M}}) + \mathcal{N}_{\text{M}}^x(\mathcal{N}_{\text{L}}^y\mathcal{D}_{\text{F}} - \mathcal{N}_{\text{F}}^y\mathcal{D}_{\text{L}}) + \mathcal{N}_{\text{L}}^x(\mathcal{N}_{\text{F}}^y\mathcal{D}_{\text{M}} - \mathcal{N}_{\text{M}}^y\mathcal{D}_{\text{F}}). \tag{3.6}$$

Note that the denominators of x_i and y_i are identical and the numerators are symmetric in the x- and y-coordinates of their predecessors, respectively. Hence, for $\circ \in \{x, y\}$, we define $\mathcal{N}_i^\circ$ to unify the notation.

We wish to argue that $\tilde{\mathcal{D}}_i$ is not the 0-polynomial. Note that every $\mathcal{N}_j^y$ with $j \in \{\text{F},\text{M},\text{L}\}$ appears in at most two summands of $\tilde{\mathcal{D}}_i$. Thus, the fact that there is only one polynomial, namely $\mathcal{N}_2^y$, which might be the 0-polynomial guarantees that one summand of $\tilde{\mathcal{D}}_i$ does not vanish. Here we use the fact that v_1 is no predecessor of any v_i with $i > 5$ and that the polynomials $\mathcal{N}_i^x, \mathcal{N}_i^y, \mathcal{D}_i$ are not the 0-polynomial for $i > 3$.

We now expand to find the desired representations of x_i and y_i. The denominator is the least common multiple of $\mathcal{D}_{\text{M}}$ and $\tilde{\mathcal{D}}_i$, none of which are the 0-polynomial. In particular, we define E_i and F_i to be two crr-free polynomials such that

$$\mathcal{D}_{\text{M}}E_i = \tilde{\mathcal{D}}_iF_i. \tag{3.7}$$

In Equations (3.4) and (3.5), we expand the left summand by E_i and the right summand by F_i. Then the coordinates of vertex v_i can be expressed by

$$\mathcal{N}_i^\circ := F_i\mathcal{D}_{\text{M}}(a_i\mathcal{N}_{\text{L}}^\circ\mathcal{D}_{\text{F}} + b_i\mathcal{N}_{\text{F}}^\circ\mathcal{D}_{\text{L}}) + \mathcal{N}_{\text{M}}^\circ(E_i - (a_i+b_i)\mathcal{D}_{\text{F}}\mathcal{D}_{\text{L}}F_i) \tag{3.8}$$

$$\mathcal{D}_i := \mathcal{D}_{\text{M}}E_i = \tilde{\mathcal{D}}_iF_i \tag{3.9}$$

Thus, each coordinate of v_i is a rational function in x_4, where the coefficients are polynomials in $\mathcal{A}$. Due to the algebraically independent area assignment, the coefficients cannot vanish and $\mathcal{D}_i$ is not the 0-polynomial. Using the fact that $\mathcal{D}_{\text{F}} \cdot \mathcal{D}_{\text{M}} \cdot \mathcal{D}_{\text{L}}$ is not the 0-polynomial, any $\mathcal{N}_j^\circ$ with $j \in \{\text{F},\text{M},\text{L}\}$ which is not the 0-polynomial, certifies that $\mathcal{N}_i^\circ$ is not the zero polynomial. Recall that only for one $j \in \{\text{F},\text{M},\text{L}\}$, namely if $j = 2$, $\mathcal{N}_j^y$ may be the 0-polynomial. This proves properties (ii) and (iii).

Moreover, (iii) immediately implies (iv): The area of face f_a can be expressed as the determinant of its three vertex coordinates. Thus, if the vertex coordinates are rational functions in x_4, so is the area of face f_a. ◀

As stated in Lemma 3.13 (iv), for every area assignment, the area of face f_a in $D(x_4)$ can be expressed as a rational function $\mathfrak{f}(x_4, \mathcal{A})$. We call $\mathfrak{f}$ the *(abstract) last face function* of T and interpret it as a rational function in x_4 where the coefficients depend on $\mathcal{A}$. Due to the algebraic independence, it holds that:

Observation 3.14. *For all $\mathcal{A} \in \mathbb{A}_I$, the degree of the numerator polynomials of the last face function $\mathfrak{f}(x_4, \mathcal{A})$ coincide. Likewise, the degree of the denominator polynomials agree.*

Thus, we define *the degrees* of the last face function $\mathfrak{f}(x_4, \mathcal{A})$ with respect to some fixed algebraic independent area assignment $\mathcal{A}$. Let $d_1(\mathfrak{f})$ and $d_2(\mathfrak{f})$ denote the degree of the numerator and denominator polynomial of $\mathfrak{f}$ in x_4, respectively. In fact, the degrees do not only coincide for all algebraically independent area assignments, but also for different embeddings of the plane graph.

Let G be some plane graph of the planar graph G^*. By $[G]$ we denote the set (of equivalence classes) of all plane graphs of G^*.

▶ **Proposition 3.15.** *Let T be a plane 4-connected triangulation with a p-order $\mathcal{P}$. Then for every plane graph $T' \in [T]$, the last face functions $\mathfrak{f}$ and $\mathfrak{f}'$ constructed by Lemma 3.13 with respect to $\mathcal{P}$ have the same degrees, i.e., $d_i(\mathfrak{f}) = d_i(\mathfrak{f}')$ for $i \in [2]$.*

Proof. We assume that $v_1v_2v_3$ is the clockwise outer face of T and $w_1w_2w_3$ is the clockwise outer face of T'. Then $v_1v_2v_3$ is a counter clockwise inner face of T' and $w_1w_2w_3$ is a counter clockwise inner face of T. Compared to T, the orientation of the faces $v_1v_2v_3$ and $w_1w_2w_3$ in T' changes; while the orientation of all other faces remains: This is easily seen when considering the drawings on the sphere, which are obtained by one-point compactification of some point in the outer face. Due to the 3-connectedness and Whitney's uniqueness theorem, the drawings T and T' on the sphere are equivalent [Whitney, 1933]. Moreover, in the drawing on the sphere $v_1v_2v_3$ and $w_1w_2w_3$ are counter clockwise. Then choosing one face as the outer face and applying a stereographic projection of the punctured sphere where a point of the outer face is deleted, results in a drawing in the plane where all faces remain counter clockwise while the outer face becomes clockwise.

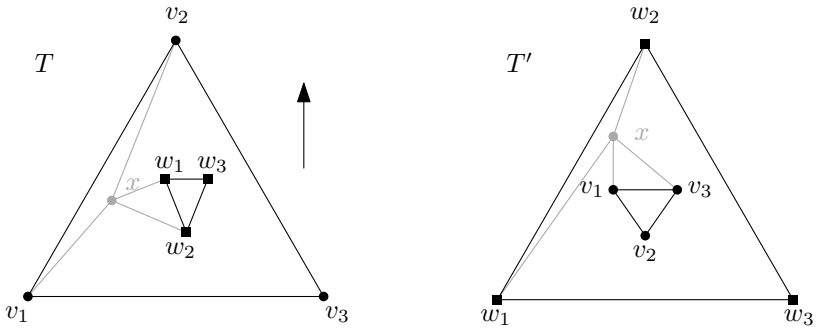

Figure 3.14: Illustration of Proposition 3.15 and its proof.

Let $\mathcal{A}$ be an algebraically independent area assignment of T. The outer face $v_1v_2v_3$ is assigned to the total area $-\Sigma\mathcal{A}$ and $w_1w_2w_3$ to some value c. For T', we consider the area assignment $\mathcal{A}'$ where all area assignments remain but $w_1w_2w_3$ obtains the total area $-\Sigma\mathcal{A}$ and $v_1v_2v_3$ some value c. Clearly, $\mathcal{A}'$ is algebraically independent since $\mathcal{A}$ is. Fortunately, the negative sign accounts for the fact that the orientation changes. Thus, when constructing realizing drawings by Lemma 3.13, T and T' are treated by the very same procedure. Therefore, $\mathfrak{f}'$ can be obtained from $\mathfrak{f}$ by swapping all occurrences of c and $-\Sigma\mathcal{A}$. Consequently, the degrees of the denominator and numerator polynomials of the last face functions $\mathfrak{f}$ and $\mathfrak{f}'$ coincide. ◀

If our method is sufficient to prove area-universality of one plane graph T, then Proposition 3.15 allows us to show area-universality for all plane graphs of $[T]$.

Let $\mathbb{A}$ denote the set of all area assignment with a total sum c, where c is transcendental. As the penultimate ingredient, we show that the subset of algebraically independent area assignments $\mathbb{A}_I$ is dense in $\mathbb{A}$.

▶ **Lemma 3.16.** *$\mathbb{A}_I$ is dense in $\mathbb{A}$.*

Proof. We prove this claim by induction and show that the set of algebraically independent k-tuples is dense. We build our proof upon the fact that the algebraic closure of a countable field is countable [Rotman, 2015, p. 343, Cor. B-2.41].

For the induction base, we consider $k = 1$. Since the algebraic closure of $\mathbb{Q}$ is countable, its complement $\mathbb{R} \setminus \mathbb{Q}$ is dense in $\mathbb{R}$.

Now we consider the induction step from $k-1$ to k. In order to show that the algebraically independent k-tuple are dense, it suffices to show that for each a in $\mathbb{R}^n$ and each ε-ball B of a, there exists an algebraic independent b in B. By induction hypothesis, we find a $(k-1)$-tuple $(b_2, \ldots, b_k)$ with algebraically independent entries, that is arbitrarily close to $(a_2, \ldots, a_k)$. Let K denote the algebraic closure of $\mathbb{Q}(b_2, ..., b_n)$, the smallest field containing $\mathbb{Q}$ and $\{b_2, \ldots, b_k\}$. As a rational function field over $\mathbb{Q}$, the field $\mathbb{Q}(b_2, ..., b_n)$ is countable. Thus, since the algebraic closure of a countable field is countable, K is countable. Consequently, in each open neighborhood of a_1, there exists a b_1 in the complement of K. Therefore, in each ε-ball of $a = (a_1, \ldots, a_n)$ there exists an algebraic independent $b = (b_1, \ldots, b_n)$. ◀

3.2.3 Almost Surjectivity and Area-Universality

In this subsection, we present a sufficient condition to guarantee area-universality. Let A and B be sets. A function $f\colon A \to B$ is *almost surjective* if all but finitely many values of B are attained, i.e., there exists a finite set $B_1 \subset B$ such that $f(A) = B \setminus B_1$. The central theorem states that almost surjectivity implies area-universality.

■ **Theorem 8.** *Let T be a plane 4-connected triangulation with a p-order $\mathcal{P}$. If the last face function $\mathfrak{f}$ constructed by Lemma 3.13 is almost surjective for all area assignments in $\mathbb{A}_I$, then T is area-universal.*

Proof. By Corollary 1, it suffices to show that an arbitrary but fixed area assignment $\mathcal{A} \in \mathbb{A}$ of T is realizable. Due to Proposition 2.13 and the fact that $\mathbb{A}_I$ is dense in $\mathbb{A}$ by Lemma 3.16, we may assume without loss of generality that $\mathcal{A}$ is contained in $\mathbb{A}_I$.

Let $(v_1, \ldots, v_n)$ be the order of the p-order and f_0 be the triangle formed by v_1, v_2, v_3. As before let $\mathbb{A}^+ := \mathbb{A}^{2\Sigma\mathcal{A}}|_{f_0 \to \mathcal{A}(f_0)}$ denote the set of area assignments of T whose total area does not exceed $2\Sigma\mathcal{A}$ and in which the face f_0 is assigned to $\mathcal{A}(f_0)$. Since $\mathcal{A}$ is algebraically independent, it holds that $\mathcal{A}(f_0) > 0$. By Proposition 2.15, $\mathcal{A}$ is realizable if every open neighborhood of $\mathcal{A}$ in $\mathbb{A}^+$ contains a realizable area assignment.

Let f_a and f_b denote the faces incident to $e_{\mathcal{P}}$ and $a_l := \mathcal{A}(f_a)$, $b_l := \mathcal{A}(f_b)$. Lemma 3.13 guarantees the existence of a finite set $\mathcal{B}$ such that for all $x_4 \in \mathbb{R} \setminus \mathcal{B}$, there exists an almost $\mathcal{A}$-realizing vertex placement $D(x_4)$. Recall that the area of f_a and f_b is not necessarily realized in $D(x_4)$. By Observation 3.11, we aim for an almost realizing vertex placement where additionally the area of f_a is realized.

By assumption, $\mathfrak{f}$ is almost surjective. Thus for every ε with $0 < \varepsilon < 1$, there exists $\tilde{x} \in \mathbb{R}$ such that $a_l \leq \mathfrak{f}(\tilde{x}) \leq a_l + \varepsilon$. Since $\mathcal{B}$ is finite, we can also find $\tilde{x} \in \mathbb{R} \setminus \mathcal{B}$ with $a_l \leq \mathfrak{f}(\tilde{x}) \leq a_l + \varepsilon$. Therefore, the face f_a has an area between a_l and $a_l + \varepsilon$ in the

almost realizing vertex placement $D(\tilde{x})$ of $\mathcal{A}$. (If f_a and f_b are both inner faces, then the face f_b has an area between $b_l - \varepsilon$ and b_l. Otherwise, if f_a or f_b is the outer face, then the total area changes and face f_b has an area between b_l and $b_l + \varepsilon$.) Thus, for some $\mathcal{A}'$ in the ε-neighborhood of $\mathcal{A}$ in $\mathbb{A}^+$, $D(\tilde{x})$ is a real solution of $\textsc{aeq}(T, \mathcal{A}', F \setminus \{f_b\})$ and Theorem 4 ensures that $\mathcal{A}'$ is realizable. Consequently, in every neighborhood of $\mathcal{A}$ in $\mathbb{A}^+$ there exists a realizable area assignment and hence, by Proposition 2.15, $\mathcal{A}$ is realizable. It follows that T is area-universal. ■

In order to prove the area-universality of our considered graphs, we use the following sufficient condition for almost surjectivity. We denote the degree of a polynomial p by $|p|$. Let $p, q\colon \mathbb{R} \to \mathbb{R}$ be real polynomials and Q the set of real roots of q. We say the polynomials p and q are *crr-free* if they do not have common real roots. For a rational function $f(x) := \frac{p(x)}{q(x)}$, we define the *max-degree* of f as the maximum degree of the numerator and denominator polynomial, i.e., $\text{max-deg}(f) := \max\{|p|, |q|\}$. Moreover, we say f is crr-free if p and q are.

▶ **Lemma 3.17.** *Let $p, q\colon \mathbb{R} \to \mathbb{R}$ be real polynomials and Q the set of real roots of q. If the rational function $f\colon \mathbb{R}\setminus Q \to \mathbb{R},\ f(x) = \frac{p(x)}{q(x)}$ is crr-free and has odd max-degree, then f is almost surjective.*

Proof. Let $c \in \mathbb{R}\setminus\{0\}$ and consider $g\colon \mathbb{R} \to \mathbb{R},\ g(x) := p(x) - cq(x)$. The leading coefficients of the polynomials p and $c \cdot q$ cancel for at most one choice of c. For all other values, the degree of g is $|g| = \max\{|p|, |q|\}$ and by assumption odd. Consequently, as a real polynomial of odd degree, g has a real root $\tilde{x}$. If $q(\tilde{x}) \neq 0$, then

$$g(\tilde{x}) = 0 \iff f(\tilde{x}) = c.$$

Suppose $q(\tilde{x}) = 0$. Then, $q(\tilde{x}) = 0 = g(\tilde{x}) = p(\tilde{x})$. Hence $\tilde{x}$ is a zero of both p and q. However, this is a contradiction to the assumption that p and q are crr-free. ◀

Combining Lemma 3.17 with Theorem 8, we obtain our final result:

■ **Corollary 9.** *Let T be a plane triangulation with a p-order $\mathcal{P}$. If the last face function $\mathfrak{f}$ of T is crr-free and has odd max-degree for one algebraically independent area assignment, then every plane graph in $[T]$ is area-universal.*

Proof. If the last face function $\mathfrak{f}$ of T has odd max-degree for some $\mathcal{A} \in \mathbb{A}_I$, then this holds true for all area assignments in $\mathbb{A}_I$ by Observation 3.14. Consequently, Lemma 3.17 guarantees that the last face function $\mathfrak{f}(\cdot, \mathcal{A})$ is almost surjective for all $\mathcal{A} \in \mathbb{A}_I$. Thus, Theorem 8 implies the area-universality of T.

For every other plane graph $T' \in [T]$, the last face function $\mathfrak{f}'$ has also odd max-degree by Proposition 3.15. Here we used the fact that $\mathfrak{f}'$ can be obtained from $\mathfrak{f}$ by exchanging two algebraically independent numbers. By the same reasoning, $\mathfrak{f}'$ is also crr-free. Thus, $\mathfrak{f}'$ is crr-free and has odd max-degree and the above argument shows that T' is area-universal. ■

In order to apply Corollary 9, we need to understand the last face function. In particular, we must trace the coordinate polynomials and their degrees.

3.2.4 Analyzing the Coordinates and their Degrees

Throughout this section, let T be a plane 4-connected triangulation with p-order $\mathcal{P}$ specified by $(v_1, v_2, \dots, v_n)$ and $\mathcal{A}$ an algebraically independent area assignment. We use Lemma 3.13 to obtain an almost realizing drawing $D(x_4)$ and Lemma 3.17 to guarantee almost surjectivity of the last face function $\mathfrak{f}$. Thus, we are interested in the max-degree of $\mathfrak{f}$.

As shown in Lemma 3.13, we can represent the coordinates (x_i, y_i) of each vertex v_i and the last face function by rational functions. Specifically, we have a representation of x_i and y_i by polynomials $\mathcal{N}_i^x, \mathcal{N}_i^y, \mathcal{D}_i$ in x_4 such that

$$x_i = \frac{\mathcal{N}_i^x}{\mathcal{D}_i} \quad \text{and} \quad y_i = \frac{\mathcal{N}_i^y}{\mathcal{D}_i}.$$

Due to Lemma 3.17, we also aim for the fact that $\mathcal{N}_i^x$ and $\mathcal{N}_i^y$ are crr-free with $\mathcal{D}_i$ and are interested in their degrees. Recall that we denote the degree of a polynomial p by $|p|$. Moreover, we say that a polynomial $p(x_1, \dots, x_k)$ *depends* on x_j if and only if $p(x_1, \dots, x_j, \dots, x_k) \neq p(x_1, \dots, 0, \dots, x_k)$. Equations (3.8) and (3.9) show that

Observation 3.18. *For $i \in \{4, \dots, n\}$, $\mathcal{N}_i^\circ$ depends on a_i and b_i, whereas $\mathcal{D}_i$ does not.*

In order to study their degree, we define $d_i^\circ := |\mathcal{N}_i^\circ| - |\mathcal{D}_i|$.

▶ **Lemma 3.19.** *Let v_i be a vertex with the three predecessors $p_{\text{F}}, p_{\text{M}}, p_{\text{L}}$ in $\mathcal{P}$. For the vertex coordinates of v_i in $D(x_4)$, it holds that the (not necessarily crr-free) polynomials $\mathcal{N}_i^\circ, \mathcal{D}_i, \tilde{\mathcal{D}}_i$, defined in Equations (3.6), (3.8) and (3.9), have the following degrees:*

$$|\mathcal{N}_i^\circ| = |\mathcal{D}_{\text{M}}| + |\mathcal{D}_{\text{F}}| + |\mathcal{D}_{\text{L}}| + |F_i| + \max\left\{d_{\text{L}}^\circ, d_{\text{F}}^\circ, d_{\text{M}}^\circ + \max\{|E_i| - |\mathcal{D}_{\text{F}}| - |\mathcal{D}_{\text{L}}| - |F_i|, 0\}\right\}$$

$$|\mathcal{D}_i| = |\mathcal{D}_{\text{M}}| + |E_i| = |\tilde{\mathcal{D}}_i| + |F_i|$$

$$|\tilde{\mathcal{D}}_i| = |\mathcal{D}_{\text{F}}| + |\mathcal{D}_{\text{M}}| + |\mathcal{D}_{\text{L}}| + \max\left\{d_{\text{F}}^x + \max\{d_{\text{M}}^y, d_{\text{L}}^y\}, d_{\text{M}}^x + \max\{d_{\text{L}}^y, d_{\text{F}}^y\}, d_{\text{L}}^x + \max\{d_{\text{F}}^y, d_{\text{M}}^y\}\right\}$$

Proof. We need to determine the degrees of the polynomials in Equations (3.6), (3.8) and (3.9). Here we use the fact that for all polynomials p, q different from the 0-polynomial it holds $|p \cdot q| = |p| + |q|$. With the convention that $|0| = -\infty$, the above identity also holds for the 0-polynomial. Moreover, unless $|p| = |q|$ and the leading coefficients are canceling, it holds that $|p + q| = \max\{|p|, |q|\}$. Since the area assignment is algebraically independent, cancelation of leading coefficients does not occur. ◀

However, in order to apply Lemma 3.17, we also need that $\mathcal{N}_i^x$ and $\mathcal{N}_i^y$ are crr-free with $\mathcal{D}_i$. In order to guarantee this, we are interested in sufficient conditions.

▶ **Lemma 3.20.** *Let $\circ \in \{x, y\}$. Suppose $\mathcal{N}_j^\circ$ and $\mathcal{D}_j$ are crr-free for all $j < i$. Then, $\mathcal{N}_i^\circ$ and $\mathcal{D}_i$ have a common zero z if and only if the following properties hold*

- *z is a zero of E_i*
- *z is independent of a_i and b_i*

and additionally

(i) z is a zero of at least two of $\{\mathcal{D}_{\text{F}}, \mathcal{D}_{\text{M}}, \mathcal{D}_{\text{L}}\}$ or
(ii) z is a zero of both of $\{\mathcal{N}_{\text{L}}^\circ \mathcal{D}_{\text{M}} - \mathcal{N}_{\text{M}}^\circ \mathcal{D}_{\text{L}}, \mathcal{N}_{\text{F}}^\circ \mathcal{D}_{\text{M}} - \mathcal{N}_{\text{M}}^\circ \mathcal{D}_{\text{F}}\}$.

Due to their technicality, we have moved the proofs of Lemma 3.20 and of the two following lemmas to Section 3.2.5. We continue to study a more specific situation.

Stacking on same angle Recall that, by Lemma 3.9, vertex v_i is inserted in the 4-face of T_{i-1}. In this section, we analyze the situation that in the p-order several vertices are repeatedly inserted in the same angle. In particular, we say vertices v_{i+1} and v_{i+2} are *stacked on the same angle* if their first and last predecessors are identical and the middle predecessor of v_{i+2} is v_{i+1}. Specifically, v_{i+1} and v_{i+2} have predecessors $(p_{\text{F}}, v_i, p_{\text{L}})$ and $(p_{\text{F}}, v_{i+1}, p_{\text{L}})$, respectively. Figure 3.15 illustrates two vertices which are stacked on the same angle.

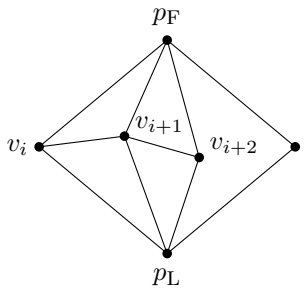

Figure 3.15: Vertices v_{i+1} and v_{i+2} are stacked on the same angle.

▶ **Lemma 3.21.** *If v_{i+1} and v_{i+2} are stacked on the same angle in the p-order $\mathcal{P}$ and if the polynomials $\mathcal{N}^{\circ}_{i+1}$ and $\mathcal{D}_{i+1}$ are crr-free, then it holds that*

$$E_{i+2} = E_{i+1} - (a_{i+1} + b_{i+1})\mathcal{D}_{\text{F}}\mathcal{D}_{\text{L}}F_{i+1}$$
$$F_{i+2} = F_{i+1}.$$

For the proof of Lemma 3.21, we refer to Section 3.2.5. For the degrees of the coordinate polynomials of v_{i+2}, we obtain the following expressions.

▶ **Lemma 3.22.** *If v_{i+1} and v_{i+2} are stacked on the same angle in the p-order $\mathcal{P}$, and if the polynomials $\mathcal{N}^{\circ}_{i+1}$,$\mathcal{D}_{i+1}$, and $\mathcal{N}^{\circ}_{i+2}$, $\mathcal{D}_{i+2}$ are crr-free, then for $\circ \in \{x, y\}$, it holds that*

$$|\mathcal{N}^{\circ}_{i+2}| = |\mathcal{D}_{i+1}| + M + d^{\circ}_{i+1}$$
$$|\mathcal{D}_{i+2}| = |\mathcal{D}_{i+1}| + M$$

with $M := \max\{|E_{i+1}|, |\mathcal{D}_{\text{F}}| + |\mathcal{D}_{\text{L}}| + |F_{i+1}|)\}$. In particular, it holds that $d^{\circ}_{i+2} = d^{\circ}_{i+1}$.

The proof of Lemma 3.22 is presented in Section 3.2.5.

3.2.5 Proofs of the Degree-Lemmas

In this section, we present the pending proofs of the previous section.

▶ **Lemma 3.20.** *Let $\circ \in \{x, y\}$. Suppose $\mathcal{N}_j^\circ$ and $\mathcal{D}_j$ are crr-free for all $j < i$. Then, $\mathcal{N}_i^\circ$ and $\mathcal{D}_i$ have a common zero z if and only if the following properties hold*

- *z is a zero of E_i*
- *z is independent of a_i and b_i*

and additionally

(i) z is a zero of at least two of $\{\mathcal{D}_\text{F}, \mathcal{D}_\text{M}, \mathcal{D}_\text{L}\}$ or
(ii) z is a zero of both of $\{\mathcal{N}_\text{L}^\circ\mathcal{D}_\text{M} - \mathcal{N}_\text{M}^\circ\mathcal{D}_\text{L}, \mathcal{N}_\text{F}^\circ\mathcal{D}_\text{M} - \mathcal{N}_\text{M}^\circ\mathcal{D}_\text{F}\}$.

Proof. The proof consists of two directions. For both recall the formulas for $\mathcal{N}_i^\circ$ and $\mathcal{D}_i$ given in Equations (3.8) and (3.9). Suppose that $\mathcal{N}_i^\circ$ and $\mathcal{D}_i$ have a common zero z. We think of z as an algebraic function of $(a, a_5, b_5, \dots, a_i, b_i)$. By Observation 3.18, the variables a_i and b_i do not occur in D_i. Consequently, z does not depend on a_i and b_i, and is thus algebraically independent of a_i and b_i. Since $\mathcal{D}_i = \mathcal{D}_\text{M}E_i$, by Equation (3.9), z is a zero of at least one of $\mathcal{D}_\text{M}$ or E_i. We distinguish three cases.

Case 1: If z is a zero of both, $\mathcal{D}_\text{M}$ and E_i, then Equation (3.8) simplifies to

$$\mathcal{N}_i^\circ[z] = -(a_i + b_i)(\mathcal{N}_\text{M}^\circ\mathcal{D}_\text{F}\mathcal{D}_\text{L}F_i)[z] = 0.$$

By the assumption of being crr-free, z is neither a zero of $\mathcal{N}_\text{M}^\circ$ nor F_i. Hence, z is a zero of $\mathcal{D}_\text{F}\mathcal{D}_\text{L}$. In conclusion, z is a zero of E_i, $\mathcal{D}_\text{M}$ as well as $\mathcal{D}_\text{F}$ or $\mathcal{D}_\text{L}$ (or both). In other words, condition (i) is fulfilled.

Case 2: If z is a zero of $\mathcal{D}_\text{M}$ and not of E_i, then Equation (3.8) reads as

$$\mathcal{N}_i^\circ[z] = (\mathcal{N}_\text{M}^\circ(E_i - (a_i + b_i))\mathcal{D}_\text{F}\mathcal{D}_\text{L}F_i)[z] = 0.$$

Since z, a_i, b_i are algebraically independent, $\mathcal{N}_i^\circ[z]$ vanishes on each summand. However, z is not a zero of E_i by assumption of Case 2 and z is not a zero of $\mathcal{N}_\text{M}^\circ$ since $\mathcal{D}_\text{M}$ and $\mathcal{N}_\text{M}^\circ$ are crr-free. Thus, we arrive at a contradiction and this case does not occur.

Case 3: If z is a zero of E_i and not of $\mathcal{D}_\text{M}$, z is not a zero of F_i; since E_i and F_i are crr-free. Consequently, Equation (3.8) implies $(\mathcal{D}_\text{M}(a_i\mathcal{N}_\text{L}^\circ\mathcal{D}_\text{F} + b_i\mathcal{N}_\text{F}^\circ\mathcal{D}_\text{L}) - (a_i + b_i)\mathcal{N}_\text{M}^\circ\mathcal{D}_\text{F}\mathcal{D}_\text{L})[z] = 0$. Reordering for a_i and b_i results in

$$\big(a_i\mathcal{D}_\text{F}(\mathcal{D}_\text{M}\mathcal{N}_\text{L}^\circ - \mathcal{N}_\text{M}^\circ\mathcal{D}_\text{L}) + b_i\mathcal{D}_\text{L}(\mathcal{D}_\text{M}\mathcal{N}_\text{F}^\circ - \mathcal{N}_\text{M}^\circ\mathcal{D}_\text{F})\big)[z] = 0$$

As argued above, z, a_i, and b_i are algebraically independent, and thus z is a zero of both summands. If z is a zero of $\mathcal{D}_\text{F}$, then it is also a zero of $\mathcal{D}_\text{L}\mathcal{D}_\text{M}\mathcal{N}_\text{F}^\circ$. However, by assumption and crr-freeness, it is not a zero of $\mathcal{D}_\text{M}\mathcal{N}_\text{F}^\circ$, and thus it is a zero of $\mathcal{D}_\text{L}$. Likewise, if z is a zero of $\mathcal{D}_\text{L}$ then it follows that z is also a zero of $\mathcal{D}_\text{F}$. Hence, (i) is satisfied.

Thus, in the following we may assume that z is not a zero of $\mathcal{D}_\text{F}\mathcal{D}_\text{L}$, but of both polynomials $(\mathcal{N}_\text{L}^\circ\mathcal{D}_\text{M} - \mathcal{N}_\text{M}^\circ\mathcal{D}_\text{L})$ and $(\mathcal{N}_\text{F}^\circ\mathcal{D}_\text{M} - \mathcal{N}_\text{M}^\circ\mathcal{D}_\text{F})$. This is condition (ii).

It remains to show the reverse direction. Since z is a zero of E_i, it follows that z is a zero of $\mathcal{D}_i$. By construction of our cases, z is a zero of $\mathcal{N}_i^\circ$. Alternatively, it is easy to check that z is also a zero of $\mathcal{N}_i^\circ$ as given in Equation (3.8) in all cases. Consequently, z is a zero of both $\mathcal{N}_i^\circ$ and $\mathcal{D}_i$. ◀

▶ **Lemma 3.21.** *If v_{i+1} and v_{i+2} are stacked on the same angle in the p-order $\mathcal{P}$ and if the polynomials $\mathcal{N}^\circ_{i+1}$ and $\mathcal{D}_{i+1}$ are crr-free, then it holds that*

$$E_{i+2} = E_{i+1} - (a_{i+1} + b_{i+1})\mathcal{D}_{\text{F}}\mathcal{D}_{\text{L}}F_{i+1}$$
$$F_{i+2} = F_{i+1}.$$

Proof. Note that the irreducibility of E_{i+1} and F_{i+1} directly implies the irreducibility of E_{i+2} and F_{i+2}: Since $F_{i+2} = F_{i+1}$, every zero of F_{i+2} is a zero of F_{i+1}. Therefore, z is a zero of E_{i+2} and F_{i+2} if and only if z is a zero of E_{i+1} and F_{i+1}. It remains to show that

$$E_{i+2}\mathcal{D}_{i+1} = F_{i+2}\tilde{\mathcal{D}}_{i+2}.$$

To do so, we will show that $\tilde{\mathcal{D}}_{i+1}$ is a factor of $\tilde{\mathcal{D}}_{i+2}$. By Equation (3.6), we obtain the following formula for $\tilde{\mathcal{D}}_{i+2}$:

$$\tilde{\mathcal{D}}_{i+2} = \mathcal{N}^x_{i+1}(\mathcal{N}^y_{\text{L}}\mathcal{D}_{\text{F}} - \mathcal{N}^y_{\text{F}}\mathcal{D}_{\text{L}}) + \mathcal{N}^y_{i+1}(\mathcal{N}^x_{\text{F}}\mathcal{D}_{\text{L}} - \mathcal{N}^x_{\text{L}}\mathcal{D}_{\text{F}}) + \mathcal{D}_{i+1}(\mathcal{N}^x_{\text{L}}\mathcal{N}^y_{\text{F}} - \mathcal{N}^x_{\text{F}}\mathcal{N}^y_{\text{L}})$$

The last summand is clearly divisible by $\mathcal{D}_{i+1}$ and, hence by $\tilde{\mathcal{D}}_{i+1}$. Therefore we focus on the first two summands, in which we replace $\mathcal{N}^\circ_{i+1}$ with the help of Equation (3.8) by

$$\mathcal{N}^\circ_{i+1} = F_{i+1}\mathcal{D}_i(a_{i+1}\mathcal{N}^\circ_{\text{L}}\mathcal{D}_{\text{F}} + b_{i+1}\mathcal{N}^\circ_{\text{F}}\mathcal{D}_{\text{L}}) + \mathcal{N}^\circ_i E_{i+2}.$$

Replacing $\mathcal{N}^\circ_{i+1}$ by the above expressions and using Equation (3.6) for $\tilde{\mathcal{D}}_{i+1}$, we obtain:

$$\begin{aligned}
&\mathcal{N}^x_{i+1}(\mathcal{N}^y_{\text{L}}\mathcal{D}_{\text{F}} - \mathcal{N}^y_{\text{F}}\mathcal{D}_{\text{L}}) + \mathcal{N}^y_{i+1}(\mathcal{N}^x_{\text{F}}\mathcal{D}_{\text{L}} - \mathcal{N}^x_{\text{L}}\mathcal{D}_{\text{F}})\\
&\quad = (F_{i+1}\mathcal{D}_i[a_{i+1}\mathcal{N}^x_{\text{L}}\mathcal{D}_{\text{F}} + b_{i+1}\mathcal{N}^x_{\text{F}}\mathcal{D}_{\text{L}}] + \mathcal{N}^x_i E_{i+2})(\mathcal{N}^y_{\text{L}}\mathcal{D}_{\text{F}} - \mathcal{N}^y_{\text{F}}\mathcal{D}_{\text{L}})\\
&\quad + (F_{i+1}\mathcal{D}_i[a_{i+1}\mathcal{N}^y_{\text{L}}\mathcal{D}_{\text{F}} + b_{i+1}\mathcal{N}^y_{\text{F}}\mathcal{D}_{\text{L}}] + \mathcal{N}^y_i E_{i+2})(\mathcal{N}^x_{\text{F}}\mathcal{D}_{\text{L}} - \mathcal{N}^x_{\text{L}}\mathcal{D}_{\text{F}})\\
&\quad = \mathcal{D}_{\text{F}}\mathcal{D}_{\text{L}}\mathcal{D}_i F_{i+1}(\mathcal{N}^y_{\text{L}}\mathcal{N}^x_{\text{F}} - \mathcal{N}^y_{\text{F}}\mathcal{N}^x_{\text{L}})(a_{i+1} + b_{i+1})\\
&\qquad + E_{i+2}(\mathcal{N}^x_i(\mathcal{N}^y_{\text{L}}\mathcal{D}_{\text{F}} - \mathcal{N}^y_{\text{F}}\mathcal{D}_{\text{L}}) + \mathcal{N}^y_i(\mathcal{N}^x_{\text{F}}\mathcal{D}_{\text{L}} - \mathcal{N}^x_{\text{L}}\mathcal{D}_{\text{F}}))\\
&\quad = \mathcal{D}_{\text{F}}\mathcal{D}_{\text{L}}\mathcal{D}_i F_{i+1}(\mathcal{N}^y_{\text{L}}\mathcal{N}^x_{\text{F}} - \mathcal{N}^y_{\text{F}}\mathcal{N}^x_{\text{L}})(a_{i+1} + b_{i+1})\\
&\qquad + E_{i+2}(\tilde{\mathcal{D}}_{i+1} - \mathcal{D}_i(\mathcal{N}^x_{\text{L}}\mathcal{N}^y_{\text{F}} - \mathcal{N}^x_{\text{F}}\mathcal{N}^y_{\text{L}}))
\end{aligned}$$

We remove the term $E_{i+2}\tilde{\mathcal{D}}_{i+1}$ which clearly divisible by $\tilde{\mathcal{D}}_{i+1}$. In the remainder we factor out $(\mathcal{N}^x_{\text{F}}\mathcal{N}^y_{\text{L}} - \mathcal{N}^x_{\text{L}}\mathcal{N}^y_{\text{F}})\mathcal{D}_i$ and recall the definitions of E_{i+2} and D_{i+1}. It remains

$$\begin{aligned}
&\mathcal{D}_{\text{F}}\mathcal{D}_{\text{L}}\mathcal{D}_i F_{i+1}(\mathcal{N}^x_{\text{F}}\mathcal{N}^y_{\text{L}} - \mathcal{N}^x_{\text{L}}\mathcal{N}^y_{\text{F}})(a_{i+1} + b_{i+1}) + E_{i+2}(-\mathcal{D}_i(\mathcal{N}^x_{\text{L}}\mathcal{N}^y_{\text{F}} - \mathcal{N}^x_{\text{F}}\mathcal{N}^y_{\text{L}}))\\
&= (\mathcal{N}^x_{\text{F}}\mathcal{N}^y_{\text{L}} - \mathcal{N}^x_{\text{L}}\mathcal{N}^y_{\text{F}})\mathcal{D}_i(\mathcal{D}_{\text{F}}\mathcal{D}_{\text{L}}F_{i+1}(a_{i+1} + b_{i+1}) + E_{i+2})\\
&= (\mathcal{N}^x_{\text{F}}\mathcal{N}^y_{\text{L}} - \mathcal{N}^x_{\text{L}}\mathcal{N}^y_{\text{F}})\mathcal{D}_i E_{i+1} = (\mathcal{N}^x_{\text{F}}\mathcal{N}^y_{\text{L}} - \mathcal{N}^x_{\text{L}}\mathcal{N}^y_{\text{F}})\mathcal{D}_{i+1}
\end{aligned}$$

By definition, $\mathcal{D}_{i+1}$ divisible by $\tilde{\mathcal{D}}_{i+1}$. The remainder consists of three summands, namely $(\mathcal{N}^x_{\text{L}}\mathcal{N}^y_{\text{F}} - \mathcal{N}^x_{\text{F}}\mathcal{N}^y_{\text{L}}) + E_{i+2} + (\mathcal{N}^x_{\text{F}}\mathcal{N}^y_{\text{L}} - \mathcal{N}^x_{\text{L}}\mathcal{N}^y_{\text{F}})$. Note that the first and last summand of the remainder are canceling. Consequently, the remainder is E_{i+2}, i.e., $\tilde{\mathcal{D}}_{i+2} = \tilde{\mathcal{D}}_{i+1}E_{i+2}$. This directly implies that $F_{i+1}\tilde{\mathcal{D}}_{i+2} = F_{i+1}\tilde{\mathcal{D}}_{i+1}E_{i+2} = \mathcal{D}_{i+1}E_{i+2}$ and therefore finishes the proof. ◀

▶ **Lemma 3.22.** *If v_{i+1} and v_{i+2} are stacked on the same angle in the p-order $\mathcal{P}$, and if the polynomials $\mathcal{N}^\circ_{i+1}$,$\mathcal{D}_{i+1}$, and $\mathcal{N}^\circ_{i+2}$, $\mathcal{D}_{i+2}$ are crr-free, then for $\circ \in \{x, y\}$, it holds that*

$$|\mathcal{N}^\circ_{i+2}| = |\mathcal{D}_{i+1}| + M + d^\circ_{i+1}$$
$$|\mathcal{D}_{i+2}| = |\mathcal{D}_{i+1}| + M$$

with $M := \max\{|E_{i+1}|, |\mathcal{D}_{\text{F}}| + |\mathcal{D}_{\text{L}}| + |F_{i+1}|)\}$. In particular, it holds that $d^\circ_{i+2} = d^\circ_{i+1}$.

Proof. Recall that, by definition $d^\circ_{i+2} = |\mathcal{N}^\circ_{i+2}| - |\mathcal{D}_{i+2}|$. Consequently, if the degree of $\mathcal{N}^\circ_{i+2}$ and $\mathcal{D}_{i+2}$ are as claimed, it follows directly that $d^\circ_{i+2} = d^\circ_{i+1}$. For $\circ \in \{x, y\}$, we define $m^\circ := |\mathcal{D}_{\text{F}}| + |\mathcal{D}_{\text{L}}| + |F_{i+1}| + \max\{d^\circ_{\text{L}}, d^\circ_{\text{F}}\}$. Together with Lemma 3.19, the degrees can be expressed as follows:

$$|\mathcal{N}^\circ_{j+1}| = |\mathcal{D}_j| + \max\left\{m^\circ, d^\circ_j + M\right\}$$
$$|\mathcal{D}_{j+1}| = |\mathcal{D}_j| + |E_{j+1}|$$

This implies the following formula for d°_{j+1}:

$$d^\circ_{j+1} = -|E_{j+1}| + \max\left\{m^\circ, d^\circ_i + M\right\}$$

Recall that by Lemma 3.21, $E_{i+2} = E_{i+1} - (a_{i+1} + b_{i+1})\mathcal{D}_{\text{F}}\mathcal{D}_{\text{L}}F_j$ and $F_{i+2} = F_{i+1}$. Consequently, it holds that $|E_{i+2}| = M$ and with the above formula it follows for the degree that $|\mathcal{D}_{i+2}| = |\mathcal{D}_{i+1}| + |E_{i+2}| = |\mathcal{D}_{i+1}| + M$, as claimed.

For the numerator, we replace d°_{i+1} in $\mathcal{N}^\circ_{i+2}$:

$$\begin{aligned}
|\mathcal{N}^\circ_{i+2}| &= |\mathcal{D}_{i+1}| + \max\left\{m^\circ, d^\circ_{i+1} + M\right\} \\
&= |\mathcal{D}_{i+1}| + \max\left\{m^\circ, M - |E| + \max\left\{m^\circ, d^\circ_i + M\right\}\right\} \\
&= |\mathcal{D}_{i+1}| + M - |E| + \max\left\{m^\circ, d^\circ_i + M\right\} \\
&= |\mathcal{D}_{i+1}| + M + d^\circ_{i+1}
\end{aligned}$$

By definition of M, $M - |E|$ is non-negative and hence, the outer-maximum in line 2 is attained for the second term. The last term in the third line is exactly d°_{i+1}. Hence the numerator degree $|\mathcal{N}^\circ_{i+2}|$ has the claimed form. This finishes the proof. ◀

3.2.6 Applications

We now use the developed method in order to prove area-universality of some graph classes. Several of the graph families rely on an operation which we call *diamond addition*. Let G be a plane graph and e an inner edge incident to two triangular faces consisting of e and the vertices u_1 and u_2, respectively. By applying a diamond addition of order k on edge e, we obtain the graph G' from G by subdividing edge e with the vertices $v_1, \ldots, v_k$, and inserting the edges (v_i, u_j) for all pairs $i \in [k]$ and $j \in [2]$. Figure 3.16 illustrates a diamond addition of order 3.

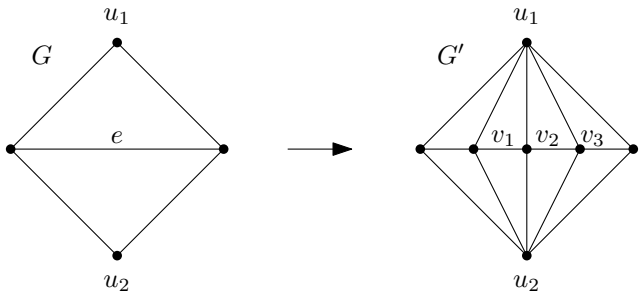

Figure 3.16: A diamond addition of order 3 on edge e which introduces the three new vertices v_1, v_2, v_3.

Accordion graphs

Here we are considering a very curious graph class that we mentioned already in the introduction, namely the accordion graphs. We show that every second graph in this class is area-universal whereas the others are not. It shows that area-universal and non-area-universal graphs may be structural very similar and how sensitive area universality is to small local changes.

These graphs can be obtained by diamond additions on the octahedron graph: Choose one edge of the central triangle of the plane octahedron graph as the *special edge*. In Figure 3.17, the special edge of the octahedron is highlighted in orange. The *accordion* graph $\mathcal{K}_\ell$ is the plane graph obtained by a diamond addition of order ℓ on the special edge of the plane octahedron graph. We speak of an *even accordion* if ℓ is even and likewise, of an *odd accordion* if ℓ is odd. Figure 3.17 illustrates the accordion graphs $\mathcal{K}_0$, $\mathcal{K}_1$, and $\mathcal{K}_2$.

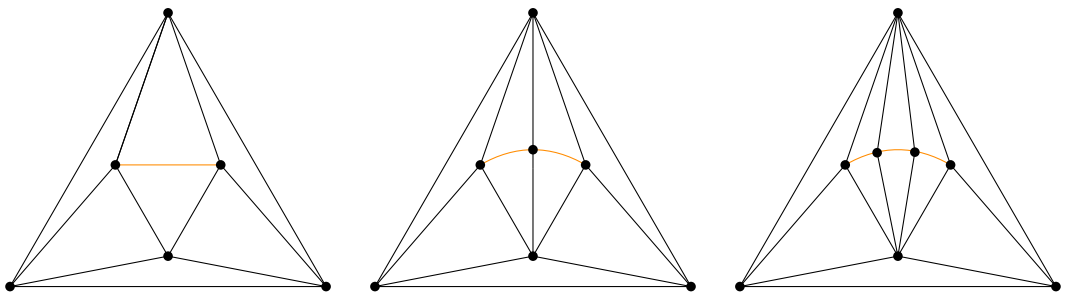

Figure 3.17: The accordion graphs $\mathcal{K}_0$, $\mathcal{K}_1$, and $\mathcal{K}_2$; The middle graph, $\mathcal{K}_1$, is an odd accordion, while $\mathcal{K}_0$ and $\mathcal{K}_2$ are even accordions.

Note that $\mathcal{K}_0$ is the octahedron itself and $\mathcal{K}_1$ is the unique plane 4-connected triangulation on seven vertices. Moreover, observe the following facts. First of all, due to its symmetry, all planar not necessarily equivalent drawings of $\mathcal{K}_\ell$ are equivalent, i.e., $[\mathcal{K}_\ell] = \mathcal{K}_\ell$. Secondly, all but two vertices of an accordion have degree four: Consult Figure 3.16 to observe that by a diamond addition on edge e of order k, the degrees of u_1 and u_2 increase by k while all other vertex degrees remain. Consequently, all vertices of an even accordion have even degree. Thus, an even accordion is an Eulerian triangulation, and hence not area-universal by Theorem 5. In contrast, we show that every odd accordion is area-universal.

■ **Theorem 10.** *An accordion graph is area-universal if and only if it is an odd accordion.*

Proof. As mentioned above, an even accordion graph is an Eulerian triangulation, and hence not area-universal by Theorem 5.

It remains to consider odd accordion graphs, all of which have a p-order. We use the p-order $\mathcal{P}$ depicted in Figure 3.18(a). We consider an arbitrary but fixed algebraically independent area assignment $\mathcal{A}$ and construct an $1/2\mathcal{A}$-almost realizing vertex placement $D(x_4)$ in a right triangle where the outer vertices are placed as follows: v_1 at $(0,0)$, v_2 at $(1,0)$, v_3 at $(1,\Sigma\mathcal{A})$, and v_4 at (x_4,a) with $a := \mathcal{A}(v_1v_2v_4)$. Consider also Figure 3.18(b). As before, we denote the two face areas incident to v_i and its predecessors by a_i and b_i for $i \geq 5$.

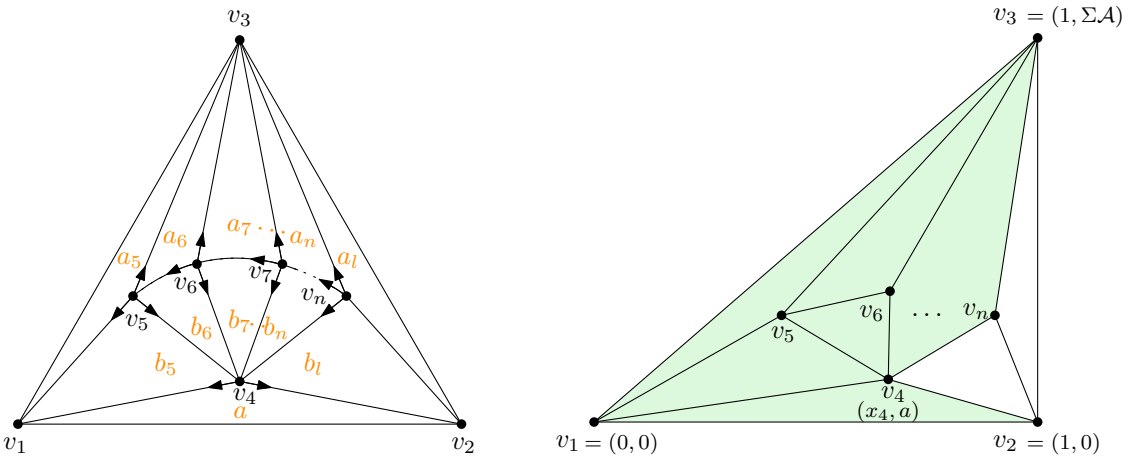

(a) A p-order $\mathcal{P}$ of an accordion graph.

(b) An almost realizing vertex placement in which the green faces are realized.

Figure 3.18: Illustration of Theorem 10 and its proof.

Note that for all vertices v_i with $i > 5$, the three predecessors of v_i are

$$p_{\text{F}} = v_3, \quad p_{\text{M}} = v_{i-1} \quad \text{and} \quad p_{\text{L}} = v_4.$$

In other words, all vertices v_i with $i > 4$ are stacked on the same angle. Consequently, for all $i > 5$, it holds that $|\mathcal{N}^\circ_{\text{F}}| = |\mathcal{D}_{\text{F}}| = |\mathcal{D}_{\text{L}}| = 0$ and $d^x_{\text{F}} = d^y_{\text{F}} = 0$, and $d^x_{\text{L}} = 1, d^y_{\text{L}} = 0$.

For v_5, we have already evaluated the crr-free vertex coordinates in Equation (3.3). Using the fact that $x_3 = 1$, we obtain the following degrees:

$$|\mathcal{N}^x_5| = 1, \quad |\mathcal{N}^y_5| = 0, \quad |\mathcal{D}_5| = |E_5| = |\tilde{\mathcal{D}}_5| = 1.$$

This implies that $d_5^x = 0$ and $d_5^y = -1$. Here we used the fact that, since $\mathcal{D}_{\text{M}} = 1$, it holds that $F_5 = 1$ and $\mathcal{D}_5 = E_5 = \tilde{\mathcal{D}}_5$. Defining $M := \max\{|E_5|, |\mathcal{D}_{\text{F}}| + |\mathcal{D}_{\text{L}}| + |F_5|\} = \max\{1, 0\} = 1$, we obtain for v_i, $i > 5$, with the help of Lemma 3.22:

$$|\mathcal{N}_{i+1}^x| = |\mathcal{D}_i| + M + d_5^x = |\mathcal{D}_i| + 1$$
$$|\mathcal{N}_{i+1}^y| = |\mathcal{D}_i| + M + d_5^y = |\mathcal{D}_i|$$
$$|\mathcal{D}_{i+1}| = |\mathcal{D}_i| + M = |\mathcal{D}_i| + 1.$$

Consequently, it holds that $|\mathcal{N}_i^x| = |\mathcal{D}_i|$ which is odd if and only if i is odd. Hence, in particular for odd accordions, it holds that $|\mathcal{N}_n^x| = |\mathcal{D}_n|$ is odd. To guarantee an almost surjective last face function, we show that the polynomials are crr-free.

✻ Claim 3.23. *For all $i \geq 5$, it holds that $\mathcal{N}_i^\circ$ and $\mathcal{D}_i$ are crr-free.*

We show this by induction on i. The induction base is settled for $i = 5$. Suppose, for a contradiction, that $\mathcal{N}_i^\circ$ and $\mathcal{D}_i$, share a common real root. Then, we are either in case (i) or (ii) of Lemma 3.20. The fact that $\mathcal{D}_{\text{F}} = \mathcal{D}_{\text{L}} = 1$ excludes case (i).

Thus, we are in case (ii). To arrive at the final contradiction, we work a little harder. Since $\mathcal{D}_{\text{F}} = \mathcal{D}_{\text{L}} = 1$, there exists z which is a zero of both $\mathcal{N}_{\text{L}}^\circ \mathcal{D}_{\text{M}} - \mathcal{N}_{\text{M}}^\circ$ and $\mathcal{N}_{\text{F}}^\circ \mathcal{D}_{\text{M}} - \mathcal{N}_{\text{M}}^\circ$. This implies that either $\mathcal{D}_{\text{M}}[z] = 0$ or $\mathcal{N}_{\text{L}}^\circ[z] = \mathcal{N}_{\text{F}}^\circ[z]$. In the first case, $\mathcal{D}_{\text{M}}[z] = 0$, it follows that $\mathcal{N}_{\text{M}}^\circ[z] = 0$. This is an immediate contradiction to the fact that $\mathcal{D}_{\text{M}}$ and $\mathcal{N}_{\text{M}}^\circ$ are crr-free.

Thus it remains to consider the latter case, namely that $\mathcal{N}_{\text{L}}^\circ[z] = \mathcal{N}_{\text{F}}^\circ[z]$. For $\circ = y$, we immediately obtain a contradiction since $\mathcal{N}_{\text{L}}^y = a < \Sigma\mathcal{A} = \mathcal{N}_{\text{F}}^y$.

For $\circ = x$ it follows that $z = 1$ since $\mathcal{N}_{\text{L}}^x = x$, $\mathcal{N}_{\text{F}}^x = 1$. Moreover, by Lemma 3.20, z is a zero of E_i. Consequently, it suffices to show that $E_i[1] \neq 0$. In order to analyze the zeros of E_i, we define for $i \in \{5, \ldots, n\}$

$$\alpha_i := a + \sum_{j=5}^{i-1} (a_j + b_j).$$

Recall that $E_5[x] = (\Sigma\mathcal{A})x - a$ by Equation (3.3). Thus, by Lemma 3.21, it holds for $i \in \{5, \ldots, n-1\}$ that

$$E_{i+1}[x] = E_i[x] - (a_i + b_i) = E_5[x] - \sum_{j=5}^{i} (a_j + b_j) = (\Sigma\mathcal{A})x - \alpha_{i+1}. \tag{3.10}$$

Since $\alpha_i < \Sigma\mathcal{A}$, it follows $E_i[1] \neq 0$ that for all $i \geq 5$. Consequently, $\mathcal{N}_i^\circ$ and $\mathcal{D}_i$ are crr-free.

Finally, we consider the last face function $\mathfrak{f}$ for the triangle of v_2, v_3, v_n. Its face area is given by

$$\mathfrak{f}(x) := \det(v_2, v_3, v_n) = \Sigma\mathcal{A}(1 - x_n) = \Sigma\mathcal{A}\left(1 - \frac{\mathcal{N}_n^x}{\mathcal{D}_n}\right).$$

Since $|\mathcal{N}_n^x|$ and $|\mathcal{D}_n|$ are odd, the max-degree of $\mathfrak{f}$ is odd. Thus, Lemma 3.17 assures that $\mathfrak{f}$ is almost surjective. By Corollary 9, the area-universality of the odd accordion follows. ■

Now, we generalize the characterization of accordion graphs to double stacking graphs. Unfortunately, it will be a little more intricate to guarantee crr-freeness.

Double stacking graphs

A double stacking graph can be obtained by two disjoint diamond addition on different inner edges of the plane octahedron graph. Denote the vertices of the plane octahedron by ABC and uvw as depicted in Figure 3.19. The *double stacking graph* $\mathcal{H}_{\ell,k}$ is the plane graph obtained from the plane octahedron by applying one diamond addition of order $\ell - 1$ on Au and one diamond addition of order $k - 1$ on vw. We label the vertices of $\mathcal{H}_{\ell,k}$ by $A, B, C, v, 1, 2, \dots \ell$ and $1', 2', \dots, k'$ as illustrated in Figure 3.19. Consequently, a double stacking graph has $(\ell + k + 4)$ vertices. Note that $\mathcal{H}_{\ell,1}$ is isomorphic to the accordion graph $\mathcal{K}_{\ell-1}$. In particular, the octahedron graph is a double stacking graph for $\ell = k = 1$.

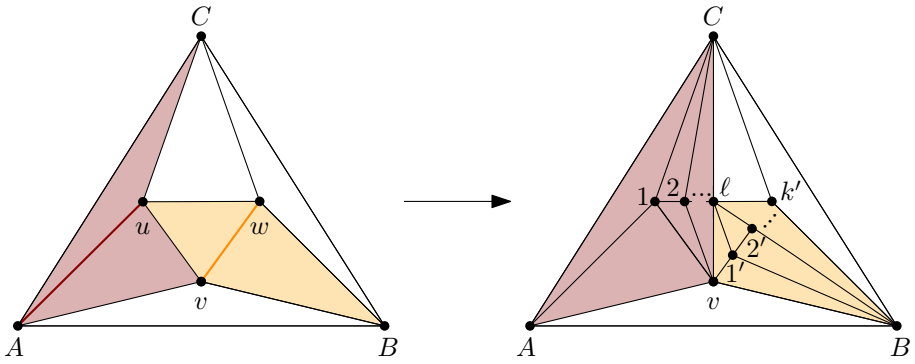

Figure 3.19: A double stacking graph.

■ **Theorem 11.** *A plane graph in* $[\mathcal{H}_{\ell,k}]$ *is area-universal if and only if* $\ell \cdot k$ *is even.*

Proof. We start to consider $\mathcal{H}_{\ell,k}$. Note that the degree of all but four vertices is exactly four; namely, the degree of B and ℓ is $k+3$, the degree of v and C is $\ell+3$. Thus, if both ℓ and k are odd, then $\mathcal{H}_{\ell,k}$ is Eulerian and thus not area-universal by Theorem 5. Since the degree depends on the planar graph, all plane graphs in $[\mathcal{H}_{\ell,k}]$ are Eulerian and not area-universal if $\ell \cdot k$ is odd.

Assume that $\ell \cdot k$ is even. In order to show the area-universality of $\mathcal{H}_{\ell,k}$, we consider the p-order $(A, B, C, v, 1, \dots, \ell, 1' \dots, k')$ in which $k'C$ is the unique undirected edge. For an algebraically independent area assignment $\mathcal{A}$, we define $a := \mathcal{A}(ABv)$ and place v_3 at $(1, \Sigma\mathcal{A})$ and v_4 at (x_4, a). Observe that the vertices $1, 2, \dots \ell$ have the predecessors C and v and are locally identical to an accordion graph. Consequently, by the analysis in the proof of Theorem 10, the coordinates of vertex ℓ can be expressed by crr-free polynomials $\mathcal{N}_\ell^\circ$ and $\mathcal{D}_\ell$ with the degrees

$$|\mathcal{N}_\ell^x| = |\mathcal{N}_\ell^y| + 1 = |\mathcal{D}_\ell| = \ell.$$

Since $\mathcal{D}_v = 1$ and $C_{1'} = E_{1'}\mathcal{D}_v = \tilde{D}_{1'}F_{1'}$ by definition, see Equation (3.7), it follows that $E_{1'} = \tilde{D}_{1'}$ and $F_{1'} = 1$. As we will see it holds that $|E_{1'}| = |\tilde{D}_{1'}| = \ell$; this implies that

$$\max\{|E_{1'}| - |\mathcal{D}_\ell| - |\mathcal{D}_B| - |F_{1'}|, 0\} = \max\{\ell - \ell - 0 - 0, 0\} = 0.$$

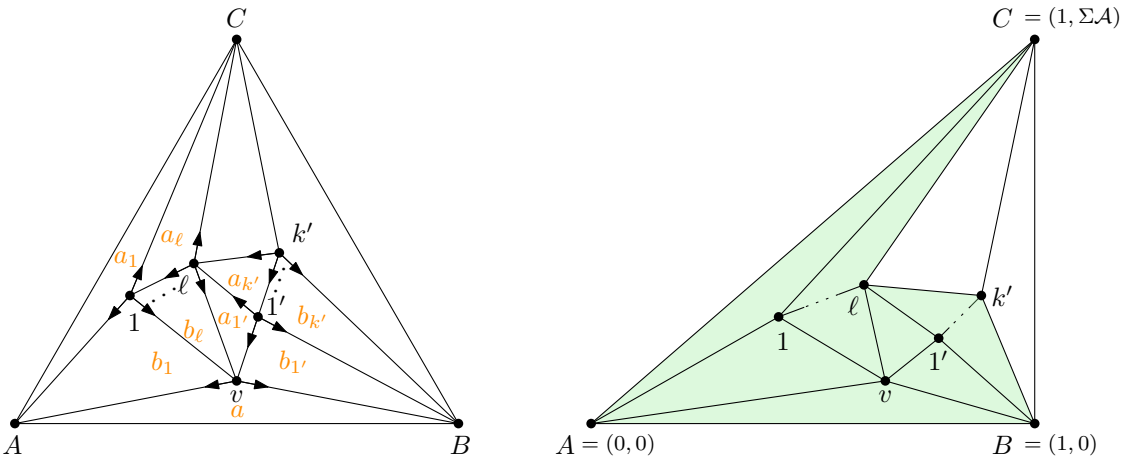

(a) A p-order of a double stacking graph. (b) An almost realizing vertex placement.

Figure 3.20: Illustration of Theorem 11 and its proof.

Note that $d_B^x = 0$, $d_B^y = -\infty$, $d_v^x = 1$, $d_v^y = 0$, $d_\ell^x = 0$, and $d_\ell^y = -1$. Lemma 3.19 yields the following degrees:

$$|\mathcal{N}_{1'}^x| = |\mathcal{D}_\ell| + \max\left\{d_\ell^x, d_B^x, d_v^x + 0\right\} = \ell + \max\left\{0, 0, 1 + 0\right\} = \ell + 1$$

$$|\mathcal{N}_{1'}^y| = \ell + \max\left\{d_\ell^y, d_B^y, d_v^y + 0\right\} = \ell + \max\left\{-1, -\infty, 0 + 0\right\} = \ell$$

$$|\mathcal{D}_{1'}| = |\tilde{\mathcal{D}}_{1'}| + |F_{1'}| = \ell$$

$$\begin{aligned}|\tilde{\mathcal{D}}_{1'}| &= |\mathcal{D}_\ell| + |\mathcal{D}_v| + |\mathcal{D}_B| + \max\left\{d_\ell^x + \max\{d_v^y, d_B^y\}, d_v^x + \max\{d_B^y, d_\ell^y\}, d_B^x + \max\{d_\ell^y, d_v^y\}\right\} \\ &= \ell + 0 + 0 + \max\left\{0 + \max\{0, -\infty\}, 1 + \max\{-\infty, -1\}, 0 + \max\{-1, 0\}\right\} = \ell\end{aligned}$$

We will later show that these polynomials are crr-free. Now, we proceed to compute the degrees of the vertex coordinates. Defining $M := \max\{|E_{1'}|, |\mathcal{D}_\ell| + |\mathcal{D}_B| + |F_{1'}|)\} = \max\{\ell, \ell + 0 + 0)\} = \ell$ and by Lemma 3.22, it follows for $j > 1$

$$|\mathcal{N}_{j'}^x| = |\mathcal{D}_{1'}| + (j-1) \cdot M + d_{1'}^x = j \cdot \ell + 1$$
$$|\mathcal{N}_{j'}^y| = |\mathcal{D}_{j'}| = |\mathcal{D}_{1'}| + (j-1) \cdot M = j \cdot \ell.$$

Assume for now, that the resulting polynomials are crr-free. As our last face we choose the triangle $k'BC$. Then the last face function $\mathfrak{f}$ evaluates to

$$\mathfrak{f}(x) := \det(k', B, C) = 1 - x_{k'} = 1 - \frac{\mathcal{N}_{k'}^x}{\mathcal{D}_{k'}}.$$

For the last vertex k', the degree of the numerator, namely $k \cdot \ell + 1$, exceeds the degree of the denominator $k \cdot \ell$ and is odd since $\ell \cdot k$ is even. Consequently, $\mathfrak{f}$ has odd max-degree and is almost surjective by Lemma 3.17. Consequently, Theorem 8 shows that $\mathcal{H}_{\ell,k}$ and every other plane graph in $[\mathcal{H}_{\ell,k}]$ is area-universal.

It remains to guarantee that the polynomials are crr-free.

▶ **Lemma 3.24.** *For all $j \geq 1$, it holds that $\mathcal{N}^{\circ}_{j'}$ and $\mathcal{D}_{j'}$ are crr-free.*

We prove this claim by induction and start with settling the base for $j = 1$ using Lemma 3.20. Suppose by contradiction that $\mathcal{N}^{\circ}_{1'}$ and $\mathcal{D}_{1'}$ share a common zero z. The fact that $\mathcal{D}_{\text{L}} = \mathcal{D}_{\text{M}} = 1$ excludes case (i). Thus, case (ii) holds and, since $\mathcal{D}_{\text{L}} = \mathcal{D}_{\text{M}} = 1$, z is a zero of the simplified polynomials $(\mathcal{N}^{\circ}_{\text{L}} - \mathcal{N}^{\circ}_{\text{M}})$ and $(\mathcal{N}^{\circ}_{\text{F}} - \mathcal{N}^{\circ}_{\text{M}}\mathcal{D}_{\text{F}})$. Recall that $\mathcal{N}^{x}_{\text{L}} = 1$ and $\mathcal{N}^{y}_{\text{L}} = 0$. Thus for $\circ = y$, it follows that z is a zero of $\mathcal{N}^{y}_{\text{L}}$ and thus also of $\mathcal{N}^{y}_{\text{M}}$. However, $\mathcal{N}^{y}_{\text{M}} = a > 0$ yields a contradiction. For $\circ = x$, $\mathcal{N}^{x}_{\text{L}} = 1$ and $\mathcal{N}^{x}_{\text{M}} = x$ imply that $z = 1$. Consequently, it holds that $\mathcal{N}^{x}_{\text{F}}[1] - \mathcal{D}_{\text{F}}[1] = 0$. Recall that in our case $\text{F} = \ell$. By Observation 3.18, $\mathcal{N}^{x}_{\text{F}} = \mathcal{N}^{x}_{\ell}$ depends on a_ℓ while $\mathcal{D}_{\text{F}}$ does not. Consequently, $\mathcal{N}^{x}_{\text{F}}[1]$ and $\mathcal{D}_{\text{F}}[1]$ are polynomials in $\mathcal{A}$; due to the algebraic independence they cannot coincide.

Now, we come to the induction step and suppose, for a contradiction, that $\mathcal{N}^{\circ}_{j'+1}$ and $\mathcal{D}_{j'+1}$ share a common real root z. By Lemma 3.20 we distinguish two cases. In all cases z is zero of $E_{j'+1}$. By Lemma 3.21, we know that for $j \in [k-1]$ it holds that $E_{j'+1} = E_{j'} - (a_{j'} + b_{j'})\mathcal{D}_\ell$. Together with $E_{1'} = a(\mathcal{N}^{x}_{\ell} - \mathcal{D}_\ell) + (1-x)\mathcal{N}^{y}_{\ell}$, we obtain

$$E_{j'+1} = a\mathcal{N}^{x}_{\ell} + (1-x)\mathcal{N}^{y}_{\ell} - \left(a + \sum_{k=1}^{j}(a_{k'} + b_{k'})\right)\mathcal{D}_\ell.$$

We claim that z does not depend on $a_{j'}$ and $b_{j'}$. Then, it follows from the algebraic independence, that z is a zero of both $a\mathcal{N}^{x}_{\ell} + (1-x)\mathcal{N}^{y}_{\ell}$ and $\mathcal{D}_\ell$.

To prove this claim we distinguish the cases suggested by Lemma 3.20. Recall that the predecessor indices $\text{F},\text{M},\text{L}$ of $j'+1$ are given by $\ell, j', 2$. If case (i) of Lemma 3.20 holds, then z is a zero of $\mathcal{D}_\ell$ and $\mathcal{D}_{j'}$ since $\mathcal{D}_2 = 1$. Then clearly z does not depend on $a_{j'}$ and $b_{j'}$ since $\mathcal{D}_\ell$ does not.

If case (ii) of Lemma 3.20 holds, then z is a zero of $\mathcal{N}^{\circ}_{2}\mathcal{D}_{j'} - \mathcal{N}^{\circ}_{j'}\mathcal{D}_2$ and $\mathcal{N}^{\circ}_{\ell}\mathcal{D}_{j'} - \mathcal{N}^{\circ}_{j'}\mathcal{D}_\ell$. We distinguish two cases for $\circ \in \{x, y\}$. For $\circ = y$, it holds that $\mathcal{N}^{y}_{2} = 0$ and $\mathcal{D}_2 = 1$. Thus, it follows that $\mathcal{N}^{y}_{j'}[z] = 0$ and $(\mathcal{N}^{y}_{\ell}\mathcal{D}_{j'})[z] = 0$. Since $\mathcal{N}^{y}_{j'}$ and $\mathcal{D}_{j'}$ are crr-free by the induction hypothesis, it holds that $\mathcal{N}^{y}_{\ell}[z] = 0$. Then as a zero of $\mathcal{N}^{y}_{\ell}$, z does neither depend on $a_{j'}$ nor on $b_{j'}$.

For $\circ = x$, $\mathcal{N}^{x}_{2} = 1$ and $\mathcal{D}_2 = 1$ imply that $\mathcal{N}^{x}_{j'}[z] = \mathcal{D}_{j'}[z]$ and $\mathcal{D}_{j'}[z](\mathcal{N}^{x}_{\ell} - \mathcal{D}_\ell)[z] = 0$. Since $\mathcal{D}_{j'}[z] \neq 0$, as otherwise $\mathcal{N}^{x}_{j'}$ and $\mathcal{D}_{j'}$ are not crr-free, it holds that $\mathcal{N}^{x}_{\ell}[z] = \mathcal{D}_\ell[z]$. Using the last fact, $E_{j'+1}[z]$ simplifies to $(1-z)\mathcal{N}^{y}_{\ell}[z] - \left(\sum_{k=1}^{j}(a_{k'} + b_{k'})\right)\mathcal{D}_\ell[z] = 0$. This implies that

$$\mathcal{N}^{x}_{\ell}[z] = \mathcal{D}_\ell[z] = \frac{1}{\sum_{k=1}^{j}(a_{k'} + b_{k'})}(1-z)\mathcal{N}^{y}_{\ell}[z]$$

Since neither $\mathcal{N}^{x}_{\ell}$ nor $\mathcal{D}_\ell$ depend on $a_{k'}$ and $b_{k'}$, these three polynomial do not coincide at z for small variations of $a_{k'}$. Thus for a dense set of algebraically independent area assignments, these three polynomials share no common real root. Consequently, we can assume that z does not depend on $a_{j'}$ and $b_{j'}$ and thus z is a zero of both $(a\mathcal{N}^{x}_{\ell} + (1-x)\mathcal{N}^{y}_{\ell})$ and $\mathcal{D}_\ell$. However, we show that this is not the case.

✻ **Claim 3.25.** *$\mathcal{D}_\ell$ and $(a\mathcal{N}^{x}_{\ell} + (1-x)\mathcal{N}^{y}_{\ell})$ are crr-free.*

Suppose z is a zero of $\mathcal{D}_\ell$ and $a\mathcal{N}_\ell^x + (1-x)\mathcal{N}_\ell^y$. Recall that by Equation (3.10) and since $\mathcal{D}_{i+1} = E_{i+1}D_i$ it follows for $i \in [\ell]$ for $i \in [\ell]$ it holds that

$$E_i = x - \alpha_i \quad \text{and} \quad \mathcal{D}_i = \prod_{j=1}^{i} E_j = \prod_{j=1}^{i}(x - \alpha_j).$$

Therefore, the zero set of $\mathcal{D}_i$ is given by $\{\alpha_i \mid i \in [\ell]\}$. We define

$$G_j[x] := a\mathcal{N}_j^x[x] + (1-x)\mathcal{N}_j^y[x]$$

and aim to show by induction on $j \in [\ell]$ that for all $i \leq j$: $G_j[\alpha_i] \neq 0$. Note that the claim is equivalent to $G_\ell[\alpha_i] \neq 0$ for all $i \leq \ell$. For the induction base, Equation (3.3) shows that $\mathcal{N}_1^x = a_1 x + b_1$ and $\mathcal{N}_1^y = a_1 a + b_1$. Consequently, it holds that $G_1[\alpha_1] = G_1[a] = a_1 a + b_1 \neq 0$. By Equation (3.8), for $i \in [\ell - 1]$, the numerator polynomials can be expressed by $\mathcal{N}_j^\circ = \mathcal{D}_j(a_j\mathcal{N}_v^\circ + b_j) + \mathcal{N}_j^\circ E_{j+1}$. This yields

$$\begin{aligned} G_j[\alpha_i] &= a\big(\mathcal{D}_j(a_j\mathcal{N}_v^x + b_j) + \mathcal{N}_j^x E_{j+1}\big)[\alpha_i] + (1-\alpha_i)\big(\mathcal{D}_j(a_j\mathcal{N}_v^y + b_j) + \mathcal{N}_j^y E_{j+1}\big)[\alpha_i] \\ &= \mathcal{D}_j[\alpha_i] \cdot (aa_j + b_j(1 + a - \alpha_i)) + E_{j+1}[\alpha_i] \cdot \big(a\mathcal{N}_j^x[\alpha_i] + (1-\alpha_i)\mathcal{N}_j^y[\alpha_i]\big) \end{aligned}$$

If $i \leq j$, then the first summand vanishes since $\mathcal{D}_j[\alpha_i] = 0$. The second summand does not vanish by induction and the fact that $E_{j+1}[\alpha_i] = \alpha_i - \alpha_{j+1} < 0$. For $i = j+1$, the second term vanishes since $E_{j+1}[\alpha_{j+1}] = 0$ and the first term does not vanish since both factors do not. Consequently, it holds that $G_\ell[\alpha_i] \neq 0$. This finishes the proof of the claim and the theorem. ■

Note that we have presented two infinite families, the area-universal family of odd accordion graphs – or more generally of (even product) double stacking graphs – and the non-area-universal family of Eulerian graphs. With the gained knowledge, we draw the following conclusions easily.

■ **Corollary 12.** *For every $n \geq 7$, there exists a 4-connected triangulation on n vertices that is area-universal.*

Proof. The double stacking graph $\mathcal{H}_{\ell,k}$ has $\ell + k + 4$ vertices and is area-universal if and only if $\ell \cdot k$ is even by Theorem 11. Thus, depending on the parity of n, either $\mathcal{H}_{2,n-6}$ or $\mathcal{H}_{1,n-5}$ has n vertices and is area-universal. ■

■ **Corollary 13.** *For every $n \geq 8$, there exists a 4-connected triangulation on n vertices that is not area-universal.*

Proof. If n is even, then $\mathcal{H}_{1,n-5}$ is not area-universal by Theorem 11. For $n = 9$, the result will follow from Theorem 14. For odd $n \geq 11$, we construct a 4-connected Eulerian triangulation on n vertices: We start with the octahedron where an octahedron is stacked into the central face. Applying an diamond addition of order $n - 9$ on one edge of the separating triangle results in a 4-connected Eulerian triangulation. ■

3.3 Small Triangulations

We now investigate the area-universality of small triangulations. Somewhat surprisingly, deciding the area-universality of small graphs is already quite difficult. The classification of small triangulation was conducted in collaboration with Henning Heinrich in the framework of his master thesis [Heinrich, 2018]. As shown in Theorem 4, the realizability of an area assignment can be decided by a quadratic equation system. Using the program Bertini, which solves equation systems numerically, Heinrich tested the realizability of all area assignments with 0 and 1, which we also call 01-assignments, for all 4-connected triangulations with at most ten vertices. In order to disprove the realizability of an area assignment we usually present arguments similar to the ones used in Section 3.1.1, i.e., we use a generalized counting argument. Combining this with our tools from Section 3.2, we are able to classify all triangulation with a p-order on up to ten vertices. In Section 3.3.4, we give a conclusion of what we can learn from small instances.

Throughout this section, we depict and encode area assignments by face colorings. A white face represents an assigned area of 0 and a gray face an assigned area of 1. We call such an area assignment a *white/gray area assignment*. A few times, we need more than two values, because of what we use several shades of gray, where a darker shade corresponds to a larger area assignment. In the following analysis, we repeatedly use the following two facts when proving non-area-universality.

▶ **Lemma 3.26.** *Let T be a plane triangulation with a white/gray area assignment where each inner vertex is adjacent to a gray face. If the number of white faces exceeds the number of inner vertices by k, then in a realizing drawing at least k edges are contracted.*

Proof. Since every inner vertex is incident to a gray face, it may realize at most one flat angle and at least some edge must be contracted. Clearly, a contracted edge edge must be incident to two white faces. By contracting one edge incident to two white faces, the number of white faces decreases by two and the number of inner vertices by one. Thus, in the resulting graph, the number of white faces exceeds the number of inner vertices by $k-1$. By induction, at least k edges must be contracted in order to obtain a graph where the number of white faces does not exceed the number of inner vertices. ◀

In the remainder we call an edge incident to two white faces a *contractible* edge. To arrive at a contradiction, we will argue that none of the contractible edges is contracted in a realizing drawing. The following property is a helpful argument.

▶ **Lemma 3.27.** *Let T be a plane triangulation with an area assignment $\mathcal{A}$ and let C be a simple cycle of T. If some face in the interior of C is assigned to a positive area in $\mathcal{A}$, then in every $\mathcal{A}$-realizing drawing of T at most $|C|-3$ edges are contracted.*

Proof. Since a triangle is the smallest polygon of positive area, the interior of C must be bounded by at least three edges. ◀

To study the triangulations on up to ten vertices, we introduce the following notation. Usually, every planar graph has several plane graphs which are not equivalent. For $\alpha \in \{a, b, c, \dots\}$, we write $\mathcal{G}_{10\alpha}$ to refer to a planar graph on ten vertices. When referring to a plane graph, we add i to represent the ith plane graph $\mathcal{G}_{10\alpha,i}$ in the ordering of our figures. Moreover, we represent the set of all plane graphs by $[\mathcal{G}_{10\alpha}]$ or $[\mathcal{G}_{10\alpha,i}]$. In our figures, we indicate area-universality by a checkmark and non-area-universality by a cross. Additionally, for non-area-universal graphs a non-realizable area assignment is depicted by a face coloring.

3.3.1 Triangulations on up to Eight Vertices

By Proposition 2.11, we may restrict our attention to 4-connected triangulations. As we will see, all of these triangulations on up to eight vertices are either Eulerian triangulations or accordion graphs. Consequently, they can be fully characterized by our results in the previous sections, namely by Theorems 5 and 10.

The octahedron graph is the smallest 4-connected triangulation and has six vertices. Therefore, all triangulations on up to five vertices are area-universal. As discussed in Section 3.1.1, the octahedron graph is Eulerian and hence not area-universal by Theorem 5.

On seven vertices there also exists exactly one 4-connected triangulation, namely the right graph depicted in Figure 3.21. As mentioned before, it is the odd accordion graph $\mathcal{K}_1$ and therefore area-universal by Theorem 10.

Figure 3.21: The unique plane 4-connected triangulations on six and seven vertices.

There are three plane 4-connected triangulations on eight vertices; for a depiction see Figure 3.22. They belong to the two planar graphs $\mathcal{G}_{8a}$ and $\mathcal{G}_{8b}$. The plane graph $\mathcal{G}_{8a,1}$, see left graph in Figure 3.22, is Eulerian, and therefore, it is not area-universal by Theorem 5. As already indicated by the notation $\mathcal{G}_{8b,1}$ and $\mathcal{G}_{8b,2}$, depicted in the middle and right of Figure 3.22, are different embeddings of the same planar graph. Note that $\mathcal{G}_{8b,1}$ is isomorphic to the double stacking graph $\mathcal{H}_{2,2}$. Consequently, Theorem 11 guarantees the area-universality of all plane graphs in $[\mathcal{H}_{2,2}] = [\mathcal{G}_{8b,1}]$.

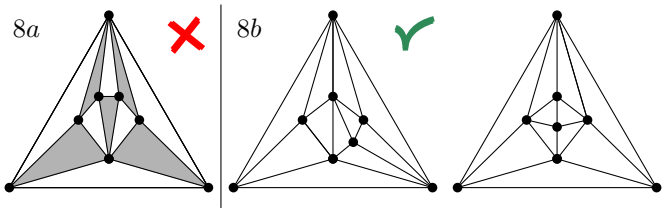

Figure 3.22: The three plane 4-connected triangulations on eight vertices.

In a nutshell, we can formulate our findings as follows:

▶ **Proposition 3.28.** *Let T be a triangulation on up to eight vertices. Then T is area-universal if and only if T does not contain an Eulerian triangulation as a subgraph.*

Proof. If T contains an Eulerian triangulation, then by Theorem 5 and Lemma 2.2, T is not area-universal.

Now assume T does not contain an Eulerian triangulation as a subgraph. By Proposition 2.11, T is area-universal if and only if all of its 4-connected components are. As our analysis shows, the only non-area-universal triangulations on up to eight vertices are the two Eulerian triangulations on six and eight vertices. Consequently, T is area-universal. ◀

We now continue our classification for triangulations on nine and ten vertices.

3.3.2 Triangulations on Nine Vertices

Figure 3.23 presents the 4-connected triangulations on nine vertices. The 13 plane triangulations belong to the four different planar graphs, which we refer to by $\mathcal{G}_{9a}, \mathcal{G}_{9b}, \mathcal{G}_{9c}$ and $\mathcal{G}_{9d}$. As explained before, we denote one of these plane graphs by $\mathcal{G}_{9\alpha,i}$ where i refers to the ith plane graph in Figure 3.23. For instance, there exist the plane graph $\mathcal{G}_{9b,i}$ for all $i \in [4]$.

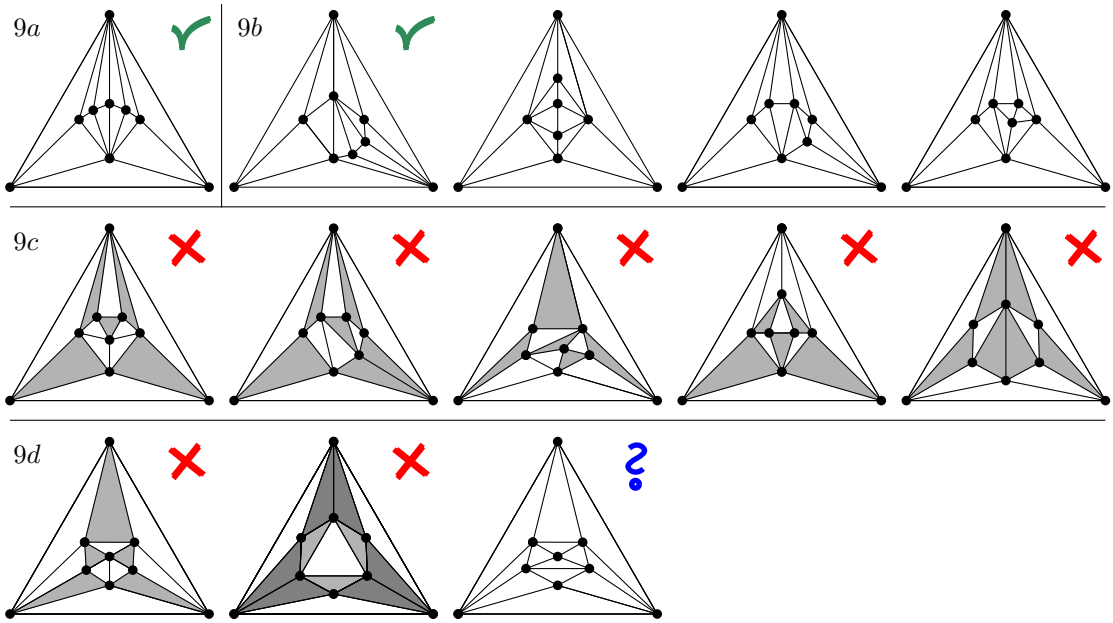

Figure 3.23: The 4-connected triangulations on nine vertices.

Note that the plane graphs of $[\mathcal{G}_{9d}]$, which we introduced in the introduction, are the smallest triangulations without p-orders. The following theorem classifies the area-universality of 4-connected triangulations on nine vertices except for $\mathcal{G}_{9d,3}$.

■ **Theorem 14.** *For the plane 4-connected triangulations on nine vertices it holds:*
(i) The plane triangulation $\mathcal{G}_{9a,1}$ is area-universal.
(ii) All plane triangulations in $[\mathcal{G}_{9b}]$ are area-universal.
(iii) All plane triangulations in $[\mathcal{G}_{9c}]$ are not area-universal.
(iv) The plane triangulations $\mathcal{G}_{9d,1}$ and $\mathcal{G}_{9d,2}$ are not area-universal.

We remark that the non-area-universality of $\mathcal{G}_{9c,5}$ has also been shown by Manfred Scheucher answering our question posed at EuroCG 2017 [Scheucher, 2017].

Proof. The plane triangulation $\mathcal{G}_{9a,1}$ is the odd accordion graph $\mathcal{K}_3$ and thus area-universal by Theorem 10. The plane triangulation $\mathcal{G}_{9b,1}$ is isomorphic to the double stacking graph $\mathcal{H}_{2,3}$. Therefore, the plane graphs in $[\mathcal{G}_{9b}]$ are area-universal by Theorem 11.

With the exception of $\mathcal{G}_{9d,3}$, we show that the remaining plane graphs $\mathcal{G}_{9c,i}$ and $\mathcal{G}_{9d,i}$ are not area-universal. We unify the argument for $\mathcal{G}_{9c,i}$ and $i \in \{1,2,3,4\}$. For a contradiction, we suppose that the white/gray area assignment $\mathcal{A}$, depicted in Figure 3.24, has a realizing drawing D. The number of white faces in $\mathcal{A}$ exceeds the number of inner vertices by two and each vertex is incident to both white and gray faces. Consequently, Lemma 3.26 ensures that D has at least two contracted edges. Moreover, it has three contractible edges; we color one orange and the other two cyan as shown in Figure 3.24. Contracting the orange

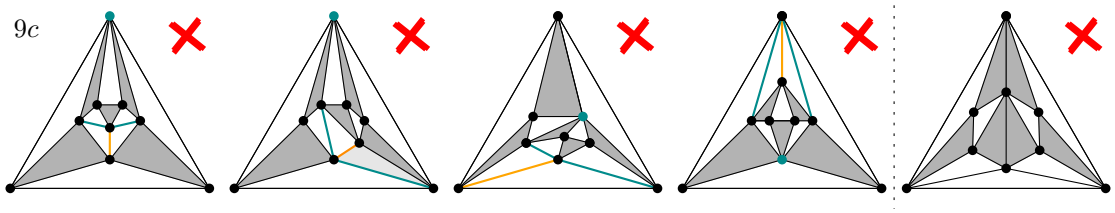

Figure 3.24: The five plane graphs of $\mathcal{G}_{9c}$ are not area-universal.

edge results in the Eulerian triangulation on eight vertices with an inner face 2-coloring as in the proof of Theorem 5. Therefore, it is not realizable. Consequently, the orange edge is not contracted in D but both of the cyan edges are. However, the two cyan edges and two edges incident to the cyan vertex form a 4-cycle C. Since the interior of C has positive area, not both cyan edges are contracted in D by Lemma 3.27. Thus, we obtain a contradiction proving that $\mathcal{G}_{9c,i}$, $i \in \{1, 2, 3, 4\}$, is not area-universal.

The white/gray area assignment of $\mathcal{G}_{9c,5}$ given in Figure 3.24 has seven white face, six inner vertices and two contractible edges. By Lemma 3.26, a realizing drawing contains a contracted edge. By symmetry, it suffices to consider one of the two contractible edge. Its contraction results in the graph depicted in Figure 3.25(a) which contains the octahedron. The induced area assignment of the octahedron is the $(0, 1, 3)$-assignment displayed in Figure 3.25(a).

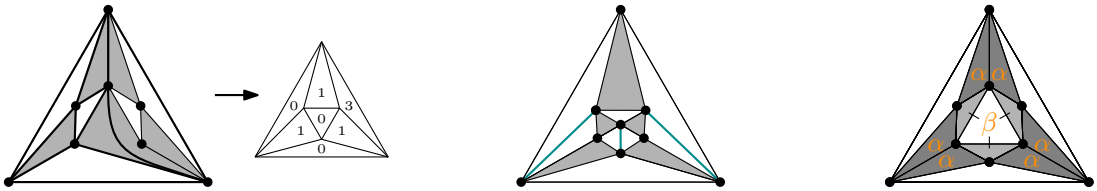

(a) Contraction of one edge in $\mathcal{G}_{9c,5}$ induces a $(0, 1, 3)$-assignment of the octahedron.

(b) $\mathcal{G}_{9d,1}$

(c) $\mathcal{G}_{9d,2}$

Figure 3.25: Illustration of the proof that $\mathcal{G}_{9c,5}$, $\mathcal{G}_{9d,1}$, and $\mathcal{G}_{9d,2}$ are not area-universal.

The following lemma shows that this area assignment of the octahedron is not realizable. It gives a more general statement on a $(0, \alpha, \beta, \gamma)$-assignment displayed in Figure 3.26(a). Here, we are interested in the case $\alpha = \beta = \gamma$.

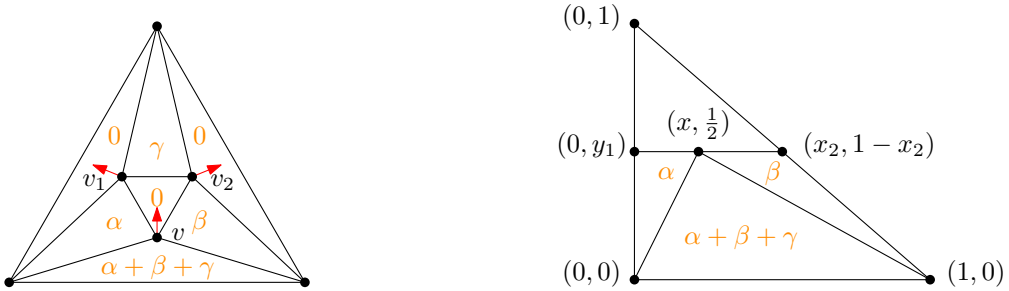

(a) The $(0, \alpha, \beta, \gamma)$-assignment.

(b) Structure of a realizing drawing.

Figure 3.26: Illustration of Lemma 3.29 and its proof.

▶ **Lemma 3.29.** *The $(0, \alpha, \beta, \gamma)$-assignment of the octahedron graph is not realizable if*

$$\gamma(\alpha + \beta + \gamma) < 8\alpha\beta.$$

In particular, it is not realizable for $\alpha = \beta = \gamma$.

Proof. Consider Figure 3.26 and suppose without loss of generality that $4(\alpha + \beta + \gamma) = 1$. Suppose, for a contradiction, that there exists an $\mathcal{A}$-realizing drawing D within the right triangle with corners $(0, 0)$, $(1, 0)$, and $(0, 1)$. Moreover, there exists a unique flat angle assignment forcing three collinear triples.

Let f denote the face of area β, we show that $\text{AEQ}(T, \mathcal{A}, F - f)$ has no real solution. In D, vertex v is placed on the line $y = \frac{1}{2}$. For each vertex, one coordinate remains to be determined; we denote the variables by x, y_1, x_2 as depicted. The remaining equations of $\text{AEQ}(T, \mathcal{A}, F - f)$ read as follows:

$$\begin{aligned} \det(A, v, v_1) = 2\alpha &\implies y_1 = \frac{2\alpha}{x} \\ \det(v_1, v_2, C) = 2\gamma &\implies x_2 = \frac{2\gamma}{1 - y_1} \\ \det(v_1, v, v_2) = 0 &\implies -y_1(x - x_2) - x_2(x + 1/2) + x = 0 \end{aligned}$$

Replacing the variables y_1 and x_2 in the third equation with the help of the first two equations, we obtain the equality:

$$\begin{aligned} & 0 = (2\gamma - 1)x^2 + x(4\alpha + \gamma) - 4\alpha(\alpha + \gamma) \\ \iff\ & x = \frac{1}{2 - 4\gamma}\left(4\alpha + \gamma \pm \sqrt{\gamma(\gamma + 8\alpha(4\alpha + 4\gamma - 1))}\right). \end{aligned}$$

Therefore, x is a real number if and only if $\gamma + 8\alpha(4\alpha + 4\gamma - 1) \geq 0$. Using the fact that $4(\alpha + \beta + \gamma) = 1$, we obtain the necessary condition that $\gamma \geq 8\alpha(4\beta)$. For an arbitrary total area, the constraint translates to $\gamma(\alpha + \beta + \gamma) \geq 8\alpha\beta$. This shows the claim. ◀

Finally, we turn our attention to the plane graphs of $\mathcal{G}_{9d}$. We start to show that $\mathcal{G}_{9d,1}$ is not area-universal. Note that in the white/gray area assignment displayed in Figures 3.23 and 3.25(b), the number of white faces exceeds the number of inner vertices by two and that every inner vertex is incident to a gray face. By Lemma 3.26 at least two contractible edges are contracted. Figure 3.25(b) displays the contractible edges in cyan. Note that every pair of contractible edges forms a 4-cycle whose interior has positive area. Hence, by Lemma 3.27, at most one contractible edge is contracted in a realizing drawing. This contradiction shows that $\mathcal{G}_{9d,1}$ is not area-universal.

For the plane graph $\mathcal{G}_{9d,2}$, computer search asserts that all area assignments consisting of 0 and 1 are realizable [Heinrich, 2018]. However, the area assignment depicted in Figure 3.25(c) is not realizable for $\alpha = 2\beta$. Unfortunately, we have no geometric argument to show this. However, Mathematica ensures that there is no real solution of the equation system $\text{AEQ}(T, \mathcal{A}, F')$. Thus, by Theorem 4, $\mathcal{G}_{9d,2}$ is not area-universal. ■

The last observation on $\mathcal{G}_{9d,2}$ shows that it is not sufficient to consider 01-assignments.

■ **Corollary 15.** *Area-universality cannot be tested by checking every 01-area assignment.*

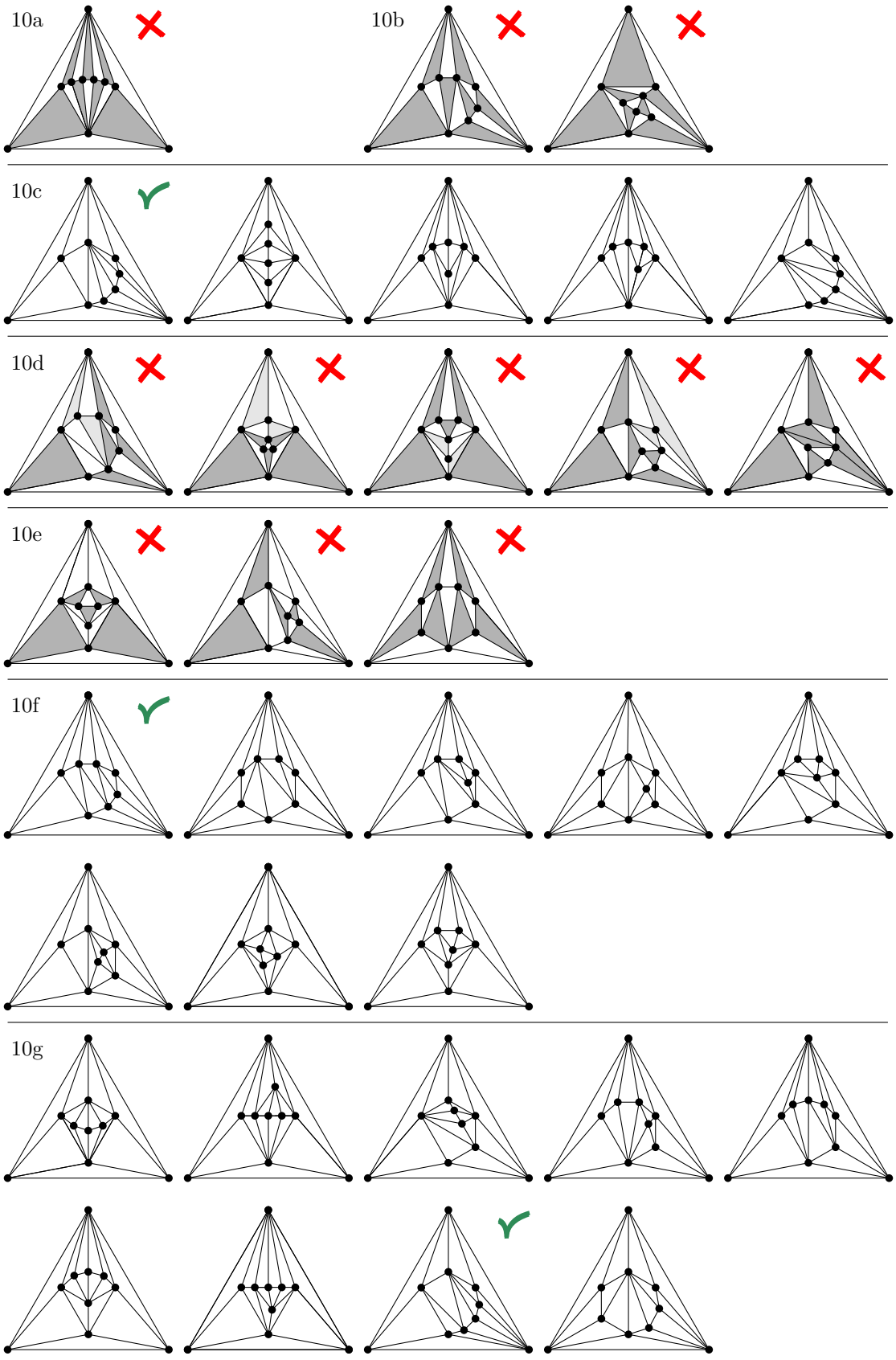

Figure 3.27: The 4-connected triangulations on ten vertices with a p-order.

3.3.3 Triangulations on Ten Vertices

There exist 47 plane 4-connected triangulations on ten vertices. They belong to ten different planar graphs. Seven of these have a p-order; we call them $\mathcal{G}_{10\alpha}$ for $\alpha \in \{a, b, \ldots, g\}$. Their 33 plane graphs are displayed in Figure 3.27. The remaining three planar graphs, which we call $\mathcal{G}_{10\alpha}$ with $\alpha \in \{i, j, k\}$, have no p-order and Figure 3.33 presents their 14 plane graphs. The following theorem fully characterizes the area-universality of the triangulations with p-orders.

■ **Theorem 16.** *For the plane 4-connected triangulations on ten vertices with a p-order the following holds:*

(i) The plane graph of $[\mathcal{G}_{10a}]$ *is not area-universal.*
(ii) All plane graphs of $[\mathcal{G}_{10b}]$ *are not area-universal.*
(iii) All plane graphs of $[\mathcal{G}_{10c}]$ *are area-universal.*
(iv) All plane graphs of $[\mathcal{G}_{10d}]$ *are not area-universal.*
(v) All plane graphs of $[\mathcal{G}_{10e}]$ *are not area-universal.*
(vi) All plane graphs of $[\mathcal{G}_{10f}]$ *are area-universal.*
(vii) All plane graphs of $[\mathcal{G}_{10g}]$ *are area-universal.*

Proof. As indicated by the inner face 2-coloring in Figure 3.27, the planar graphs $\mathcal{G}_{10a}$ and $\mathcal{G}_{10b}$ are Eulerian triangulations and thus not area-universal by Theorem 5. Since $\mathcal{G}_{10c,1}$ is the double stacking graph $\mathcal{H}_{2,4}$, Theorem 11 shows that all plane triangulations in $[\mathcal{G}_{10c,1}]$ are area-universal.

Next, we show that no plane graph $\mathcal{G}_{10d,i}$ is area-universal. In order to have less contractible edges and thus fewer cases to analyze, we assign the light gray faces in Figure 3.27 to an area of small $\varepsilon > 0$; as before white faces are assigned to an area of 0 and gray faces to 1. In fact, the area assignment where light faces have area 0 remains not realizable by Corollary 3. We start to show that $\mathcal{G}_{10d,1}$ is not area-universal: The number of white faces exceeds the number of inner vertices. Hence, by Lemma 3.26, in a realizing drawing an edge is contracted. Indeed, there exists a unique contractible edge. Its contraction yields the graph depicted in Figure 3.28(a) which contains the octahedron graph with a $(0, 1, \varepsilon)$-assignment. By Theorem 5 and Corollary 3, this area assignment is not realizable for small enough $\varepsilon > 0$. Consequently, $\mathcal{G}_{10d,1}$ is not area-universal.

After coloring the outer face of $\mathcal{G}_{10d,1}$ gray, this argument is applicable for all plane graphs of $[\mathcal{G}_{10d}]$ in which the outer face corresponds to a gray face of $\mathcal{G}_{10d,1}$, namely for the graphs $\mathcal{G}_{10d,i}$ with $i \in [4]$. To see this, consider the octahedron subgraph after contraction of the contractible edge. In the induced area assignment only two faces play a special role; one has area 2ε and the other face contains three gray faces one of which may be the outer face. By Proposition 3.3 and Corollary 3, this area assignment is not realizable if a gray face

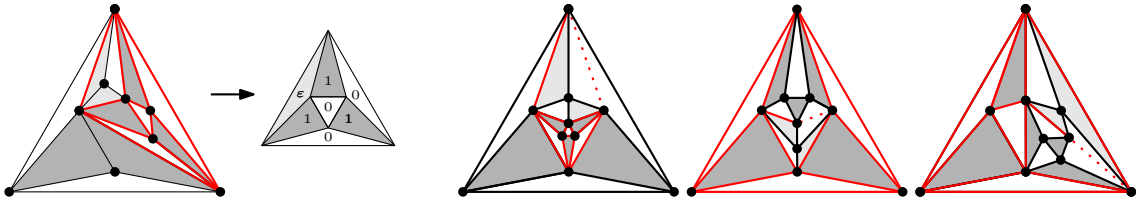

(a) $\mathcal{G}_{10d,1}$ (b) $\mathcal{G}_{10d,i}$ for $i \in \{2, 3, 4\}$

Figure 3.28: Non-area-universality of $\mathcal{G}_{10d,i}$ for $i \leq 4$.

is an outer face. [In case, you want to convince yourself by hand, consult Figure 3.28(b).]

It remains to analyze the plane graph $\mathcal{G}_{10d,5}$. Consider the depicted white/gray area assignment in Figure 3.29(a). It has eight white faces and seven inner vertices. Therefore, by Lemma 3.26, at least one edge must be contracted; we color one cyan and the other orange. Contracting either one of the possible edges, we obtain a $(0, 1, 3)$-assignment of the octahedron as depicted in Figures 3.29(b) and 3.29(c). Lemma 3.29 guarantees that this area assignment of the octahedron is not realizable. Therefore, $\mathcal{G}_{10d,5}$ is not area-universal. This finishes our analysis of $\mathcal{G}_{10d}$.

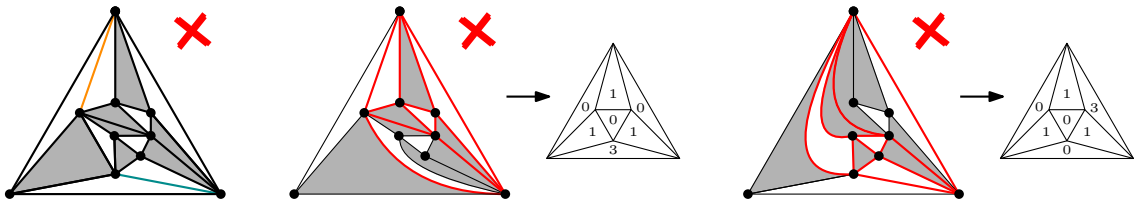

(a) $\mathcal{G}_{10d,5}$ (b) Contraction of the cyan edge. (c) Contraction of the orange edge.

Figure 3.29: The plane graph $\mathcal{G}_{10d,5}$ after contraction of a contractible edge.

Now, we turn our attention to $\mathcal{G}_{10e}$. The plane graphs $\mathcal{G}_{10e,1}$ and $\mathcal{G}_{10e,2}$ can be handled by the same argument. The area assignments depicted in Figures 3.30(a) and 3.30(b) have six contractible edges. We color two of them orange, two cyan and two blue as illustrated. Suppose, for a contradiction, that there exists a realizing drawing D. Since the number of white faces exceeds the number of inner vertices by three, at least three edges must be contracted in D by Lemma 3.26. Note that the orange and cyan edges from a 4-cycle with positive area. Thus at most one of these edges is contracted in D. Consequently, both blue edges are contracted in D. However, their contraction results in an inner face 2-coloring of the Eulerian triangulation on eight vertices and we obtain the final contradiction. Thus, neither $\mathcal{G}_{10e,1}$ nor $\mathcal{G}_{10e,2}$ are area-universal.

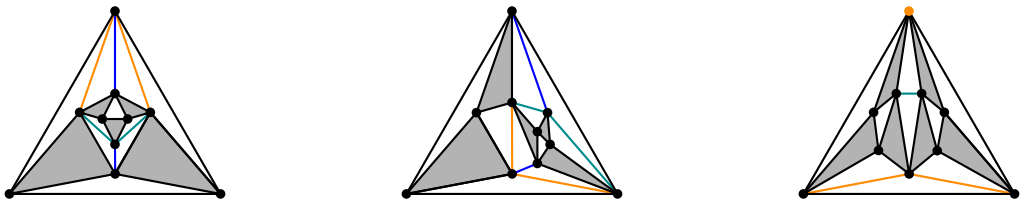

(a) $\mathcal{G}_{10e,1}$ (b) $\mathcal{G}_{10e,2}$ (c) $\mathcal{G}_{10e,3}$

Figure 3.30: No plane graph of $\mathcal{G}_{10e}$ is area-universal.

The area assignment of $\mathcal{G}_{10e,3}$ allows for three contractible edges; two of which we color orange and one of which we color cyan, see also Figure 3.30. Contraction of the cyan edge results in the non-realizable area assignment of $\mathcal{G}_{9c,5}$. Therefore, the cyan edge is not contracted in a realizing drawing D. Since the number of white faces exceeds the number of inner vertices by two, both orange edges are contracted in D. However, the orange edges form a 4-cycle together with the non-incident outer vertex which is highlighted in orange. Since the interior of the 4-cycle has positive area, this yields contradiction and shows that $\mathcal{G}_{9c,5}$ is not area-universal. Consequently, no plane graph in $[\mathcal{G}_{9c}]$ is area-universal.

Now, we consider the plane graphs of $\mathcal{G}_{10f}$. First, we show that $\mathcal{G}_{10f,1}$ is area-universal with the p-order depicted in Figure 3.31. We place v_3 at $(1,1)$ and use a computer algebra system to determine the degrees of the crr-free vertex coordinates, see Table 3.1.

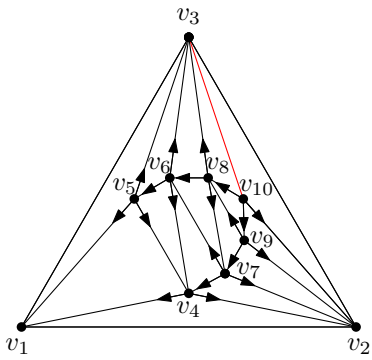

Figure 3.31: A p-order of $\mathcal{G}_{10f,1}$.

Table 3.1: Degrees of vertex coordinates.

i	$\lvert\mathcal{N}_i^x\rvert$	$\lvert\mathcal{N}_i^y\rvert$	$\lvert\mathcal{D}_i\rvert$
4	1	0	0
5	1	0	1
6	2	1	2
7	3	2	2
8	5	4	5
9	8	7	7
10	13	12	12

Choosing the triangle $v_2v_3v_{10}$ as the last face, the last face function evaluates to

$$\mathfrak{f}(x_4) := \det(v_2, v_3, v_{10}) = 1 - x_{10} = 1 - \frac{\mathcal{N}_{10}^x}{\mathcal{D}_{10}}.$$

Since $|\mathcal{N}_{10}^x| = 13 > 12 = |\mathcal{D}_{10}|$ and $|\mathcal{N}_{10}^x|$ is odd, and the last face function $\mathfrak{f}$ is almost surjective by Lemma 3.17. Thus, Corollary 9 implies the area-universality of $\mathcal{G}_{10f,i}$ for all i.

Finally, it remains to consider $\mathcal{G}_{10g}$ and we start with $\mathcal{G}_{10g,8}$ with the p-order displayed in Figure 3.32. We place v_3 at $(1,1)$ and use a computer algebra system to compute the degrees of the crr-free polynomials. The results are summarized in Table 3.2.

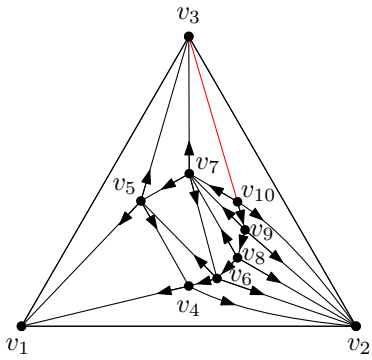

Figure 3.32: A p-order of $\mathcal{G}_{10g,8}$.

Table 3.2: Degrees of vertex coordinates.

i	$\mathcal{N}_i^x$	$\mathcal{N}_i^y$	$\mathcal{D}_i$
4	1	0	0
5	1	0	1
6	2	1	1
7	3	2	3
8	5	4	4
9	8	7	7
10	11	10	10

With triangle $v_2v_3v_{10}$ as the last face, we obtain the last face function

$$\mathfrak{f}(x_4) := \det(v_2, v_3, v_{10}) = 1 - x_{10} = 1 - \frac{\mathcal{N}_{10}^x}{\mathcal{D}_{10}}.$$

Since $|\mathcal{N}_{10}^x| = 11 > 10 = |\mathcal{D}_{10}|$, the last face function $\mathfrak{f}$ has odd max-degree and is almost surjective by Lemma 3.17. Thus, Corollary 9 implies the area-universality of the plane graphs of $\mathcal{G}_{10g,i}$ for all i. This finishes our analysis of the 4-connected triangulations with a p-order on ten vertices. ■

Observe that our developed methods enabled us to completely characterize the area-universality of all 4-connected triangulations with a p-order on up to ten vertices. Unfortunately, this is not the case for the triangulations without a p-order. There exist 14 plane 4-connected triangulations on ten vertices without a p-order. They belong to the three planar graphs $\mathcal{G}_{10h}, \mathcal{G}_{10i}$, and $\mathcal{G}_{10j}$. For an illustration consider Figure 3.33. Heinrich's computer search asserts that all of these plane graphs are 01-*universal*, that is all of their 01-assignments are realizable [Heinrich, 2018]. However, we have no tool to prove their area-universality nor did we find other non-realizable assignments.

¿ Question ? : Which of the 4-connected triangulation on ten vertices without a p-order are area-universal?

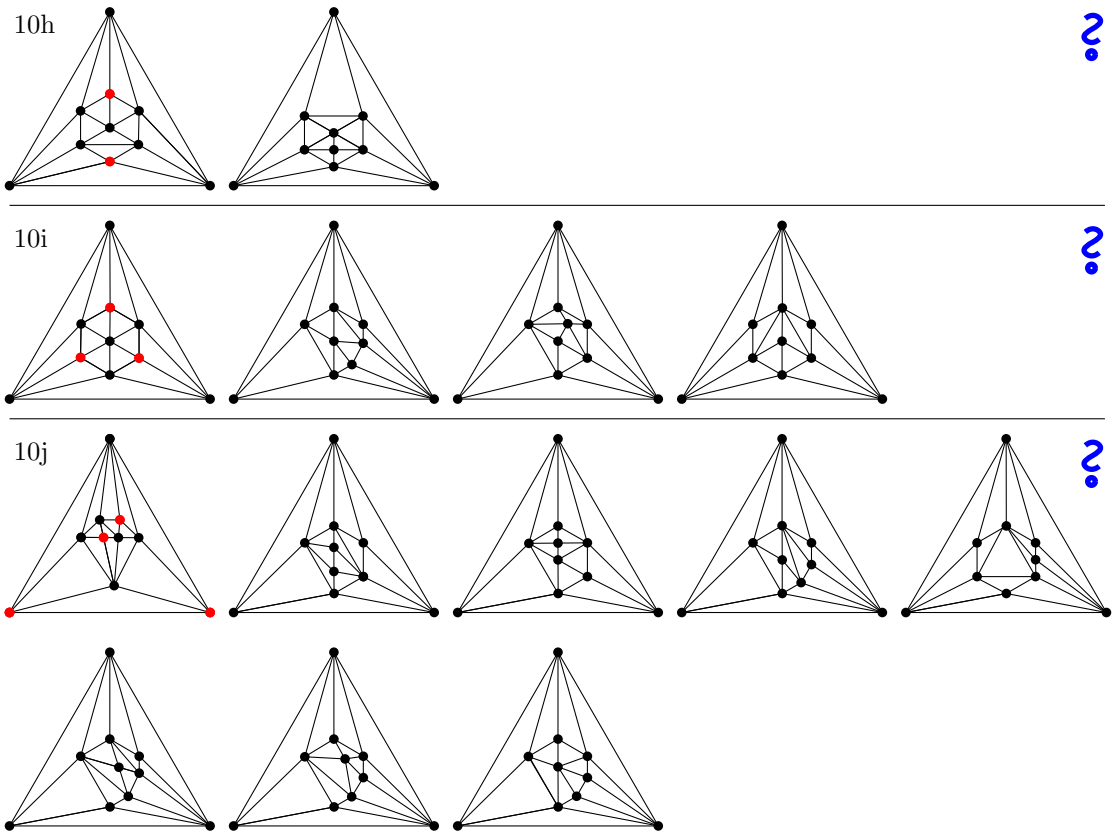

Figure 3.33: Plane graphs on ten vertices without a p-order. Their status is open.

Remark. It is easy to check that these triangulations have no p-order by considering the vertices of degree four. In Figure 3.33, the vertices of degree four are highlighted in red for one plane graph of each class. Recall that, by Lemma 3.8, triangulations with a p-order have an edge such that its removal results in a 3-degenerate graph. Thus, for the existence of a p-order in a 4-connected triangulation T, it is necessary that T contains two neighboring vertices of degree 4. This immediately shows that $\mathcal{G}_{10h}$ and $\mathcal{G}_{10i}$ have no p-order. Moreover, $\mathcal{G}_{10j}$ has a unique candidate edge, namely the one incident to the two vertices of degree four. However, removing it and its neighbors, results in a graph with minimum degree four.

3.3.4 Summary of Gained Insights from Small Triangulations

We summarize our findings and end with conclusions drawn from our characterization of small triangulations. First of all, it is evident that we found no example where two embeddings of the same planar graph behave differently, i.e., we do not know of a graph where one embedding is area-universal and another is not. This enforces the following question:

¿ Question ? : Is area-universality a property of planar graphs rather than plane graphs?

For graphs with p-orders, we have indeed seen that if the last face function is almost surjective for one plane graph then this holds true for all embeddings. Therefore, if some embedding of a planar graph fulfills the conditions of Corollary 9, the area-universality of all embeddings follows. Consequently, an example, showing that area-universality is a property of plane graphs, either belongs to a planar triangulation without a p-order, or to a planar graph such that the last face function of all p-orders is not almost surjective – even though at least one embedding is area-universal.

Studying the area-universality of $\mathcal{G}_{9d,2}$, we learned that area-universality cannot be tested by checking all 01-area assignment. Recall that Heinrich [Heinrich, 2018] tested all 01-assignments by numerically solving the area equation systems with Bertini. However, $\mathcal{G}_{9d,2}$ has an 012-assignment which is not realizable.

Conclusion. 01-*universality does not imply area-universality.*

Interestingly, computer search suggests that every plane triangulations on ten vertices with a p-order is 01-universal. However, this does not hold in general since we proved the non-area-universality of $\mathcal{G}_{9d,1}$ with the help of a non-realizable 01-assignment in Theorem 14. Moreover, we can say that the p-order is no indicator of area-universality since there exists area-universal and non-area-universal graphs with a p-order.

Furthermore, as shown in Corollary 12 and Corollary 13 for all n there exists a 4-connected triangulation which is area-universal as well as one that is not area-universal. We say a graph is *near 3-degenerate*, if there exists an edge, such that after its deletion the graph is 3-degenerate. Thus, the following fact holds:

Conclusion. *None of the following is a sufficient criterion for area-universality of plane graphs, not even for triangulations:*

- *high-connectivity (4 and 5)*
- *parity of the number of vertices*
- *near-3-degeneracy*

Interestingly, all known area-universal graphs are *near 3-degenerate*, that is, there exists an edge, such that after its deletion the graph is 3-degenerate. This holds true for subgraphs of stacked triangulations, plane cubic graphs, double stacking graphs, as well as graphs with p-orders. Therefore, we wonder if near-3-degeneracy is a necessary condition for area-universality.

¿ Question ? : Are all area-universal graphs near-3-degenerate?

To answer this question in the negative, new tools must be developed.

3.3.5 Excursus to Near-Triangulations

Up until now, every non-area-universal graph contains a non-area-universal triangulation as a subgraph. In this section, we make a small excursus to inner triangulations. An *inner triangulation* is a plane 2-connected graph in which every inner face is a triangle. Deleting an outer edge of a triangulation, results in a *near-triangulation*, i.e., an inner triangulation where the outer face has degree four. Here we discuss the following question:

¿ Question ? : Is every near-triangulation without separating triangles area-universal?

We are able to answer the question in the negative with the help of a relative of $\mathcal{G}_{9c,4}$. In fact, we may remove one edge from $\mathcal{G}_{9c,4}$ and the resulting graph remains to be not area-universal.

▶ **Proposition 3.30.** *The graph $\mathcal{G}_{9c,4}$ has an edge e such that $\mathcal{G}_{9c,4}-e$ is not area-universal.*

Proof. Figure 3.34(a) depicts the plane graph $\mathcal{G}_{9c,4}$ with one deleted edge. We show that the illustrated white/gray area assignment of this graph G is not realizable. For a contradiction, suppose there exists a realizing drawing. Note that the area assignment has two symmetric contractible edges. By contracting the right contractible edge, we obtain the graph G' and the area assignment displayed in Figure 3.34(b). Since it contains an octahedron graph with a non-realizable area assignment by Theorem 5, no edge is contracted in D. Thus, due to the six white triangular faces and six inner vertices, there exists a unique flat angle assignment. Figure 3.34(c) illustrates a drawing respecting the flat angles. It is easy to see, that the white convex quadrilateral has vanishing area if and only if the vertices on the outer segments are placed on the top outer vertex. However, this placement corresponds to the contraction of the contractible edges. This is a contradiction and shows that $\mathcal{G}_{9c,4}-e$ is not area-universal. ◀

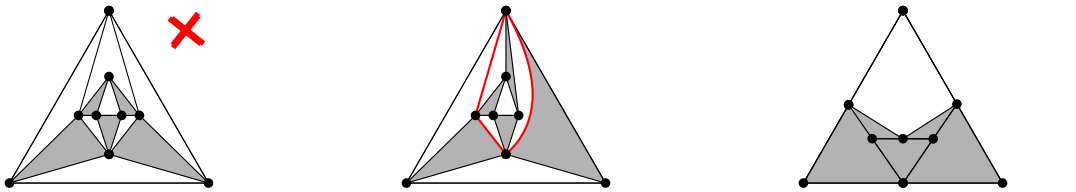

(a) The plane $\mathcal{G}_{9c,4}-e$.

(b) $\mathcal{G}_{9c,4}-e$ after contraction contains the octahedron.

(c) A drawing of $\mathcal{G}_{9c,4}-e$ with realized flat angles.

Figure 3.34: Illustration of Proposition 3.30 and its proof.

With this example at hand, the non-equivalent plane graph of $\mathcal{G}_{9c}-e$ where the 4-face is the outer face is of special interest. Figure 3.35(a) depicts this graph, which we refer to as the *butterfly graph*. The butterfly graph is either area-universal providing us with a certificate that area-universality is a property of plane graphs or it is not area-universal and thus, answering the above question in the negative. As it turns out, the butterfly graph is not area-universal. In particular, this is the first non-area-universal planar graph which is not a triangulation – or does not contain a non-area-universal triangulation as a subgraph.

▶ **Proposition 3.31.** *The butterfly graph is not area-universal.*

Proof. Let $\mathcal{A}$ denote the white/gray area assignment depicted in Figure 3.35(a). First, we argue that an $\mathcal{A}$-realizing drawing has no contracted edge. Note that every contractible

(a) The butterfly graph.

(b) The butterfly graph with one contracted outer edge.

Figure 3.35: Illustration of Proposition 3.31 and its proof.

edge of the butterfly graph is an outer edge. By symmetry, it is sufficient to consider one outer edge. Contracting the right outer edges results in the graph depicted in Figure 3.35(b). This induces a $\{0, 1, 3\}$-assignment of the octahedron graph which is not realizable by Lemma 3.29. At this point, we do offer a nice geometric proof that the area assignment is not realizable. However, it is easy to check with a computer algebra system that the equation system $\text{AEQ}(T, \mathcal{A}, F')$ has no real solution. Thus, the area assignment is not realizable by Theorem 4. ◀

In fact, the butterfly graph is a smallest non-area-universal near-triangulation. To see this we show that 3-degenerate near-triangulations are area-universal. Recall that a graph is 3-degenerate if and only if it has an ordering of its vertices $v_1, v_2, \ldots, v_n$ such that v_i has degree at most three in the subgraph induced by $v_1, v_2, \ldots, v_i$. Moreover, a triangulation is 3-degenerate if and only if it is a stacked triangulation. Consequently, we have seen already that 3-degenerate triangulations are area-universal in Observation 1.1. This property generalizes to 3-degenerate near-triangulations.

■ **Theorem 17.** *Every plane 3-degenerate near-triangulation T is area-universal.*

Proof. We show that every area assignment $\mathcal{A}$ of T is realizable. To do so, we first argue that we may assume that T has no separating triangle: Suppose that T contains a separating triangle t. Let T_{I} and T_{E} denote the two plane graphs obtained by decomposing T along t. Then T_{I} is a stacked triangulation and thus area-universal by Observation 1.1. Thus, Lemma 2.10 states that T is area-universal if and only if T_{E} is area-universal. Consequently, we assume that T has no separating triangle.

Since T is 3-degenerate, there exists an ordering of the vertices $v_1, v_2, \ldots, v_n$ where v_i has degree at most 3 in T_i, the subgraph of T induced by the vertices $\{v_1, \ldots, v_i\}$.

✱ **Claim 3.32.** *A face of T_i is either a triangle or the outer face.*

Proof. The claim follows from a double counting argument. Let f be an inner face of T_i with degree d. The interior of f in T is an inner triangulation T' with an outer face of degree d. Thus, T' has $3n' - 3 - d$ edges. Since no inner edge of T' belongs to T_i, the interior of T' can be constructed by inserting vertices of degree at most 3. Therefore, T' has at most $3(n' - d) + d = 3n' - 2d$ edges. This holds true only if $d \leq 3$. ◀

The claim implies that the neighbors of v_i in T_i appear consecutive on the boundary of some face in T_{i-1}; otherwise T_i has an inner face which is not a triangle. Moreover, since T contains no separating triangle, it follows immediately that v_i is an outer vertex in T_i. We call the plane graph depicted in Figure 3.36(a) the diamond. For our construction, we make use of the following fact.

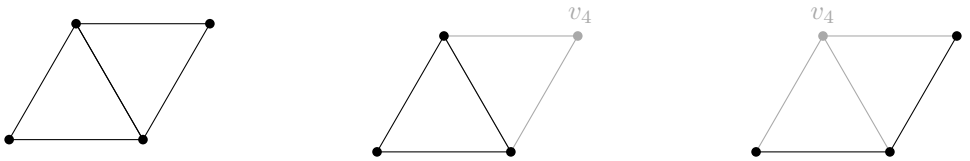

(a) The diamond graph. (b) Case: T_3 is a triangle. (c) Case: T_3 is a path.

Figure 3.36: Illustration of the proof of Claim 3.33.

*** Claim 3.33.** *T_4 is a diamond and for each $i \geq 5$, v_i has three neighbors in T_i.*

Proof. By Euler's formula, a near triangulation has $3n-7$ edges. We associate each edge with the smallest i such that v_i is incident to it. Clearly, the last $n-3$ vertices in the vertex ordering contribute at most $3(n-3)$ edges. Thus, T_3 has two or three edges. Suppose that T_3 is a triangle. By the edge count, there exists a unique vertex v_j which has degree two in T_j while all other vertices v_i with $i > 3$, have degree three in T_i. If $j \neq 4$, then v_4 has degree three and T_4 is isomorphic to K_4. However, K_4 yields a separating triangle and thus a contradiction. Consequently, it holds that $j = 4$ and therefore, T_4 is the diamond graph. This situation is depicted in Figure 3.36(b).

Now suppose that T_3 is a path with two edges. Then, by the edge count, each vertex v_i with $i > 3$, has degree three in T_i. Since T is simple, the middle predecessor of v_4 is the vertex of degree two in T_3. Thus, we obtain that T_4 is the diamond graph. This case is illustrated in Figure 3.36(c). ◀

We are now ready to construct a realizing drawing of T. The idea of the proof is simple. We place T_4 wisely in the plane and argue that we can insert v_i without introducing crossings and such that the two incident triangles in T_i are realized.

For the initial placement of T_4, we may assume, without loss of generality, that the vertices v_1, v_2, v_3 induce a path. We place the vertices of T_4 such that they form a non-convex quadrangle Q_4 with a reflex angle at v_4. Consider also Figure 3.37(a). Moreover, we guarantee that the area of the triangle $v_1v_4v_3$ exceeds ΣA; for instance by placing the vertices as follows: $v_1 = (0, \Sigma\mathcal{A})$, $v_2 = (0,0)$ and $v_3 = (3,0)$. This placement of the vertices guarantees that during our further construction the three predecessors of v_i are not collinear. The boundary of the outer face of T_4 defines the quadrangle Q_4.

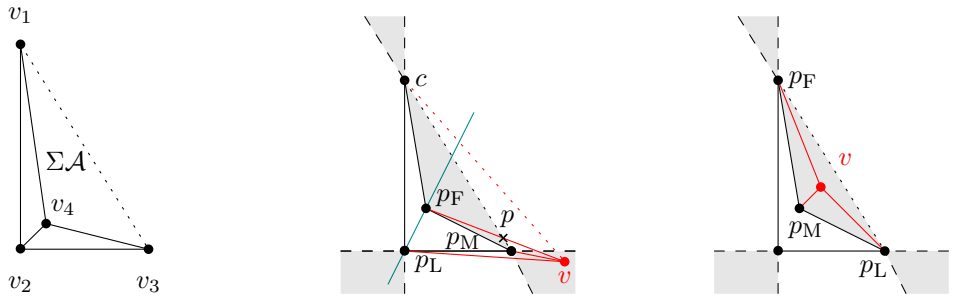

(a) Placement of T_4. (b) p_M is a convex corner. (c) p_M is a reflex corner.

Figure 3.37: Illustration of the construction.

For placing v_{i+1}, suppose that we are given a realizing drawing of T_i which is bounded by a non-convex quadrilateral Q_i with a big reflex angle. We say that the reflex angle of Q_i is *big* if the triangle consisting of the reflex corner and its two neighbors exceeds the area

of all faces that do not belong to T_i but to T. Since Q_i has 3 convex corners and one reflex corner, no three corners are collinear.

Denote the three neighbors of v_{i+1} in T_{i+1} by p_{F}, p_{M}, p_{L} such that they appear in clockwise orientation on the boundary of T_i (and Q_i), as depicted in Figures 3.37(b) and 3.37(c). Clearly, the three neighbors of v_{i+1} are consecutive on the boundary of Q_i. As in Lemma 3.12, we place v_{i+1} in the unique position realizing the area of its two incident inner triangles. Here we use the fact that the three predecessors of v_{i+1} are not collinear. We define Q_{i+1} as the quadrangle Q_i where p_{M} is replaced by v_{i+1}. We have to ensure that the produced drawing of T_{i+1} is crossing-free and that Q_{i+1} is a non-convex quadrilateral with a big reflex angle. Therefore, we distinguish two cases.

Figure 3.37(b) illustrates the case when p_{M} is a convex corner of Q_i. Then vertex v_{i+1} is placed in the intersection of the half spaces which are defined by the segments $p_{\text{F}}p_{\text{M}}$ and $p_{\text{M}}p_{\text{L}}$ and their *outside* with respect to Q_i, respectively. Let c denote the corner of Q_i which does not coincide with a predecessor of v_{i+1}. Clearly, the line through p_{F} and p_{L} separates c and v. Therefore, Q_{i+1} is crossing-free. To show that the reflex angle is still big, it suffices to consider the case that v_{i+1} is adjacent to the vertex with the reflex angle; otherwise the area of the big angle remains. Without loss of generality, we consider the situation depicted in Figure 3.37(b). Note that v_{i+1} is placed outside of the triangle $cp_{\text{F}}p_{\text{M}}$. Let p denote the intersection point of cp_{M} and $p_{\text{F}}v_{i+1}$. Then already the triangle $cp_{\text{F}}p$, which is contained in the triangle $cp_{\text{F}}v_{i+1}$, exceeds the area of all faces that do not belong to T_{i+1} but to T.

If p_{M} is a reflex corner of Q_i, then vertex v_{i+1} is placed within the triangle $p_{\text{F}}p_{\text{M}}p_{\text{L}}$. Moreover, the area of the big angle decreases by exactly the area of the two new triangles. Thus, Q_{i+1} is a non-convex quadrangle with a big reflex angle which is bounding a realizing drawing of T_{i+1}. ■

Now, we are ready to prove our claim.

▶ **Proposition 3.34.** *The butterfly graph is a smallest non-area-universal near-triangulation.*

Proof. By the average degree, every near-triangulation on less than seven vertices is 3-degenerate. However, the smallest near-triangulation which is not 3-degenerate has eight vertices and is depicted in Figure 3.38. As indicated, it is a subgraph of the double stacking graph $\mathcal{H}_{2,2}$ and thus area-universal by Theorem 11. For the four near triangulations on nine vertices, it holds that one is a subgraph of $\mathcal{H}_{2,2}$, one is the non-area-universal butterfly and two have open status. ◀

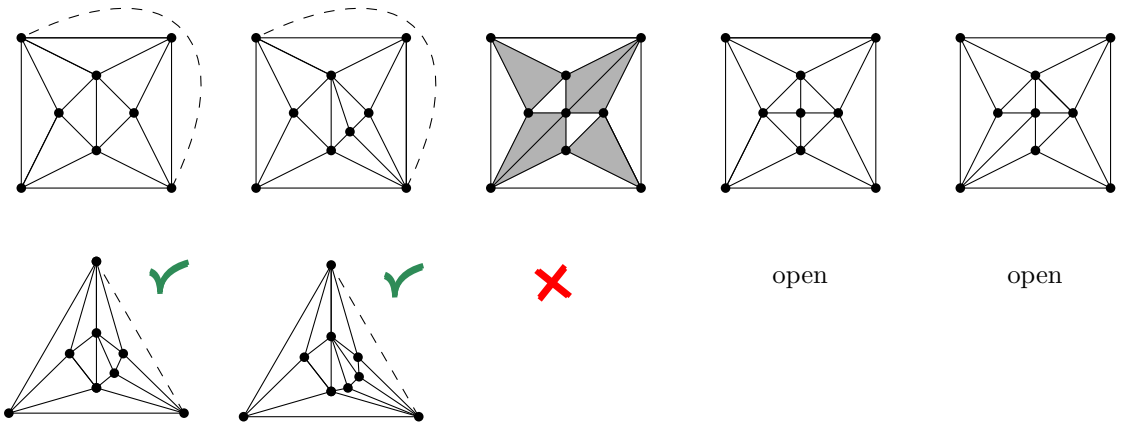

Figure 3.38: The smallest near-triangulations that are not near-3-degenerate.

4 | Quadrangulations

This chapter is based on joint work with William Evans, Stefan Felsner, and Stephen Kobourov. The results will most likely also appear as [Evans et al., 2018]. We study the area-universality of plane quadrangulations, i.e., maximal plane bipartite graphs. In particular, we tackle the following interesting and challenging conjecture:

Conjecture. *Every plane bipartite graphs is area-universal.*

While we do not completely settle this conjecture, we develop methods to prove area-universality via reductions to the area-universality of related graphs. This allows us to establish area-universality for large classes of plane quadrangulations. Our methods are strong enough to prove area-universality of all plane quadrangulations with up to 13 vertices.

We have already introduced operations that preserve area-universality in Chapter 2. In Section 4.1, we use one of these operations, the edge contraction, to show the area-universality of grid graphs and large classes of angle graphs. In Section 4.2, we study strong area-universality, i.e., area-universality within a prescribed outer face, and present strong area-universal graph families. Moreover, we prove area-universality when a graph can be composed into strong area-universal graphs. In Section 4.3, we use the developed tools to show that all quadrangulations with at most 13 vertices are area-universal. Note that we study convex drawings of quadrangulations in Section 6.1.

4.1 Area-Universal Quadrangulations via Edge Contractions

In this section, we discuss some implications of the edge contractions of Lemma 2.3. For the readers convenience, we repeat it here:

▶ **Lemma 2.3.** *Let G be a plane graph which can be transformed into an area-universal plane graph G' by inserting vertices, inserting edges, and performing face-maintaining edge contractions. Then G is area-universal.*

Also recall that an edge contraction is face-maintaining if the number of faces remains, that is at most all but three edges of a face are contracted. We say that a set of edges of a plane graph is *face-independent* if it contains at most one edge per face. If G is a triangle-free plane graph, then every face-independent set of edges is face-maintaining.

In fact, for every quadrangulation there exists a face-maintaining edge contraction to an *inner triangulation*. Clearly, this inner triangulation is not necessarily area-universal.

▶ **Proposition 4.1.** *Every plane quadrangulation Q has a face-maintaining edge contraction to an inner triangulation where the outer face has degree* 3 *or* 4*.*

The proof is based on the following lemma. We call a matching of a graph *near perfect* if it misses at most one vertex.

▶ **Lemma 4.2.** *For a simple plane quadrangulation Q, its dual graph Q^* has a perfect matching if n is even and a near perfect matching if n is odd. In the latter case, there exists a near perfect matching that misses the outer face of Q.*

Proof. Let V, E, and F be the vertices, edges, and faces of Q. Recall that in a quadrangulation with n vertices, Euler's formula implies that Q has $2n-4$ edges, and $n-2$ faces. The proof is based on Tutte's characterization of graphs with perfect matchings: Q^* has a perfect matching if and only if for each set of faces $S \subset F$, the number of connected components with an odd number of vertices in $Q^*[F-S]$ is at most $|S|$. Here $Q^*[F-S]$ denotes the subgraph of Q^* induced by $F-S$.

First we consider the case that Q has an even number of vertices. Let $S \subset F$ be a subset of faces in Q and consider the incidence graph of components in $Q^*[F-S]$ and vertices S in Q^*. If $S = \emptyset$, then there exists exactly one component consisting of all $n-2$ faces. Since n is even, there is no odd component.

Now consider a set $S \neq \emptyset$. Observe that every non-empty set of faces has at least 4 boundary edges. Since Q is simple and bipartite, every cycle is at least of length 4. Therefore, in the incidence graph, the degree of every component is at least 4 and the degree of every face at most 4. Double counting the edges of the incidence graph yields the inequality $4|S| \geq 4|C|$. Consequently, the number of components is at most $|S|$. In particular, the number of odd components is bounded by $|S|$.

Now we consider the case that Q has an odd number of vertices. Let $f_\circ \in F$ be the outer face. We claim that $Q^*[F-f_\circ]$ has a perfect matching. We show that for every subset of faces $S \subset F$ containing $f_\circ$, the number of odd components in $Q^*[F-S]$ is strictly smaller than $|S|$. By the above double counting argument, the number of components is still at most $|S|$. It therefore remains to consider the case of equality where all components are odd. Clearly, the components and S partition of the set of faces. For $k := |S|$, let $C_1, C_2, \ldots, C_k$ be the components. Then it holds that

$$\sum_{i=1}^{k} |C_i| + |S| = n - 2.$$

By assumption, $|C_i|$ is odd for every i. Note that independent of the parity of k, the left hand side has an even number of odd summands and is therefore an even number. This contradicts to the fact that $n-2$ is odd. ◀

With this lemma, we prove the proposition as follows.

Proof of Proposition 4.1. By Lemma 4.2, Q^* has a near perfect matching M^*. Let M denote the edges dual to M^* in Q. Note that every face of Q is incident to at most one edge of M. Hence, M is a set of face-independent edges. Moreover, with the possible exception of the outer face, every face is incident to at least one edge of M. Consequently, contracting the edges of M yields an inner triangulation where the outer face has degree 3 if n is even and 4 if n is odd. ◀

4.1.1 Table Cartograms

As a first application of Lemma 2.3, we show an alternative proof for the area-universality of grid graphs. The *grid* $G(m, n)$ is the Cartesian product $P_m \times P_n$ of paths P_m and P_n on m and n vertices, respectively. Figure 4.1(a) illustrates the grid $G(9, 6)$. Evans et al. [Evans et al., 2017] showed area-universality of grid graphs in the context of *table cartograms* where additionally the outer face is required to be a rectangle. Our new proof does not yield a rectangular outer face. However, it is very simple.

▶ **Proposition 4.3.** *The grid graph $G(m, n)$ is area-universal.*

Proof. Figure 4.1 illustrates the proof for the case that n even. We contract the edges of every second column of $G(m, n)$ to a *super vertex*. The super vertices are labeled by $1, \ldots, k$ from left to right. Then, we add vertices and edges to enhance the resulting graph to a triangulation G as depicted in Figure 4.1(b).

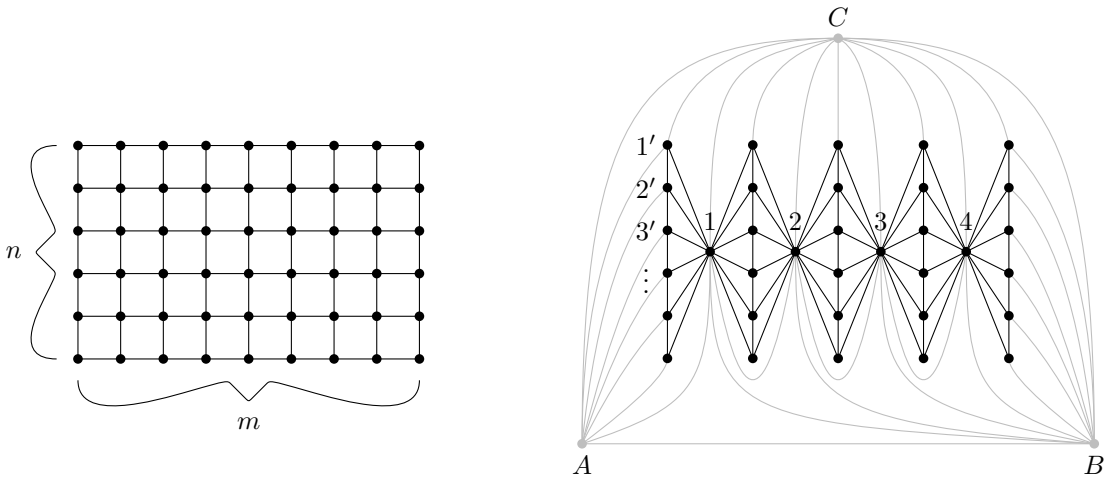

(a) The grid graph $G(m, n)$ for $n = 6$ and $m = 9$.

(b) A planar 3-tree 'containing' $G(m, n)$.

Figure 4.1: Illustration of the proof of Proposition 4.3.

In particular, we add three new vertices A, B, C and insert the edges (i, B), (i, C) and $(i, i+1)$ such that $(i, i+1, C)$ form triangles containing the vertices of a column. Adding one additional edge incident to C, the graph in the interior of a triangle $(i, i+1, C)$ is a stacked triangulation: The vertices can be inserted from top to bottom. Moreover, observe that the induced subgraph of $A, B, C, 1, \ldots, k$ is a stacked triangulation which can be constructed by inserting the vertices in the order $1, \ldots, k$.

It remains to consider the interior of triangles $A1C$ and kBC. If n is odd, the triangle kBC is a face. Otherwise, we treat it symmetrically to $A1C$. We enhance the interior of $A1C$ to a stacked triangulation by inserting edges from all inner vertices to A and one extra edge to C. Thus, G is a stacked triangulation and therefore area-universal.

Consequently, every grid graph can be transformed into a subgraph of an area-universal graph by face-maintaining edge contractions and Lemma 2.3 implies that grids are area-universal. ◀

4.1.2 Angle Graphs of Triangulations

The *angle graph* of a plane graph G is the graph Q with vertex set consisting of the vertices and faces of G and edges corresponding to face-vertex incidences. If G is 2-connected, then Q is a quadrangulation. Clearly, the angle graph is bipartite where the two bipartition classes are given by the vertices V and the faces F of G. Here we consider angle graphs of triangulations. For an example, consider the stacked triangulation in Figure 4.2(a) and its angle graph Figure 4.2(c).

For a plane graph G and its angle graph Q, we often consider the *union (graph)* $G + Q$, consisting of the union of the vertex and edge sets of G and Q, respectively. Note that the union is again a plane graph: Indeed, the vertex set of $G + Q$ coincides with the vertex set of Q. Hence, $G + Q$ can be understood as the quadrangulation Q where the edges between the vertices of one bipartition class, namely V, are inserted.

We will repeatedly construct realizing drawings of Q with the help of a drawing of $G+Q$. To do so, we introduce the notion of a *refined area assignment*. Let G_1 be a subgraph of G_2. Then, every face of f of G_1 corresponds to a collection of faces C_f in G_2. We say an area assignment $\mathcal{A}_1$ of G_1 *is refined* by an area assignment $\mathcal{A}_2$ of G_2 if $\mathcal{A}_1(f) = \sum_{s \in C_f} \mathcal{A}_2(s)$. Reversely, we also say $\mathcal{A}_2$ of G_2 *refines* $\mathcal{A}_1$ of G_1.

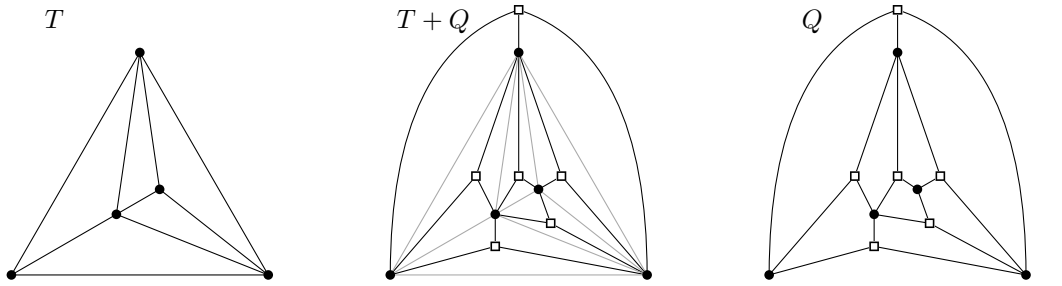

(a) A triangulation T. (b) The union $T + Q$. (c) The angle graph Q of T.

Figure 4.2: The angle graph Q of a triangulation T and their union $T + Q$. Since T is a stacked triangulation and thus area-universal, Q is area-universal by Proposition 4.4; Q is the unique quadrangulation with 11 vertices and minimum degree 3.

▶ **Proposition 4.4.** *The angle graph Q of an area-universal triangulation T is area-universal.*

Proof. We show that the union $T + Q$ is area-universal: The graph $T + Q$ can be seen as T where a vertex of degree 3 is inserted in every face. By Lemma 2.8 and the area-universality of T, $T + Q$ is area-universal. Consequently, Q is the subgraph of an area universal graph and thus area-universal by Lemma 2.2. ◀

Remark. The very same approach shows that angle graphs of equiareal triangulations are equiareal. However, the argument does not generalize from area-universal triangulations to other area-universal graphs since we use the fact that every face of the quadrangulation corresponds to exactly two faces in the union.

As a straight-forward consequence of Proposition 4.4, angle graphs of stacked triangulations are area-universal. For an example consider Figure 4.2. We can also show area-universality of angle graphs of some non-area-universal triangulations. For instance, the angle graph of the octahedron is depicted in Figure 4.3(a), and its area-universality is quite easy to see.

▶ **Proposition 4.5.** *The angle graph Q of the octahedron graph G is area-universal.*

Proof. The graph Q can be transformed to an area-universal graph by four face-maintaining edge contractions and insertion of four edges as depicted in Figure 4.3(b). The resulting graph is the stacked triangulation illustrated in Figure 4.3(c). A vertex with label i can be inserted in a triangle if all vertices with smaller labels are already inserted. Consequently, Lemma 2.3 implies the area-universality of Q. ◀

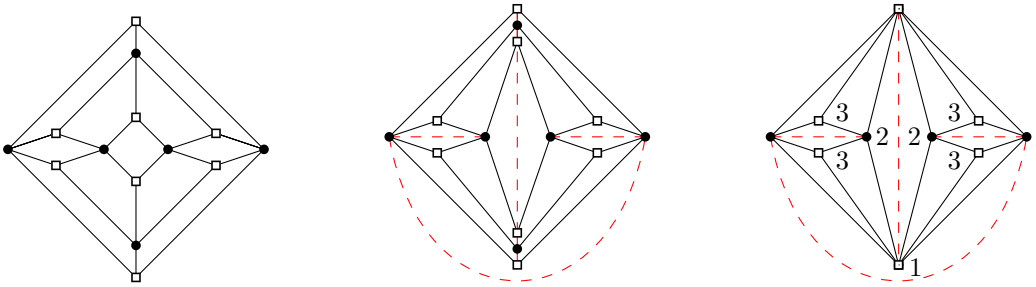

(a) Angle graph of octahedron. (b) Inserted and contracted edges. (c) A stacked triangulation.

Figure 4.3: Illustration of Proposition 4.5 and its proof.

More generally, it suffices for the triangulation to be *close to* area-universal. As we will see in Chapter 5, every plane graph has an area-universal subdivision. For a plane graph G, the minimum number of inserted subdivision vertices such that the subdivided graph becomes area-universal is the *subdivision number* of G, denoted by $s(G)$. If G is area-universal, then clearly $s(G) = 0$. We will see that the octahedron graph has subdivision number 1 (Proposition 5.4). Therefore, the following theorem generalizes Proposition 4.4.

■ **Theorem 18.** *If T is a plane triangulation with subdivision number $s(T) \leq 1$, then its angle graph Q is area-universal.*

Proof. Figure 4.4 illustrates this proof for the octahedron graph. Let e be an edge of T such that subdividing e yields the area-universal graph $T_\circ$. Our strategy is as follows: Given an area assignment $\mathcal{A}$ of Q, we define a refining area assignment $\mathcal{A}'$ of the union $U := Q + T_\circ$. Then, there exists a unique area assignment $\mathcal{A}_\circ$ of $T_\circ$ such that $\mathcal{A}'$ refines also $\mathcal{A}_\circ$. With the help of an $\mathcal{A}_\circ$-realizing drawing of $T_\circ$, which exists since $T_\circ$ is area-universal, we find an $\mathcal{A}'$-realizing drawing D' of U. Deleting $T_\circ$ from D' yields an $\mathcal{A}$-realizing drawing of Q.

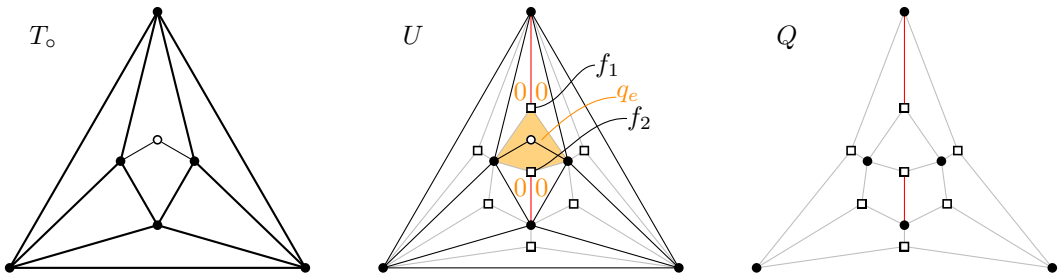

(a) The subdivision $T_\circ$. (b) The union $U := T_\circ + Q$. (c) The angle graph Q of T.

Figure 4.4: Illustration of the proof of Theorem 18 when T is the octahedron graph.

For the definition of $\mathcal{A}'$, note that every face of Q corresponds to two faces in U. Let q_e denote the face of Q that is split by the subdivided edge e in U. We denote the two faces adjacent to e in T by f_1 and f_2. For all faces q in Q except the four faces q_1, q_2, q_3, and q_4 sharing an edge with q_e, we arbitrarily partition the area $\mathcal{A}(q)$ between the two corresponding faces in U. For q_i, $i \in [4]$, assign the area $\mathcal{A}(q_i)$ to the triangular face of U which is neither incident to f_1 nor to f_2 as illustrated in Figure 4.5. This defines the area assignment $\mathcal{A}'$. We define $\mathcal{A}_\circ$ as the area assignment of $T_\circ$ that is refined by $\mathcal{A}'$ of U.

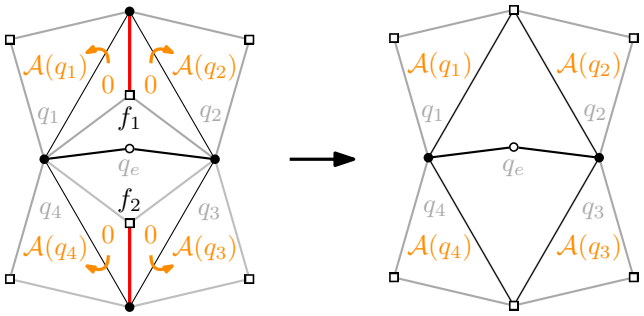

Figure 4.5: Faces in U in the neighborhood of the subdivided edge e.

Let $D_\circ$ be an $\mathcal{A}_\circ$-realizing drawing of $T_\circ$. Since each vertex $f \in F - \{f_1, f_2\}$ of U acts as a vertex of degree 3 stacked into a face of $T_\circ$, we can insert them in $D_\circ$ such that they realize the areas of $\mathcal{A}'$ by Lemma 2.8. For an $\mathcal{A}'$-realizing drawing of U it remains to insert f_1 and f_2. Due to the definition of A', the red edges in Figure 4.5 incident to f_1 and f_2 must be contracted in every $\mathcal{A}'$-realizing drawing of U. Consequently, we insert f_1 and f_2 at the end vertex of the red edges, respectively. This yields an $\mathcal{A}'$-realizing drawing of U. Since $\mathcal{A}'$ refines $\mathcal{A}$, deleting the edges of $T_\circ$ yields an $\mathcal{A}$-realizing drawing of Q. ■

In fact, the proof of Theorem 18 can be applied in more general settings. It is not hard to see that the same argument works if the subdivision vertices are *isolated*, i.e., in the dual graph T^* the set of faces incident to a subdivision vertex induces a matching.

■ **Corollary 19.** *Let T be a triangulation with an area-universal subdivision $T_\circ$ that has isolated subdivision vertices. Then the angle graph Q of T is area-universal.*

Moreover, we can allow for diamond additions of arbitrary order.

■ **Theorem 20.** *Let T be a triangulation obtained from an area-universal graph T' by several disjoint diamond additions of an arbitrary order. Then the angle graph Q of T is area-universal.*

Proof. We consider a diamond addition of order k applied on an edge (u, w) of T'. Let $T'_\circ$ denote the triangulation T' where the edge (u, w) is subdivided by k vertices as in T; in other words the edge (u, w) is replaced by a path P with $k+1$ edges. Let A and B denote the two common neighbors of u and w in T', respectively. We consider the union $U := Q + T'_\circ$ and define H as the restriction of U to the interior of $AuBw$. Figure 4.6(a) depicts H for a diamond addition of order 3.

Given an area assignment $\mathcal{A}$ of Q, we construct an area assignment $\mathcal{A}'$ of T' and an area assignment $\mathcal{A}_U$ of U that refines both $\mathcal{A}$ and $\mathcal{A}'$. Observe that every face q of Q is either a face of U or corresponds to two faces of U. In the latter case, we partition the prescribed area of q equally between its two faces in U and obtain the area assignment $\mathcal{A}_U$ of U. We

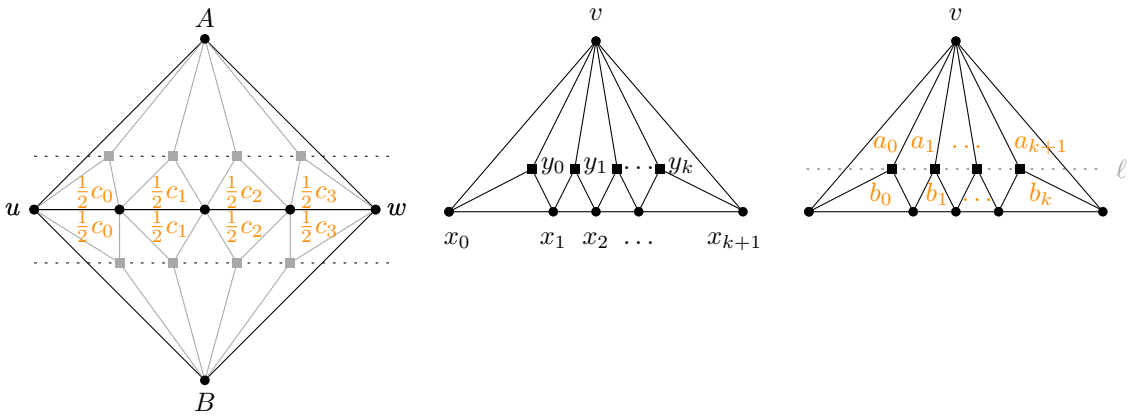

(a) The graph H for a diamond addition of order 3 and $\mathcal{A}_H$.

(b) A tent graph T_k.

(c) An $\mathcal{A}$-realizing drawing of T_k.

Figure 4.6: Illustration of Lemma 4.6 and its proof.

will make use of the equal partition for faces incident to P. We denote $\mathcal{A}_U$ restricted to H by $\mathcal{A}_H$. We define $\mathcal{A}'$ of T' as the area assignment refined by $\mathcal{A}_U$, where we identify P and (u, w) for the containment relation. From an $\mathcal{A}'$-realizing drawing D' of T', we construct an $\mathcal{A}_U$-realizing drawing of U as follows: Firstly, we add all face vertices not adjacent to P by Lemma 2.8; recall that they act as vertex of degree 3 in a triangle. Secondly, we reinsert H.

We show the realizability of $\mathcal{A}_H$ by considering the top and bottom half of H independently. A tent graph T_k is a plane graph with outer face $v, x_0, x_1, x_2, \ldots, x_{k+1}$ and inner vertices $y_0, y_1, \ldots, y_k$ where y_i is incident to x_i, x_{i+1} and v. Figure 4.6 illustrates T_4. Observe that decomposing H along P results in two tent graphs T_k.

▶ **Lemma 4.6.** *Every area assignment $\mathcal{A}$ of a tent graph T_k has an $\mathcal{A}$-realizing drawing within each triangle that has area $\Sigma\mathcal{A}$ and corners v, x_0, x_{k+1}. Moreover, the length of every segment $x_i x_{i+1}$ is proportional to the area of the incident triangle.*

Proof. We denoted the assigned areas of T_k by a_i and b_i, respectively, as depicted in Figure 4.6(c). We position x_i on the segment $x_0 x_{k+1}$ such that

$$\frac{b_i}{\|x_{i+1} - x_i\|} = \frac{\sum_i b_i}{\|x_{k+1} - x_0\|}.$$

Then, in a realizing drawing the vertices y_i lie on a line ℓ parallel to the segment $x_0 x_{k+1}$. We place y_i with the following procedure. Defining y_{-1} as the intersection of the segment $v x_0$ with the line ℓ, we suppose that y_{i-1} is placed already when we consider y_i for $i \geq 0$. Move y_i rightwards on the line ℓ starting at y_{i-1} and observe the area of the face $v y_{i-1} x_i y_i$. Clearly, it starts at 0 and increases continuously. The intermediate value theorem guarantees a position, where the area equals a_i. We place y_i at the corresponding position and continue with y_{i+1}. Due to the correct total area, the area of a_{k+1} is realized if all other face areas are correct. Thus, we obtain an $\mathcal{A}$-realizing drawing of T_k. ◀

We use Lemma 4.6 to reinsert each of the two tent graphs of H. By definition of $\mathcal{A}_\circ$, the subdivision vertices on (u, w) are placed consistently for the top on bottom part. Here we use the fact the assigned areas were split equally into two. Since A_U refines $\mathcal{A}$, we obtain an $\mathcal{A}$-realizing drawing of Q by deleting the edges of $T'_\circ$. ■

With a more careful analysis, we may also handle special configurations when a triangle of T is incident to more than one subdivision vertex.

■ **Theorem 21.** *Let T be a triangulation with a face $f_\circ$ such that subdividing each edge incident to $f_\circ$ (at most once) yields an area-universal graph $T_\circ$. Then the angle graph Q of T is area-universal.*

Proof. For simplicity and with slight abuse of notation, we denote the face corresponding to $f_\circ$ in $T_\circ$ also by $f_\circ$ and the three faces incident to subdivision vertices by f_1, f_2, f_3 as illustrated in Figure 4.7(a). In the following, we show how to deal with exactly three subdivision vertices since inserting an extra subdivision vertex never harms the area-universality.

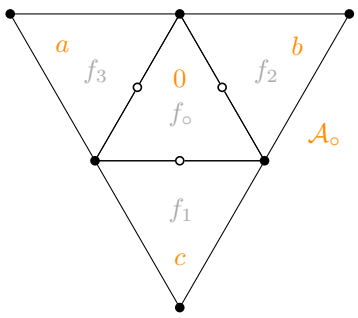

(a) Neighborhood of $f_\circ$ in $T_\circ$ and $\mathcal{A}_\circ$.

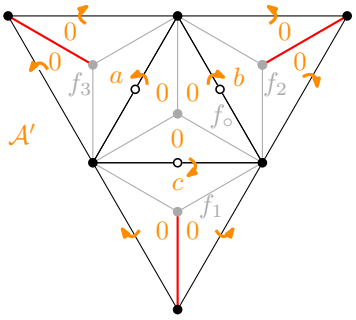

(b) Neighborhood of $f_\circ$ in $Q + T_\circ$ and $\mathcal{A}'$.

Figure 4.7: Illustration of the proof of Theorem 21 for three subdivision vertices.

For an area assignment $\mathcal{A}$ of Q, we construct an area assignment $\mathcal{A}_\circ$ of $T_\circ$. Then from an $\mathcal{A}_\circ$-realizing drawing $D_\circ$ of $T_\circ$, we construct an $\mathcal{A}$-realizing drawing of Q. In the first step, we define an area assignment $\mathcal{A}_U$ of the union $Q + T_\circ =: U$. Note that every face of Q corresponds to two faces in U. Except for the faces incident to $f_\circ$, we arbitrarily partition the area $\mathcal{A}(q)$ of each face q of Q between its two faces in U. For the faces incident to $f_\circ$, we assign their area to the subface of U not incident to $f_\circ$ as depicted in Figure 4.7(b).

In the second step, we define the area assignment $\mathcal{A}_\circ$ of $T_\circ$ such that $\mathcal{A}_U$ of U refines $\mathcal{A}_\circ$ of $T_\circ$. Since $T_\circ$ is area-universal, there exists an $\mathcal{A}_\circ$-realizing drawing $D_\circ$ of $T_\circ$. Observe that most face-vertices of Q act as vertices of degree 3 in a triangle of U. Hence, these vertices do not influence the area-universality of U by Lemma 2.8 and we may easily insert them in $D_\circ$ such that they realize the area of $\mathcal{A}_U$. For an $\mathcal{A}_U$-realizing drawing of U, it remains to insert the face vertices f_1, f_2, f_3 and $f_\circ$. By definition of $\mathcal{A}_U$, we place f_1, f_2, f_3 such that the edges which are highlighted in red in Figure 4.7(b) are contracted. In order to place $f_\circ$ in $D_\circ$, we work a little harder.

Given a polygon P, we say a point p *sees* another point q if the segment pq is contained in P. Note that $f_\circ$ is incident to three (black) vertices from T and three (white) subdivision vertices. Given a straight-line drawing of $T_\circ$, we say a point of $f_\circ$ is a black center if it sees the three black vertices.

▶ **Lemma 4.7.** *In every $A_\circ$-realizing drawing $D_\circ$ of $T_\circ$, the polygon $f_\circ$ has a black center.*

Proof. Consider any triangulation of $f_\circ$ in $D_\circ$. Figure 4.8 depicts the interesting cases. If the triangulation contains a white-black diagonal, then the incident white vertex is a black center; it is adjacent to two black vertices by outer vertices and to the last by the diagonal.

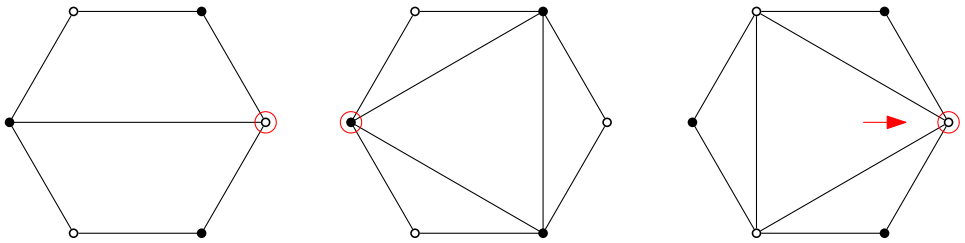

Figure 4.8: Triangulations of $f_\circ$ for finding a black center in $f_\circ$.

There exist exactly two triangulations which do not contain a white black-diagonal, namely the triangulations consisting of white-white or black-black diagonals. In the case of a ack-black diagonals, any black vertex is a black center.

In the case of white-white diagonals, we use the fact that $f_\circ$ has area 0. Since all triangles of the triangulation have no area, the corresponding vertex triples are collinear. We distinguish two cases: If two white vertices coincide, then the point of coincidence is a black center: Each white vertex is adjacent to two black vertices. Together two white vertices cover all three black vertices. If no two white vertices coincide, then the central triangle needs a flat angle. Let v denote the white vertex where the flat angle of the central face is realized. We claim that v is a black center: Clearly, it sees its adjacent two black vertices. Moreover, there exist two collinear triples sharing two distinct points, namely the white triple and the triple disjoint from v. Thus all four vertices are collinear. ◀

Lemma 4.7 guarantees that the polygon $f_\circ$ in $D_\circ$ has a black center at which we place the face-vertex $f_\circ$ of Q. Since $\mathcal{A}_U$ of U refines $\mathcal{A}$ of T, we obtain an $\mathcal{A}$-realizing drawing of Q by deleting the edges of $T_\circ$. ■

Remark. To show the area-universality of the angle graph Q of a triangulation T with subdivision number $s(T) \leq 2$, we need to consider the relative placement of the subdivision vertices. If the two subdivision vertices are independent, Corollary 19 guarantees the area-universality of Q. It remains to consider the cases where the two subdivision vertices share a common neighbor v and have incident neighboring faces. Figure 4.9 displays these cases. If the two subdivision vertices are incident to a common face, then Theorem 21 shows the area-universality of Q. If v has degree 4, then Proposition 4.8 shows that the middle graph of Figure 4.9 is strongly realizable. Unfortunately, this method seems hopeless if v has higher degree.

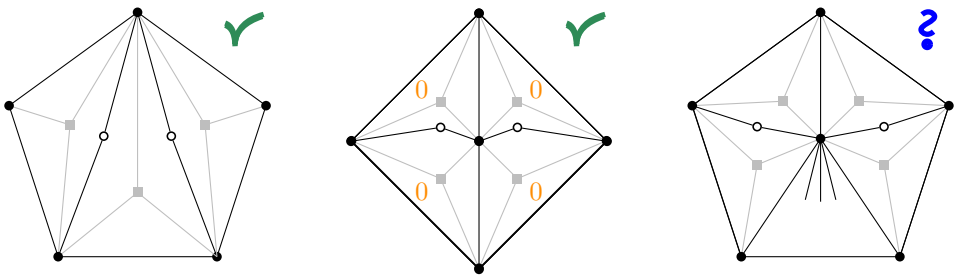

Figure 4.9: Three cases of two dependent subdivision vertices and their angle graphs.

▶ **Proposition 4.8.** *Every area assignment $\mathcal{A}$ of the graph G, depicted in Figure 4.10(a), where the faces incident to outer edges have area 0, has a realizing drawing within any quadrangle q of area $\Sigma\mathcal{A}$.*

Proof. We denote the outer vertices by A, B, C, D and the non-zero face areas by a, b, c, d as shown in Figure 4.10(a). By symmetry of G, we may assume that q contains the diagonal AC. We distinguish two cases. If the areas b and d do not exceed the triangles ABC and CDA, respectively, we partition a and c into areas a_1, a_2 and c_1, c_2 such that $a_1/c_1 = a_2/c_2$ and $x := \text{AREA}(ABC) - b = a_1 + c_1$ with $0 \leq x \leq a + c$. Then we apply Lemma 4.6 to the resulting left and right tent graph. Due to the same ratio, the inner vertex v is placed in the same point.

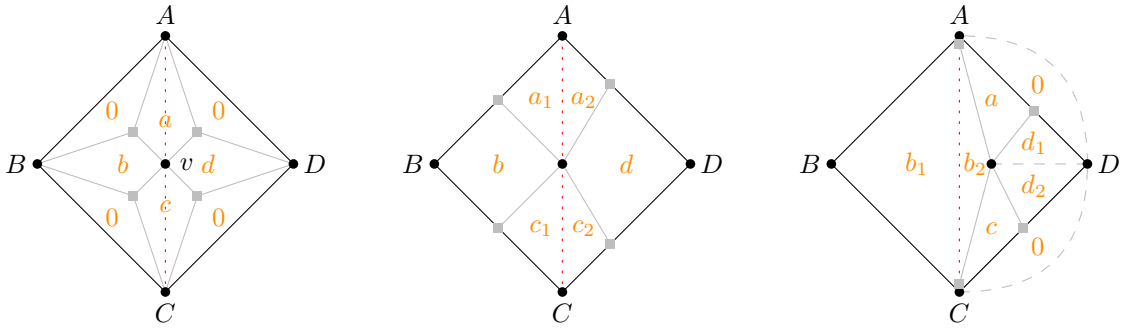

(a) Strong realizability for v of degree 4. (b) Case 1: b and d are small. (c) Case 2: b or d are big.

Figure 4.10: Strong realizability for v of degree 4.

Now, we consider the case that b or d exceed the area of ABC or BDA, respectively. By symmetry, we assume that b exceeds the area of triangle ABC. This case is illustrated in Figure 4.10(c) and reduces to a stacked triangulation: First of all, we identify the left two vertices with A and C, respectively, and define $b_1 = \text{AREA}(ABC)$ and $b_2 := b - b_1$. Then v must be placed within ACD. Inserting the artificial edge (v, D) and the three edges of the triangle ACD, results in a stacked triangulation with outer face ACD. Consequently, we can realize the areas b_2, a, c, d as wished. ◀

When combined with knowledge from Chapter 5, the above results imply the area-universality of the following classes of angle graphs.

■ **Corollary 22.** *The angle graph Q of a plane triangulation T is area-universal if*

- *T is a stacked triangulation,*
- *T is 4-connected and has at most ten vertices, or*
- *any (possibly a different) embedding of T is a double stacking graph, i.e., $T \in [\mathcal{H}_{\ell,k}]$.*

Proof. Since stacked triangulations are area-universal as seen in Observation 1.1, Proposition 4.4 implies the area-universality of its angle graphs. Corollaries 34 and 35 show that triangulations with at most nine vertices and all plane graphs in $[\mathcal{H}_{\ell,k}]$ have subdivision number at most 1. Consequently, Theorem 18 implies that their angle graphs are area-universal. Moreover, plane 4-connected triangulations on ten vertices can be obtained by at most two disjoint diamond additions as shown in Lemmas 5.13 and 5.14. Thus, their area-universality follows from Theorem 20. ■

4.2 On Strongly Area-Universal Quadrangulations

In this section, we study strongly area-universal quadrangulations. Note that for $n > k$, the area of a convex n-gon strictly exceeds the area of a contained k-gon. Therefore, we immediately obtain that the graph depicted in Figure 4.11 is not strongly area-universal.

Observation 4.9. *Not all plane bipartite graphs are strongly convex area-universal.*

In particular, if the outer face is a regular hexagon, the left quadrangle can never contain more that $2/3$ of the total area. Consequently, every area assignment a, b where the quadrangle has area $a > 2/3$ is not realizable in a regular hexagon with total area 1.

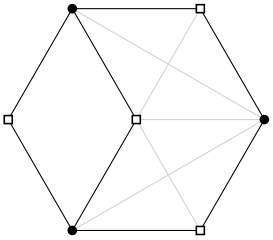

Figure 4.11: This plane bipartite graph is not strongly area-universal.

▶ **Proposition 4.10.** *If a plane quadrangulation G has an area assignment $\mathcal{A}$ such that every realizing drawing has a convex outer face, then there exists a plane quadrangulation H that is not area-universal.*

Proof. Suppose we are given a quadrangulation G and an area assignment $\mathcal{A}$ such that every $\mathcal{A}$-realizing drawing has a convex outer face. Then, we construct H as follows: Let G_1 and G_2 be two copies of G. Choose two outer vertices of G belonging to the same bipartition class of G and identify their twin in G_1 and G_2, respectively. The resulting graph is depicted in Figure 4.12. If G was 3-connected, we additionally inserting a cube graph in the central face of H such that H is also 3-connected.

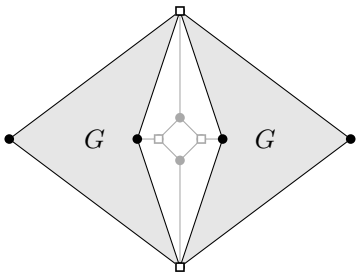

Figure 4.12: Construction of a non-area-universal quadrangulation Q from a graph G with an area assignment that needs a convex outer face.

Assigning a positive area to the central face and $\mathcal{A}$ to each copy of G, we claim that H has no realizing drawing. Suppose, by contradiction, that there exists a realizing drawing. Due to the positive area of the central face, at most one copy of G in H has a convex outer face, without loss of generality assume G_1 has convex outer face. Thus G_2 has an A-realizing drawing where the outer face is not convex. A contradiction. ◀

4.2.1 Angle Graphs of Wheels

Now, we consider angle graphs of wheels, which are also known as *pseudo-double wheels*. The *pseudo-double wheel* S_k is a plane graph with $2k+2$ vertices and consists of a cycle with vertices $v_1, v_2, \dots v_{2k}$ and a vertex v adjacent to all vertices on the cycle with odd index and a vertex w adjacent to all vertices on the cycle with even index. Depending on their index we call the vertices of the cycle *odd* or *even*. Figure 4.13(a) displays S_5. From the definition (and the Jordan curve theorem), it is immediate that all embeddings of the underlying planar graph of S_k are equivalent. Note that the pseudo-double wheel with $(2k+2)$ vertices is the angle graph of the wheel graph W_k which consists of a cycle C_k with an additional vertex incident to vertices of C_k. Figure 4.13(b) illustrates this fact. The smallest pseudo-double wheel S_3 is also known as the *cube graph*.

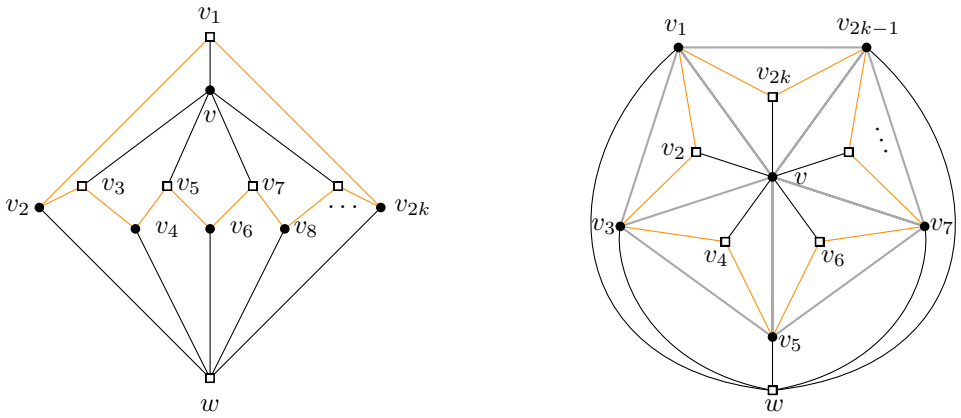

(a) A pseudo-double wheel.

(b) A wheel and its angle graph.

Figure 4.13: Pseudo-double wheels are angle graphs of wheels.

In this section, we show that the cube graph and more generally, that all pseudo-double wheels are strongly area-universal.

■ **Theorem 23.** *The pseudo-double wheel S_k, $k \geq 3$, is strongly area-universal.*

Clearly, we can combine Lemma 2.5 and Theorem 23 in order to construct other strongly area-universal graphs. A graph is a *stacked pseudo-double wheel* if there exists a set of faces such that decomposition along these faces yields several pseudo-double wheels. A *generalized stacked pseudo-double wheel* can be decomposed into pseudo-double wheels and copies of Q_5, which is strongly area-universal by Proposition 2.4. By definition, a stacked pseudo-double wheel is a generalized stacked pseudo-double wheel. For an example of a stacked cube graph consider Figure 4.14.

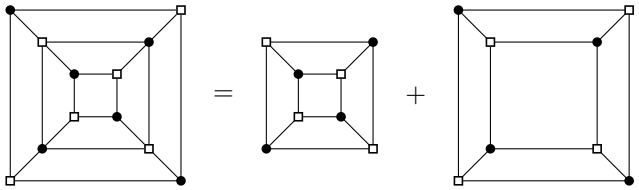

Figure 4.14: This graph is a stacked cube graph and strongly area-universal by Corollary 24.

■ **Corollary 24.** *Every generalized stacked pseudo-double wheel is strongly area-universal.*

To prove Theorem 23, we first study a subgraph of S_k, namely the plane graph $c(S_k)$, called the *core*, which is obtained by deleting v_0. Figure 4.15 illustrates the core of S_5. For simplicity, we define $A := v_2$ and $B := v_{2k}$.

▶ **Lemma 4.11.** *Let $c(S_k)$ be the core of a plane pseudo-double wheel with an area assignment $\mathcal{A}$. Let q be a quadrangle of area $\Sigma\mathcal{A}$ containing the diagonal AB whose corners are identified with the vertices A, w, B, v. Then, $c(S_k)$ has an $\mathcal{A}$-realizing drawing within q.*

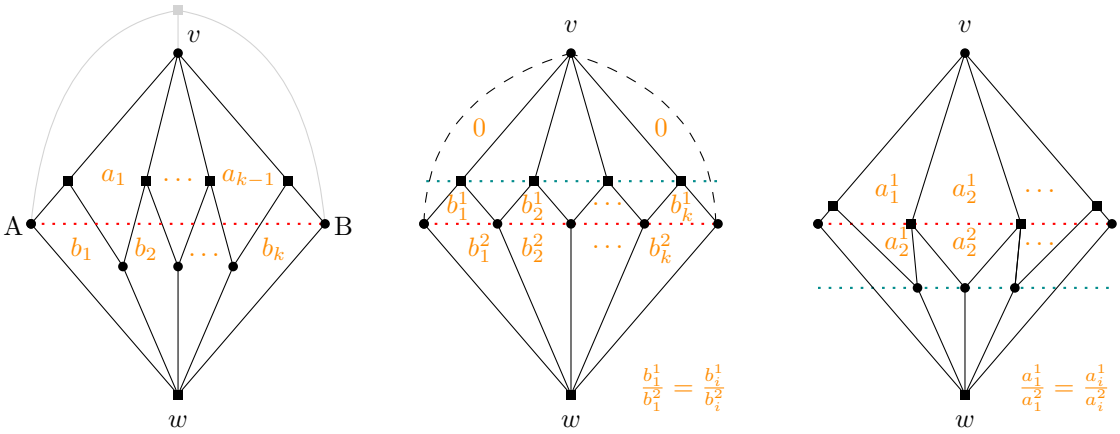

(a) The core $c(S_k)$ of S_k. (b) Drawing in case (i). (c) Drawing in case (ii).

Figure 4.15: Illustration of the proof of Lemma 4.11.

Proof. We distinguish two cases. We call the faces of $c(S_k)$ incident to w, the *bottom faces* and the faces incident to v the *top faces* of $c(S_k)$. We denote the face areas by a_i for the top and by b_i for the bottom faces and distinguish two cases. Consider also Figure 4.15(a).

Case (i): If $\sum_i b_i > \text{AREA}(\triangle AwB)$, we position the even vertices on the segment AB. Note that adding the edges of consecutive even vertices and Av and Bv (and deleting w) results in a tent graph. We partition the face area b_i of each bottom face into b_i^1 and b_i^2 such that the ratio b_i^1/b_i^2 coincides for all i and $\sum_i b_i^2 = \text{AREA}(\triangle AwB)$. By Lemma 4.6, the tent graph has a realizing drawing within the triangle vAB. Due to the same ratio, the vertex placement on AB also realizes the area for triangles incident to w. Figure 4.15(b) visualizes the realizing drawing of $c(S_k)$.

Case (ii): If $\sum_i a_i > \text{AREA}(\triangle vAB)$, we position the odd vertices on the segment AB. Note that the graph in the bottom triangle is a tent graph. Therefore, we partition the area a_i of a top faces into a_i^1 and a_i^2 such that the ratio a_i^1/a_i^2 coincides for all i and $\sum_i a_i^1 = \text{AREA}(\triangle vAB)$. As in case (i), we use Lemma 4.6 to find a realizing drawing of the tent graph. Figure 4.15(c) visualizes the realizing drawing of $c(S_k)$. ◀

We use Lemma 4.11 to settle three out of four cases of Theorem 23.

Proof of Theorem 23. For an area assignment $\mathcal{A}$ of S_k, we consider an arbitrary but fixed quadrangle q of area $\Sigma\mathcal{A}$ whose corners are identified with $v_1v_2wv_{2k}$. We distinguish two cases depending on the shape of q.

In case 1, q contains the segment v_2v_{2k}. We distinguish two subcases based on the assigned areas a and b of the faces incident to v_1 relative to the area of the triangle $v_1v_2v_{2k}$.

In case 1(i), it holds that $a + b \leq \text{AREA}(v_1v_2v_{2k})$ and Figure 4.16(a) visualizes the resulting layout. We position v such that the triangles v_1v_2v and v_1vv_{2k} realize a and b,

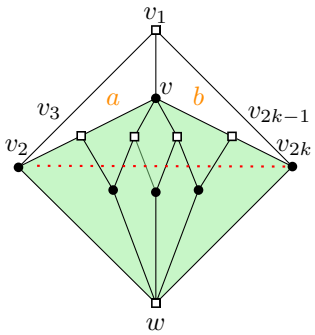

(a) Case 1(i): top faces are small.

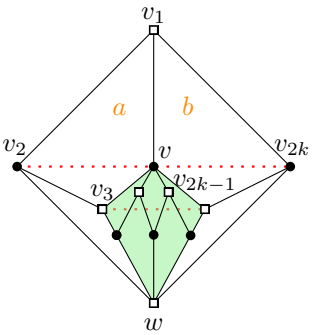

(b) Case 1(ii): top faces are big.

Figure 4.16: Realizing drawings in case 1, when the segment v_2v_{2k} is contained in q. Both subcases reduce to Lemma 4.11.

respectively. Hence, we may position the vertex v_3 anywhere on the segment vv_2; and likewise v_{2k-1} anywhere on vv_{2k-3}. Since the remaining graph corresponds to the core S_k, we use Lemma 4.11 to realize it in the quadrangle vv_2wv_{2k}.

In case 1(ii), we have $a + b > \text{AREA}(v_1v_2v_{2k})$ and Figure 4.16(b) illustrates the realizing drawing. We position v on the segment v_2v_{2k} such that v_3 and v_{2k-1} lie on a line parallel to the segment v_1v_{2k-3}. Moreover we realize the area of the two faces with outer edges as triangles by placing v_3 and v_{2k-1}. Note that graph induced by the vertices in the interior of vv_3wv_{2k-1} corresponds to the core of a smaller pseudo-double wheel. Consequently, Lemma 4.11 yields a realizing drawing.

In case 2, q contains the segment v_1w. We call the faces incident to v_2 the *left faces* and the faces incident to v_{2k} the *right faces*. We say the left (right) faces are *small* if the sum of their assigned areas is at most the area of the triangle v_1v_2w (v_1wv_{2k}). Otherwise, we call the left (right) faces *big*. Note that either the left or right faces must be small. By symmetry, we assume without loss of generality, that the left faces are small. Then we realize the left faces by triangular faces, by positioning v_3 accordingly.

In case 2(i), the right faces are small. We contract the edge vv_1 and realize the right faces with triangular faces by placing v_{2k-1}. Denoting the areas of the inner faces by x_i as illustrated in Figure 4.17(a), there exists an $4 \leq i \leq 2k-1$ such that

$$a + c + \sum_{j=4}^{i-1} x_j \leq \text{AREA}(v_1v_2w) \quad \text{and} \quad \sum_{j=i+1}^{2k-1} x_j + b + d \leq \text{AREA}(v_1wv_{2k}).$$

The exact layout depends on whether x_i is the area of a top or bottom face f of the core. For a top face, the unique odd vertex of f is placed at w; for a bottom face, the unique even vertex of f is placed at v. Afterwards we insert the remaining vertices. For $j < i$, we iteratively insert v_j such that it realizes the face face area x_j by triangular face with a flat angle at v_{j+1} from left to right. For $j > i$, we follow the same strategy but in decreasing order.

In case 2(ii), the right faces are big. Place v_{2k-1} on v_1w such that the area of the quadrangle $v_1v_3v_{2k-1}v_{2k}$ exceeds b but is not enough to also realize all the faces of the core, i.e., the striped faces incident to v in Figure 4.17(b). After artificially subdividing wv_{2k-1}, the remaining graph can be handled by Lemma 4.11 with outer face vv_3wv_{2k-1}. ■

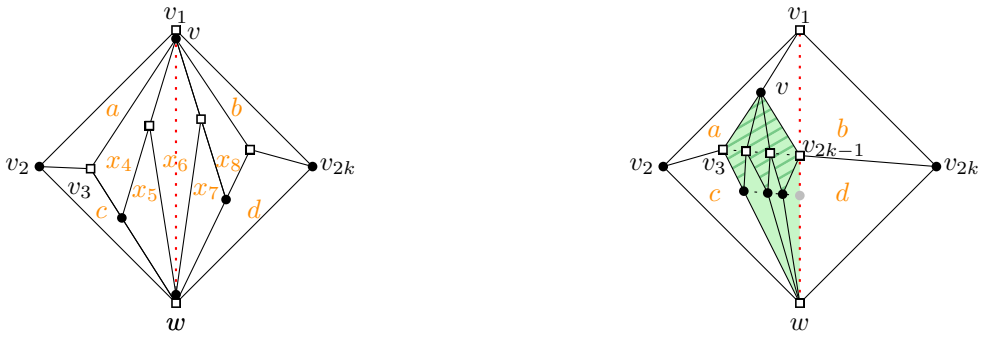

(a) Case 2(i): right faces are small.

(b) Case 2(ii): right faces are big.

Figure 4.17: Realizing drawings in case 2, when the segment v_1w is contained in q.

4.3 Small Quadrangulations

We conclude the chapter on small quadrangulations by showing that the developed methods are strong enough to prove area-universality for quadrangulations with up to 13 vertices. We also use our insights on area-universal triangulations gained in Chapter 3.

■ **Theorem 25.** *Every quadrangulation on at most 13 vertices is area-universal.*

Proof. Firstly, by Lemma 2.5 and the area-universality of Q_5 shown in Proposition 2.4, we can restrict our attention to quadrangulations with minimum degree 3.

Observation 4.12. *A minimal quadrangulation that is not area-universal has minimum degree 3.*

Thus, the smallest quadrangulation of interest is the cube graph on eight vertices. Figure 4.18 displays the planar quadrangulations on up to 13 vertices with minimal degree 3. Since all embeddings of pseudo-double wheels are equivalent, Theorem 37 proves their (strong) area-universality. It remains to consider the planar quadrangulations which are not pseudo-double wheels; specifically, one quadrangulation on eleven, two on twelve, and three on thirteen vertices, cf. Figure 4.18. We show that all of these quadrangulations are subgraphs of area-universal graphs, and thus area-universal by Lemma 2.5.

The quadrangulation T on 11 vertices is a subgraph of a stacked triangulation. This can be seen by inserting all edges between two white vertices sharing a face. The new edges induce the stacked triangulation on five vertices; each black vertex is stacked into one of these faces. Consequently T is a stacked triangulation. Since every embedding of T is area-universal by Observation 1.1, the same follows for its subgraph.

For the three planar quadrangulations on 12 vertices, the first is the pseudo-double wheel S_5; the second graph is a stacked cube graph and thus area-universal by Corollary 24. The remaining quadrangulation on 12 vertices and the first two on 13 vertices are subgraphs of an area-universal double stacking graph with some additional vertices of degree 3 stacked into triangular faces. Thus, their area-universality follows from Lemma 2.2 and Theorem 11. In Figure 4.18 the vertices which remain after iterative removal of degree 3 vertices are highlighted in red. The graph on 12 vertices reduces to the double stacking graph $\mathcal{H}_{2,2}$; the two graphs on 13 vertices to the odd accordion $\mathcal{K}_1 = \mathcal{H}_{1,2}$. The last quadrangulation on 13 vertices is a generalized stacked cube graph and thus area-universal by Corollary 24. ■

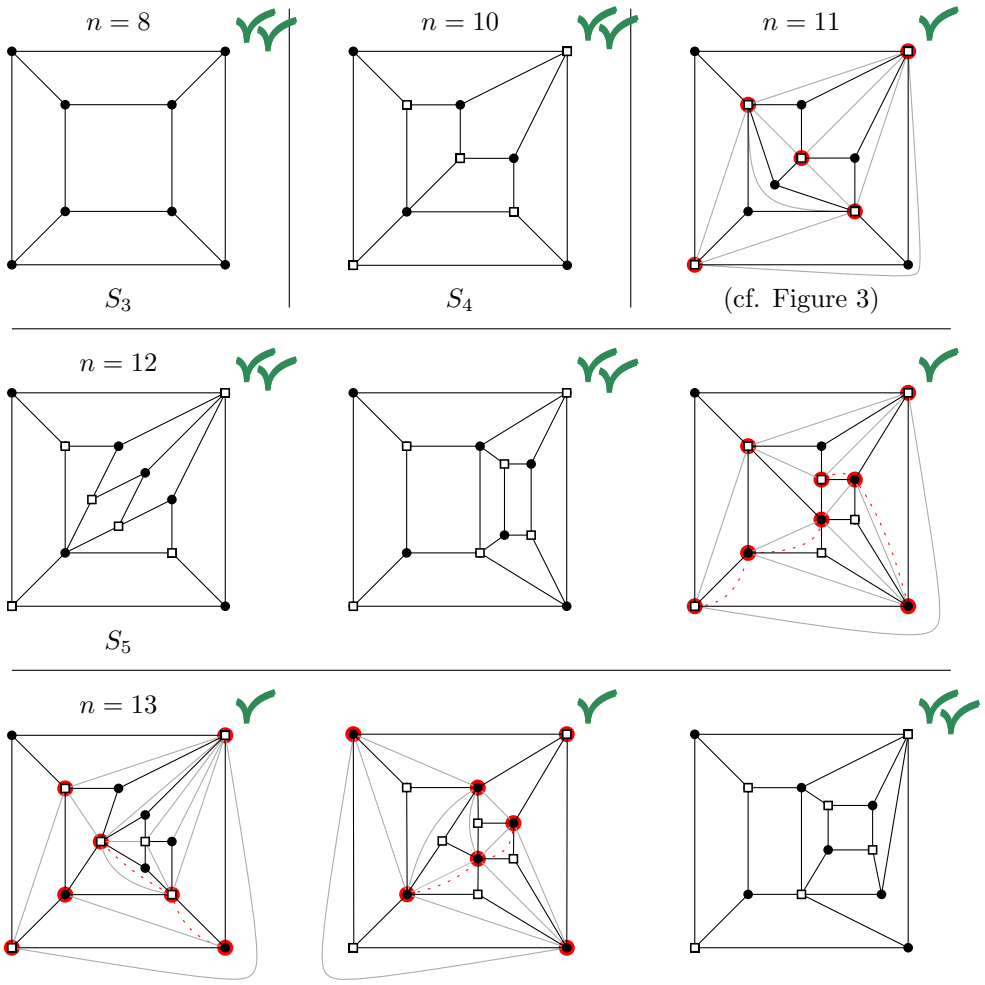

Figure 4.18: The planar quadrangulations on up to 13 vertices with minimum degree 3; only one representative for each set of plane graphs belonging to the same planar graph is illustrated. A single checkmark indicates the area-universality and a double checkmark indicates the strong area-universality of all embeddings of the depicted graph.

5 | Drawings with Bends

In this section, we relax the straight-line property and aim for realizing each area assignment of every plane graph. As discussed in Section 3.1, this is impossible with straight-line drawings. Therefore, we study realizing drawings with bended edges.

In Section 5.1, we consider general plane graphs and show that one bend per edge is sufficient. Afterwards, in Section 5.2, we improve this result for plane bipartite graphs by constructing realizing drawings where only half of the edges have a bend. Together with parts of Section 3.1, the results of these two sections can also be found in [Kleist, 2016, Kleist, 2018a]. Finally, in Section 5.3, we study the bend number of small triangulations.

5.1 Plane Graphs

By relaxing the straight-line property, we now present realizing drawings for each area assignment of every plane graph. In a *polyline drawing* of a graph, every edge is represented by a polygonal chain and a point where an edge changes its directions is called a *bend*. Interpreting the bend as a subdivision vertex, the polyline drawing corresponds to a straight-line drawing of a subdivision of the graph. In this sense, the notions of planar, crossing-free and realizing drawings immediately translate to polyline drawings. Moreover, we call a polyline drawing of a plane graph a *k-bend drawing* if each edge has at most k bends. In this section, we show that one bend per edge is sufficient to guarantee realizing drawings.

■ **Theorem 26.** *Let G be a plane graph and $\mathcal{A}\colon F' \to R_{>0}$ an area assignment of G. Then, there exists a non-degenerate 1-bend drawing of G realizing $\mathcal{A}$.*

Proof. Without loss of generality, we assume that G is a plane triangulation: If G is not a triangulation, there exists a triangulation T such that G is an induced subgraph. For each face of G, partition the assigned area between its subfaces in T and obtain the area assignment $\mathcal{A}'$ of T. Given an $\mathcal{A}'$-realizing 1-bend drawing of T, delete the artificial vertices and edges. The result is an $\mathcal{A}$-realizing 1-bend drawing of G.

We construct the final drawing of G in four steps (see definitions below):

1. Take a $\perp$-contact representation $\mathcal{C}$ which yields a rectangular layout $\mathcal{L}$.
2. Obtain a weak equivalent rectangular layout $\mathcal{L}'$ realizing the areas.
3. Define a degenerate drawing $D_\perp$.
4. Construct a non-degenerate drawing $D_\perp^*$ from $D_\perp$.

The steps are visualized for the octahedron graph in Figure 5.1.

In the first step, we construct a $\perp$-contact representation $\mathcal{C}$ of G. A *$\perp$-shape* is the union of a horizontal and vertical segment such that the lower end of the vertical segment lies in the horizontal segment. We call this point of intersection the *heart* of the $\perp$-shape. Each of

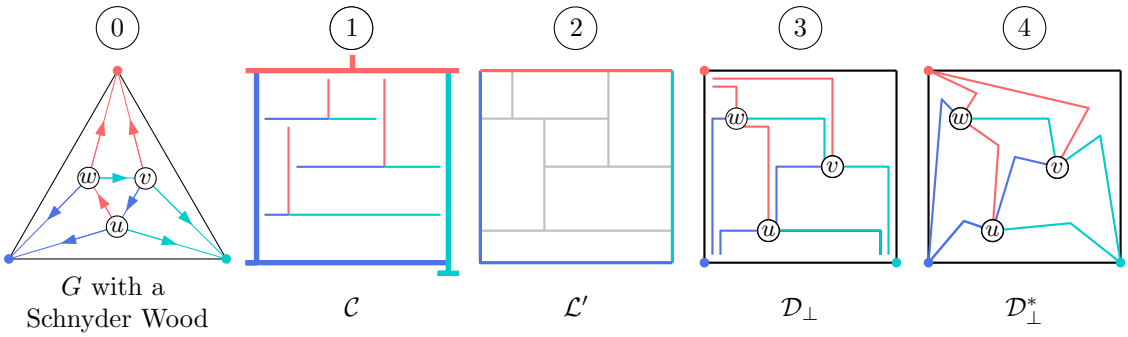

Figure 5.1: Construction of a realizing 1-bend drawing in four steps.

the other three ends of the segments is an *end* of the $\perp$-shape. A *$\perp$-contact representation* of a graph $G = (V, E)$ is a family of $\perp$-shapes $\{\perp_v : v \in V\}$ where $\perp_u$ and $\perp_v$ intersect if and only if $(u, v) \in E$. Moreover, if $\perp_u$ and $\perp_v$ intersect then the intersection must consist of a single point which is an end of either $\perp_u$ or $\perp_v$.

■ **Theorem 27** ([de Fraysseix et al., 1994])**.** *Every plane triangulation has a $\perp$-contact representation such that each inner face is represented by a rectangular region.*

Following the ideas of de Fraysseix et al. [de Fraysseix et al., 1994], $\mathcal{C}$ can be constructed as described in detail by Alam et al. [Alam et al., 2013, Section 3.1]. Observe that the $\perp$-shapes of three outer vertices may be pruned to segments such that the outer face is the complement of a rectangle. Moreover, note that every horizontal segment has a unique vertical segment touching it from above. The segments of the $\perp$-shapes of inner vertices partition the outer rectangle into finitely many rectangles; such a partition is called a *rectangular layout*. By Theorem 27, $\mathcal{C}$ yields a rectangular layout $\mathcal{L}$ in which every rectangle r corresponds to a face f_r of G. In a *generic* rectangular layout no four rectangles meet in one point. In this case, we may define a *segment* of $\mathcal{L}$ as a maximal segment belonging to the boundary of the rectangles. Indeed, $\mathcal{C}$ can be constructed such that all horizontal and vertical segments of $\mathcal{C}$ have their private supporting line. Therefore, the segments of $\mathcal{C}$ are segments of $\mathcal{L}$ and are interiorly disjoint.

In the second step, we want to achieve correct areas in a weakly equivalent layout. Two rectangular layouts are *weakly equivalent* if there exist bijections between their horizontal and vertical segments, respectively, which preserve the *ends on*-relation, i.e., a segment s ends on a segment t in one layout if and only if the same holds for their images in the other layout. We make use of the following theorem.

■ **Theorem 28** ([Eppstein et al., 2012])**.** *For every rectangular layout with area assignment $\mathfrak{a}$ on the inner rectangles, there exists a weakly equivalent rectangular layout realizing the areas of $\mathfrak{a}$.*

For this theorem several variants and proofs are known; we refer to [Wimer et al., 1988, Eppstein et al., 2012, Felsner, 2014]. For each rectangle r corresponding to the face f_r, we set $\mathfrak{a}(r) := \mathcal{A}(f_r)$. By Theorem 28, we obtain a weakly equivalent rectangular layout $\mathcal{L}'$ in which the area of each rectangle r is $\mathfrak{a}(r)$. Due to the weak equivalence of $\mathcal{L}$ and $\mathcal{L}'$, the layout $\mathcal{L}'$ can be viewed as a $\perp$-contact representation $\mathcal{C}'$, which now realizes the areas. The weakly equivalent layout $\mathcal{L}'$ is unique and may have four rectangles meeting in a point. This corresponds to the fact that two segments of $\mathcal{L}$ end in the same point of a segment

in $\mathcal{L}'$ from different sides. For our further construction, we consider these two segments as two segments of $\mathcal{L}'$.

In the third step, we obtain a 1-bend drawing of G from $\mathcal{C}'$, which may be degenerate. We define the drawing $D_\perp$ with the help of $\mathcal{C}'$ as follows:

- Place each vertex v in the heart of $\perp_v$; for a pruned $\perp$-shape, the heart is the bottom or left endpoint of the segment.
- An edge $e = (u, v)$ is supported by the segments of C' in the following way: Since the two vertices u and v share an edge, $\perp_u$ and $\perp_v$ have a point of contact c in which a vertical and a horizontal segment meet. We draw the edge e from the heart of $\perp_u$ along a segment of $\perp_u$ to the contact point c and then along a segment of $\perp_v$ to the heart of $\perp_v$, see Figure 5.2. The edge e has c as its unique bend point.

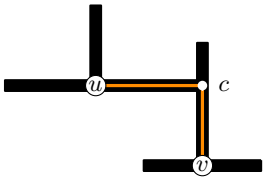

Figure 5.2: Definition of $D_\perp$.

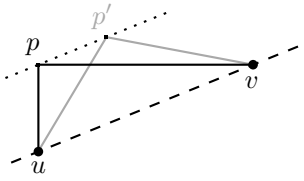

Figure 5.3: A parallel shift from p to p'.

Note that two edges may intersect along segments but never form a proper crossing. Hence the properties of a degenerate drawing of G are fulfilled. By construction, each edge consists of a horizontal and a vertical segment and, hence, has at most one bend.

Observation 5.1. *$D_\perp$ is a degenerate 1-bend drawing of G realizing $\mathcal{A}$.*

For the fourth step, it remains to remove the degeneracies of $D_\perp$. For an edge e, we interpret its bend point p_e as a vertex of degree 2, and refer to the two incident edges of p_e as its horizontal and vertical segments. As part of the degeneracies, bend points intersect non-incident edges. We handle this issue by parallel shifts. A *parallel shift* of a bend point p in a drawing D yields a (degenerate) drawing D' of G in which only the position of p and its edges changed: Let p and p' denote the positions of the bend in D and D', respectively, and let u and v denote its the two neighbors. A (degenerate) drawing D' of D is obtained by a parallel shift of p if the segment pp' is parallel to the segment uv. For an illustration consider Figure 5.3. A bend point p is *shiftable* in D if there exists a parallel shift of p. For instance, the topmost blue bend in Figure 5.4(a) is not shiftable since every shift of it results in a proper crossing.

Observation 5.2. *A parallel shift of a bend point keeps all face areas invariant.*

The contact representation $\mathcal{C}'$ induces a coloring and an orientation of the inner edges: each edge corresponds to a contact point of two segments of two $\perp$-shapes. Orient the edge such that it is an outgoing edge for the vertex belonging to the segment whose endpoint is the contact point. Color the edge red, blue, or green, depending on the type of end which belongs to the contact point: Red for the top end of the vertical segment, blue for the left endpoint of a horizontal segment, and green for the right endpoint of a horizontal segment. Such a coloring and orientation is called a *Schnyder wood* of G.

We analyze the structure of the neighborhood for a vertex v in $D_\perp$, see Figure 5.4(a). By construction, v has three outgoing edges such that all incoming edges partially run on one of these outgoing edges. (There may a unique red incoming red edge for each vertex without a bend.) As noted before, in C' every horizontal segment has a unique vertical

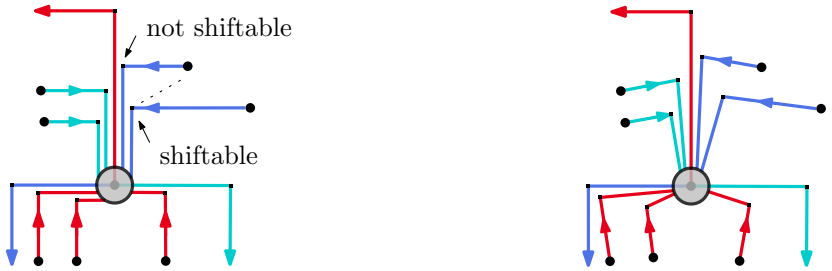

(a) The structure of the neighborhood of a vertex in the degenerate drawing $D_\perp$.

(b) The structure of the neighborhood of a vertex in the final 1-bend drawing.

Figure 5.4: The structure of the neighborhood of a vertex in $D_\perp$ and in the final drawing.

segment touching it from above and the point of contact corresponds to the heart of the $\perp$-shape. By definition of $D_\perp$, a vertex is placed in this contact point. Thus, in $D_\perp$ every horizontal segment has no segment touching it from above. Therefore, the bend point of the lowest green and blue incoming edges is shiftable upwards. Due to the fact that every rectangle has positive area, some space is guaranteed. Therefore, we can parallel shift the bend point such that its edges are free of degeneracies. In particular, the bend point does not intersect non-incident edges anymore. Consequently, the bend point of the second lowest incoming edge of v becomes shiftable. We iterate this process for all v such that all blue and green bend vertices are free of degeneracies. Afterwards, only red bend points are involved in degeneracies.

For every vertex, we consider the incoming red edges, which may have a left or a right bend with respect to the orientation. Consider the rightmost right bend point (and likewise the leftmost left bend point). Its horizontal segment has no segment touching it from below since it is rightmost (leftmost) and the vertical segment are free of degeneracies, since by the first step there is no green or blue bend point on a red segment. Consequently, the rightmost right bend (leftmost left) vertex is shiftable to the bottom. We shift it parallel downwards such that no new degeneracies are introduced. Hence, the number of degeneracies decreased. Moreover, this process achieved that the second rightmost (leftmost) bend point becomes shiftable. By iterating, we remove all degeneracies. Finally, we obtain a 1-bend drawing of G realizing the areas prescribed by $\mathcal{A}$. ■

5.1.1 Bounding the Bend Number

Knowing that one bend per edge is always sufficient, we wonder how many bends may be necessary to realize an area assignment of a plane graph? By the *bend number* of a plane graph G, $b(G)$ in short, we denote the minimum number of bends which is always sufficient and sometimes necessary to realize any given area assignment of G.

Phrased differently, Theorem 26 establishes area-universality for 1-subdivisions of plane graphs. In particular, it implies that for every plane graph, there exists an area-universal subdivision. The *(area-universal) subdivision number* of a plane graph G, $s(G)$ in short, is the minimum number of subdivision vertices which need to be inserted such that the subdivision of G is area-universal. If G is area-universal, then $s(G) = 0$. Clearly, the bend number is upper bounded by the subdivision number. However, equality of both parameters is not clear since for the bend number the bended edges can be chosen with respect to the area assignment whereas for the subdivision number the bended edges must coincide for all

area assignments. Theorem 26 assures that

▶ **Proposition 5.3.** *For every plane graph $G = (V, E)$ it holds that $0 \leq b(G) \leq s(G) \leq |E|$.*

For a graph class $\mathcal{G}$, we define the bend and subdivision number as the maximum number attained by some graph of the class, i.e.,

$$b(\mathcal{G}) := \max_{G \in \mathcal{G}} b(G) \quad \text{and} \quad s(\mathcal{G}) := \max_{G \in \mathcal{G}} s(G).$$

Consequently, Theorem 5 and Theorem 26 yield that for the class $\mathcal{G}_m$ of plane graphs with m edges it holds that $s(\mathcal{G}_m) \in \Theta(m)$.

■ **Corollary 29.** *For the class $\mathcal{G}_m$ of plane graphs with m edges, it holds that*

$$\lfloor m/12 \rfloor \leq b(\mathcal{G}_m) \leq s(\mathcal{G}_m) \leq m.$$

Proof. The upper bound follows from Theorem 26. For the lower bound consider $\lfloor m/12 \rfloor$ disjoint copies of the octahedron graph and insert $m - 12\lfloor m/12 \rfloor$ edges to obtain a graph G_m on m edges. Since the octahedron graph is not area-universal by Theorem 5, it follows that there exists an area assignment of G_m where each copy of the octahedron graph has at least one bend in every realizing polyline drawing. Thus, $b(G_m) \geq \lfloor m/12 \rfloor$. ■

We note here that the lower bound of Corollary 29 cannot be improved with the octahedron.

▶ **Proposition 5.4.** *The plane octahedron graph G has bend and subdivision number 1.*

Proof. Since, by Theorem 5, G is not area-universal, it clearly holds that $1 \leq b(G) \leq s(G)$. It remains to show that $s(G) \leq 1$. We claim that subdividing an edge of the central triangle results in an area-universal graph $G_\circ$. Figure 5.5 illustrates this subdivision. Inserting two

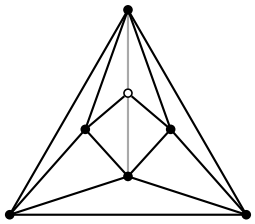

Figure 5.5: An area-universal subdivision $G_\circ$ of the octahedron.

further edges results in the accordion graph $\mathcal{K}_1$, which is area-universal by Theorem 10. Thus, as a subgraph of an area-universal graph, $G_\circ$ is area-universal by Lemma 2.2. ◀

For the curious reader, we would like to mention that the bounds of Corollary 29 also hold when we restrict the class of plane graphs to triangulations. Note here that the number of edges in a triangulation is always a multiple of 3.

▶ **Lemma 5.5.** *For every $k \geq 24$, there exists a plane triangulation G_m on $3k =: m$ edges such that*

$$\lfloor m/12 \rfloor \leq b(G_m) \leq s(G_m).$$

Proof. Before we construct G_m, we show that there exists an Eulerian triangulation on n vertices for every $n \geq 8$. (In fact, there exists one if and only if $n \in \{3, 6\}$ or $n \geq 8$.) Given an Eulerian triangulation on n vertices, a diamond addition of order 2 on any inner edge results in an Eulerian triangulation on $n + 2$ vertices. Starting with the octahedron graph, we obtain Eulerian triangulations on $2n$ vertices for every $n \geq 3$. Moreover, we can take two copies of the octahedron graph and identify the boundary of some inner face of one copy with the outer face of the other copy. This yields an Eulerian triangulation on nine vertices. Thus there exists Eulerian triangulations on $2n + 1$ vertices for $n \geq 4$.

Now, we construct G_m. Let G denote the plane octahedron graph. For simplicity, we first consider the case that $m = 12\ell$ for some $\ell \geq 6$. We start our construction with an Eulerian triangulation on $\ell + 2$ vertices and consider an inner face 2-coloring with ℓ white faces. Then, we insert a copy of the octahedron graph G into every white face f of T by identifying three outer vertices of G with the vertices of f. This yields a graph H consisting of ℓ octahedron graphs which are pairwise edge-disjoint. Therefore, H has $12\ell = m$ edges.

By Theorem 5, the octahedron graph G is not area-universal. Hence, there exists an area assignment $\mathcal{A}_0$ which has no realizing straight-line drawing. Let $\mathcal{A}$ be an area assignment of H such that the restriction to any copy of G results in $\mathcal{A}_0$; the remaining faces of H obtain some arbitrary value. Thus in every $\mathcal{A}$-realizing polyline drawing D of G, each copy of the octahedron graph has at least one edge with a bend. Since the octahedron graphs are edge-disjointness, at least ℓ of the 12ℓ edges have a bend and the claim holds for $m = 12\ell$.

For every m which is not a multiple of 12, we consider the largest ℓ such that $12\ell < m$ and construct H for $m' = 12\ell$ as before. We then stack as many degree 3 vertices into black faces as needed to obtain a graph with m edges. Here we use the fact that $m - 12\ell$ is a multiple of 3, since $m = 3k$. ◀

For quite some time we wondered whether the class of 4-connected triangulations on m edges has the same behavior or if the following holds true:

¿ Question ? : For the class of 4-connected triangulations $\mathcal{T}$, does there exist a constant c such that $b(\mathcal{T}) \leq s(\mathcal{T}) \leq c$?

Recently, we encountered the non-area-universal butterfly graph depicted in Figure 3.35(a). With this example at hand, we can answer the question in the negative and show that the subdivision number may also be linear in the number of edges.

▶ **Proposition 5.6.** *For every $m = 3k$, $k \geq 14$, there exists a plane 4-connected triangulation T_m on m edges such that*

$$\lfloor m/21 \rfloor \leq b(T_m) \leq s(T_m).$$

Proof. Let G be the butterfly graph. For simplicity, we first consider the case that $m = 21n$ for some $n \geq 2$. We start our construction with the plane quadrangulation Q_n on $2n + 2$ vertices whose dual graph is a cycle. Figure 5.6(a) depicts Q_n. Since the dual graph of Q_n is bipartite, we may 2-color the faces of Q_n with black and white such that neighboring faces have different colors. Without loss of generality, we may assume that the outer face is white. Note that the number of white and black faces is n.

In every black face of Q_n, we insert a copy of G. In every white face of Q_n, we insert an edge connecting the two vertices of degree 2 in Q_n. Clearly, the resulting graph H is a triangulation. Since G has no separating triangle and no chords, it is easy to check that H has no separating triangle. Thus H is a 4-connected triangulation.

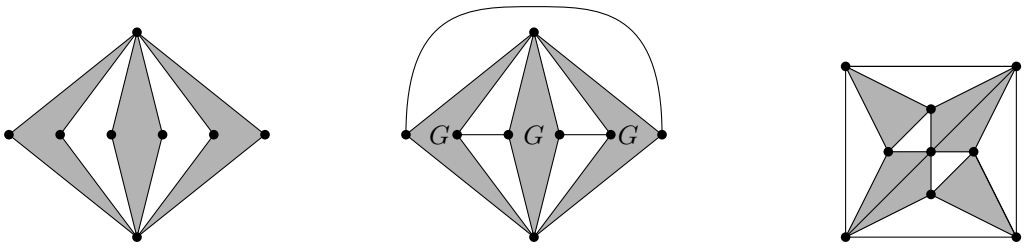

(a) The quadrangulation Q_n. (b) The triangulation H. (c) The butterfly graph.

Figure 5.6: A lower bound construction for the class of 4-connected triangulations.

Since we added n copies of G, H has $2n + 2 + 5n = 7n + 2$ vertices and $21n = m$ edges. Since G is not area-universal by Proposition 3.31 and every two of the n copies of G in H are edge-disjoint, it holds that $s(H) \geq n = \frac{1}{21} \cdot m$.

For every m which is not a multiple of 21, we consider the largest n such that $21n < m$, i.e., $n := \lfloor m/21 \rfloor$ and construct H as before. Then, we apply a diamond addition of order $(m-21n)/3$ on the edge inserted in the outer face of Q_n. In this way we obtain a graph H' with m edges such that $s(H') \geq n = \lfloor m/21 \rfloor > \frac{1}{21} \cdot m - 1$. This proves the claim. ◀

Consequently, the class of 4-connected triangulations also has a linear bend number.

■ **Corollary 30.** *For the class $\mathcal{T}_m$ of plane 4-connected triangulations on m edges, it holds*

$$\lfloor m/21 \rfloor \leq b(\mathcal{T}_m) \leq s(\mathcal{T}_m) \leq m.$$

Likewise, Corollary 30 can also not be improved with the help of the butterfly graph.

▶ **Proposition 5.7.** *The butterfly graph G has $b(G) = s(G) = 1$.*

Proof. We show that subdividing an outer edge e of the butterfly graph graph results in an area-universal subdivision. Figure 5.7(a) illustrates this subdivision. We start to study the near-triangulation G' depicted in Figure 5.7(b) which we obtain by deleting e and inserting e'. Observe that G' is 3-degenerate: A vertex with label i in G' has degree at

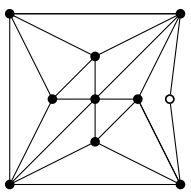

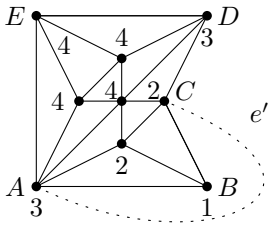

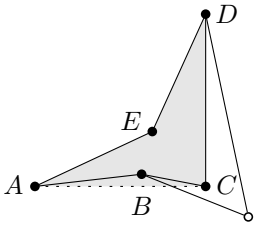

(a) An area-universal subdivision of the butterfly graph. (b) The 3-degenerate near-triangulation G'. (c) Inserting e in a realizing drawing of G'.

Figure 5.7: Illustration of Proposition 5.7 and its proof.

most 3 after removal of all vertices with smaller labels. Consequently, by Theorem 17, G' is area-universal. Given a realizing drawing for G', we delete e' and insert e with at most one bend. In the construction of a realizing drawing in Theorem 17, we may choose the reflex outer vertex such that e is not incident to it. Then, the outer vertex C of G' enclosed by e is a convex corner with convex neighbors as depicted in Figure 5.7(c) and we can easily add e with one bend such that it has a face area of any given size. ◀

5.2 Plane Bipartite Graphs

In this section, we improve the upper bound on the number of bends that always suffice for plane bipartite graphs. We show that at most half of the edges need a bend. Indeed, we can place the bends on the same edges independent of the area assignment. Hence, we obtain a bound on the subdivision number.

■ **Theorem 31.** *Let $G = (X \cup Y, E)$ be a plane bipartite graph. Then, $s(G) \leq |E|/2$.*

Proof. First, we consider the case that G is a quadrangulation and show that an arbitrary but fix area assignment $\mathcal{A}$ has an $\mathcal{A}$-realizing 1-bend drawing of G with at most $|E|/2$ bends. Moreover, we place the bends on the same edges independent of $\mathcal{A}$. The proof consists of four steps, illustrated in Figure 5.8. The main difference to the proof of Theorem 26 lies in Step 1. Moreover, Steps 3 and 4 are a little more intricate. The procedure is as follows:

0. (Augment G to a quadrangulation.)
1. Take a segment contact representation $\mathcal{C}$ yielding a rectangular layout $\mathcal{L}$.
2. Obtain a weak equivalent rectangular layout $\mathcal{L}'$ realizing the areas.
3. Define a degenerate drawing D on $\mathcal{L}'$.
4. Construct a non-degenerate drawing D^* from D by parallel shifts.

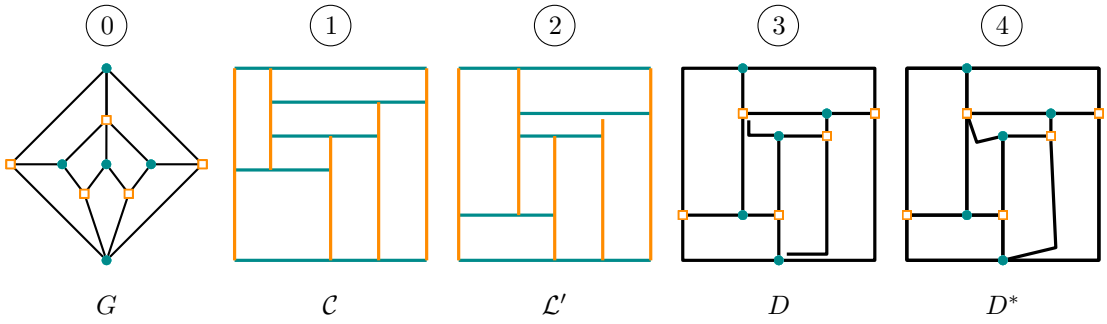

Figure 5.8: Construction of a 1-bend drawing realizing the prescribed areas in four steps.

In the first step, we take a *segment contact representation* of $G = (X \cup Y, E)$. This is a family $\{s_v | v \in X \cup Y\}$ of horizontal and vertical segments where s_v and s_u intersect if and only if $(u, v) \in E$. Moreover, each non-empty intersection consists of a single point which is an endpoint of at least one of the segments.

■ **Theorem 32** ([de Fraysseix et al., 1991, Hartman et al., 1991])**.** *Every plane quadrangulation has a segment contact representation such that each inner face is represented by a rectangle.*

Let $\mathcal{C}$ be a segment contact representation of G. We assume that the vertices of X are represented by vertical segments. The segments of $\mathcal{C}$ partition a rectangle into rectangles, and hence, $\mathcal{C}$ yields a rectangular layout $\mathcal{L}$. In the second step, we obtain a weakly equivalent rectangular layout $\mathcal{L}'$ realizing the areas by Theorem 28; let $\mathcal{C}'$ denote the corresponding segment contact representation. In the third step, we define a degenerate drawing D from $\mathcal{C}'$. The challenge is to place the vertices such that, firstly, we insert the bends on the same edges, secondly, we save one bend per vertex, and thirdly, we can remove the degeneracies by parallel shifts. We distinguish two cases depending on the minimal degree δ of G. Note that in a quadrangulation δ is 2 or 3.

Case 1: $\delta(G) = 3$. Since every segment has only two endpoints but at least three contacts, every segment has an inner contact point. For a vertical segment s_v, an inner contact point is *right* if it is the endpoint of a horizontal segment touching s_v from the right. Otherwise, it is *left*. Likewise, we distinguish inner *top* and *bottom* contact points of horizontal segments. We construct D from $\mathcal{C}'$ as follows:

- A vertex $v \in X$ is placed on topmost right inner contact point of the segment s_v if it exists; otherwise v is placed on the topmost left inner contact point.
- A vertex $v \in Y$ is placed on leftmost bottom inner contact point of the segment s_v if it exits; otherwise v is placed on the leftmost top inner contact point.
- An edge $e = (v, w) \in E$ is drawn from v along s_v to the contact point of s_v and s_w, and then along s_w to w.

Note that with this definition the vertices are placed on the same contact points independent of the area assignment. This allows us to obtain an area-universal subdivision of G. By placing a vertex on an inner contact point of its segment, the corresponding edge has no bend. Hence, we save one bend per vertex and the number of bends is at most $|E| - |V|$.

Observation 5.8. *D is a degenerate 1-bend drawing of G realizing $\mathcal{A}$ with at most $|E|-|V|$ bends.*

In the fourth step, we remove the degeneracies by parallel shifts of bend points. By the placement of the vertices, a vertical segment s_v has no right bend point above v and a horizontal segment s_v has no bottom bend point left of v. This property is our *invariant* 4_0. For a vertex $v \in X$ ($v \in Y$) with a vertical (horizontal) segment s_v, we partition the inner bend points into three sets: $\mathcal{B}_1(s_v)$, the set of right (bottom) bend points on s_v, $\mathcal{B}_2(s_v)$, the set of left (top) bend points on s_v which are below (right of) v, and $\mathcal{B}_3(s_v)$, the set of remaining bend points, i.e., left (top) bend vertices on s_v which are above (left of) v, see also Figure 5.9(a). For a segment s_v and all $i \in \{1, 2, 3\}$, a bend point $b \in B_i(s)$ is *smaller* than $b' \in B_i(s)$ if b is closer to v in D than b'. We remove the degeneracies in three steps. For $i \in [3]$, Step 4_i is defined as follows:

Step 4_i: For each $v \in X \cup Y$, do: while $\mathcal{B}_i(s_v)$ is not empty, choose the smallest $b \in \mathcal{B}_i(s_v)$, parallel shift b, and delete b from $\mathcal{B}_i(s_v)$.

If Step 4_i is completed successfully, then *invariant* 4_i holds, namely that every segment has no bend points in $B_j(s_v)$ for $0 \leq j \leq i$. Indeed invariant 4_i is necessary in order to perform Step 4_{i+1}. Clearly, invariant 4_3 guarantees a non-degenerate 1-bend drawing of G which realizes $\mathcal{A}$ and has at most $|E| - |V|$ bends. Hence it remains to show that the smallest $b \in \mathcal{B}_i(s_v)$ is shiftable if invariant 4_{i-1} holds. Consider a vertex $v \in X$ with vertical segment s_v and the smallest $b \in \mathcal{B}_1(s_v)$, see Figure 5.9(b). By invariant 4_0, the horizontal edge of b is free of bottom contact points. Since b is the smallest in $\mathcal{B}_1(s_v)$, the vertical edge

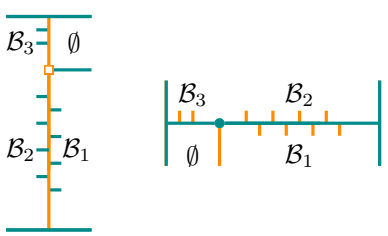

(a) Definition of D and $\mathcal{B}_i$.

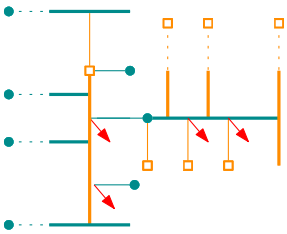

(b) Illustration of Step 4_1 and Step 4_2.

Figure 5.9: Illustration of Step 3 and Step 4 in Case 1 of the proof of Theorem 31.

of b is free of right contact points. Therefore, b is shiftable bottom-rightwards. Moreover, after shifting and deleting b, the new smallest bend point becomes shiftable. The argument for $v \in Y$ is analogous. More generally, for $i \in \{1, 2, 3\}$, the smallest bend point $b \in \mathcal{B}_i(s_v)$ is shiftable since both of its edge are free of bend points to one side; for one edge this is guaranteed by the invariant 4_{i-1}, for the other edge by the fact that b is the smallest bend point in $b \in \mathcal{B}_i(s_v)$.

Case 2: $\delta(G) = 2$. If it exists, choose an inner vertex of degree 2 and remove the segment s_v in $\mathcal{C}'$. This results in a quadrangulation where two faces are unified to one new face. Assign the sum of the two face areas to the new face. Delete inner vertices of degree 2 until all inner vertices are of degree at least 3. This yields a graph G' with area assignment $\mathcal{A}'$. Proceed with G' as in Case 1 with some extra care. If one or several outer vertices have degree 2, we place them on distinct positions on their segments; for instance in clockwise order. Moreover, we make the parallel shifts small enough, such that the following *special* property is fulfilled in an $\mathcal{A}'$-realizing drawing of G': up to a tiny ε with $n\varepsilon \ll A_{\min}$, each face f of G' contains an axis-aligned rectangle with area $\mathcal{A}'(f) - \varepsilon$, where $A_{\min} := \min_{f \in F'(G)} \mathcal{A}(f)$.

We use the special property to reinsert the degree 2 vertices in reverse order of deletion and obtain a sequence of drawings $(G'_k)_k$. We use the invariant that G'_k is a non-degenerate drawing where each face area is realized by an axis-aligned rectangle up to $k\varepsilon$. Consider the $(k+1)^{\text{th}}$ vertex v of degree 2 and the face f in G_k where v must be inserted. Assume f has area $a_1 + a_2$ and must be split into two faces f_1 and f_2 of area a_1 and a_2. By assumption, it holds that $a_1, a_2 \geq A_{\min}$ and f contains an axis-aligned rectangle R of area $a_1 + a_2 - k\varepsilon$. Assume that $v \in X$. By the intermediate value theorem, there exists a vertical segment s within R such that s dissects f into two parts of area a_1 and a_2, respectively. Place v on one endpoint of s and a bend point b on the other endpoint of s as illustrated in Figure 5.10. Note that the areas of f_1 and f_2 are realized by a rectangle up to $k\varepsilon$. In order to remove the degeneracies, use parallel shifts of v and b which are small enough to guarantee that f_i contains a rectangle of area $a_i - (k+1)\varepsilon$. This ends our treatment of Case 2.

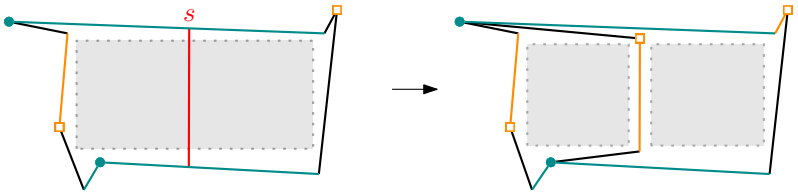

Figure 5.10: Insertion of an inner vertex of degree 2 in Case 2.

If G is not a quadrangulation, then we consider a quadrangulation Q with G as an induced subgraph. For each face in G, we partition its area assignment among its subfaces in Q and obtain $\mathcal{A}'$. Clearly, an $\mathcal{A}'$-realizing 1-bend drawing of Q induces an $\mathcal{A}$-realizing 1-bend drawing of G. However, the number of bends may exceed $|E|/2$. Therefore, we ensure to save one bend per vertex by placing the vertices on inner contact points which belong to edges of G. To do so, delete all segments belonging to artificial vertices in $\mathcal{C}$. If necessary, remove vertices of low degree iteratively as in Case 2. Afterwards, place vertices, remove degeneracies and reinsert vertices of G with low degree as in Case 1 and Case 2. Note that degree 1 vertices may also appear, but can easily be reinserted.

A planar bipartite graph has at most $(2|V| - 4)$ edges. Therefore, the number of edges with bends is at most $|E| - |V| \leq |V| - 4$ and without bends at least $|V|$. Consequently, in all cases the number of bends is less than $|E|/2$. ■

If in the third step of the last proof, the vertices are placed in fortunate positions, one can save some additional bends. In particular, every corner of the outer rectangle has two first contact points, one on each incident segment; if in both of these a vertex is placed, then one bend can be saved. For the cube graph this allows to save four bends and shows that the cube graph as a partial 3-tree is not only area-universal but also *convex area-universal*, i.e., every area assignment has a realizing drawing with convex faces.

▶ **Proposition 5.9.** *The cube graph is convex area-universal.*

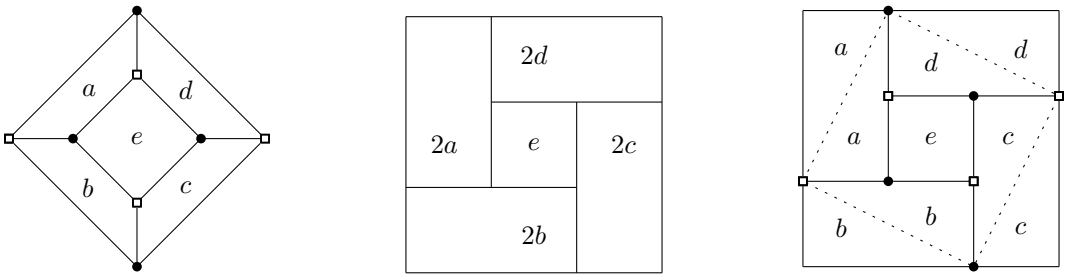

(a) The cube graph with an area assignment $\mathcal{A}$.

(b) A rectangular layout realizing $\mathcal{A}'$.

(c) A convex straight-line drawing realizing $\mathcal{A}$.

Figure 5.11: Illustration of the proof of Proposition 5.9

Proof. Let $\mathcal{A}$ be an area assignment of the cube graph as illustrated in Figure 5.11(a). Then $\mathcal{A}'$ denotes the area assignment where the areas of the four boundary faces are doubled with respect to $\mathcal{A}$. Theorem 31 guarantees the existence of an $\mathcal{A}'$-realizing 1-bend drawing realizing and Figure 5.11(b) illustrates a corresponding layout $\mathcal{L}'$. Observe that already the drawing D defined from $\mathcal{L}'$ in the third step of the proof of Theorem 31 is non-degenerate. Moreover, as illustrated in Figure 5.11(c), every outer edge has exactly one bend and all inner edges are segments. Replacing the outer edges by segments halves the area of the boundary faces and thus gives an $\mathcal{A}$-realizing straight-line drawing with convex faces. ◀

We study the concept of convex area-universality closer in Section 6.1. In particular, we will see several alternative proofs of the convex area-universality of the cube graph. However, before we do so, we investigate the bend number of small triangulations.

5.3 Small Graphs

In this section, we study the bend and subdivision numbers of small triangulations. We will see that they have fairly small subdivision numbers. In particular, 4-connected triangulations on up to ten vertices have a subdivision number of at most 1 with one exception. To obtain our bounds, we show a fruitful connection between diamond additions and the subdivision number. We start with an obvious fact which we already used in Proposition 5.4 to determine the bend number of the octahedron graph.

▶ **Proposition 5.10.** *Let G be a plane graph such that applying a diamond addition of some order on an edge e of G results in an area-universal graph G', then $s(G) \leq 1$.*

Proof. We show that inserting one subdivision vertex on e in G results in an area-universal graph $G_\circ$. Clearly, as a subgraph of G', $G - e$ is area-universal. Note that decomposing $G_\circ$

along the shortest cycle enclosing the subdivided edge e results in the area-universal graph $G - e$ and the strongly area-universal graph Q_5. Thus, Lemma 2.5 implies the area-universality of $G_\circ$. ◀

The reverse direction is of similar flavor, but a little more intricate.

■ **Theorem 33.** *Let G be a plane graph obtained from an area-universal graph G' by one or several disjoint diamond additions whose orders sum to k, then $s(G) \leq k$.*

Proof. Let $\mathcal{A}$ be an area assignment of G. We show how to obtain an $\mathcal{A}$-realizing drawing with at most k bends. We place the bends on the same edges, independent of the area assignment and thus obtain a bound on the subdivision number. Each face f of G' corresponds to a collection C_f of faces of G. We consider an area assignment $\mathcal{A}'$ of G' such that $\mathcal{A}'(f) := \sum_{s \in C_f} \mathcal{A}(s)$, i.e., $\mathcal{A}$ refines $\mathcal{A}'$. Since G' is area-universal, there exists an $\mathcal{A}'$-realizing drawing D'.

We now aim to add the vertices introduced in one of the diamond additions. Let $e = (u, w)$ be an edge in G' on which a diamond addition is applied. Without loss of generality, we suppose that e is horizontal in D'. We name the vertices, which are to be inserted on e, by $v_1, \ldots, v_\ell$ from left to right. For notational convenience, we define $v_0 := u$, $v_{\ell+1} := w$ and denote the area of the incident top left and bottom left triangle of v_i by a_i and b_i, respectively. Since D' is $\mathcal{A}'$-realizing, the triangle uwA has area $a := \sum_i a_i$ and the triangle wuB has area $b := \sum_i b_i$.

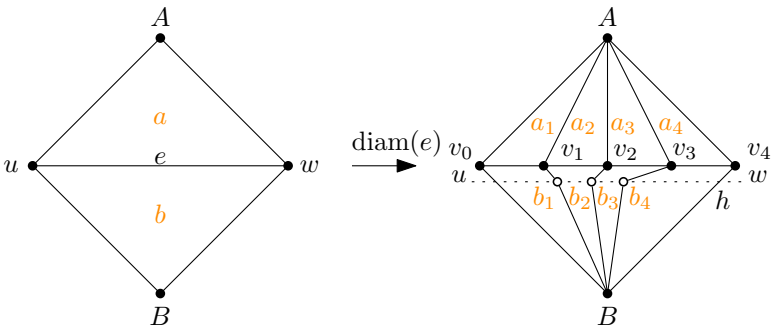

Figure 5.12: Illustration of Theorem 33 for a diamond addition of order 3.

Let $b_{\min} := \min_j\{b_j\}$ the minimal area of a bottom triangle. We define h to be a line in D' strictly below and parallel to e such that a triangle formed by e and a point on h has area less than $b_{\min}$. This is possible since the area assignment is positive. We insert the vertices from left to right. For $i \in [\ell]$, lets assume v_{i-1} is placed on e. Then in order to place v_i, we move a point p on e and stop when the triangle $v_{i-1}pA$ has area a_i. The existence of such a point p follows from continuity of the area of $v_{i-1}pA$ and the intermediate value theorem. We place v_i at p.

In order to realize b_i, we place bend points w_i of edge v_iB on h. (To unify notation, we also insert a helper point w_0 on the intersection of the segment Bv_0 and the line h.) For $i \in [\ell]$, lets assume w_{i-1} is placed on h. We move a point q on h and stop when the 5-gon $v_{i-1}w_{i-1}Bqv_i$ has area b_i. For the existence of a point q we use the fact that the area of a triangle $v_{i-1}v_iq$ never exceeds b_i by construction of the line h. Then the existence of such a point q follows from the intermediate value theorem.

By this construction, all areas a_i, b_i are realized for $i \leq \ell$. The last triangles obtain the remaining area, which is correct due to the correct total area of the top and bottom triangle in G, i.e., $a - \sum_{i=1}^{\ell} a_i = a_{\ell+1}$ and $b - \sum_{i=1}^{\ell} b_i = b_{\ell+1}$. This finishes the proof. ■

Theorem 33 is particularly interesting since almost all small triangulations can be obtained by few diamond additions from area-universal graphs. In particular, for plane triangulations with at most nine vertices, we immediately obtain a very small subdivision number. To do so, we need the following lemma.

▶ **Lemma 5.11.** *Every plane 4-connected triangulation T with $n \leq 9$ vertices can be obtained by one diamond addition from an area-universal graph.*

Proof. Note that all plane 4-connected triangulations on at most eight vertices are either area-universal or accordion graphs. Thus, we can concentrate on the triangulations on nine vertices. We showed in Theorem 14 that $\mathcal{G}_{9a}$ and $\mathcal{G}_{9b}$ are area-universal. Therefore, it remains to consider the plane graphs of $\mathcal{G}_{9c}$ and $\mathcal{G}_{9d}$.

We show that the plane graphs of $\mathcal{G}_{9c}$, can be obtained from the accordion $\mathcal{K}_1$ with an additional vertex of degree three is stacked into some face; we denote this graph by G. Thus G is area-universal by Theorem 10 and Lemma 2.8. Note that $\mathcal{G}_{9c}$ has two pairs of adjacent vertices of degree four, namely the red and orange vertices in Figure 5.13. Since no orange and red vertex share a face, at least one pair consists of inner vertices for $\mathcal{G}_{9c,i}$. Reversing a diamond addition by deleting an orange (or red) vertex and inserting an edge as indicated, namely such that its partner has degree 3, results in G. Consequently, each plane graph $\mathcal{G}_{9c,i}$ can be obtained from some embedding of G by one diamond addition.

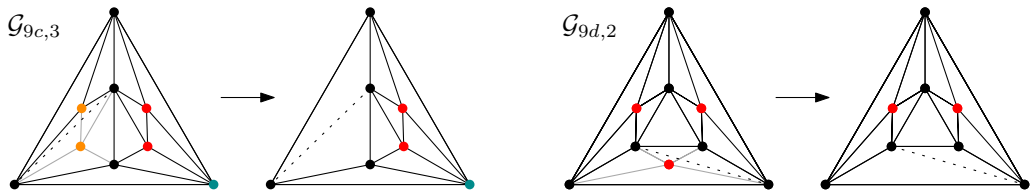

Figure 5.13: Illustration of the proof of Lemma 5.11.

Now, we show that $\mathcal{G}_{9d,i}$ can be obtained from the double stacking graph $\mathcal{H}_{2,2}$ which is area-universal by Theorem 11: Note that $\mathcal{G}_{9d}$ has three non-adjacent vertices of degree 4, which are highlighted in red in Figure 5.13. Thus, every plane graph $\mathcal{G}_{9d,i}$ has at least one inner vertex v of degree 4. Reversing the diamond addition by deleting v and inserting any diagonal, results in the double stacking graph $\mathcal{H}_{2,2}$. This is illustrated for the very symmetric plane graph $\mathcal{G}_{9d,2}$ in Figure 5.13. ◀

This lemma has several nice implications for the small bend number and also for the equiareality of small graphs. Here, we combine it with Theorem 33.

■ **Corollary 34.** *For a plane 4-connected triangulation T on at most 9 vertices it holds that $b(T) \leq s(T) \leq 1$.*

Proof. By Lemma 5.11, T can be obtained from an area-universal graph by one diamond addition. Consequently, Theorem 33 implies the bound on the subdivision number. ■

Moreover, and not surprisingly, we can use Proposition 5.10 or Theorem 33 to show equiareality of double stacking graphs. For later reference we use the following simple observation: By definition of $\mathcal{H}_{\ell,k}$, applying an diamond addition of order 1 on an appropriate edge of $\mathcal{H}_{\ell,k}$ results in $\mathcal{H}_{\ell+1,k}$. In any case, there exist at least two appropriate edges which do not share a common face. Consequently, for every H in $[\mathcal{H}_{\ell,k}]$ at least one of these edges is an inner edge. This shows the following:

Observation 5.12. *For $\ell \geq 2$, a plane graph H in $[\mathcal{H}_{\ell,k}]$ can be obtained by one diamond addition from a graph in $[\mathcal{H}_{\ell-1,k}]$. Symmetrically, if $k \geq 2$ from a graph in $[\mathcal{H}_{\ell,k-1}]$.*

This observation has the following consequence.

■ **Corollary 35.** *For every plane graph H in $[\mathcal{H}_{\ell,k}]$, it holds $b(H) = s(H) \equiv \ell \cdot k \pmod 2$.*

Proof. By Theorem 11, H is area-universal if and only if $\ell \cdot k$ is even. Consequently, for $\ell \cdot k$ even it holds that $b(H) = s(H) = 0$ and otherwise $1 \leq b(H) \leq s(H)$. Thus, it remains to show that $s(H) \leq 1$ if ℓ and k are both odd. By Observation 5.12 and Theorem 11, H can be obtained form an area-universal graph by one diamond addition. Thus, Theorem 33 implies the claim.

[Alternatively, applying one diamond addition to H results in an area-universal graph and Proposition 5.10 implies the claim.] ■

We now want to show that 4-connected triangulations on ten vertices also have small bend numbers. In particular, we show that

■ **Theorem 36.** *For a plane 4-connected triangulation T with ten vertices it holds that $b(T) \leq s(T) \leq 2$. Specifically, for all graphs other than $\mathcal{G}_{10i}$, it holds that $b(T) \leq s(T) \leq 1$.*

To do so, we first study how to obtain these graphs from area-universal triangulations by diamond additions and distinguish triangulation with and without p-order. By a *reverse* diamond addition, we remove an inner vertex of degree 4, together with its incident edges and insert one of the diagonals in the resulting 4-face.

▶ **Lemma 5.13.** *The plane 4-connected triangulations on ten vertices with a p-order can be obtained by one diamond addition from an area-universal graph.*

Proof. The 4-connected triangulation on ten vertices with a p-order are illustrated in Figure 3.27. The statement is vacuous for area-universal graphs. Recall that Theorem 16 assures that all plane graphs of $\mathcal{G}_{10c}$, $\mathcal{G}_{10f}$, and $\mathcal{G}_{10g}$ are area-universal. Moreover, $\mathcal{G}_{10a,1}$ and $\mathcal{G}_{10b,1}$ are double stacking graphs and thus, Observation 5.12, can be obtained by one diamond addition from an area-universal graph.

It thus remains to consider $\mathcal{G}_{10d}$ and $\mathcal{G}_{10e}$. The proof is illustrated in Figure 5.14. In both graphs, there exist two pairs of adjacent vertices of degree four, namely the red and orange vertices in Figure 5.14. Since no orange and no red vertex share a face, either both red or both orange vertices are inner vertices. Deleting any of these four vertices and inserting one edge such that their partner has degree 3, results in an plane graph of $\mathcal{G}_{8b}$ where additionally, the partner is a vertex of degree 3 stacked into some face. The cyan vertex has odd degree and guarantees that is a plane graph in $[\mathcal{G}_{8b}]$. Since $\mathcal{G}_{8b} = [\mathcal{H}_{2,2}]$ consists of area-universal graphs by Theorem 11, the claim follows for every plane graph of $\mathcal{G}_{10d}$ and $\mathcal{G}_{10e}$. ◀

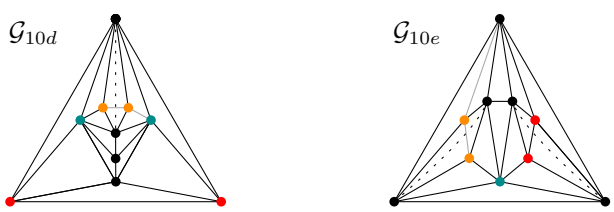

Figure 5.14: $\mathcal{G}_{10d,i}$ and $\mathcal{G}_{10e,i}$ can be obtained by one diamond addition from some $\mathcal{G}_{8b,j}$.

Unfortunately, the situation for the triangulations without p-orders is more diverse.

▶ **Lemma 5.14.** *The plane 4-connected triangulation G on ten vertices without a p-order can be obtained from an area-universal graph by at most*

- *two disjoint diamond additions of order 1 if $G = \mathcal{G}_{10h,1}$,*
- *two disjoint diamond additions of order 1 if $G \in \mathcal{G}_{10i}$,*
- *one diamond addition of order 1 if $G \in \mathcal{G}_{10j}$.*

Moreover, unless $\mathcal{G}_{10h,2}$ or $\mathcal{G}_{9d,3}$ are area-universal, $\mathcal{G}_{10h,2}$ cannot be obtained from an area-universal graph by diamond additions.

Proof. In most cases, the considered graph is obtained by diamond additions from some embedding of the double stacking graph on eight vertices, namely $\mathcal{H}_{2,2} = \mathcal{G}_{8b,1}$. Recall that there exist exactly two different planar 4-connected triangulations on eight vertices, namely the Eulerian triangulation and the planar graph of $\mathcal{H}_{2,2}$. Hence, a vertex of odd degree certifies a plane graph of $[\mathcal{H}_{2,2}]$; all of which are area-universal by Theorem 11.

As Figure 5.15(a) illustrates, $\mathcal{G}_{10h,1}$ can be obtained from a plane graph of $[\mathcal{H}_{2,2}]$ by two diamond additions. We delete the two red vertices with a reverse diamond addition; the cyan vertex certifies an odd vertex degree. This shows the claim for $\mathcal{G}_{10h,1}$.

The graph $\mathcal{G}_{10h,2}$ has a unique inner vertex of degree 4; this vertex is displayed in red in Figure 5.15(c). However, its removal either leads to $\mathcal{G}_{9d,3}$, which has open status, or to $\mathcal{G}_{9d,1}$, which is not area-universal. Thus, it cannot be obtained from an area-universal graph unless $\mathcal{G}_{9d,3}$ or $\mathcal{G}_{10h,2}$ itself are area-universal.

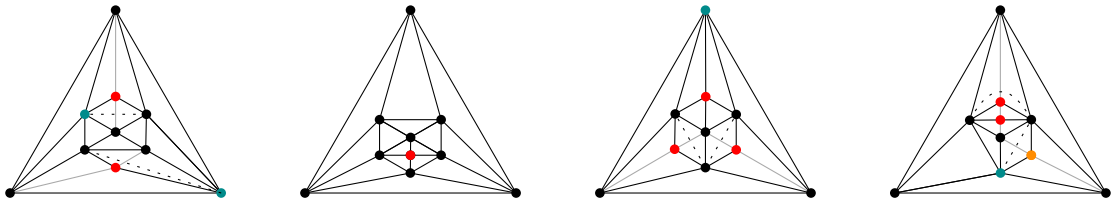

(a) $\mathcal{G}_{10h,1}$ (b) $\mathcal{G}_{10h,2}$ (c) $\mathcal{G}_{10i}$ (d) $\mathcal{G}_{10j}$

Figure 5.15: Illustration of Lemma 5.14 and its proof.

For $\mathcal{G}_{10i}$, consider the three red vertices highlighted in Figure 5.15. Since no two of them share a face, at least two are inner vertices in every embedding. We apply a reverse diamond addition on two inner red vertices as depicted. Again, this results in a triangulation of $[\mathcal{H}_{2,2}]$ as one of the three cyan vertices certifies an odd degree.

For $\mathcal{G}_{10j}$, consider the three colored vertices in red and orange of degree 4. In every embedding at least one of them is an inner vertex, since the orange vertex shares no face with any of the two red vertices. If the orange vertex is inner, then a reverse diamond addition as illustrated results in a graph from $[\mathcal{H}_{2,3}] = [\mathcal{G}_{9b,2}]$, see also Figure 3.23. If one of the red vertices is inner, then we apply a reverse diamond addition such that the other red vertex has degree 3. Its removal produces a graph of $[\mathcal{H}_{2,2}]$ since the cyan vertex guarantees an odd degree. ◀

Lemmas 5.13 and 5.14 enable us to show that plane triangulations with ten vertices have small subdivision number.

■ **Theorem 36.** *For a plane 4-connected triangulation T with ten vertices it holds that $b(T) \leq s(T) \leq 2$. Specifically, for all graphs other than $\mathcal{G}_{10i}$, it holds that $b(T) \leq s(T) \leq 1$.*

Proof. Theorem 33 together with Lemma 5.13 and Lemma 5.14 guarantee that the subdivision number is bounded by 1 for all plane 4-connected triangulations on ten vertices except for $\mathcal{G}_{10h}$ and $\mathcal{G}_{10i}$.

It remains to show that for all i, it holds that $s(\mathcal{G}_{10h,i}) \leq 1$. We claim that the subdivision of $\mathcal{G}_{10h,1}$, depicted in Figure 5.16, is area-universal. Deleting the subdivision vertex and inserting the other diagonal e of the remaining 4-face results in the plane graph $\mathcal{G}_{10f,5}$, which is area-universal by Theorem 16. Given a realizing drawing of $\mathcal{G}_{10f,5}$, we delete e and use Proposition 2.4 to insert the subdivided edge. Since Theorem 16 guarantees that every embedding of $\mathcal{G}_{10f}$ is area-universal, this argument also works for $\mathcal{G}_{10h,2}$. ■

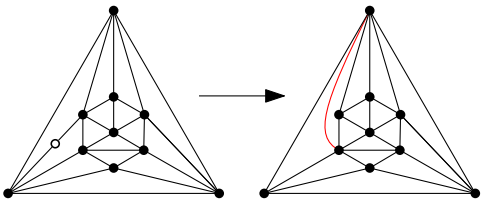

Figure 5.16: This subdivision of $\mathcal{G}_{10h,1}$ is area-universal; since $\mathcal{G}_{10f,5}$ is area-universal.

We have just seen that the small triangulations have a very small bend number. In particular, all small graphs with a p-order have a subdivision number bounded by 1. Recall that every triangulation T with a p-order is *near-3-degenerate*, i.e., there exists an edge e such that $T - e$ is 3-degenerate. We wonder if this holds in general:

¿ Question ? : Is the subdivision number of triangulations with p-orders bounded by 1? By a constant? Or even more general, is the subdivision number of a plane graph G which is 3-degenerate bounded by a constant?

Indeed, for one embedding of a near-3-degenerate triangulation this holds true: Let T be a plane graph with an outer edge e such that $T - e$ is 3-degenerate. Then, by Theorem 17, the graph $T - e$ is area-universal. Since T can be obtained from Q_5 and T_e, Proposition 2.4 implies that subdividing e in T yields an area-universal plane graph.

6 | Related Concepts

In this chapter, we examine several concepts related to area-universality. We have already studied shape restriction in the context of strongly area-universality. In Section 6.1, we investigate convex realizing drawings which are visually very appealing. Unfortunately, they do not always exist neither for plane cubic graphs nor for quadrangulations. However, we present families which allow for convex realizing drawings. In Section 6.2, we consider equiareal drawings in which all faces have the same area. We introduce operations that preserve equiareality and show that all 4-connected triangulations on up to ten vertices have an equiareal drawing. In Section 6.3, we are liberal and also allow negative areas in the area assignments. We show that every plane cubic graph has a realizing drawing, which is not necessarily crossing-free.

6.1 Convex Area-Universality

A drawing of a planar graph is *convex* if each face is the bounded by a convex polygon. As a visually appealing property of drawings, convexity has been studied extensively in graph drawing. Most classically, Tutte's spring embeddings [Tutte, 1963, Tutte, 1960] guarantee convex drawings for every 3-connected planar graph. In this section, we seek for convex realizing drawings, i.e., given an area assignment $\mathcal{A}$ of a plane graph G, we seek an $\mathcal{A}$-realizing drawing of G which is also convex.

Definition. *A plane graph is* convex area-universal *if for all area assignments there exists a convex realizing drawing.*

Since every triangle is convex, straight-line drawings of a triangulations are convex. Thus, it holds that:

Observation 6.1. *A triangulation is area-universal if and only if it is convex area-universal.*

In this sense, convex area-universality generalizes the area-universality of triangulations to plane graphs. Clearly, we must restrict our study to graphs which allow for convex drawings. Here, we consider two graph classes which are sparser than triangulations and therefore have some potential to be convex area-universal: 3-connected cubic graphs and quadrangulations. However, we will show that it is too much to ask for convex area-universality in both cases. Nevertheless, we are able to present some convex area-universal graph classes.

In fact, we have already seen that the cube graph, which is cubic and bipartite, is convex area-universal. Here we present two more elementary proofs.

▶ **Proposition 5.9.** *The cube graph is convex area-universal.*

Proof. We denote the outer vertices of the cube by v_i and the inner vertices by w_i for $i \in [4]$, and the areas of an assignment $\mathcal{A}$ by a, b, c, d, e. Figure 6.1(a) illustrates the labeling.

Proof 1: Choose a triangle $\triangle$ of area $\Sigma\mathcal{A}$ and place the outer vertices v_1, v_2, v_3 on the three corners and v_4 on the segment v_1v_3. Figure 6.1(b) depicts the resulting realizing drawing. Position w_2 such that the face areas a and b are realized by triangular faces with a flat angle at w_1 and w_3. Then place w_3 and v_4 on the segments w_2v_3 and v_1v_3, respectively, such that the area c is realized by the triangle $w_3v_3v_4$. Lastly, w_1 and w_4 can be positioned such that the remaining area is split into d and e as needed.

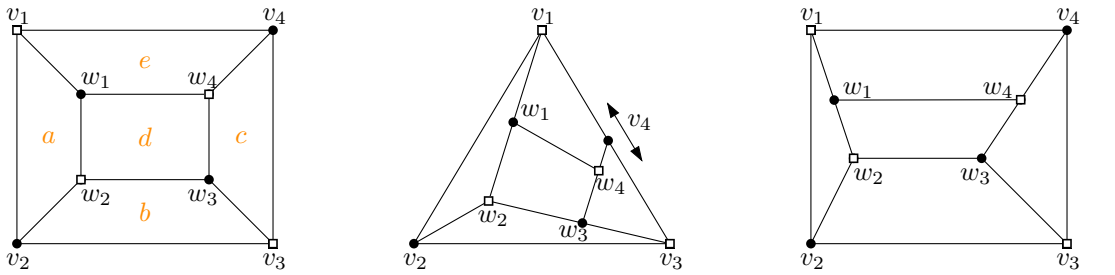

(a) The cube graph.

(b) A convex realizing drawing within a triangle.

(c) A convex realizing drawing within a rectangle.

Figure 6.1: Illustration of the convex area-universality of the cube.

Proof 2: Figure 6.1(c) presents the resulting layout of this proof. Consider a rectangle of area $\Sigma\mathcal{A}$. It holds that $a + c \leq 1/2\Sigma\mathcal{A}$ or $b + e \leq 1/2\Sigma\mathcal{A}$. By symmetry of the cube graph, we may assume that the first inequality holds and that v_1v_2 is a vertical segment as in Figure 6.1(c). Then we realize the areas a and c by triangular faces with corners w_2 and w_3. By our assumption, the x-coordinate of w_2 is at most the x-coordinate of w_3. Moreover, for both vertices, we can choose any y-coordinate in order to realize a and c. Thus, we move w_2 and w_3 to the same y-coordinate such that the area b is realized by a trapezoid. Then there exists a horizontal segment which partitions the remaining area into d and e. We place w_1 and w_4 at the intersections of the segment and the existing edges. Note that all faces are trapezoids and thus convex. ◀

We now generalize this result into two directions. First of all, the cube graph is convex area-universal for every fixed outer face. Secondly, this does not only hold for the cube graph but for all pseudo-double wheels, the angle graphs of wheels. Afterwards we will see that, in general, it is too much to ask for convex realizing drawings of quadrangulations.

6.1.1 Strongly Convex Area-Universal Quadrangulations

In this section, we give an example of a strongly convex area-universal graph family. We say a graph is *strongly convex area-universal* if for every area assignment $\mathcal{A}$ and every convex outer face $f_\circ$ with total area $\Sigma\mathcal{A}$, there exists an $\mathcal{A}$-realizing drawing within $f_\circ$.

Recall that a *pseudo-double wheel* S_k has $2k + 2$ vertices and consist of a cycle with vertices $v_1, v_2, \ldots v_{2k}$ and a vertex v adjacent to all vertices on the cycle with odd index and a vertex w adjacent to all vertices on the cycle with even index, see Figure 6.2(a). We have seen in Section 4.2.1 that pseudo-double wheels are the angle graphs of wheels and that the cube graph is the pseudo-double wheel S_3.

■ **Theorem 37.** *The pseudo-double wheel S_k, $k \geq 3$, is strongly area-universal.*

Proof. For a given area assignment $\mathcal{A}$, we denote the areas incident to the outer edges by a, b, c, d and the remaining areas by $x_4, x_5, \ldots, x_{2k-1}$ with $x_{2k-1} = c$ as depicted in Figure 6.2(a). Let q be a convex quadrangle of area $\Sigma\mathcal{A}$ and corners A, B, C, D identified with the outer vertices of S_k. Observe that at least one of the two inequalities hold:

$$a + b \leq \text{AREA}(ABC) \quad \text{or} \quad c + d \leq \text{AREA}(ACD).$$

By symmetry, we assume without loss of generality that the first inequality holds. Hence, we may place v_3 in the triangle ABC such that the areas a and b are realized by the triangles $v_1v_2v_3$ and v_2wv_3. Now we distinguish two cases. The two resulting layouts are illustrated in Figure 6.2.

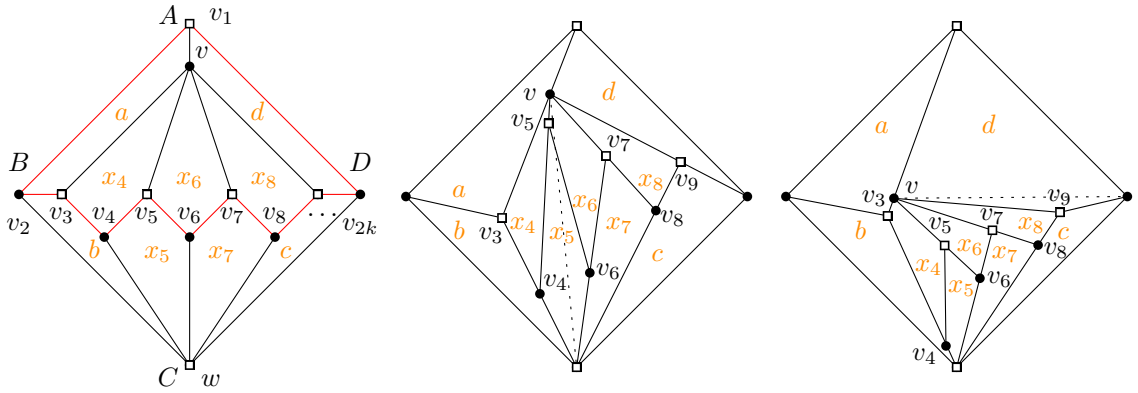

(a) Pseudo-double wheel S_k. (b) Realizing drawing in case 1. (c) Realizing drawing in case 2.

Figure 6.2: Illustration of the proof of Theorem 37.

In case 1, it holds that $d \leq \text{AREA}(Av_3D)$. Figure 6.2(b) visualizes the resulting drawing. Then, we realize the area d by a triangle AvD. We split the remaining quadrangle vv_3CD into two parts by the diagonal vC and determine $i \in [2k-1]$ such that

$$\sum_{j=4}^{i-1} x_j \leq \text{AREA}(vv_3C) \quad \text{and} \quad \sum_{j=i+1}^{2k-1} x_j \leq \text{AREA}(vCD).$$

By construction, v_4 and v_{2k-1} must be placed on a specific segment. Placing v_j, we realize the area x_j by a triangle for all $j < i$. Specifically, x_j is realized by the triangle $uv_{j-1}v_j$ where $u := v$ if j is even and $u := w$ if j is odd. The angle at v_{j+1} is straight and thus v_{j+1} can be places anywhere on the segment uv_j. Likewise for all $j > i$, we realize the area x_j by the triangle uv_jv_{j+1} with $u := v$ if j is even and $u := w$ if j is odd, by positioning v_j accordingly. It remains the quadrangle $vv_{i-1}wv_{i+1}$ of area x_i. Vertex v_i is placed at v if i is odd and at w if i is even.

In case 2, it holds that $d > \text{AREA}(Av_3D)$. Figure 6.2(c) visualizes the resulting drawing. We place v at v_3 and v_4 at w. We place v_{2k-1} such that the area c and d are realized. In decreasing order, we place v_i such that x_i is realized by the triangle uv_iv_{i+1} with $u := v$ if i is even and $u := w$ if i is odd. (Alternatively, inserting the edges (v, v_{2j}) and (w, v_{2j+1}) yields a stacked triangulation within vwv_{2k}.) ■

6.1.2 Quadrangulations are not Convex Area-Universal

In this section we discuss the following question:

¿ Question ? : Are 3-connected quadrangulations convex area-universal?

The restriction to 3-connectedness stems from the fact that not all 2-connected quadrangulations allow for convex drawings; whereas Tutte's spring embeddings [Tutte, 1963] guarantee convex drawings of 3-connected planar graphs. Even though we hoped for a positive result, we answer the question in the negative.

■ **Theorem 38.** *There exists a 3-connected quadrangulation which is not convex area-universal.*

Proof. We show that the 3-connected quadrangulation Q, depicted in Figure 6.3(b), has an area assignment which does not allow for a convex drawing in any (even non-convex) outer face. Our construction is based on a non-realizable area assignment of the octahedron graph. As before we encode the area assignment with a white/gray face coloring of the octahedron illustrated in Figure 6.3(a). Theorem 5 and Corollary 3 guarantee that the following area assignment is not realizable.

▶ **Proposition 6.2.** *For small enough $\varepsilon > 0$, the octahedron graph has no drawing where the white faces have area of at most ε and the gray faces have area of at least 1.*

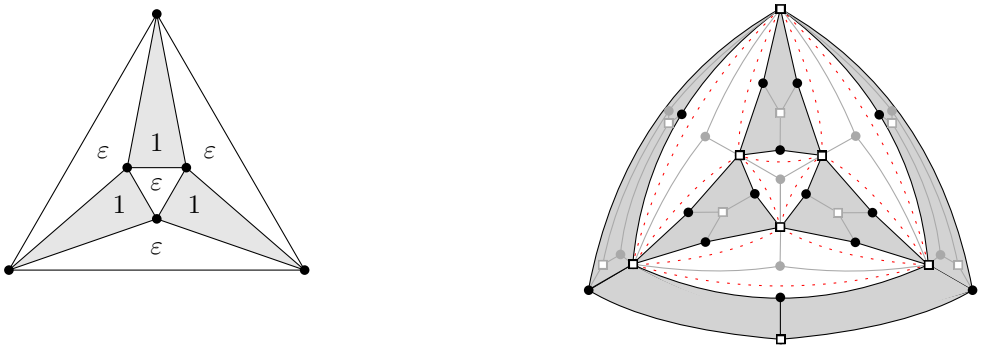

(a) A non-realizable area assignment of the octahedron graph.

(b) The quadrangulation Q and its black subgraph Q'.

Figure 6.3: Illustration of Theorem 38 and its proof.

We will give an area assignment of Q such that a convex realizing drawing of Q induces a realizing drawing of this non-realizable area assignment of the octahedron. To do so, we first consider the black subgraph Q' of Q depicted in Figure 6.3(b); it is a 1-subdivision of the octahedron graph together with a framing quadrangle and three additional edges. We call the two classes of the vertex bipartition the *squared* and *circled* vertices.

▶ **Lemma 6.3.** *For small enough $\varepsilon > 0$, Q' has no drawing where the white faces have area ε, the gray faces have area 1, and each white face is convex.*

Proof. For a contradiction suppose that there exists a drawing D with the above properties. By convexity, a segment between two squared vertices of a white face f is contained in f. Therefore, these segments and the square vertices yield a drawing D' of the octahedron, illustrated in Figure 6.3(b) by the red dotted graph, in which the area of each white face is at most ε and of each gray face at least 1. However, D' contradicts Proposition 6.2. ◀

Finally, we enhance Q' to the 3-connected triangulation Q by carefully inserting edges and vertices such that the (red dotted) segments between two squared vertices are still contained in a white face if it is convex. In particular, the new edges are only joined to squared vertices. Dividing the areas of the white and gray regions arbitrarily yields area assignment of Q such that any convex realizing drawing contradicts Lemma 6.3. ■

Remark. Since we did not use the shape of the outer face in the proof of Theorem 38, Q does not have a realizing drawing of the considered area assignment where each inner face is convex.

Remark. The construction of Q in the proof of Theorem 38 is based on the octahedron graph. Since the analogous result of Proposition 6.2 holds for any Eulerian triangulation by Theorem 5, the same idea allows to construct further non-convex area-universal quadrangulations from any Eulerian triangulation.

6.1.3 Cubic Graphs are not Convex Area-Universal

Clearly, one can wonder about convex area-universality for further graph classes. In this section we consider convex realizing drawings of plane cubic graphs. However, we show the analogous result of Theorem 38, i.e., convex drawings do not exist in general.

■ **Theorem 39.** *There exists a 3-connected plane cubic graph that is not convex area-universal.*

Proof. Let G denote the plane cubic graph and $\mathcal{A}$ the area assignment depicted in Figure 6.4(a). Suppose, for a contradiction, that there exists a convex $\mathcal{A}$-realizing drawing D of G. By convexity and the fact that the faces incident to outer edges have area 0, each inner vertex must be placed on an outer edge in D. Note that the neighbor of an outer vertex must be placed on two outer segments simultaneously and hence it coincides with the outer vertex. Consequently, we obtain a hexagon inscribed in a triangle as depicted in Figure 6.4(b).

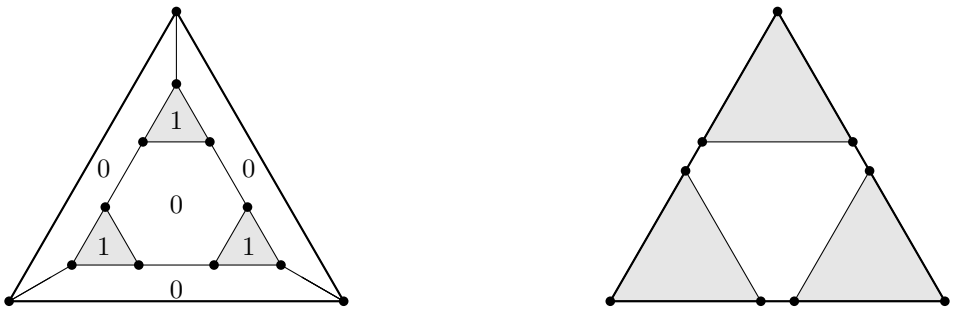

(a) The cubic graph G with area assignment $\mathcal{A}$.

(b) A hexagon inscribed in a triangle.

Figure 6.4: This cubic graph has no convex drawing realizing the prescribed face areas.

Hence, it remains to place two vertices per outer segment. The central hexagonal face is minimal if the two vertices coincide. Therefore, the problem reduces to finding a realizing drawing of the octahedron graph with an non-realizable white/gray area assignment as in the proof of Theorem 5. ■

6.2 Equiareality

There exist various concepts for *visually appealing* graph drawings. Several commonly used quality measures concern the lengths of edges. For instance, uniformity of edge lengths is a desirable quality and has been studied for planar graphs in the context of *matchstick graphs* [Harborth, 1994, Kurz and Pinchasi, 2011, Abel et al., 2016]. A *matchstick graph* is a graph that has a planar straight-line drawing where all edges are of the same length. The name originates from the fact that a matchstick graphs can be represented by placing non-crossing matchsticks in the plane.

In a similar flavor, we consider drawings where all inner faces are of the same size. This concept was introduced by Ringel [Ringel, 1990].

Definition. *A plane graph is* equiareal *if there exists a drawing where all inner faces have the same area.*

Clearly, every area-universal graph is equiareal. Figure 6.5 presents several equiareal drawings. They indicate that these drawings are quite aesthetic and seem to reflect symmetries nicely. The drawings have been produced by computer experiments with the airpressure method. For an introduction to the airpressure method consider Chapter 8.

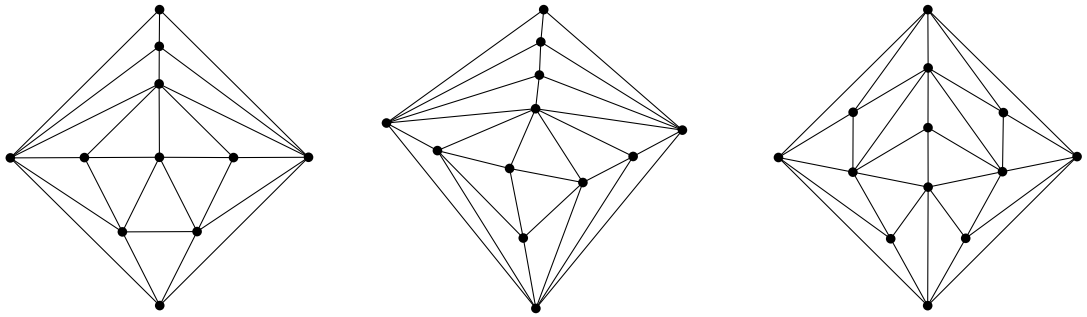

Figure 6.5: Some equiareal drawings of 4-connected near-triangulations.

Our first observation concerns the fact that equiareality is indeed a property of plane graphs rather than planar graphs. Recall that no such example is known for area-universality.

▶ **Proposition 6.4.** *Equiareality is a property of plane graphs.*

Proof. The two plane graphs G and G' depicted in Figures 6.6(a) and 6.6(b) are different embeddings of the same planar graph. We claim that one is equiareal while the other is not. On the one hand, an equiareal drawing G is given in Figure 6.6(c). Thus G is equiareal. On the other hand, Ringel [Ringel, 1990] showed that G' is not equiareal as we discussed in Section 3.1.1. ■

Recall that the non-area-universality of the graphs relied on the fact that some faces have large area while others have small area. By splitting faces of large area into several faces, the non-area-universal graphs yield examples of further non-equiareal graphs. However, this face splitting is forbidden when we restrict to the class of 4-connected graphs. Naturally, we wonder:

¿ Question ? : Is every 4-connected triangulation equiareal?

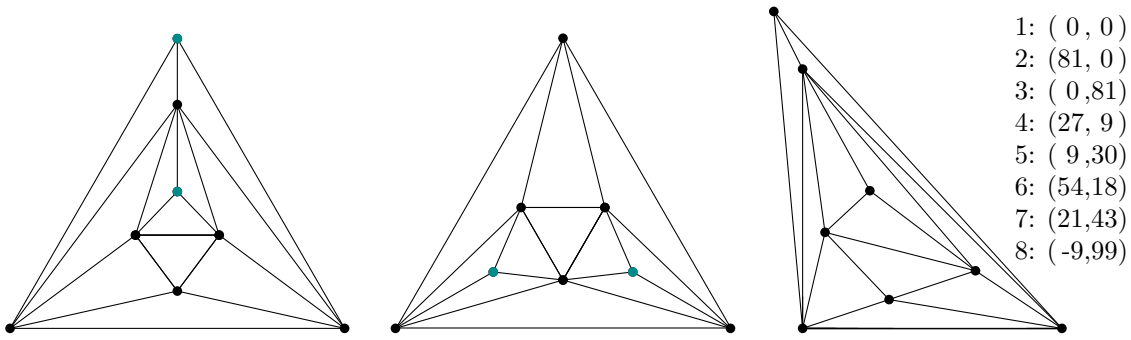

(a) G is equiareal. (b) G' is not equiareal. (c) An equiareal drawing of G.

Figure 6.6: Equiareality is a property of plane graphs.

For a start, we discuss an equiareal preserving operation. As seen in the previous section diamond addition sometimes maintains area-universality. Here we observe a similar behavior for equiareality. To do so, we consider two diamond additions as *disjoint* if the subdivided triangles are different.

■ **Theorem 40.** *Let G be a plane graph which is obtained from an area-universal graph G' by one or several disjoint diamond additions. Then G is equiareal.*

Proof. We construct an equiareal drawing of G with the help of a special realizing drawing of G'. Let $E_\diamond$ denote the set of edges of G' on which a diamond addition is applied in order to obtain G. Let $e \in E_\diamond$. Let t^1 and t^2 be the two faces incident to e and σ the order of the diamond addition applied on e. We define an area assignment $\mathcal{A}$ of G' such that $\mathcal{A}(t^1) = \mathcal{A}(t^2) = \sigma + 1$. In this way, we prescribe the area of each face incident to an edge of $E_\diamond$. Since the diamond additions are disjoint, no face is incident to two edges of $E_\diamond$. For all remaining inner faces f of G, we define $\mathcal{A}(f) = 1$.

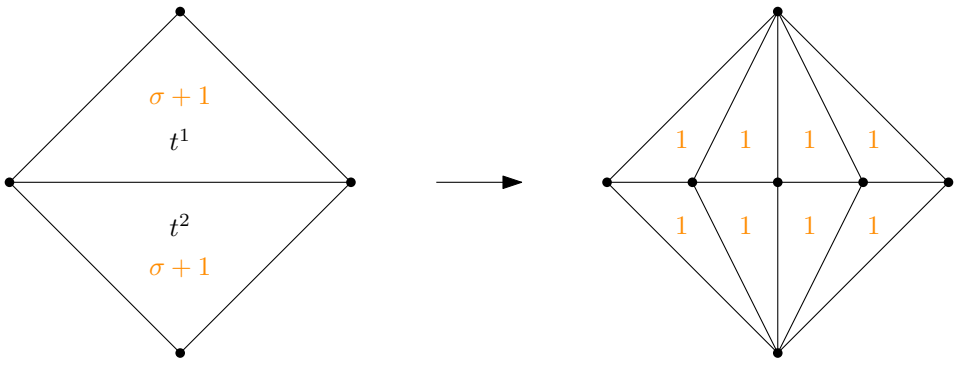

Figure 6.7: Illustration of Theorem 40 and its proof for a diamond addition of order three. The edge e is partitioned into 4 segments of equal length.

Since G' is area-universal there exists an $\mathcal{A}$-realizing drawing D' of G'. We perform the diamond addition on D' in order to obtain a drawing of G in the following manner: We partition each edge $e \in E_\diamond$ in $\sigma + 1$ segments of equal length and place the σ vertices on the endpoints of these segments. Figure 6.7 illustrates this construction. Consequently, each of the two triangles t^1 and t^2 is partitioned into $\sigma + 1$ triangles of equal size. Therefore, each face of G' has area 1 and we have an equiareal drawing of G. ■

We can apply Theorem 40 to show equiareality of double stacking graphs. This implies that there exist 4-connected equiareal triangulations on n vertices for every n.

■ **Corollary 41.** *Every plane triangulation in* $[\mathcal{H}_{\ell,k}]$ *is equiareal.*

Proof. Let H be a plane graph in $[\mathcal{H}_{\ell,k}]$ with $\ell \cdot k > 1$. By Observation 5.12, H can be obtained by one diamond addition from a graph in $[\mathcal{H}_{\ell-1,k}]$ if $\mathcal{H}_{\ell-1,k}$ exists or otherwise from a graph in $[\mathcal{H}_{\ell-1,k}]$. Theorem 11 ensures the area-universality of all graphs in $[\mathcal{H}_{\ell,k}]$ when $\ell \cdot k$ is even. Therefore, H is either already area-universal, and thus also equiareal, or can be obtained by one diamond addition from an area-universal graph. In the latter case, Theorem 40 ensures its equiareality. ■

Moreover, Theorem 40 provides us with a simple proof that a non-equiareal 4-connected triangulation has at least eleven vertices.

■ **Corollary 42.** *Every plane 4-connected triangulation* T *with* $n \leq 10$ *is equiareal.*

Proof. For $n \leq 9$, the claim follows from Lemma 5.11 and Theorem 40. For $n = 10$, the claim follows from Lemmas 5.13 and 5.14 and Theorem 40 except for the plane graph $\mathcal{G}_{10h,2}$ which is illustrated in Figure 6.8(a).

Most likely, $\mathcal{G}_{10h,2}$ cannot be obtained from an area-universal graph by disjoint diamond additions. Therefore, we give an explicit equiareal drawing which is depicted in Figure 6.8(b): Starting from a realizing drawing for the illustrated $(1, 2, 5)$-assignment of the octahedron, we insert a vertex of degree 3 in the face of area 5 which splits the area into two triangles of area 2 and one triangle of area 1. In Figure 6.8(b) this vertex is highlighted in orange.

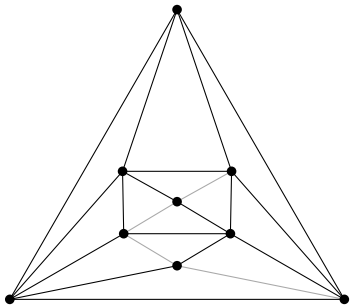

(a) The plane graph $\mathcal{G}_{10h,2}$.

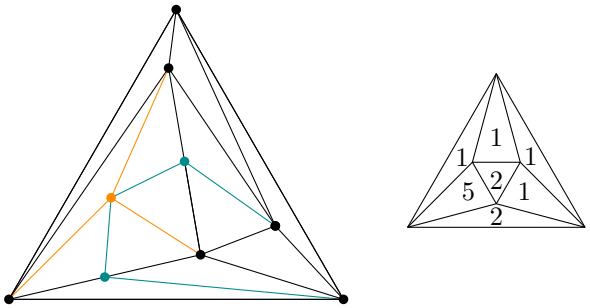

(b) An equiareal drawing of $\mathcal{G}_{10h,2}$ constructed from a $(1, 2, 5)$-assignment of the octahedron graph.

Figure 6.8: The plane graph $\mathcal{G}_{10h,2}$ and an equiareal drawing of it.

The insertion results in four faces of area 2. Applying two diamond additions by inserting the vertices on the midpoints of their edge, we obtain a realizing drawing of $\mathcal{G}_{10h,2}$. The vertices added in the last step are colored in cyan in Figure 6.8(b). ■

Finally, we discuss the equiareality of the triangulation on 13 vertices depicted in Figure 6.9(a). We mentioned in the introduction that Sabriego and Stump investigated the question whether all 4-connected triangulations are equiareal. In particular, they tried to heuristically find a 4-connected triangulations which is not equiareal. They tested one plane graph of every planar triangulation on up to 13 vertices (and some with 14 vertices). For the triangulation on 13 vertices, which is depicted in Figure 6.9(a), their heuristic did not find a close to equiareal drawing. Therefore, they wondered whether it is not equiareal.

However, with our developed machinery, it is easy to see that the triangulation is equiareal.

▶ **Proposition 6.5.** *The plane triangulation T depicted in Figure 6.9(a) is equiareal.*

Proof. Note that T can be obtained by two disjoint diamond additions from the graph T' depicted in Figure 6.9(b). Since T' is the accordion graph $\mathcal{K}_1$ on seven vertices where a vertex of degree 3 is stacked into one face, T' is area-universal by Proposition 3.28. Consequently, T can be obtained from an area-universal graph by several disjoint diamond additions and is thus equiareal by Theorem 40. ◀

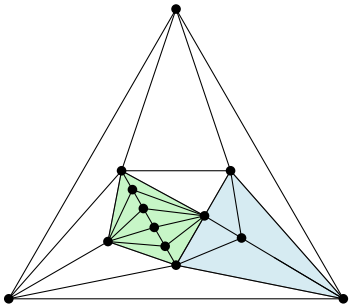

(a) A plane triangulation on 13 vertices.

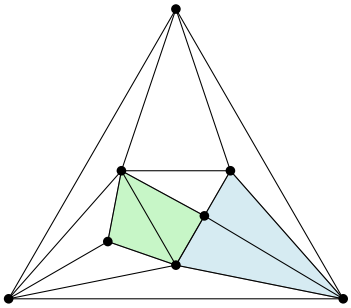

(b) The accordion graph $\mathcal{K}_1$ with a vertex of degree 3 stacked into one face.

Figure 6.9: Illustration of Proposition 6.5 and its proof.

6.3 Negative Areas and Plane Cubic Graphs

This section is based on joint work with Alexander Igamberdiev. We alter our problem in two directions. In one aspect we are more demanding and in the other aspect more generous. In particular, we want to consider generalized area assignments which also allow for negative face areas. However, this forces us to refrain from planarity.

To do so, we need some notation. A *generalized area assignment* of a plane graph G is a function $\mathcal{A}\colon F' \to \mathbb{R}$. We also have to clarify what we mean by the area of a face in a drawing with crossings. Let G be a plane graph with vertex placement D. For an inner face $f = (v_1, \ldots, v_k)$ of G, we define the area of f in D with the *shoelace formula* as in Equation (2.2):

$$2 \cdot \textsc{area}(f, D) = \sum_{i=2}^{k-1} \mathrm{Det}(v_1, v_i, v_{i+1}).$$

We say a generalized area assignment $\mathcal{A}$ is *realizable* if there exists a vertex placement D such that for each inner face f it holds that $\textsc{area}(f, D) = \mathcal{A}(f)$. We show that every generalized area assignment of a plane cubic graph is realizable.

■ **Theorem 43.** *Let G be a plane cubic graph and $\mathcal{A}\colon F' \to \mathbb{R}$ a generalized area assignment. Then $\mathcal{A}$ is realizable.*

We prove this statement in three steps. First, we show the claim for the triangular prism, depicted in Figure 6.10, then for 3-connected plane cubic graphs and finally for plane cubic graphs which are at most 2-connected.

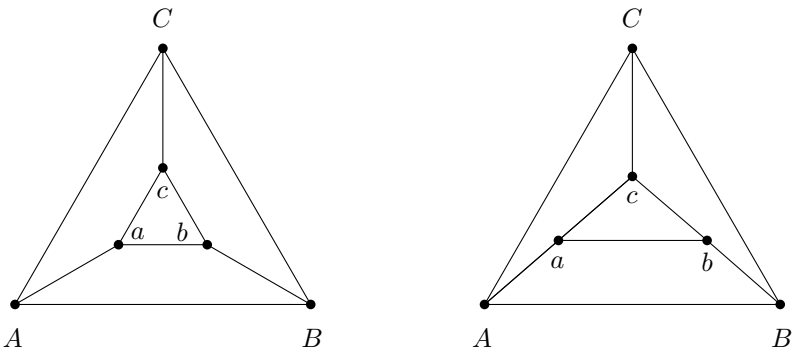

Figure 6.10: The triangular prism and a layout realizing all positive area assignments.

▶ **Lemma 6.6.** *Every generalized area assignment of the triangular prism is realizable.*

Proof. We label the vertices of the triangular prism as depicted in Figure 6.10 and realize one face area after the other. We start by realizing the central face abc by any triangle of correct area, for example, we set $a = (0, 0)$, $b = (2, 0)$ and $c = (0, \mathcal{A}(abc))$ as in Figure 6.11. Note that this definition respects the sign of the area.

Secondly, we realize the bottom face $ABba$. For this we identify A and a and place B on the line supported by b and c such that the face area of $ABba$ is realized. Note that ac and Bc serve as the base segment for the remaining two faces. Hence, we may place C in the intersection point of the two height lines. This finishes the proof.

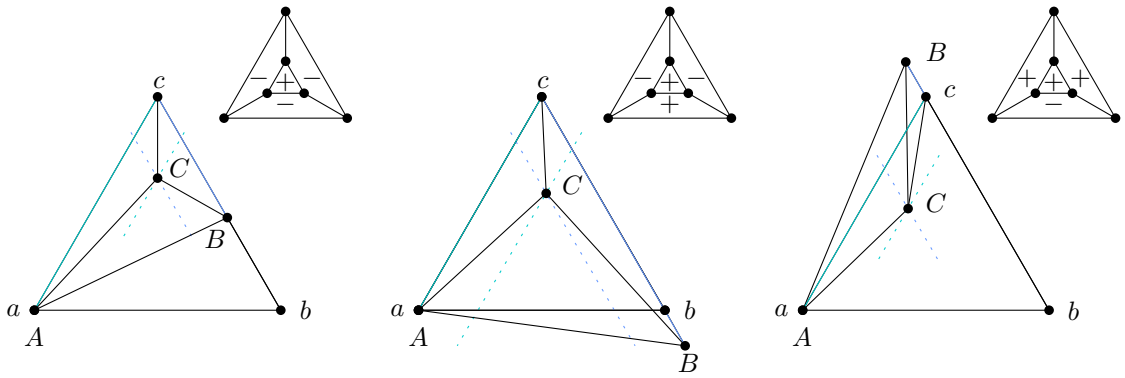

Figure 6.11: Different layouts of the triangular prism to realize all generalized area assignment. If the central face has positive area, there are three depicted layouts and additionally, the one when all areas have positive sign.

Figure 6.11 displays the different layouts when the central face is positive (and at least one face is negative.) The other three layouts can be obtained by taking the mirror image of the graph and reversing the sign of the area assignment. ◀

6.3.1 3-connected Plane Cubic Graphs

Next, we show that all plane 3-connected cubic graphs may realize any generalized area assignment. We use the following observation.

Observation 6.7. *Let D be a vertex placement of a plane graph G with a vertex v of degree 3. Let ℓ denote a line through two neighbors w_1 and w_2 of v. Let u denote the third neighbor of v and f_i the face incident to u, v, w_i. Moving v on the line through v parallel to ℓ, except for the two faces f_1 and f_2 incident to v, all faces areas are maintained.*

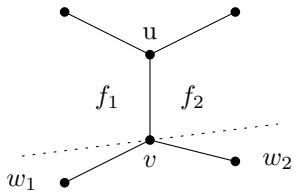

Figure 6.12: By moving v on the indicated line, area between f_1 and f_2 can be exchanged.

Here, we show the following theorem.

▶ **Proposition 6.8.** *For a plane 3-connected plane cubic graph every generalized area assignment $\mathcal{A}\colon F' \to \mathbb{R}$ is realizable.*

The proof is inductive and uses the fact that plane cubic graphs can be constructed by iteratively inserting edges starting from the triangular prism. Here an *edge-insertion* is an operation of the following type, see also Figure 6.13: Given a plane cubic graph, choose a face f and two of its edges e_1 and e_2. For $i \in [2]$, subdivide e_i with v_i and insert a new edge (v_1, v_2). Note that this operation maintains 3-connectedness. In fact, every cubic graph can be constructed with this operation.

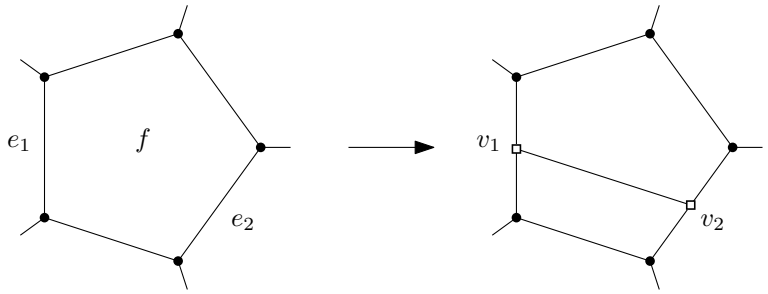

Figure 6.13: An edge-insertion into a face of a plane cubic graph.

.

▶ **Lemma 6.9** ([Igamberdiev et al., 2017]). *Every 3-connected plane cubic graph, different from K_4, can be constructed from triangular prism by a sequence of inner edge insertions, i.e., no edge is inserted in the outer face.*

Now, we are ready to prove the theorem for 3-connected graphs.

Proof of Proposition 6.8. We show the claim by induction with the help of Lemma 6.9. Since it excludes K_4, we show the claim separately: Let a_1, a_2, a_3 be an area assignment to the three inner triangles of K_4. Fix a triangle whose area equals the total area $h := \sum a_i$, for example, $(0,0)$, $(2,0)$ and $(0,h)$. It is easy to check that placing the inner vertex at $(2/h \cdot a_2, a_1)$ fulfills all conditions.

The induction base for the triangular prism is established by Lemma 6.6.

For the induction step, we realize a generalized area assignment $\mathcal{A}$ of G which can be obtained from G' by an edge insertion into f where $e_1 := (u_1, w_1)$ and $e_2 := (u_2, w_2)$ are subdivided by vertices v_1 and v_2. Inserting the edge gives two new faces which we call f_u and f_w, respectively. We consider an $\mathcal{A}'$-realizing vertex placement D' of G' which coincides with $\mathcal{A}$ except for the fact that $\mathcal{A}'(f) := \mathcal{A}(f_u) + \mathcal{A}(f_w)$.

The idea of the construction is visualized in Figure 6.14: In D', we place v_1 on the edge e_1 such that v_1 does not lie on the line ℓ supported by e_2. This is possible if and only if both edges do not have the same supporting line. Consider the triangulation of f_u and f_w where v_1 is the center. The area of the polygon f_u and f_w can be corrected by the area of the triangles $v_1v_2u_2$ and $v_1v_2w_2$, respectively. Since v_1 does not lie on ℓ, moving v_2 along ℓ continuously (and monotonically) changes the area of the triangle $v_1v_2u_2$. Consequently, there is a unique position for v_2 on the line ℓ such that f_u has correct area. Since $\mathcal{A}'(f) := \mathcal{A}(f_u) + \mathcal{A}(f_w)$ and f has area in $\mathcal{A}'(f)$ in G', the area of f_w is also correct for this position of v_2.

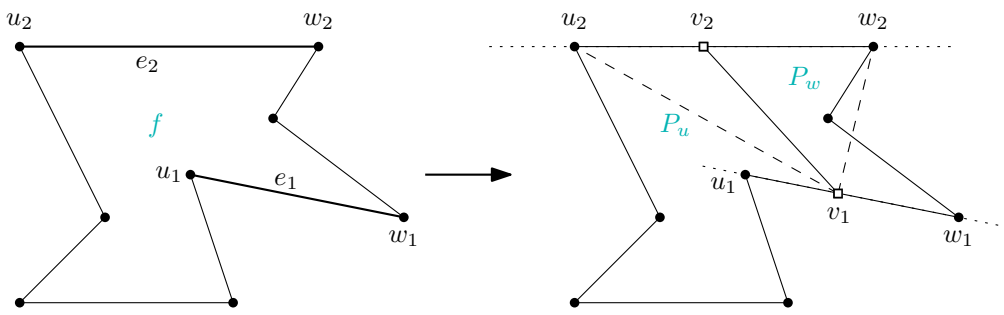

Figure 6.14: Illustration of the induction step.

We ensure that e_1 and e_2 do not have the same supporting line by a stronger induction hypothesis: There exists a realizing drawing where no two edges of any inner face are collinear.

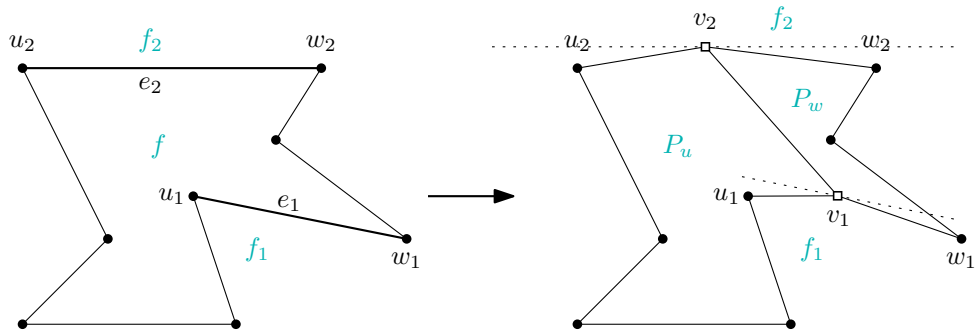

Figure 6.15: Illustration of the stronger induction step such that no face has collinear edges.

In the current idea, there exist two issues with collinear edges. Firstly, by subdividing an edge, the two new edges have the same supporting line. Secondly, the new inserted edge may be collinear with an existing edge. As before, let f be a face in G' with edges e_1 and e_2. Let f_1 and f_2 denote the other faces incident to e_1 and e_2 as depicted in Figure 6.15. In $\mathcal{A}$, we shift a small $\varepsilon > 0$ of the area of f_1 to f_2 and use the strong induction hypothesis to consider a realizing drawing for this modified area assignment. In order to obtain a realizing drawing of $\mathcal{A}$ we may place v_1 and v_2 on lines ℓ_1 and ℓ_2 parallel to e_1 and e_2, respectively. Since the number of edges is bounded, only finitely many points on these two lines are *problematic*, i.e., cause pairs of collinear edges. For a fixed position of v_1 on ℓ_1, there exists a unique position of v_2 on ℓ_2. Observe that if v_1 moves continuously between two problematic points on ℓ_1, v_2 also moves continuously on ℓ_2. Therefore, there exists an unproblematic position of v_1 which yields an unproblematic position of v_2. ◀

6.3.2 General Plane Cubic Graphs

Now, we prove the claim for all plane cubic graphs.

■ **Theorem 43.** *Let G be a plane cubic graph and $\mathcal{A}\colon F' \to \mathbb{R}$ a generalized area assignment. Then $\mathcal{A}$ is realizable.*

Proof. Proposition 6.8 establishes the proof for 3-connected plane graphs. Therefore, we now show how to obtain the result for less connected graphs.

If G is at most 1-connected we easily obtain the result by induction: Let v be a vertex such that $G[V - v]$ is not connected. Let V_1 be the vertex set of one component of $G[V - v]$ and consider $G_1 := G[V_1 + v]$ and $G_2 := G[V \backslash V_1]$. By induction we obtain realizing drawings for G_1 and G_2. Identifying v in both drawings yields a realizing drawing of G.

It remains to consider the case that G is 2-connected. Since G is cubic, there also exists a cut containing only 2 edges. (If v_1 and v_2 form a separator, consider the edges from v_1 and v_2 to at least two components. By pigeon hole principle, v_i has only one edge to at least one component. In all cases we find a cut consisting of two edges.) Let G_1 and G_2 denote the components after deletion of the edges of a 2-cut, see also Figure 6.16.

Observe that G_i contains two vertices of degree 2 and is therefore not cubic. We call these two vertices the anchors of G_i. If the anchors are not adjacent in G_i, then we insert the edge between them and obtain a cubic graph.

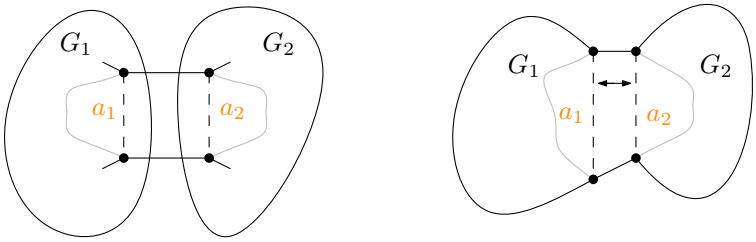

Figure 6.16: Illustration of the proof of Theorem 43 for 2-connected plane cubic graphs with non-adjacent anchors.

Suppose that the trick works in both graphs G_1 and G_2. Then we split the area assignment arbitrarily among the three new faces, see also Figure 6.16. Given a realizing drawing for G_i, we rotate the drawing such that the line through the anchors is vertical. Then we adjust the distance of the vertical lines through the anchors in the drawing of G_1 and G_2 such that the central 4-face has the prescribed area.

If the anchor vertices of G_i are adjacent in G_i, then we delete the anchors from G_i and define their two unique neighbors in the remaining graph as the new anchor vertices. Note that a common neighbor of the two anchors of G_i serves as a separator in G. Consequently, the anchors have two unique neighbors. We repeat this operation until the anchor vertices share no edge. Since the graph is finite, the procedure stops. Finally, G_1 and G_2 are connected by a sequence of 4-faces as depicted Figure 6.17 and their anchors are not adjacent.

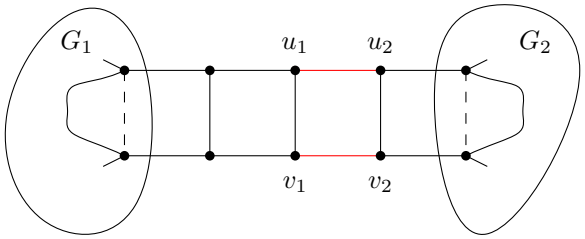

Figure 6.17: Illustration of the proof of Theorem 43 for 2-connected plane cubic graphs with adjacent anchors.

We find realizing vertex placements for G_i by induction. For the central part we may take a representation where all pairs of vertices which where anchor pairs are placed on a vertical line. Then we glue all parts as before. ■

7 | Computational Complexity

This chapter is based on joint work with Michael Dobbins, Tillmann Miltzow, and Paweł Rzążewski. The results also appear in [Dobbins et al., 2018]. We are interested in the computational complexity of deciding if a given plane graph is area-universal and denote this problem by Area Universality.

Area Universality
Input: Plane graph $G = (V, E)$.
Question: Is G area-universal?

Even though the computational complexity of Area Universality is still open, we have an intriguing conjecture. To support our conjecture we show hardness of several variants of Area Universality indicating that our conjecture might reflect the truth. The chapter is organized as follows: We start with an introduction to our considered computational complexity class. Afterwards we show hardness of three variants.

7.1 Introduction to the Complexity Class $\forall\exists\mathbb{R}$

When investigating natural geometric problems, one often discovers that an instance can be described as a first-order formula over the reals in prenex form containing only existential quantifiers:

$$\exists X_1, X_1, \ldots, X_n \colon \Phi(X_1, X_2, \ldots, X_n).$$

The variables encode the configuration of the geometric objects and the quantifier-free formula Φ describes the relations between them. A value assignment X satisfying Φ corresponds to a solution of the original geometric problem.

More precisely,Φ is a quantifier-free boolean formula built of constants 0 and 1, arithmetic operators $(+, -, \times)$, relation symbols $(<, \leq, =, \neq)$, logic symbols $(\wedge, \vee, \neg, \Leftrightarrow)$, variable symbols, and parentheses, using standard syntactic rules. All variables are assumed to be real numbers, all arithmetic operators and relational symbols are interpreted as operators and relations over $\mathbb{R}$. Moreover, the quantifiers range over all reals. Indeed, every boolean formula of this type which additionally contains quantifiers can always be transformed such that all quantifiers appear in the beginning. If a formula has this appearance, it has the so-called *prenex form*.

The computational problem Existential Theory of the Reals (ETR) takes a boolean formula in prenex form as an input and asks whether it is true or not. The

complexity class ∃ℝ consists of all problems that reduce in polynomial time to ETR. Here we consider the classical Karp reductions in the Turing model. Interestingly, many natural geometric problems are not only contained in ETR, but also appear to be ∃ℝ-complete. A prominent example is the stretchability of pseudoline arrangements; see also [Matoušek, 2014, Mnëv, 1988, Schaefer and Štefankovič, 2017].

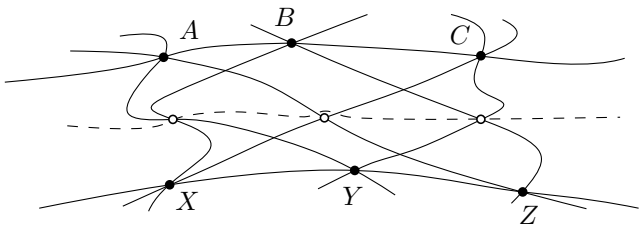

Figure 7.1: A non stretchable pseudoline arrangement.

A *pseudoline arrangement* in the plane is a set of unbounded x-monotone Jordan curves where every pair of curves intersects in exactly one crossing point. A pseudoline arrangement is *stretchable* if there exists an arrangement of straight lines with the same face structure. Stretchability is a computational problem which asks whether a given pseudoline arrangement is stretchable. The ∃ℝ-completeness of Stretchability reflects the deep algebraic connections between line arrangements and real algebra. This connection has important consequences. The first consequence is that there is little hope to find a simple combinatorial algorithm for Stretchability, since simple combinatorial algorithms to decide ETR are not known. In fact, without certain algebraic tools allowing to bound the length of integer coordinate representations, we would not even know if Stretchability is decidable (see [Matoušek, 2014]). However, it is not just difficult to decide whether a given pseudoline arrangement is stretchable. It requires algebraic arguments. For instance, the non-stretchability of the (smallest non-stretchable) pseudoline arrangement depicted in Figure 7.1 is based on Pappus's Hexagon Theorem [Levi, 1926], dating back to the 4th century.

■ **Theorem** (Pappus's Hexagon Theorem)**.** *Let A, B, C be three points on a straight line and let X, Y, Z be three points on another line. If the lines $\overline{AY}, \overline{BZ}, \overline{CX}$ intersect the lines $\overline{BX}, \overline{CY}, \overline{AZ}$, respectively, then the three points of intersection are collinear.*

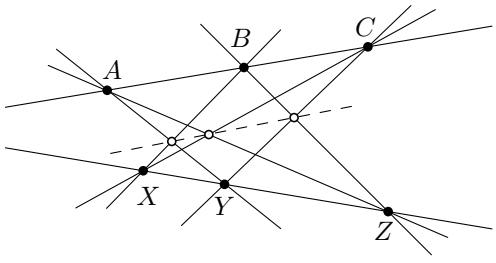

Figure 7.2: Illustration of Pappus's Hexagon Theorem.

Although the statement of Pappus's Hexagon Theorem is intrinsically geometric, it is non-trivial to prove and most known proofs have some algebraic flavor, see [Richter-Gebert, 2011, Chapter 1].

As mentioned before, geometric problems that are $\exists\mathbb{R}$-complete usually ask for the existence of certain objects, satisfying properties that are easy to check. However, the nature of Area Universality seems to be different. We therefore define the complexity class $\forall\exists\mathbb{R}$ as the set of all problems that reduce in polynomial time to Universal Existential Theory of the Reals (UETR). The input of UETR is a first order formula over the reals in prenex form, which starts with a block of universal quantifiers followed by a block of existential quantifiers and is otherwise quantifier-free. We ask if the formula is true.

Universal Existential Theory of the Reals (UETR)
Input: A formula over the reals of the form
$(\forall\, Y_1, Y_2, \ldots, Y_m)\,(\exists\, X_1, X_2, \ldots, X_n) : \Phi(X_1, X_2, \ldots, X_n, Y_1, Y_2, \ldots, Y_m)$,
where Φ is a quantifier-free formula with variables $Y_1, Y_2, \ldots, Y_m, X_1, X_2, \ldots, X_n$.
Question: Is the input formula true?

It is straightforward to show that Area Universality belongs to $\forall\exists\mathbb{R}$. We have seen all necessary ideas already in Section 2.3. The idea of the proof is to use a block of universal quantified variables to describe the area assignment and a block of existential quantified variables to describe the placement of the vertices of a drawing of G.

▶ **Proposition 7.1.** Area Universality *is in* $\forall\exists\mathbb{R}$.

Proof. Let G be a plane graph with n vertices and k faces. We describe a formula $\Psi \in$ UETR of polynomial size such that G is area-universal if and only if Ψ is true. We use the universal quantifiers for the areas and the existential quantifiers for the coordinates of the vertices. We represent the coordinates of a vertex v_i by (x_i, y_i). We have seen the essential part of the quantifier free formula already in Chapter 2. Recall that, by Proposition 2.17, for every area assignment $\mathcal{A}$ of G there exists a system $\mathcal{E}(G, \mathcal{A})$ of polynomial equations (of polynomial size) which has a real solution if and only if $\mathcal{A}$ is realizable. A tuple of real numbers $(a_1, \ldots, a_k)$ is an area assignment if and only if all entries are positive; we write $\mathcal{A} := (a_1, \ldots, a_k)$. Hence, our instance of UETR reads as follows:

$$\forall(a_1, \ldots, a_k) \in \mathbb{R}\ \exists(x_1, \ldots, x_n, y_1, \ldots, y_n) \in \mathbb{R}\colon (a_1 > 0) \wedge \cdots \wedge (a_k > 0) \implies \mathcal{E}(G, \mathcal{A})$$

Instead of $\mathcal{E}(G, \mathcal{A})$, we can also use the boolean-free formula $\mathcal{E}'(G, \mathcal{A})$ as defined in the proof of Proposition 2.17. ◀

We believe that the following stronger statement holds.

Conjecture. Area Universality *is* $\forall\exists\mathbb{R}$*-complete.*

While this conjecture, if true, would show that Area Universality is a really difficult problem in an algebraic and combinatorial sense, it would also give the first known natural geometric problem that is complete for $\forall\exists\mathbb{R}$. In the following, we explain how $\forall\exists\mathbb{R}$ fits well into the zoo of complexity classes.

7.1.1 Connections to the Polynomial Hierarchy

ETR is often considered to be a real counterpart of Satisfiability (Sat), where we ask if a given existential *logic* formula is true. Hence, in Sat we are seeking for a solution of a logic

formula and in ETR for the solution of a real formula. A *logic formula* is built of constants 0 and 1, logic symbols ($\wedge, \vee, \neg, \Leftrightarrow, \Rightarrow$), variable symbols, parentheses, and quantifiers ($\exists$ and $\forall$), using standard syntactic rules. Compared to a logic formula, a formula over the reals also allows for arithmetic operators ($+, -, \times$), and relation symbols ($<, \leq, =, \neq$).

Moreover, as $\exists\mathbb{R}$ is the complexity class containing all problems reducible in polynomial time to ETR, the celebrated Cook-Levin theorem [Cook, 1971, Levin, 1973] shows that NP is the class of problems reducible in polynomial time to Sat.

In both, ETR and Sat, only one block of existential quantifiers is used. Allowing universal and existential quantifiers for the boolean variables makes a problem algorithmically more difficult. This leads to the definition of the so-called *polynomial hierarchy* of complexity classes. Informally speaking, the problems on increasing levels of the polynomial hierarchy can be reduced to checking if a formula with increasing number of alternating quantifier blocks is true (see [Arora and Barak, 2009, Chapter 5]).

For instance, the complexity class Π_2^p is contained in the second level of the polynomial hierarchy. Π_2^p consists of the problems which reduce in polynomial time to Π_2-Taut of checking if a logic formula of the form

$$(\forall\, Y_1, Y_2, \ldots, Y_m)\,(\exists\, X_1, X_2, \ldots, X_n) : \Phi(X, Y),$$

where Φ is quantifier-free, is true. Even though the complexity class might look pure logical, some natural combinatorial problems appear to be complete for Π_2^p. An example of such a problem is 3-Choosability, also known as 3-List-Colorability [Gutner, 1996]. In 3-Choosability, we are given a graph G, and want to decide if for any assignment of a list of three colors to each vertex of G, there exists a proper coloring of the vertices of G where the colors are chosen from the lists.

The complexity class $\forall\exists\mathbb{R}$ can be seen as the real counterpart of the complexity class Π_2^p. Moreover, it is obvious that $\exists\mathbb{R}$ is contained in $\forall\exists\mathbb{R}$, see also Figure 7.3. Since it is easy to observe and well-known that NP is contained in $\exists\mathbb{R}$, with the analogous approach we can observe that Π_2^p is contained in $\forall\exists\mathbb{R}$. Establishing the the containment of $\forall\exists\mathbb{R}$ in PSPACE is highly nontrivial [Basu et al., 2006]. For all we know, all these complexity classes could collapse, as we do not know whether NP and PSPACE constitute two different or the same complexity class. However, $\exists\mathbb{R} \neq \forall\exists\mathbb{R}$ can be believed with similar confidence as $\mathrm{NP} \neq \Pi_2^p$.

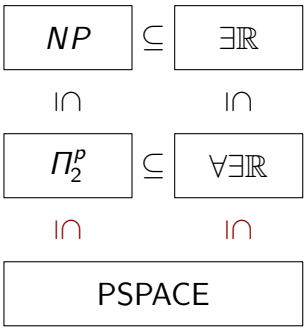

Figure 7.3: Containment relations of the complexity classes.

Although to the best of our knowledge, $\forall\exists\mathbb{R}$ and $\exists\forall\mathbb{R}$ have never been formally introduced, the idea has been around. In particular, the literature on algorithms deciding if a formula of the first order theory of the reals is true, focuses on formulas in prenex form and a key parameter for their difficulty is the number of quantifier alternations [Renegar, 1992].

Blum et. al. [Blum et al., 1998] also introduce a hierarchy of complexity classes analogous to the complexity class NP, but over the reals (or other rings). Their canonical model of computation is the so-called Blum-Shub-Smale machine (BSS). The main difference is that BSS accepts real numbers as input. However, the classes $\exists\mathbb{R}$, $\forall\exists\mathbb{R}$, $\exists\forall\mathbb{R}$ work with ordinary Turing machines, which only take strings over a finite (binary) alphabet as input.

7.2 Hard Variants

As a first step towards proving our conjecture, we consider three variants of Area Universality, each approaching the conjecture from a different direction. To do so, we introduce restricted variants of ETR and UETR which are still complete. These are presented in Section 7.2.1 and may also be useful to show hardness for other problems.

As a starting point we drop the planarity restriction. For a plane graph $G = (V, E)$, the *face hypergraph* of G has vertex set V, and its hyper-edges correspond to the sets of vertices which form the faces of G. Consequently, the face hypergraph of a plane triangulation is 3-uniform since all faces are triangles. We define the *area of a triple of points* in the plane to be the area of the triangle formed by these three points. Clearly, Area Universality can be equivalently formulated in the language of face hypergraphs. This relation motivates the following relaxation of the problem.

Area Universality for Triples*
Input: A set V of vertices, a set of triples $F \subseteq \binom{V}{3}$, and a partial area assignment $\mathcal{A}' \colon F' \to \mathbb{R}_{\geq 0}$ for some $F' \subseteq F$.
Question: Is it true that for every $\mathcal{A} \colon F \to \mathbb{R}_{\geq 0}$ with $\mathcal{A}(f) = \mathcal{A}'(f)$ for all $f \in F'$, there exist a placement of V in the plane, such that the area of each $f \in F$ is $\mathcal{A}(f)$?

In Section 7.2.2, we show that this problem is hard.

■ **Theorem 44.** Area Universality for Triples* *is* $\forall\exists\mathbb{R}$*-complete.*

For the proof of Theorem 44, we use gadgets similar to the *von Staudt constructions* used to show the $\exists\mathbb{R}$-hardness of order-types, see [Matoušek, 2014].

Our second result concerns a variant, where we investigate the complexity of realizing a specific area assignment. Prescribed Area denotes the following problem: Given a plane graph G with an area assignment $\mathcal{A}$, does there exist a crossing-free drawing of G that realizes $\mathcal{A}$? We study a partial extension version of Prescribed Area, where some vertex positions are fixed and we seek for a realizing placement of the remaining vertices.

Prescribed Area Partial Extension
Input: A plane graph $G = (V, E)$, an area assignment $\mathcal{A} \colon F' \to \mathbb{R}_{>0}$, and fixed positions for a subset of vertices $V' \subseteq V$.
Question: Does there exist a realizing drawing of G respecting the given positions for all $v \in V'$?

In Section 7.2.3, we show that this problem is hard.

■ **Theorem 45.** Prescribed Area Partial Extension *is* $\exists\mathbb{R}$*-complete.*

The last two results consider the analogous question for simplicial complexes in three dimensions. Recall that a *3-simplex* $s \subseteq \mathbb{R}^3$ is the convex hull of at most four affinely independent points. We denote the *vertices* of s by $\mathrm{vert}(s)$ and call the convex hull of a subset of $\mathrm{vert}(s)$ a *face* of s. A *simplicial complex* $\mathcal{S}$ in $\mathbb{R}^3$ is a set of 3-simplices such that

firstly, any face of a simplex from $\mathcal{S}$ is also a simplex in $\mathcal{S}$ and secondly, the intersection of two simplices $s, t \in \mathcal{S}$ is either $\emptyset$ or a face of s and t.

An *abstract simplicial complex* is a family Σ of non-empty finite sets over a ground set $V = \bigcup \Sigma$, which is closed under taking non-empty subsets. We say Σ is *pure* when all of the maximal sets in Σ have the same number of elements. Moreover, Σ is *realizable* in $\mathbb{R}^3$ when there is a simplicial complex $\mathcal{S}$ in $\mathbb{R}^3$ that has a vertex for each element of V and a simplex corresponding to each set in Σ. A *crossing-free drawing* of Σ is a mapping of every $i \in V$ to a point $p_i \in \mathbb{R}^3$ such that the following holds: For any pair of sets $\sigma_1, \sigma_2 \in \Sigma$ there is a separating hyperplane $h = \{x \in \mathbb{R}^3 : \langle a, x\rangle = b\}$ such that $\langle a, p_i\rangle \leq b$ for all $i \in \sigma_1$ and $\langle a, p_i\rangle \geq b$ for all $i \in \sigma_2$. A *volume assignment* for Σ is a function $\mathcal{V} : T \to \mathbb{R}_{\geq 0}$ on the collection T of all 4-element sets in Σ. A crossing-free drawing of Σ *realizes* a volume assignment $\mathcal{V} : T \to \mathbb{R}_{\geq 0}$ when for each $\tau \in T$, the convex hull of the points $\{p_i : i \in \tau\}$ has volume $\mathcal{V}(\tau)$. The analogous question of Prescribed Area can be stated as follows:

Prescribed Volume
Input: A pure abstract simplicial complex Σ realizable in $\mathbb{R}^3$; a volume assignment $\mathcal{V}$.
Question: Does there exist a crossing-free drawing of Σ that realizes $\mathcal{V}$?

Likewise, the analogous question of Area Universality reads as:

Volume Universality*
Input: A pure abstract simplicial complex Σ realizable in $\mathbb{R}^3$ and a volume assignment $\mathcal{V}' : T' \to \mathbb{R}_{\geq 0}$ for some of the 4-element sets $T' \subseteq T$ of Σ.
Question: Is it true that for every $\mathcal{V}\colon T \to \mathbb{R}_{\geq 0}$ with $\mathcal{V}(\tau) = \mathcal{V}'(\tau)$ for all $\tau \in T'$, there exists a crossing-free drawing of Σ that realizes $\mathcal{V}$?

Note that crossing-free 3-dimensional simplicial complexes are a natural generalization of planar triangulations. The fact that the tetrahedra only intersect in common faces corresponds to the non-crossing condition in planar drawings. Indeed, Prescribed Volume generalizes Prescribed Area for triangulations in the following sense:

▶ **Proposition 7.2.** *There is a polynomial time algorithm that takes as input any plane triangulation T with positive area assignment $\mathcal{A}$ and outputs a simplicial complex $\mathcal{S}$ with volume assignment $\mathcal{V}$ such that $\mathcal{A}$ is realizable for T if and only if $\mathcal{V}$ is realizable for $\mathcal{S}$.*

Additionally, these analogues of Prescribed Area and Area Universality are hard. First we show that Prescribed Volume is hard.

■ **Theorem 46.** Prescribed Volume *is $\exists\mathbb{R}$-complete.*

Then, we extend its proof in order to obtain the following result:

■ **Theorem 47.** Volume Universality* *is $\forall\exists\mathbb{R}$-complete.*

Both proofs are presented in Section 7.2.4.

7.2.1 Hard Variants of ETR and UETR

In this section, we introduce restricted variants of ETR and UETR which enable us to show hardness. Recently, Abrahamsen et al. showed that the following problem is also $\exists\mathbb{R}$-complete [Abrahamsen et al., 2018]. In particular, note that we can restrict multiplication to inversion and assume that a YES-instance has a solution within a bounded positive interval.

ETR-INV
Input: A formula over the reals of the form $(\exists\, X_1, X_2, \ldots, X_n) : \Phi(X_1, X_2, \ldots, X_n)$, where Φ is a conjunction of constraints of the following form: $X = 1$ (introducing constant 1), $X + Y = Z$ (addition), $X \cdot Y = 1$ (inversion), with $X, Y, Z \in \{X_1, \ldots, X_n\}$. Additionally, Φ is either unsatisfiable, or has a solution, such that all variables are in the interval $[1/2, 2]$.
Question: Is the input formula true?

In order to define some even more restricted variant of ETR-INV, we introduce the concept of an *incidence graph* of a formula. By definition of ETR-INV, we can consider a formula Φ of the form $\Phi = C_1 \wedge C_2 \wedge \ldots \wedge C_m$, where each C_i is a quantifier-free formula of the first order-theory of the reals with variables $X_1, X_2, \ldots, X_n$, which uses arithmetic operators and comparisons but no logic symbols. An *incidence graph* of Φ is the bipartite graph with vertex set $\{X_1, X_2, \ldots, X_n\} \cup \{C_1, C_2, \ldots, C_m\}$ that has an edge X_iC_j if and only if the variable X_i appears in the subformula C_j.

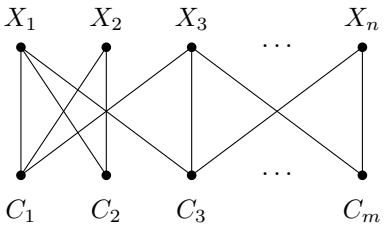

Figure 7.4: The incidence graph of the formula $\Phi = (X_1 + X_2 = X_3) \wedge (X_1 \cdot X_2 = 1) \wedge (X_1 + X_4 = X_3) \wedge (X_4 \cdot X_3 = 1)$.

By PLANAR-ETR-INV we denote the restriction of ETR-INV, where the incidence graph of Φ is planar, and Φ is either unsatisfiable, or has a solution where all variables are within the interval $(0, 5)$. We show that this variant of ETR is still hard.

■ **Theorem 48.** PLANAR-ETR-INV *is* $\exists\mathbb{R}$*-complete.*

Proof. Consider an instance $(\exists\, X_1, X_2, \ldots, X_n) : \Phi(X)$ of ETR-INV. Let G be (not necessarily crossing-free) straight-line drawing of the incidence graph of Φ in the plane. Suppose that G is not crossing-free and consider a pair of crossing edges. Let (X, C_X) and (Y, C_Y) denote the edges where X, Y denote the variables and C_X and C_Y the constraints. We introduce three new existential variables X', Y', Z and three constraints:

$$X + Y = Z, \qquad X + Y' = Z, \qquad X' + Y = Z.$$

Observe that these constraints ensure that $X = X'$ and $Y = Y'$. Therefore, we may modify the constraints C_X such that X' replaces X; likewise we replace Y by Y' in C_Y. Moreover, the drawing of G can be modified such that the new incidence graph G' has strictly fewer crossings. To do so, we choose a small enough empty box around the crossing and modify the drawing within this box as depicted in Figure 7.5.

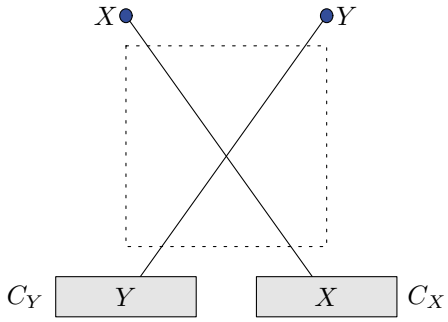

(a) The edges (X, C_x) and (Y, C_Y) cross.

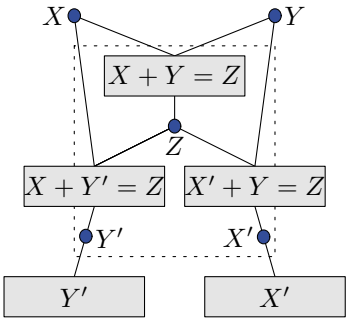

(b) Modified drawing without the crossing.

Figure 7.5: Illustration of the proof of Theorem 48.

In particular, G' looses the considered crossing and no new crossing is introduced. We repeat this procedure until the incidence graph of the modified formula is crossing-free. Finally, note that $0 < 1 \leq Z = X + Y \leq 2 + 2 = 4 < 5$ whenever $1/2 \leq X, Y \leq 2$. Note that the number of new variables and constraints is at most $O(|\Phi|^4)$, since the degree of each subformula in ETR-INV is at most three. ■

Now we introduce a restricted variant of UETR where the variables range of the positive reals and the constraints are in conjunctive form.

Constrained-UETR
Input: A formula over the reals of the form $(\forall\, Y_1, \ldots, Y_m \in \mathbb{R}_{>0})\, (\exists\, X_1, \ldots, X_n \in \mathbb{R}_{>0}) : \Phi(X, Y)$, where Φ is a conjunction of constraints of the form: $X = 1$ (introducing constant 1), $X + Y = Z$ (addition), $X \cdot Y = Z$ (multiplication), with $X, Y, Z \in \{X_1, \ldots, X_n, Y_1, \ldots, Y_m\}$.
Question: Is the input formula true?

This problem can be seen as a simplified $\forall\exists\mathbb{R}$-version of a variant of ETR called Ineq, where we ask if a conjunction of polynomial equations and inequalities has a real solution. Ineq is known to be $\exists\mathbb{R}$-complete [Matoušek, 2014, Schaefer and Štefankovič, 2017]. Similarly, we show the $\forall\exists\mathbb{R}$-completeness of Constrained-UETR.

■ **Theorem 49.** Constrained-UETR *is* $\forall\exists\mathbb{R}$*-complete.*

Our main tool is the following result by Schaefer and Štefankovič. We state it in a slightly different way, which is more suitable to our notation.

▶ **Lemma 7.3** ([Schaefer and Štefankovič, 2017])**.** *Let $\Phi(X)$ be a quantifier-free formula of the first order theory of the reals, with the vector of variables $X = (X_1, X_2, \ldots, X_n)$. In polynomial time, we can construct for some $k = O(|\Phi|)$ a polynomial $F\colon \mathbb{R}^{n+k} \to \mathbb{R}$ of degree 4, whose coefficient have bitlength $O(|\Phi|)$ such that*

$$\{x \in \mathbb{R}^n :\ \Phi(x) \text{ is true}\} = \{x \in \mathbb{R}^n :\ (\exists u \in \mathbb{R}^k)\ F(x, u) = 0\}.$$

With this lemma at hand, we are ready to prove the theorem.

Proof of Theorem 49. First of all, observe that Constrained-UETR is contained in $\forall\exists\mathbb{R}$, since the formula $(\forall Y_1, Y_2, \ldots, Y_m \in \mathbb{R}_{>0})(\exists X_1, X_2, \ldots, X_n \in \mathbb{R}_{>0})\colon \Phi(X, Y)$ is equivalent to the following instance of UETR:

$$(\forall Y_1, \ldots, Y_m \in \mathbb{R})(\exists X_1, \ldots, X_n \in \mathbb{R})\colon \left(\bigwedge_{i=1}^{m} (Y_i > 0) \Rightarrow \bigwedge_{i=1}^{n} (X_i > 0) \wedge \Phi(X, Y)\right).$$

To prove the hardness of Constrained-UETR, we consider an instance of UETR of the form $\Psi = (\forall Y_1, Y_2, \ldots, Y_m \in \mathbb{R})(\exists X_1, X_2, \ldots, X_n \in \mathbb{R})\colon \Phi(X, Y)$ and create an equivalent Constrained-UETR formula

$$\overline{\Psi} = (\forall Y_1, Y_2, \ldots, Y_{\overline{m}} \in \mathbb{R}_{>0})(\exists X_1, X_2, \ldots, X_{\overline{n}} \in R^{+})\colon \overline{\Phi}(X, Y),$$

such that the size of the new formula $\overline{\Psi}$ is polynomial in the size of Ψ. The reduction consists of several steps.

Transforming Φ into a single polynomial. First, we apply Lemma 7.3 to simplify Φ. Let $F\colon \mathbb{R}^{n+m+k} \to \mathbb{R}$ be the obtained polynomial for some $k \in O(|\Phi|)$. We define a UETR formula Ψ' as follows:

$$\Psi' = (\forall Y_1, \ldots, Y_m \in \mathbb{R})(\exists X_1, \ldots, X_n \in \mathbb{R})(\exists U_1, \ldots, U_k \in \mathbb{R})\colon F(Y, X, U) = 0.$$

First note that Ψ' is equivalent to Ψ. To see this, we define

$$S = \{(y, x) \in \mathbb{R}^{m+n} : \Phi(x, y)\} \quad \text{and} \quad S' = \{(y, x) \in \mathbb{R}^{m+n} : (\exists u \in \mathbb{R}^k) F(y, x, u) = 0\},$$

as in Lemma 7.3. We know that $S' = S$ and Ψ is true if and only if the orthogonal projection of S onto the first m coordinates equals $\mathbb{R}^m$. Similarly, Ψ' is true if and only if the orthogonal projection of $S = S'$ onto the first m coordinates equals $\mathbb{R}^m$.

Transforming F into a conjunction of constraints. We transform F into an equivalent conjunction of constraints. First note that we can rewrite F as a sum of monomials $F = f_1 + \ldots + f_\ell$ in polynomial time, because F has degree at most 4. We show how to replace each monomial f by an equivalent set of constraints, each of which is either the introduction of the constant 1, an addition or a multiplication. Consider a mononomial

$$f = s \cdot c \cdot Z_1 \cdot Z_2 \cdot \ldots \cdot Z_t$$

of F, where $s \in \{-1, 1\}$ is the sign, c is a positive integer of bitlength $O(|\Phi'|) = O(|\Phi|)$, and $Z_1, \ldots, Z_t$ are not necessarily distinct variables. For convenience, we introduce the existentially quantified variables I_0, I_1, I_{-1}, I_2, whose values will be forced to be 0, 1, -1, and 2, respectively, by the following constraints:

$$I_0 = I_0 + I_0, \qquad I_1 = 1, \qquad I_0 = I_{-1} + I_1, \qquad \text{and} \qquad I_2 = I_1 + I_1.$$

We start by describing a variable holding the value sc, using only the above constraints. Let $c_\ell c_{\ell-1} \dots c_0$ be binary expansion of c, i.e., $c = \sum_{i=0}^{\ell} c_i \cdot 2^i$ where each c_i is either 0 or 1. We introduce new existentially quantified variables and the constraints described below; the index of each variable represents its intended value. The idea is to use the recursion

$$c_\ell \dots c_t = 2 \cdot c_\ell \dots c_{t-1} + c_t.$$

We encode the multiplication and addition of the recursion in two steps. The constraints are as follows:

$$\begin{aligned} V_{2c_\ell} &= I_2 \cdot I_{c_\ell} \\ V_{2c_\ell + c_{\ell-1}} &= V_{2c_\ell} + I_{c_{\ell-1}} \\ V_{4c_\ell + 2c_{\ell-1}} &= I_2 \cdot V_{2c_\ell + c_{\ell-1}} \\ &\vdots \\ V_c &= V_{\sum_{i=1}^{\ell} c_i \cdot 2^i} + I_{c_0} \\ V_{sc} &= I_s \cdot V_c \end{aligned}$$

Observe that $V_{sc} = sc$. Next, we introduce new existential variables V_f, V_{Z_1} and $V_{Z_1 Z_2 \dots Z_k}$ for all $2 \leq k \leq t$, and add the following constraints:

$$\begin{aligned} V_{Z_1} &= Z_1 \\ V_{Z_1 Z_2 \dots Z_k} &= V_{Z_1 Z_2 \dots Z_{k-1}} \cdot Z_k \text{ for all } 2 \leq k \leq t \\ V_f &= V_{sc} \cdot V_{Z_1 Z_2 \dots Z_t}. \end{aligned}$$

The last constraint ensures that the value of V_f is equal to the value of f. We repeat the same procedure for every monomial f.

Recall that $F = f_1 + f_2 + \ldots + f_\ell$, where $f_1, f_2, \ldots, f_\ell$ are monomials. We introduce new existential variables and the following constraints for $2 \leq k \leq \ell - 1$:

$$\begin{aligned} V_{f_1 + f_2 + \ldots + f_k} &= V_{f_1 + f_2 + \ldots + f_{k-1}} + V_{f_k} \\ I_0 &= V_{f_1 + f_2 + \ldots + f_{\ell-1}} + V_{f_\ell} \end{aligned}$$

This way we construct $\Psi'' = (\forall Y'_1, \ldots, Y'_{m'} \in \mathbb{R})(\exists X'_1, \ldots, X'_{n'} \in \mathbb{R})\colon \Phi''(X', Y')$, which is equivalent to Ψ, its size is polynomial in $|\Psi|$, and Φ'' is a conjunction of the introduction of the constant 1, addition and multiplication constraints.

Changing the ranges of the quantifiers. Next, we guarantee that the quantifiers range over the positive reals. For each variable Z of Ψ'', we introduce two positive variables Z^+ and Z^-. If Z is universally quantified, then so are both Z^+ and Z^-; analogously, if Z is existentially quantified, then so are Z^+ and Z^-. Every appearance of Z in Φ'' is substituted

by $(Z^+ - Z^-)$; let Φ''' be the formula obtained in such a way. It is easy to observe that the constructed formula is equivalent to Ψ'. However, the structure of constraints is destroyed.

Restoring the form of the constraints. Finally, we restore the form of the constraints. Therefore, we re-introduce the existential variable I_1 with constraint $I_1 = 1$. Then, we transform every constraint in Φ''' in the following way: A constraint $(Z^+ - Z^-) = 1$ is transformed into $Z^+ = Z^- + I_1$.

An addition constraint $(X^+ - X^-) + (Y^+ - Y^-) = (Z^+ - Z^-)$ is equivalent to the expression $X^+ + Y^+ + Z^- = X^- + Y^- + Z^+$. We introduce new positive, existentially quantified variables and the constraints:

$$\begin{aligned} V_{X^+ + Y^+} &= X^+ + Y^+ \\ V_{X^- + Y^-} &= X^- + Y^- \\ V_{X^- + Y^- + Z^+} &= V_{X^- + Y^-} + Z^+ \\ V_{X^+ + Y^+} + Z^- &= V_{X^- + Y^- + Z^+}. \end{aligned}$$

A multiplication-constraint $(X^+ - X^-) \cdot (Y^+ - Y^-) = (Z^+ - Z^-)$ is equivalent to the expression $X^+Y^+ + X^-Y^- + Z^- = X^+Y^- + X^-Y^+ + Z^+$. We introduce new positive, existentially quantified variables and the constraints for each pair $\circ, \times \in \{+, -\}$

$$V_{X^\circ Y^\times} = X^\circ \cdot Y^\times$$

as well as the constraints:

$$\begin{aligned} V_{X^+Y^+ + X^-Y^-} &= V_{X^+Y^+} + V_{X^-Y^-} \\ V_{X^+Y^- + X^-Y^+} &= V_{X^+Y^-} + V_{X^-Y^+} \\ V_{X^+Y^- + X^-Y^+ + Z^+} &= V_{X^+Y^- + X^-Y^+} + Z^+ \\ V_{X^+Y^- + X^-Y^+} + Z^- &= V_{X^+Y^- + X^-Y^+ + Z^+}. \end{aligned}$$

Note that finally all constraints are of the desired form and the variables are strictly positive. Thus we produced a formula

$$\overline{\Psi} = (\forall Y_1, Y_2, \ldots, Y_{\overline{m}} \in \mathbb{R}_{>0})(\exists X_1, X_2, \ldots, X_{\overline{n}} \in \mathbb{R}_{>0}) \colon \overline{\Phi}(X, Y),$$

in which $\overline{\Phi}$ is a conjunction of the introduction of a constant, additions, and multiplications. Moreover, $\overline{\Psi}$ is equivalent to Ψ. Observe that the number of introduced variables and the length of $\overline{\Phi}$ are polynomial in $|\Phi|$. This completes the proof. ■

With this tool at hand, we are able to show hardness for several variants of area-universality. We start to consider Area Universality for Triples*.

7.2.2 Hardness of Area Universality for Triples*

We now prove Theorem 44.

■ **Theorem 44.** Area Universality for Triples* *is* $\forall\exists\mathbb{R}$*-complete.*

Proof. For the membership, we form an instance of $\forall\exists\mathbb{R}$. For each triple, we consider one equation as in Equation (2.1) and form the instance by taking their conjunctions.

For proving hardness, we reduce from Constrained-UETR. For every instance Ψ of Constrained-UETR, we give a set of points V and unordered triples T, along with a partial area assignment $\mathcal{A}'$. Let Ψ be a formula of the form:

$$\Psi = (\forall Y_1, \dots, Y_m \in \mathbb{R}_{>0})(\exists X_1, \dots, X_n \in \mathbb{R}_{>0})\colon \Phi(X, Y).$$

Recall that Φ is a conjunction of constraints of the form $Z = 1$, $Z_i + Z_j = Z_k$, and $Z_i \cdot Z_j = Z_k$.

First, we show how to express Φ. Our gadgets are similar to the ones for showing $\exists\mathbb{R}$-hardness of Order Type (see Matoušek [Matoušek, 2014]).

All variables are represented by points on one line; which we denote by ℓ for the rest of the proof. First, we enforce points to be on ℓ. Afterwards we construct gadgets to mimic addition and multiplication.

To force points on a line, we start by introducing the three points p_0, p_1, and r and define $\mathcal{A}'(p_0, p_1, r) := 1$. The positive area of the triple ensures that the points are not collinear and pairwise different. We measure in units of $\|p_0p_1\|$ and interpret p_0 as 0 and p_1 as 1. Denoting a line through two points a and b by $\ell_{a,b}$, we set $\ell := \ell_{p_0,p_1}$, see also Figure 7.6. To force a point x on ℓ, we set $\mathcal{A}'(x, p_0, p_1) := 0$. Note that this does not introduce any other constraint on the position of x on ℓ.

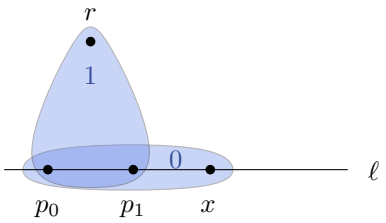

Figure 7.6: Forcing points on a line.

Each variable X is represented by a point x on ℓ. Additionally, since all variables are non-zero, we introduce a triple of positive area forcing x to be different from p_0. Note that in general, we can ensure that two points x_1, x_2 are distinct, by introducing a new point q and adding a triple (x_1, x_2, q) with $\mathcal{A}'(x_1, x_2, q) := 1$. Now, we define the absolute value of X by $\|p_0x\|$. If x is on the same side of p_0 as p_1, then the value of X is positive, otherwise it is negative. We accept currently both positive and negative values, but later we force the original variables to be positive.

Let us describe the gadgets for addition and multiplication. We start with the addition constraint $X + Y = Z$. Let x, y, z be the points encoding the values of X, Y, Z, respectively. Recall that these points lie on ℓ and do not coincide with p_0. We introduce a point q_1 and prescribe the areas $\mathcal{A}'(p_0, x, q_1) = \mathcal{A}'(y, z, q_1) = 1$. Figure 7.7 illustrates the addition gadget.

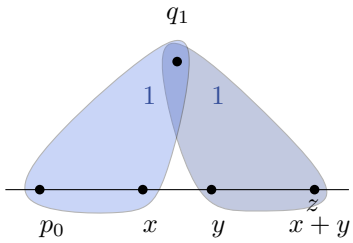

Figure 7.7: The addition gadget.

Since the two triangles have the same area and height, the distance between y and z must agree with the distance between p_0 and x. Thus, the value of Z is either $X+Y$ or $X-Y$. Analogously, we introduce a point q_2 and define $\mathcal{A}'(p_0, y, q_2) = \mathcal{A}'(x, z, q_2) = 1$, implying that Z is either $Y+X$ or $Y-X$. This is satisfied either if $Z = X+Y$ (the intended solution) or if $Z = X-Y = Y-X$. The second solution implies that $X = Y$ and thus $Z = 0$. This contradicts to the fact that $z \neq p_0$ and hence shows the correctness of the addition gadget.

As a preparation to the multiplication gadget, we show how to enforce on the four pairwise different points p, p', s, s' that $\ell_{p,p'}$ is parallel to $\ell_{s,s'}$, without adding additional constraints on any of the four points. Figure 7.8 displays the desired situation.

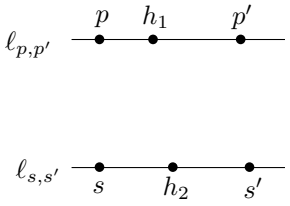

Figure 7.8: Gadgets for the construction of a parallel line.

We insert two new points h_1 on the line $\ell_{p,p'}$ and h_2 on the line $\ell_{s,s'}$ by defining $\mathcal{A}'(p, p', h_1) = \mathcal{A}'(s, s', h_2) = 0$. We aim for a trapezoid with points p, h_1, s, h_2 such that ph_1 is parallel to sh_2. For this, we prescribe the areas $\mathcal{A}'(p, h_1, s) = \mathcal{A}'(p, h_1, h_2) = 1$ and the areas $\mathcal{A}'(s, h_2, p) = \mathcal{A}'(s, h_2, h_1) = 2$, as illustrated in Figure 7.9(a). Indeed, s and h_2 must lie on the same side of the line ℓ_{p,h_1}: Assume for a contradiction that ℓ_{p,h_1} separates s and h_2. If p and h_1 are on the same side of ℓ_{s,h_2} then the triangle (s, h_2, p) is contained in or contains the triangle (s, h_2, h_1), see Figure 7.9(b). However, both triangles are supposed to have the same area and $p \neq h_1$. A contradiction.

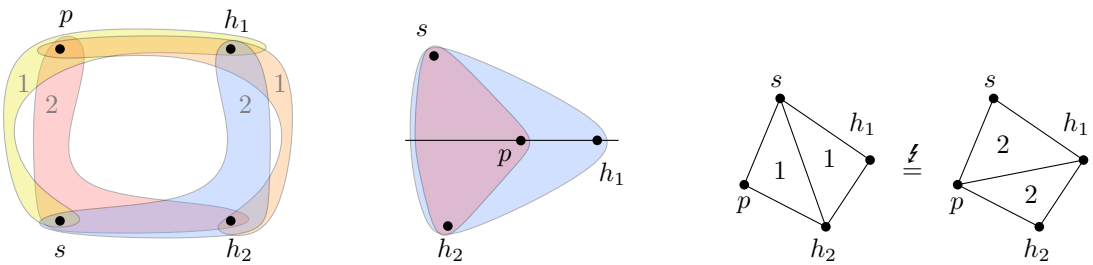

(a) (b) (c)

Figure 7.9: Forcing a trapezoid.

Consequently, ℓ_{s,h_2} separates p and h_1 and the quadrangle can be partitioned by each of the two diagonals sh_2 and ph_1. See Figure 7.9(c) to observe the following contradiction:

$$2 = \mathcal{A}(p, h_1, s) + \mathcal{A}(p, h_1, h_2) = \mathcal{A}(s, h_2, h_1) + \mathcal{A}(s, h_2, p) = 4.$$

Thus s and h_2 lie on the same side of ℓ_{p,h_1}. By the prescribed areas, s and h_2 have the same distance to ℓ_{p,h_1}. Therefore, the segments ph_1 and sh_2 and the lines $\ell_{p,p'}$ and $\ell_{s,s'}$ are parallel. Moreover, no other constraints are imposed on the points p, p', s, s'.

To construct a multiplication gadget for the constraint $X \cdot Y = Z$, let x, y, z ($\neq p_0$) be the points encoding the values of X, Y, Z, respectively. First we introduce two points p, p' which do not lie on ℓ, but the three points p_0, p, p' are collinear by setting $\mathcal{A}'(p_0, p, p') = 0$. We enforce the following pairs of lines to be parallel by the construction of a parallel line: $\ell_{p_1,p}$ with $\ell_{y,p'}$ and $\ell_{x,p}$ with $\ell_{z,p'}$. Figure 7.10 displays the multiplication gadget. By the intercept theorem, the following ratios coincide – also for negative variables:

$$|p_0p|/|p_0p'| = |p_0p_1|/|p_0y| = |p_0x|/|p_0z|.$$

By the definition of x, y, z, we obtain $1/Y = X/Z$, which implies that $X \cdot Y = Z$.

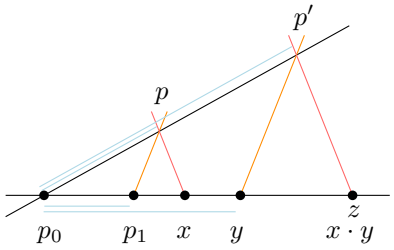

Figure 7.10: The multiplication gadget.

Next, we introduce the universally quantified variables $Y_1, Y_2, \ldots, Y_m$. For every Y_i, let y_i be the point encoding its value, we know that y_i is on ℓ and $y_i \neq p_0$. We introduce a triple $f_i = (p_0, r, y_i)$, whose area is universally quantified. Recall that r is a point with $\mathcal{A}'(p_0, p_1, r) = 1$. Now we show how to enforce each original variable X to be positive. We add an existentially quantified variable S_X and the constraint $X = S_X \cdot S_X$. The variable S_X may not be positive, but this is not required. This finishes the reduction which clearly runs in polynomial time.

It remains to argue that Ψ is true if and only if our constructed instance of Area Universality for Triples* is realizable. Let $V(Y_1), \ldots, V(Y_m) \in \mathbb{R}_{>0}$ be some values of the universally quantified variables. Then for every $i \in \{1, \ldots, m\}$, $\mathcal{A}(p_0, r, y_i)$ enforces the positions of y_i to correspond to $V(Y_i)$. Consequently, the position of the point encoding the value of S_{Y_i} is either $\sqrt{(V(Y_i)}$, or $-\sqrt{(V(Y_i))}$ (both alternatives are plausible). Fixing a value of X_i fixes S_{X_i} to be either $\sqrt{V(X_i)}$ or $-\sqrt{V(X_i)}$ (both plausible), so it only remains to show that if there exist values $V(X_1), \ldots, V(X_n)$ such that $\Phi(Y, X)$ holds, then there is an $\mathcal{A}$-realizing placement of the points $x_1, \ldots, x_n$ and vice versa. This follows immediately from the correctness of the gadgets and the fact that auxiliary points for S_{X_i} and S_{Y_j} can be set arbitrarily and are independent for each gadget. This shows hardness of Area Universality for Triples*. ■

We now come to further hard variant.

7.2.3 Hardness of Prescribed Area Partial Extension

In this section, we prove Theorem 45 by reducing from Planar-ETR-inv.

■ **Theorem 45.** Prescribed Area Partial Extension *is* $\exists\mathbb{R}$*-complete.*

Proof. Let $\Psi = (\exists X_1, \ldots, X_n) : \Phi(X_1, \ldots, X_n)$ be an instance of Planar-ETR-inv. Recall that we can assume that if Ψ is a yes-instance, then it has a solution, in which the values of the variables are in the interval $(0, \lambda)$ for $\lambda = 5$. We construct a plane graph $G_\Psi = (V, E)$, an area assignment $\mathcal{A}$ of G_Ψ, and fixed positions for a subset V' of vertices, such that G_Ψ has a realizing drawing respecting the prescribed vertex positions if and only if Φ is satisfiable by real values from the interval $(0, \lambda)$.

Consider the incidence graph of Φ and fix an orthogonal plane drawing on an integer grid. As indicated in Figure 7.11, we consider a crossing-free degenerate drawing where the edges are allowed to share grid lines as long as they do not properly cross. Such a drawing can be computed by a $\perp$-contact-representation as in Theorem 27.

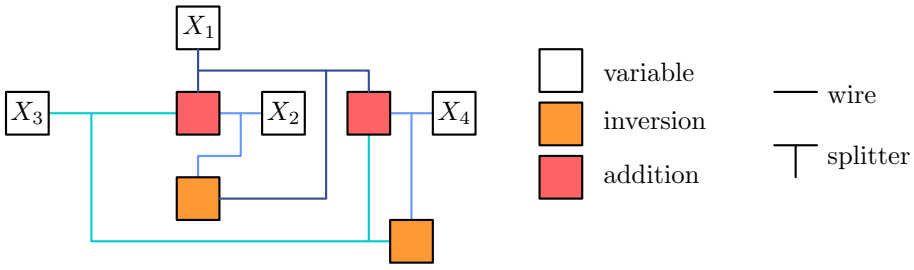

Figure 7.11: An orthogonal drawing on an integer grid of the incidence graph G_Ψ of the instance $\Psi = (X_1 + X_2 = X_3) \wedge (X_1 \cdot X_2 = 1) \wedge (X_1 + X_4 = X_3) \wedge (X_4 \cdot X_3 = 1)$.

We design several types of gadgets: *variable gadgets* representing the variables, as well as *inversion* and *addition gadgets*, realizing the corresponding constraints. Moreover, we construct *wires* and *splitters* in order to copy and transport information. Some vertices will have prescribed positions; these are called *fixed* and the remaining vertices are *flexible*.

The *variable gadget* for a variable X consists of eight fixed vertices and one flexible vertex v_x, see Figure 7.12(a). The variable gadget has two inner faces. The outer face of the variable gadget forms a rectangle of area 6. The vertices a, b, v_x form a triangle of area $1/2$. Observe that the prescribed area of the triangle abv_x forces v_x to lie on the line containing the segment cd. Therefore, due to planarity, v_x must lie in the interior of the segment cd. As before, the Euclidean distance of two points p, q is given by $\|pq\|$, and $\lambda\|dv_x\|$ specifies the value of X. We symbolize $\|dv_x\|$ by a bold gray line in Figure 7.12(a). Now, we introduce a constant 1 with a constraint $X = 1$ by using a variable gadget. We define v_x to be fixed and place it in such a way that $\|dv_x\| = 1/\lambda$. In the following, we sometimes assume that a flexible vertex is forced to lie on a specified segment. Note that this property can be induced by a variable gadget.

The *wire gadget* consists of several box-like fragments: four fixed vertices positioned as the corners of an axis-parallel unit square and two opposite fixed edges, see Figure 7.12(b). Each of the other two sides of the square is subdivided by a flexible vertex, these two vertices are joined by an edge. Each of the two quadrangular faces has a prescribed area of $1/2$. Note that if one of the flexible vertices is collinear with its fixed neighbors, so is the other one. The planarity constraint ensures that each flexible vertex lies between the corresponding fixed vertices. Moreover, the segment representing the value of the variable

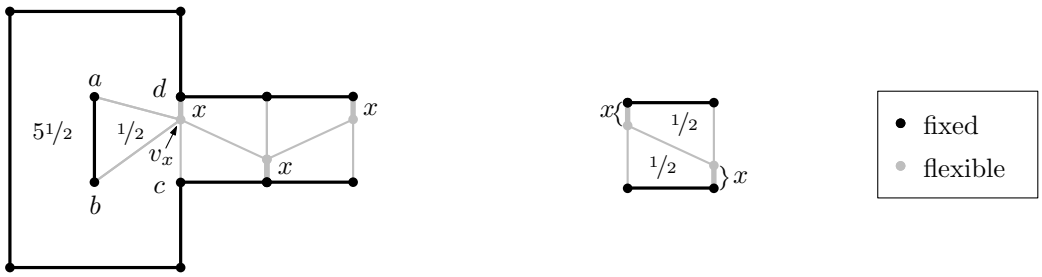

(a) The variable gadget (with a wire attached). (b) The wire gadget.

Figure 7.12: The variable gadget and wires.

changes from top to bottom or vice versa. Hence, if necessary, we may use an odd number of fragments in order to invert the side where the value is represented. Wires are used to connect other gadgets.

The *splitter gadget* contains a central fixed square of area 1, where each side is adjacent to a triangle of area 1/2 with a third flexible vertex. Figure 7.13(a) depicts the splitter gadget. Each triangle forces the flexible vertex on a line. These flexible vertices and their neighbors on the boundary of the splitter gadget are identified with the appropriate vertices in a variable gadget or a wire; this is how we connect the splitter with other gadgets. Observe that the value of one variable fixes the values of all variables by pushing the area circularly. Note that each face of area 1 has exactly two flexible vertices which are forced to lie on specific segments. Thus if one of them is determined, the other is also uniquely determined in a realizing drawing. Note that we may use the splitter gadget not only for splitting wires, but also for realizing left and right turns.

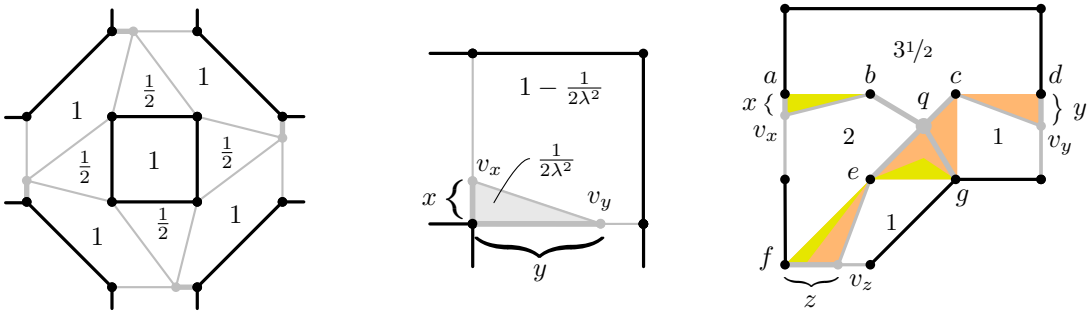

(a) The splitter gadget which also enables left and right turns. (b) The inversion gadget. (c) The addition gadget.

Figure 7.13: The splitter, inversion, and the addition.

It remains to introduce gadgets for the inversion and addition constraints. First consider an inversion constraint $X \cdot Y = 1$. The *inversion gadget*, illustrated in Figure 7.13(b), consists of four fixed vertices arranged in a unit square, two flexible vertices v_x and v_y, and seven edges. By linking the inversion gadget with variable gadgets or wires, we can ensure that v_x and v_y belong to the segment of their fixed neighbors. Let x be the distance from the bottom left corner to v_x, and y be the distance from the bottom left corner to v_y. Suppose that these distances represent, respectively, the values of variables X and Y in the way described in the paragraph about variable gadgets; this is obtained by identifying them with appropriate vertices of such a gadget or a wire. Namely, the value of X is $\lambda \cdot x$,

and the value of Y is $\lambda \cdot y$. To realize the area $1/(2\lambda^2)$ of the triangle formed by v_x, v_y, and their common neighbor, the lengths x and y are forced to satisfy the equation

$$\frac{xy}{2} = \frac{1}{(2\lambda^2)}.$$

This implies that the value of $X \cdot Y$ is $\lambda x \cdot \lambda y = 1$. Consequently, the inversion constraint is satisfied.

Finally, we construct an *addition gadget* for an addition constraint $X + Y = Z$. We introduce nine fixed vertices placed on an integer grid on the boundary of our gadget, as depicted in Figure 7.13(c). Moreover, we introduce four fixed vertices b, c, e, g in the interior of our gadget on integer points and three flexible vertices v_x, v_y, v_z encode the values of variables X, Y, Z, respectively. The vertices v_x, v_y, v_z are identified by appropriate flexible vertices in variable or wire gadgets; this ensures that they are forced to lie on the segments of their fixed outer neighbors. Finally, we introduce a flexible vertex q adjacent to the four inner fixed vertices b, c, e, g. Consequently, the addition gadget has four inner faces f_1, f_2, f_3, f_4 to which we assign the areas $\mathcal{A}(f_1) = 3.5, \mathcal{A}(f_2) = 2, \mathcal{A}(f_3) = 1$, and $\mathcal{A}(f_4) = 1$.

Let $x := \|av_x\|$ and $y := \|dv_y\|$ and $z := \|fv_z\|$. Since v_x, v_y, v_z encode the values of the variables X, Y, and Z, respectively, we know that $X = \lambda x$, $Y = \lambda y$, and $Z = \lambda z$. Moreover, the area of the triangle av_xb is $a_x := x/2$, the area of the triangle cdv_y is $a_y := y/2$ and the area of efv_z is $a_z := z/2$. We want to show that there exists a realizing drawing if and only if $X + Y = Z$. In a realizing drawing, the area of f_1 is

$$A(f_1) = 3 + A(av_xb) + A(cv_yd) + A(bqc) = 3 + a_x + a_y \overset{!}{=} 3.5 = \mathcal{A}(f_1).$$

Consequently, the area of the triangle bqc is forced to be $1/2 - a_x - a_y$. Note if Ψ is a positive instance, we may assume that $Z = X + Y < \lambda$, thus the area of the triangle bqc is positive. On the other hand, if $X + Y > \lambda$, it is easy to see that there is no way to put flexible points in a way that conforms prescribed areas. An easy but crucial point is that $A(bqc) + A(egq) = 1/2 = A(beq) + A(gcq)$. Combining this with the fact that the triangle bqc has area $1/2 - a_x - a_y$, we obtain that area of the triangle egq is forced to $a_x + a_y$. Observe that the area of f_3 forces the area of triangle cqg to equal a_y. It is easy to see that the area of f_4 equals $A(f_4) = 1/2 + A(egq) + (1/2 - A(efv_z)) = 1 + a_x + a_y - a_z$. Its prescribed area of 1 therefore enforces that $a_x + a_y = a_z$.

If on the other hand, the constraint $a_x + a_y = a_z$ is fulfilled, we take the placement of q such that f_1 and f_3 are fulfilled. By f_3, the area of the triangle cqg equals a_y and it holds

$$A(f_2) = 2 - A(av_xb) - A(cqg) + A(efv_z) = 2 - a_x - a_y + a_z = 2 = \mathcal{A}(f_2).$$

By the correct total area, f_4 has area $\mathcal{A}(f_4)$. The correctness of the addition gadget follows.

Finally, during the construction, we might have introduced inner faces without specified areas. Since the total area of each gadget is fixed, we *measure* the area of these introduced faces and set these as the prescribed area. Consequently, we created a planar graph G_Ψ, a subset of vertices with fixed positions, and an area assignment $\mathcal{A}$, such that G_Ψ has a realizing drawing for $\mathcal{A}$ and respecting the fixed positions if and only if Ψ is true. The correctness of the construction follows directly from the correctness of the individual gadgets. Moreover, the size of G_Ψ is polynomial in $|\Psi|$. Thus the proof is complete. ■

Next, we consider the variants with simplicial complexes in three dimensions.

7.2.4 Realizing the Volume of Simplicial Complexes

We start with some basic definitions and observations. Recall that a *simplex* $s \subseteq \mathbb{R}^d$ is the convex hull of at most $d+1$ affinely independent points, the *vertices* of s are denoted by $\text{vert}(s)$. By affinely independent, we mean that there is no set of $\{r_i \in \mathbb{R} \mid i \in [k]\}$ such that $r_1 + \cdots + r_k = 1$ and $v_0 = r_1 v_1 + \cdots + r_k v_k$ where $\{v_0, \ldots, v_k\} = \text{vert}(s)$. For a simplex s, the convex hull of a subset of $\text{vert}(s)$ is a *face* of s. A *simplicial complex* $\mathcal{S}$ is a set of simplices in $\mathbb{R}^d$ that satisfies the following conditions:

- Any face of a simplex from $\mathcal{S}$ is also a simplex in $\mathcal{S}$.
- The intersection of two simplices $s, t \in \mathcal{S}$ is either $\emptyset$ or a face of simplices s and t.

An *abstract simplicial complex* is a collection of finite sets Σ that is closed under inclusion. That is, if $\sigma \in \Sigma$ and $\tau \subseteq \sigma$ then $\tau \in \Sigma$. Note that to define an abstract simplicial complex Σ it suffices to only specify the maximal sets of Σ. We say Σ is a *pure* d-dimensional abstract simplicial complex when all maximal sets in Σ have exactly $d+1$ elements. Moreover, an abstract simplicial complex Σ is *realizable* in $\mathbb{R}^d$ when there is a simplicial complex $\mathcal{S} \subseteq \mathbb{R}^d$ that has a simplex $\tilde{\sigma}$ for each set $\sigma \in \Sigma$ and $\tilde{\tau} \in \mathcal{S}$ is a face of a simplex $\tilde{\sigma} \in \mathcal{S}$ if and only if $\tau \subseteq \sigma$. We say $\mathcal{S}$ *realizes* Σ. Note that every simplicial complex $\mathcal{S}$ realizes the abstract simplicial complex consisting of the set of vertices of each simplex of $\mathcal{S}$.

A *crossing-free drawing* of Σ is a mapping of every $i \in V$ to a point $p_i \in \mathbb{R}^3$, such that the following holds: For any pair of sets $\sigma_1, \sigma_2 \in \Sigma$ there is a separating hyperplane $h = \{x \in \mathbb{R}^3 : \langle a, x\rangle = b\}$ such that $\langle a, p_i\rangle \leq b$ for all $i \in \sigma_1$ and $\langle a, p_i\rangle \geq b$ for all $i \in \sigma_2$. Note also that a crossing-free drawing of an abstract simplicial complex is not necessarily a simplicial complex, since some simplices may be degenerate, or may intersect along their boundary where they do not share a common face.

A *volume assignment* for Σ is a function $\mathcal{V} : T \to \mathbb{R}_{\geq 0}$ on the collection T of all 4-element sets in Σ. A crossing-free drawing of Σ *realizes* a volume assignment $\mathcal{V} : T \to \mathbb{R}_{\geq 0}$ when for each $\tau \in T$, the convex hull of the points $\{p_i : i \in \tau\}$ has volume $\mathcal{V}(\tau)$.

Basic properties Let $\mathcal{S} = (V, F)$ be a simplicial 3-complex, i.e., a simplicial complex in $\mathbb{R}^3$. Lets first recall that the volume of a tetrahedron $t = \{a, b, c, d\}$ can be expressed in terms of the area of one triangle $\triangle := \{a, b, c\}$ and its respective height h:

$$\text{vol}(t) = 1/3 \cdot \text{area}(\triangle) \cdot h.$$

As suggested by abstract simplicial complexes, we think of a simplex s mostly as the set of its vertices $\text{vert}(s)$. However, talking about area or volume, we refer to the volume of the convex hull of $\text{vert}(s)$. Given two simplices s and t, we define $s \oplus t$ as the simplex consisting of the convex hull of $\text{vert}(s) \cup \text{vert}(t)$. For a simplicial complex $\mathcal{S}$ and a vertex v, we define the *cone of v over $\mathcal{S}$* by

$$\mathcal{S} \oplus v := \{s \oplus v \mid s \in \mathcal{S}\}.$$

In particular, we are interested in cones $T \oplus v$ over a plane triangulation T and a vertex v. We also say v is an *apex* for T in $T \oplus v$. Let $\mathcal{V}$ be a volume assignment of a simplicial complex $\mathcal{S}$ containing $T \oplus v$ for some plane triangulation T and apex v. We define *the induced area assignment* $\mathcal{A}_v$ of v on T as follows: For each triangle abc of T, we set $\mathcal{A}_v(\{a, b, c\}) := \mathcal{V}(\{a, b, c, v\})$.

▶ **Lemma 7.4.** *Let T be a plane triangulation and $\mathcal{S}$ be a simplicial complex containing $T \oplus v$ for some vertex v. Let $\mathcal{V}$ be a volume assignment of $\mathcal{S}$. If T is coplanar in a $\mathcal{V}$-realization of $\mathcal{S}$, then the induced area assignment $\mathcal{A}_v$ is realizable for T.*

Proof. For each triangle abc of T and its corresponding tetrahedron $abcv$ with height h it holds that: $\text{vol}(abcv) = 1/3 \cdot \text{area}(abc) \cdot h$. If T is coplanar, then the height h of all tetrahedra with respect to this plane coincides. Hence, the volume of the tetrahedra translates immediately to the area of the triangles (scaled by $1/3h$). If the volume assignment $\mathcal{V}$ is realized for $\mathcal{S}$, then the induced area assignment $\mathcal{A}_v$ scaled by $\lambda := 1/3h$ is realized for T. By scaling the plane accordingly, we find an $\mathcal{A}_v$-realizing drawing of T. ◀

Consider a simplicial complex $\mathcal{S}$ with volume assignment $\mathcal{V}$, a plane triangulation T and a vertex v of $\mathcal{S}$ but not of T such that $T \oplus v$ is contained in $\mathcal{S}$. We define the (weak) dual graph G^* of T: The vertex set of G^* consists of the inner faces of T and the edge set of G^* represents adjacent faces. We call an edge e in G^* *good*, if in every $\mathcal{V}$-realization of $\mathcal{S}$, the two adjacent triangles of e are coplanar. The *coplanar graph* of T (with respect to $\mathcal{V}$) is the subgraph of G^* consisting of good edges.

▶ **Lemma 7.5.** *Let T be plane triangulation, v be a vertex, and $\mathcal{S}$ be a simplicial complex containing $v \oplus T$. Then T is coplanar in all $\mathcal{V}$-realization of $\mathcal{S}$ if and only if the coplanar graph of T is connected.*

Proof. Suppose T is coplanar in all $\mathcal{V}$-realization of $\mathcal{S}$. Then clearly all edges of D are good. Consequently, the coplanar graph of T is connected.

Suppose the coplanar graph of T is connected. Then, by transitivity of coplanarity, T is coplanar in all $\mathcal{V}$-realization of $\mathcal{S}$. ◀

Reduction from Prescribed Area for Triangulations

We show that the realizability of an area assignment of any triangulation can be reduced to an instance of Prescribed Volume.

▶ **Proposition 7.2.** *There is a polynomial time algorithm that takes as input any plane triangulation T with positive area assignment $\mathcal{A}$ and outputs a simplicial complex $\mathcal{S}$ with volume assignment $\mathcal{V}$ such that $\mathcal{A}$ is realizable for T if and only if $\mathcal{V}$ is realizable for $\mathcal{S}$.*

Proof. For a plane triangulation T, we define a simplicial complex $\mathcal{S}_T$ in the following way: Take two copies of T and glue them along an outer edge resulting in the graph F. Consider Figure 7.14(a) for an illustration. We introduce two new vertices x and y and define $\mathcal{S}_T := (x \oplus F) \cup (y \oplus F)$. Note that x and y are apices for their neighborhoods. For a given area assignment $\mathcal{A}$ of T, we consider the following volume assignment of $\mathcal{S}_T$:

$$\mathcal{V}_{\mathcal{A},0}(s) := \begin{cases} \mathcal{A}(t) & \text{for } s = t \oplus x \\ 0 & \text{for } s = t \oplus y \end{cases}$$

We show that the area assignment $\mathcal{A}$ is realizable for T if and only if the volume assignment$\mathcal{V}_{\mathcal{A},0}$ is realizable for $\mathcal{S}_T$.

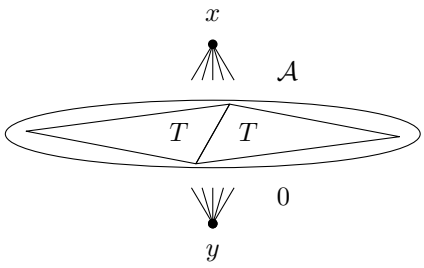

(a) Construction of the simplicial complex $\mathcal{S}_T$ and the volume assignment $\mathcal{V}_{\mathcal{A},0}$.

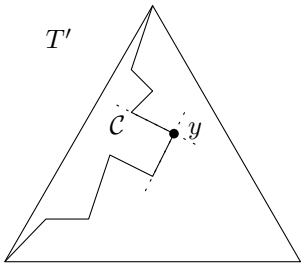

(b) If a copy T' of T is not coplanar, then y coincides with an inner vertex of T'.

Figure 7.14: Illustration of Proposition 7.2 and its proof.

If $\mathcal{A}$ is realizable for T, then we consider a realizing drawing of T and its copy in the plane. Placing vertex x at height 3 above the plane and vertex y at height 0 below the plane yields a $\mathcal{V}$-realization for $\mathcal{S}_T$.

Now assume that $\mathcal{V}_{\mathcal{A},0}$ is realizable for $\mathcal{S}_T$. We show that the vertices of at least one copy of T in any $\mathcal{V}_{\mathcal{A},0}$-realization of $\mathcal{S}_T$ are coplanar. To this end, let us assume that the vertices of one of the copies T' of T in F are not coplanar. We will call an inner edge e of T' a *crease edge* when the two triangles adjacent to e are not coplanar. We claim that y must be at an inner vertex of T'.

Observe that the area of each triangle of T' is positive, since each of the tetrahedra formed by a triangle of T' with the vertex x has positive volume. Hence, for every triangle t of T', we must have that y is in the plane spanned by t.

Let $\mathcal{C}$ denote the partition of the triangles of T' where each part consists of a maximal subset of coplanar triangles of T'. Since the vertices of T' are not coplanar, $\mathcal{C}$ has several parts and the boundaries of these parts must include at least one inner vertex. Hence, there is a closed walk W in T' around the boundary of a part of $\mathcal{C}$ that includes at least one inner vertex, see Figure 7.14(b). Since, the walk W is around the boundary of a part of $\mathcal{C}$, all the edges of W that are inner edges of T' are in fact crease edges.

For any crease edge $e = t_1 \cap t_2$ adjacent to the two triangles t_1 and t_2, the planes spanned by t_1 and t_2 intersect in a line ℓ. Since y is contained in both of these planes, y lies on the line ℓ. Observe that ℓ is also the line spanned by the edge e.

Since all triangles have positive area, the walk W must include some inner vertex w where it bends. That is, the edges e_1 and e_2 of W that are incident to w are not collinear. Since y is on both the line spanned by e_1 and the line spanned by e_2, we must have that $y = w$ at the point where these lines meet. Thus, y is at an inner vertex of T'.

Since each of the tetrahedra formed by a triangle of F with the vertex x has positive volume and these tetrahedra are non-crossing, none of the inner vertices of F coincide. Therefore, y can be an inner vertex of at most one of the copies T that constitute F, which means that the vertices of a copy T'' of T in F are coplanar.

Since the vertices of T'' are contained in a common plane P, each triangle t of T'' has area $3/h \cdot \mathcal{V}_{\mathcal{A},0}(t \oplus x)$ where h is the distance between x and P. Thus, if $\mathcal{V}_{\mathcal{A},0}$ is realizable, then scaling T'' by $\frac{h}{3}$ as above provides a realization of $\mathcal{A}$. ◀

Now, we are ready to prove the 3-dimensional generalization of prescribed area of triangulations hard.

7.2.5 Hardness of Prescribed Volume

In this section, we present a proof of the following statement.

■ **Theorem 46.** Prescribed Volume *is* $\exists\mathbb{R}$*-complete.*

Proof. We have to show the containment and the hardness. We start with the containment. Let $\mathcal{S}$ be a pure simplicial complex on the ground set V; we denote the maximal sets, namely the set of tetrahedra, by T and consider a volume assignment $\mathcal{V}\colon T \to \mathbb{R}_{\geq 0}$. We describe an ETR-formula Ψ that is true if and only if $\mathcal{S}$ has a crossing-free $\mathcal{V}$-realization. We define Ψ as follows:

$$\exists_{i\in V}(X_i, Y_i, Z_i)\ \exists_{\tau,\tau'\in T}(X_{\tau,\tau'}, Y_{\tau,\tau'}, Z_{\tau,\tau'}, B_{\tau,\tau'}) : \left(\bigwedge_{\tau,\tau'\in T} \textsc{CrossFree}(\tau,\tau')\right) \wedge \left(\bigwedge_{\tau\in T} \textsc{Volume}(\tau, \mathcal{V}(\tau))\right)$$

For two tetrahedra τ and τ', the predicate $\textsc{CrossFree}(\tau,\tau')$ shall guarantee that there exists a hyperplane separating τ and τ'. We define the predicate as the conjunction for each $i \in \tau$,

$$X_{\tau,\tau'}X_i + Y_{\tau,\tau'}Y_i + Z_{\tau,\tau'}Z_i + B_{\tau,\tau'} \geq 0$$

and for each $j \in \tau'$,

$$X_{\tau,\tau'}X_j + Y_{\tau,\tau'}Y_j + Z_{\tau,\tau'}Z_j + B_{\tau,\tau'} \leq 0.$$

In these inequalities $X_{\tau,\tau'}, Y_{\tau,\tau'}, Z_{\tau,\tau'}$, and $B_{\tau,\tau'}$ represent the coefficients of a hyperplane separating the two tetrahedra τ and τ'.

Analogous to Equation (2.1), the condition $\textsc{Volume}(\tau, \mathcal{V}(\tau))$ for a tetrahedron $\tau = \{h, i, j, k\}$ is given by the determinant equation

$$\det\begin{pmatrix} X_h & X_i & X_j & X_k \\ Y_h & Y_i & Y_j & Y_k \\ Z_h & Z_i & Z_j & Z_k \\ 1 & 1 & 1 & 1 \end{pmatrix} = 6\mathcal{V}(\tau).$$

This finishes the proof of the containment.

It remains to show the $\exists\mathbb{R}$-hardness. To do so, we reduce from ETR-inv. Let

$$\Psi = \exists X_1 \dots X_n : \Phi(X_1, \dots, X_n)$$

be an instance of ETR-inv, where Ψ is a conjunction of constraints expressing additions, inversions or the introduction of a constant. Since we will extend this proof in order to also prove Theorem 47, we handle the inversion constraints as general multiplications constraints (in order to be able to reduce from Constrained-UETR later on).

We construct a simplicial complex $\mathcal{S} = (V, F)$ and a volume assignment $\mathcal{V}$ for the tetrahedra in F, such that $\mathcal{S}$ has a $\mathcal{V}$-realization if and only if Φ is satisfiable. We start with a description of our essential building block.

Coplanar gadget The coplanar gadget forces several triangles of *equal area* to lie in a common plane as illustrated in Figure 7.15(a). These triangles will be free to one half space and hence, accessible for our further construction. In particular, all but one vertex of this gadget lie in the same plane. We call this plane the *(base) plane* of the coplanar gadget.

For the description of the construction, consider Figure 7.15(b). The coplanar gadget consists of three layers of tetrahedra. The first layer forces the triangles to be of equal size and the remaining two layers force coplanarity. We start with the plane triangulation T_k depicted in the top of Figure 7.15(b). Informally, T_k can be described as a row of alternating triangles where one vertex is stacked into every face. The parameter k denotes the number of red triangles in the top row. For the simplicial complex, we introduce a vertex v and a tetrahedron $v \oplus t$ for each triangle $t \in T_k$ and assign it to a volume of 1. In other words, v is an apex for T_k and $\mathcal{V}(t \oplus v) = 1$ for all $t \in T_k$.

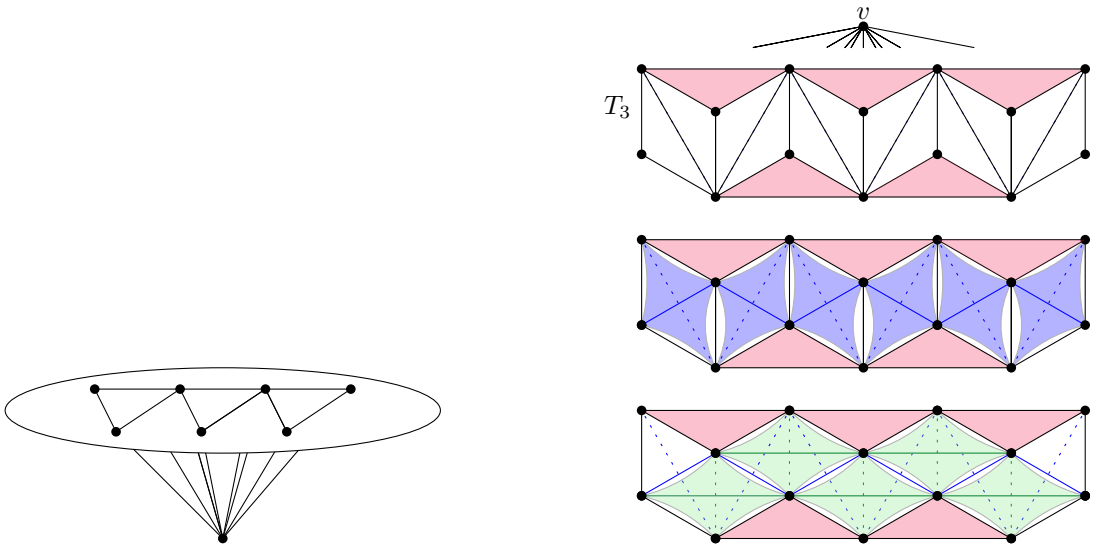

(a) The coplanar gadget. (b) The layers of the coplanar gadget.

Figure 7.15: The coplanar gadget and its construction.

Now, we describe the two layers enforcing co-planarity. Observe that the dual graph of the white triangles of T_k is an even path P. Consider a maximum matching M in P. For each matching edge e, we introduce a tetrahedron of volume 0 consisting of the two triangles of e in M, see the blue tetrahedra in Figure 7.15(b). In any realization, these quadruples of points are now coplanar due to the volume assignment. For the third layer, we consider the path P without M. This is also a matching and for each of its edges, we introduce a tetrahedron of volume 0 consisting of the two triangles in $P \setminus M$, see the green tetrahedra in Figure 7.15(b). Consequently, the coplanar graph of T_k is connected and hence, by Lemma 7.5, the vertices of T_k are coplanar in every volume realization. Lemma 7.4 in turn implies that the areas of all triangles in T_k are of equal size due to their tetrahedra with v. Note that the effective area depends on the distance of the plane to v.

When we refer to a *triangle* of the base plane, we always refer to one of the red triangles. The coplanar gadget bears its name due to the following functionality: By inserting a tetrahedron for each point of a set X with a private triangle from the base plane, the points of X are forced to lie in a common plane, i.e., to be coplanar. Moreover, this set of points is then *accessible* from almost all sides. We will make use of this fact to force points on a line.

Forcing points on a line We use the coplanar gadget to force a set of points representing the values of the variables to lie on a common line ℓ. In order to do so, we take two coplanar gadgets and enforce that their base planes E and E_ℓ are not parallel. This can be achieved by choosing two triangles Δ_1, Δ_2 of equal area on E and two distinct points v_1, v_2 from E_ℓ and inserting two tetrahedra $v_1 \oplus \Delta_1$ and $v_2 \oplus \Delta_2$ of different volume, e.g., 1 and 2.

Now consider a set of points $\{x_1, \ldots, x_n\}$. For each x_i, we introduce two tetrahedra: one with a triangle on E and the other with a triangle on E_ℓ, see Figure 7.16. We prescribe their volumes to be 1. Since the planes E and E_ℓ are not parallel, but the triangles on each plane have the same area, all x_i must lie in the intersection of two planes parallel to E and E_ℓ, respectively. We call this line of intersection ℓ.

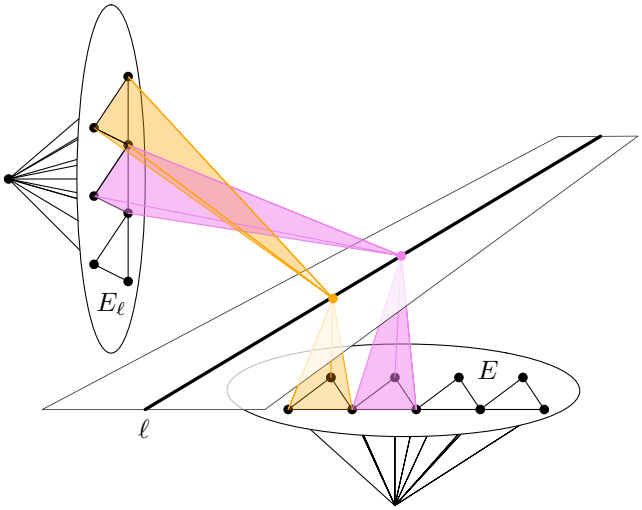

Figure 7.16: Forcing points to lie on a line ℓ.

The points $\{x_1, \ldots, x_n\}$ represent the values of our variables X_i in the following way. We introduce two special points p_0 and p_1 on the line ℓ and two other free points q, q' not necessarily on ℓ. The tetrahedron p_0, p_1, q, q' of volume 1 ensures that p_0 and p_1 are distinct. Without loss of generality we assume that $\|p_0 p_1\| = 1$. The value of variable X_i is represented by $\|p_0 x_i\|$. As before, we interpret p_0 as 0 and p_1 as 1.

Parallel gadget The parallel gadget is an extension of the coplanar gadget in order to force two sets of points to lie in two parallel planes that can vary independently of each other, see also Figures 7.17 and 7.18.

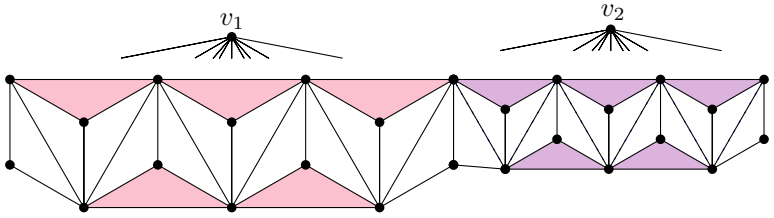

Figure 7.17: The triangulation T_{2k} consists of part T^1 with red triangles of equal area and the part T^2 with violet triangles of equal area. For $i \in \{1, 2\}$, each T^i has a private apex v_i.

Let U_1 and U_2 be two vertex sets. Consider a coplanar gadget with base plane B. In the first layer of the construction, we choose a triangulation T_{2k} for some k; the other two layers consist of degenerate tetrahedra forcing the triangulation to be coplanar in the same way as the degenerate tetrahedra of the coplanar gadget. The triangulation T_{2k} is broken into two parts, each isomorphic to T_k, as illustrated in Figure 7.17.

We denote these parts by T^1 and T^2, respectively. For each part T^i, there is an apex vertex v_i and a simplex $v_i \oplus t$ for each $t \in T^i$, and all of these simplices are assigned to a volume of 1. Consequently, the triangles of T_{2k} are coplanar and the triangles from T^i have the same area. Note that the areas of the triangles of T^1, the red triangles in Figure 7.17, are independent from the areas of the triangles of T^2, the violet triangles in Figure 7.17. We then add vertices $u \in U_i$ and for each triangle t_i of T^i a simplex $u \oplus t_i$ that is assigned volume 1. As in the coplanar gadget the vertices $u \in U_i$ from the same set are coplanar and the planes of coplanarity are each parallel to the plane that contains the triangulation T.

Clearly, we can generalize this construction to force h sets of points to lie in h parallel planes for any constant h.

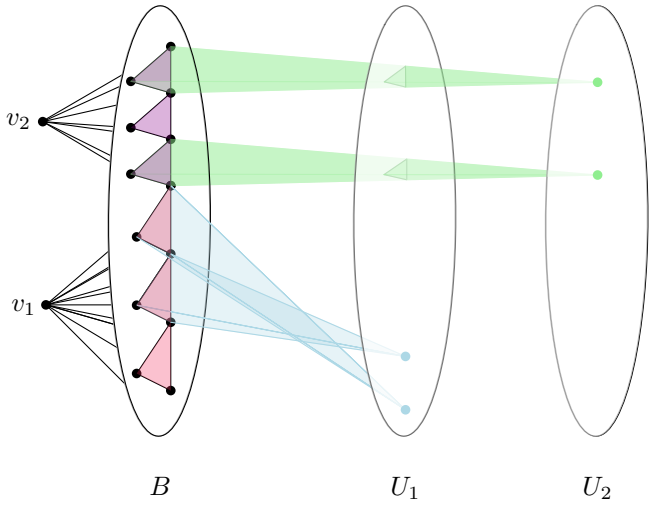

Figure 7.18: The parallel gadget. The points of U_1 and U_2 are both in a common plane parallel to B. However, these two planes are independent.

Addition and Multiplication gadget For both, the addition and multiplication gadgets, we mimic the ideas of the von Staude constructions. A crucial step is to construct a line parallel to a given line through a specified point. Let ℓ_1 be a line forced by coplanar gadgets with the already mentioned plane E and a new plane E_1. Let p be some point. We construct a line ℓ_2 parallel to ℓ_1 through p by introducing a parallel gadget extending the base plane E_1. We force points to be on ℓ_2 by tetrahedra with triangles on E_1 belonging to the parallel gadget and E (if they do not already exist). Figure 7.19 illustrates the parallel line construction.

In case we need to enforce that ℓ_1 and ℓ_2 do not coincide, we insert a tetrahedron t with volume 1 consisting of two new points on ℓ_1, a new point on ℓ_2 and an arbitrary new point. This tetrahedron t is displayed in cyan in Figure 7.19. Due to the positive volume of t, the four vertices of $\mathrm{vert}(t)$ are distinct and affinely independent. Consequently, in any $\mathcal{V}$-realization, ℓ_1 and ℓ_2 are two parallel and distinct lines.

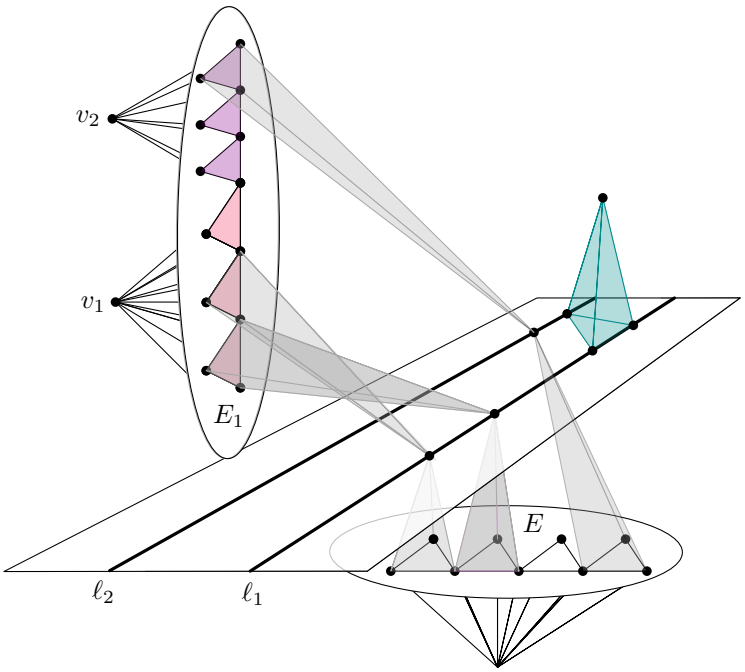

Figure 7.19: Constructing a parallel line. The cyan tetrahedron enforces ℓ_1 and ℓ_2 to be distinct.

Addition gadget For the *addition gadget* consider Figure 7.20. Suppose we want to enforce the constraint $X + Y = Z$. Thus the value of two points x and y on the line ℓ should add up to the value of the point z also on ℓ. We introduce a line ℓ' parallel to ℓ through a new point u_1 and ensure that the two lines are distinct as described above (analogous to the cyan tetrahedron in Figure 7.19). Using the parallel gadget we can later enforce more points to lie on ℓ'.

Then, we introduce a line ℓ_g through p_0 and u_1 and a parallel line ℓ'_g through y. Again, we use the parallel gadget. These two lines are green in Figure 7.20. We introduce the intersection point u_2 of ℓ' and ℓ'_g. Then we construct the line ℓ_r through u_1 and x and introduce the parallel line ℓ'_r through u_2; these two lines are displayed in red in Figure 7.20. The intersection point of ℓ and ℓ'_r is identified with z. Since the lines are parallel, it follows that $\|u_1u_2\| = \|p_0y\| = \|xz\|$ and hence, z is representing the value $\|p_0z\| = \|p_0x\| + \|p_0y\|$. This finishes our description of the addition gadget.

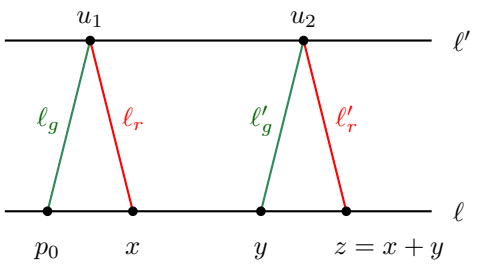

Figure 7.20: The addition gadget.

Multiplication gadget Now, we come to the *multiplication gadget*. (Note that an inversion gadget would suffice. However, as mentioned before, we extend this construction to prove $\forall\exists\mathbb{R}$-hardness for Volume Universality*. For this reduction we need the multiplication gadget, since we are going to reduce from Constrained-UETR.)

We will mimic the multiplication gadget from von Staude, which we previously used to prove Theorem 44, see Figure 7.10. We start by introducing a new coplanar gadget with base plane E_∞ to create a line ℓ_∞ intersecting ℓ in p_0 and spanning a plane with ℓ parallel to E. The points on ℓ_∞ are forced by the planes E and E_∞. We ensure that ℓ_∞ and ℓ do not coincide by introducing a tetrahedron of positive volume consisting of p_0, a new point on ℓ, a new point on ℓ_∞, and an arbitrary new point.

For the construction of the multiplication gadget, we choose a special point $\tilde{p}_1$ on ℓ_∞ and introduce the line $p_1\tilde{p}_1$. A parallel gadget with base plane E_p (together with E) forces a line parallel to $p_1\tilde{p}_1$ through y. These lines are depicted by green lines in Section 7.2.5.

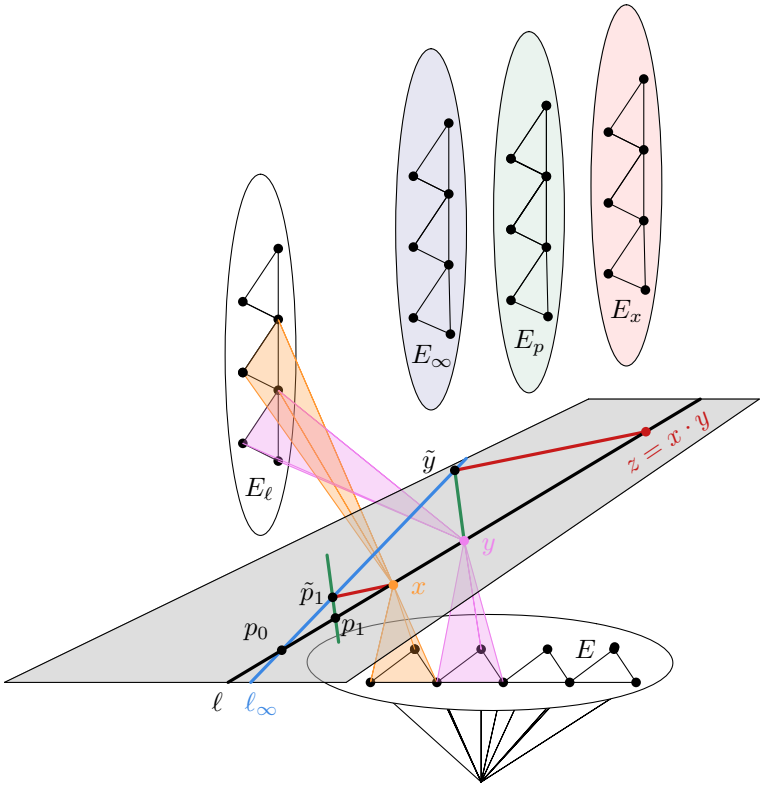

Figure 7.21: The multiplication gadget.

For each multiplication constraint including a fixed variable x, we need to introduce one private plane E_x. It forces lines parallel to $x\tilde{p}_1$ (through $\tilde{y}$). These lines are depicted by red lines in Section 7.2.5. We have already argued in the proof of Theorem 44, that the intercept theorem implies the correctness of this multiplication gadget. In particular, it holds that

$$\frac{\|\tilde{p}_1 p_0\|}{\|\tilde{y} p_0\|} = \frac{\|p_1 p_0\|}{\|y p_0\|} = \frac{\|x p_0\|}{\|z p_0\|}.$$

Thus $\|xp_0\| \cdot \|yp_0\| = \|zp_0\|$. Note that this gadget works for both cases $x \leq y$ and $x > y$.

This finishes the construction of $\mathcal{S}$ and its volume assignment $\mathcal{V}$. Next we will show that this yields a reduction.

▶ **Proposition 7.6.** *There exists a $\mathcal{V}$-realization of $\mathcal{S}$ if and only if Ψ is a* YES*-instance.*

Proof. If there exists a $\mathcal{V}$-realization of $\mathcal{S}$ then by construction of the coplanar gadget, all x_i are on a common line ℓ. By construction of the addition and multiplication gadgets all constraints of Ψ are satisfied. Hence setting $X_i := \|p_0 x_i\|$ is a satisfying assignment, and it follows that Ψ is a YES-instance.

Now, suppose that Ψ is a YES-instance. To do so, we describe an explicit placement of the previously described objects. We give explicit coordinates for the objects that are responsible for the encoding of the variables and the calculations. However, we place most of the coplanar and parallel gadgets very far away in some 'generic' directions. In this way, almost all tetrahedra are long and skinny. This ensures that they do not intersect, as those directions are sufficiently different. The following thought experiment might help to give an intuition: Consider a set Q of points in $\mathbb{R}^3$ and a set R of rays emitting from Q. When we choose the directions of the rays in a generic direction, no two rays intersect. In fact we expect that they have some positive distance. The long and skinny tetrahedra can be thought of as thickened rays.

As a start, we assume that there exist values for $X_1, \dots, X_k$ fulfilling the addition and multiplication constraints. By slight abuse of notation, we will also denote the values of $X_1, \dots, X_k$ by the same symbol. We have to show that there exists a $\mathcal{V}$-realization of $\mathcal{S}$. In order to do so, we place the point $x_i = (X_i, 0, 0)$ for all $i \in [k]$ and choose the x-axis as the line ℓ. We then build a coplanar gadget with base plane $E = \{(X, Y, -1)\}$ and a second coplanar gadget with base plane $E_\ell = \{(X, -1, Z)\}$, see also Figure 7.22.

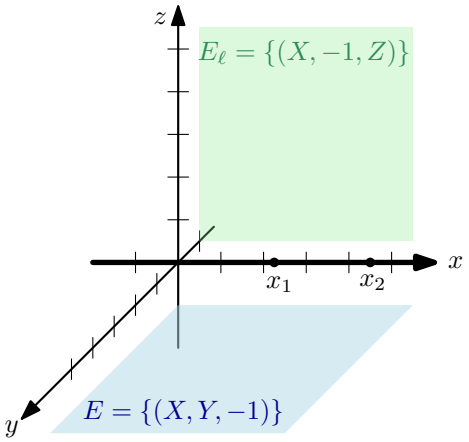

Figure 7.22: Placement of the points and the first base planes.

We can then add all the tetrahedra forcing the points x_i to be on the line ℓ. We position the triangulation T in the plane E so that triangles t_i where we attach tetrahedra with a vertex at the points x_i are positive in the second coordinate and so that successive triangles have larger second coordinate everywhere. Specifically, we can choose points $a_0, \dots, a_{2k}$ and $b_0, \dots, b_{2k-1}$, as shown in Figure 7.23(a), given explicitly by

$$a_i = \begin{cases} (0, i, -1) & \text{for } i \text{ even} \\ (9, i, -1) & \text{for } i \text{ odd} \end{cases} \qquad \text{and} \qquad b_i = (a_{i-1} + a_i + a_{i+1})/3.$$

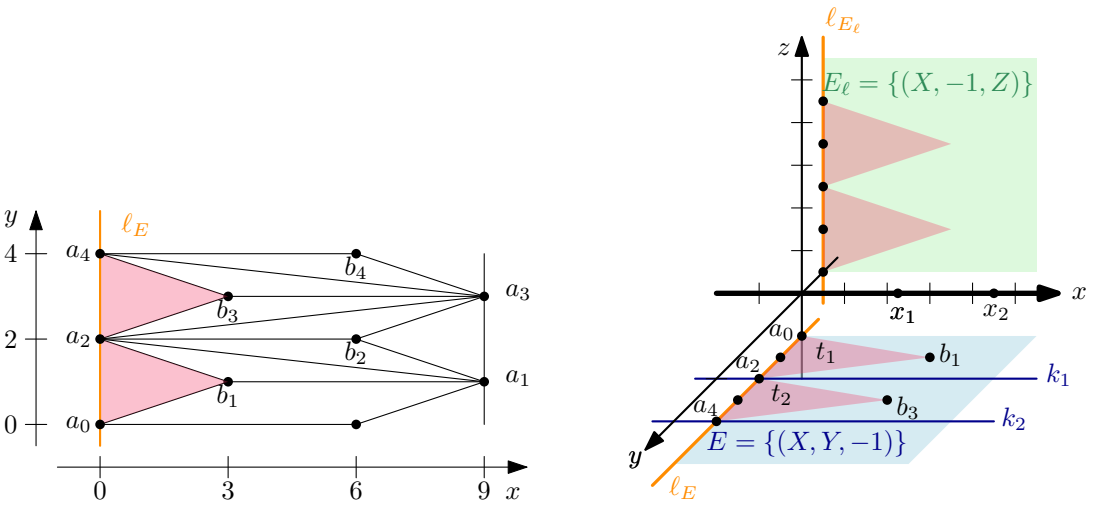

(a) Placing the triangulation.

(b) Addition of the tetrahedra.

Figure 7.23: Placing the coplanar gadgets for E and E_ℓ.

Let t_i be the triangle with vertices $\{a_{2i}, b_{2i+1}, a_{2i+2}\}$. Note that t_i has area 3. We then place the apex v of T at $(0, 0, -2)$. Let us denote the line through all $a_2, a_4, \ldots, a_{2k}$ as the *skeleton-line* ℓ_E of the triangles in E. As depicted in Figure 7.23(b), the line ℓ_E is orthogonal to ℓ. Now we add the simplices given in the definition of the coplanar gadget. Observe these tetrahedra have pairwise disjoint interior for all positions of x_i on ℓ. To be more specific, let $T_i = t_i \oplus x_i$ and $T_j = t_j \oplus x_j$ be two such tetrahedra with $i < j$. We define a plane P that separates the interior of the two tetrahedra as follows. Let k_i be the line $(X, 2i, -1)$ parallel to ℓ. The unique plane that contains ℓ and k_i defines P.

Similarly, we position the triangulation T_ℓ in E_ℓ such that each triangle t'_i is positive in the third coordinate which is increasing with i. In other words, the skeleton line ℓ_{E_ℓ} of T_ℓ is orthogonal to both ℓ_E and ℓ. We can achieve this in the same way as for T by swapping the second and third coordinates, as illustrated in Figure 7.23(b). We may extend the triangulation T_ℓ to include vertices that are negative in the third coordinate, and attach a tetrahedron to two of these triangles, t'_0 and t'_{-1} as given above, with a vertex at a_0 and a_1 respectively. Then these tetrahedra have volumes 1 and 2. Observe these tetrahedra all have pair-wise disjoint interior.

For the addition and multiplication gadget we assume that the formula Φ is "long enough", i.e., its length $n := |\Phi|$ is at least C, for some sufficiently large constant C. Otherwise we may replace n with a sufficiently large constant where needed in the construction.

For each multiplication constraint $C_i \equiv [X \cdot Y = Z]$ in Φ, we attach a copy of the multiplication gadget. Each multiplication gadget introduces two new points, $\tilde{a}_i$ and $\tilde{b}_i$ that correspond to the points $\tilde{p}_1$ and $\tilde{y}$ in the definition of the multiplication gadget, respectively, and additionally one new line ℓ_i that corresponds to the line ℓ_∞ in the definition of the multiplication gadget. We choose the lines ℓ_i such that successive lines have greater slope. Specifically, we choose $\ell_i = \{X, iX, 0\}$ to have slope i, see also Figure 7.24.

By the multiplication constraint, the triangulation E_ℓ was extended. Moreover, we introduce the tetrahedra connected to the extended triangles of T_ℓ and to the points $\tilde{a}_i, \tilde{b}_i$ in order to force these points to be in the plane parallel to E_ℓ through the line ℓ. Note that we are free to choose $\tilde{a}_i$ on the line ℓ_i. However, each choice determines $\tilde{b}_i$, provided that both points have a positive first coordinate.

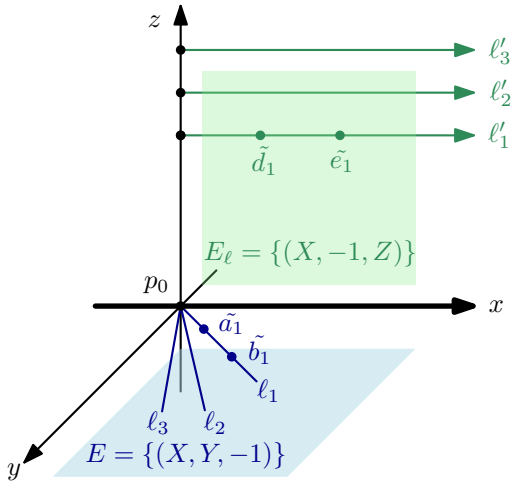

Figure 7.24: Placing points of the multiplication gadgets.

For each addition constraint $C \equiv [X + Y = Z]$ in Φ, we introduced a copy of the addition gadget. Recall that each addition gadget introduces two new points $\tilde{d}_i$ and $\tilde{e}_i$ that respectively correspond to u_1 and u_2 in the definition of the addition gadget. We put the points $\tilde{d}_i$ and $\tilde{e}_i$ on the ray $\ell'_i = \{(X, 0, n + i) : X > 0\}$. Note that these rays do not intersect the lines ℓ_i from the multiplication gadgets, as illustrated in Figure 7.24. Again we extend T_ℓ and add tetrahedra connecting a triangle of T_ℓ to each of these points. Note that we are free to choose $\tilde{d}_i$ on the ray $\{(X, 0, n + i) : X > 0\}$, and this determines $\tilde{e}_i$.

It remains to place the coplanar and parallel gadgets introduced for an an addition or a multiplication constraint. Here, we specify a *special* (generic) direction. To do so, we define $d_i = (i, n \cdot i, 1)$, then we add a triangulation T_i starting with the point $n^3 d_i$. We may choose all planes of the triangulations T_i to have slope at most 1 with respect to the second coordinate plane. This means that the tetrahedra connecting points in the second coordinate plane to those triangles that are within a constant radius of $n^3 d_i$ have a height of order n^4. Therefore, their triangles have an area of order n^{-4}. Since the triangulation has only finitely many triangles, the entire triangulation can be placed within a distance of order n^{-4} from the point $n^3 d_i$. Thus, for n large enough, for each point x among $x_i, \tilde{a}_i, \tilde{b}_i, \tilde{d}_i, \tilde{e}_i$, the tetrahedra connecting x to the coplanar and parallel gadgets will only intersect at x.

Consider a pair of distinct vertices x, x' among the vertices $x_i, \tilde{a}_i, \tilde{b}_i, \tilde{d}_i, \tilde{e}_i$ and two tetrahedra t, t' connecting those vertices to a parallel or coplanar gadget. If both x and x' are on the line ℓ, then t and t' do not intersect. Thus, suppose that x' is not on ℓ. The tetrahedra t and t' are contained in cylinders C, C' of radius of order at most n^{-4}. The projection of the cylinder C to the transverse plane of C' is a strip of width of order n^{-4} that has slope of order at least n^{-2} with respect to the line on which the point x' is chosen. Thus, if we fix the position of x, there is an interval of length of order at most n^{-2} where we cannot place x' without t and t' intersecting. Therefore, if we choose the points $\tilde{a}_i$ and $\tilde{d}_i$ successively, each time we place a point, if we consider positions that are spaced n^{-2} apart, at most a factor of n of these will cause a forbidden intersection with a tetrahedron already placed. Thus, we only have to consider a factor of n such positions to be guaranteed a position that does not cause a forbidden intersection. Thus, we have found a crossing-free drawing of $\mathcal{S}$. This completes the proof of Proposition 7.6. ◀

Finally, we argue that the underlying abstract simplicial complex of $\mathcal{S}$ is realizable.

▶ **Proposition 7.7.** *$\mathcal{S}$ is realizable in $\mathbb{R}^3$ as a simplicial complex without volume constraints.*

Proof. To see this, we just follow the same construction as above, but we start with points x_i placed arbitrarily along the first coordinate axis. We add the coplanar gadgets that force the points to be on ℓ, but we perturb the vertices of the triangulation slightly to realize the abstract simplicial complex defined by the coplanar gadget as a simplicial complex. In the case of the triangulation T this is done by moving each point b_i to the point $b_i + (0, 0, 1/2)$, and similarly for T_ℓ. In general this may be done by moving the inner points of the triangulation away from the apex v of the coplanar or parallel gadget. Next, we add the points $\tilde{a}_i, \tilde{b}_i, \tilde{c}_i, \tilde{d}_i, \tilde{e}_i$ in the upper half of the second coordinate plane without regard to collinearities or parallel lines. Then, we add the coplanar and parallel gadgets used in the addition and multiplication gadgets as above, but we modify the coplanar and parallel gadgets to be simplicial complexes by relaxing the coplanarity of the triangulation in the same way as with T. ◀

This completes the proof of Theorem 46. ■

As promised, we now expand the presented proof in order to show hardness of the universality variant.

7.2.6 Hardness of Volume Universality*

In this section we prove the following theorem.

■ **Theorem 47.** Volume Universality* *is $\forall\exists\mathbb{R}$-complete.*

Proof. We show that Volume Universality* is contained in $\forall\exists\mathbb{R}$ by describing an arbitrary instance as an UETR-formula. This is analogous to the containment of Prescribed Volume in $\exists\mathbb{R}$. We are given a pure abstract simplicial complex realizable in $\mathbb{R}^3$ over a ground set V with maximal sets T and a partial assignment of the volumes $\mathcal{V} : T' \to \mathbb{R}_{\geq 0}$. The corresponding formula is defined as follows, where the predicates CrossFree and Volume are defined as in the proof of Theorem 46:

$$\underset{\tau\in T}{\forall}(A_\tau)\ \underset{i\in V}{\exists}(X_i, Y_i, Z_i)\ \underset{\tau,\tau'\in T}{\exists}(X_{\tau,\tau'}, Y_{\tau,\tau'}, Z_{\tau,\tau'}, B_{\tau,\tau'}):$$
$$\left(\bigwedge_{\tau\in T} A_\tau \geq 0\right) \wedge \left(\bigwedge_{\tau\in T'} \mathcal{V}(\tau) = A_\tau\right) \Rightarrow$$
$$\left(\bigwedge_{\tau,\tau'\in T} \textsc{CrossFree}(\tau,\tau')\right) \wedge \left(\bigwedge_{\tau\in T} \textsc{Volume}(A_\tau,\tau)\right)$$

To prove hardness, we reduce from Constrained-UETR. Let Ψ be a formula of the form:

$$\Psi = (\forall Y_1, \ldots, Y_m \in \mathbb{R}_{>0})(\exists X_1, \ldots, X_n \in \mathbb{R}_{>0}) \colon \Phi(Y_1, \ldots, Y_m, X_1, \ldots, X_n).$$

Recall that Φ is a conjunction of constraints of the form $X = 1$, $X + Y = Z$ and $X \cdot Y = Z$. We extend the construction from the proof of Theorem 46. Since we already introduced gadgets for the constraints, it only remains to introduce the universally quantified variables.

For every Y_i, let y_i be the point encoding its value. We force y_i to lie on ℓ with the planes E and E_ℓ. As before $\|p_0 y_i\|$ represents the value of Y_i, see also Figure 7.25.

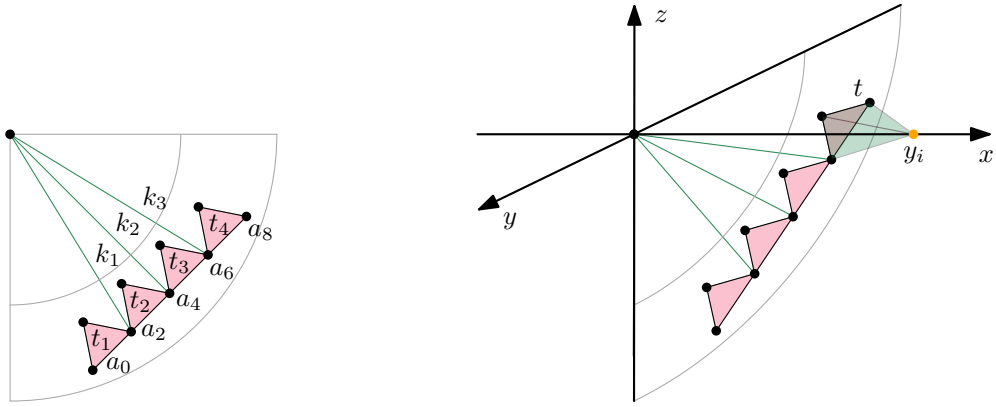

(a) Depiction of the base plane E_Y.

(b) Placement of E_Y in space.

Figure 7.25: The coplanar gadget with base plane E_Y is used to insert the universally quantified variables Y_i.

Moreover, we introduce a coplanar gadget with base plane E_Y. We ensure that ℓ intersects E_Y by identifying the point p_0, which is contained in E_Y and in ℓ. Consequently, each plane parallel to E_Y intersects ℓ in exactly one point.

We introduce a tetrahedron of volume 1, connecting one of the triangles on E_Y to the point p_1 representing the value 1. For each universally quantified variable, we introduce a tetrahedron of *flexible* volume Y_i consisting of a triangle of E_Y and the point y_i. For each value of Y_i, the point y_i is uniquely determined (since it lies on ℓ and the height of the tetrahedron is prescribed). In particular, the value of Y_i is $\|p_0 y_i\|$.

It remains to show that the defined simplicial complex $\mathcal{S}$ has the wished properties.

▶ **Proposition 7.8.** *$\mathcal{S}$ is volume-universal if and only if Ψ is a* YES*-instance.*

Proof. Suppose Ψ is a NO-instance. Then there exist the values $Y_1, \ldots, Y_m \in \mathbb{R}_{>0}$ such that for all values $X_1, \ldots, X_n \in \mathbb{R}_{>0}$ the formula Φ is false. Suppose for a contradiction that $\mathcal{S}$ is volume-universal. Then, in particular, there exists a realization for the chosen values $Y_1, \ldots, Y_m$. By the correctness of the addition and multiplication gadgets, it follows that setting X_i to $\|p_0 x_i\|$ is a satisfying assignment. This contradicts the fact that our choice of values $Y_1, \ldots, Y_m$ certifies Ψ to be a NO-instance.

Now, suppose Ψ is a yes-instance. Consider fixed but arbitrary $Y_1, \ldots, Y_m \in \mathbb{R}_{>0}$. Hence, we consider the constructed simplicial complex where all tetrahedra have fixed volume. We construct a realization exactly as is Theorem 46. It only remains to add the new points y_i and their tetrahedra to the planes E_Y, E and E_ℓ. We set the plane $E_Y = \{(0, Y, Z)\}$. The triangulation T_Y of E_Y is placed such that it is contained in $\{(0, y, z) : y, z \leq 0\}$; in particular, it is is placed within a quarter circle as depicted in Figure 7.25(a). We choose the triangulation small enough such that the line k_i in E_Y through a_{2i} and the origin separates two adjacent triangles.

First we observe that no two tetrahedra of a point y_i intersects in their interior. For this let t, t' be two such tetrahedra. We note that their underlying triangles are separated in the E_Y plane by at least one of the k_i's. Define P as a plane containing such a k_i and the x-axis. The plane P separates t and t'.

It remains to show that no newly introduced tetrahedron intersects any previous tetrahedron. We define the octants

$$O(+++) = \{(x, y, z) : x \geq 0, y \geq 0, z \geq 0\},$$

$$O(+-+) = \{(x, y, z) : x \geq 0, y \leq 0, z \geq 0\},$$

$$O(++-) = \{(x, y, z) : x \geq 0, y \geq 0, z \leq 0\},$$

$$O(+--) = \{(x, y, z) : x \geq 0, y \leq 0, z \leq 0\}.$$

For an illustration consider Figure 7.26. Except for the apex tetrahedra, it is easy to observe that all (interesting) tetrahedra of E_Y are contained in the octant $O(+--)$. Likewise, the interesting tetrahedra of E are in the octant $O(++-)$ and the tetrahedra of E_ℓ are in the octant $O(+-+)$. Moreover, the tetrahedra for the addition and the multiplication gadgets are contained in the octant $O(+++)$. This certifies that none of the new tetrahedra intersect any of the previous ones. ◀

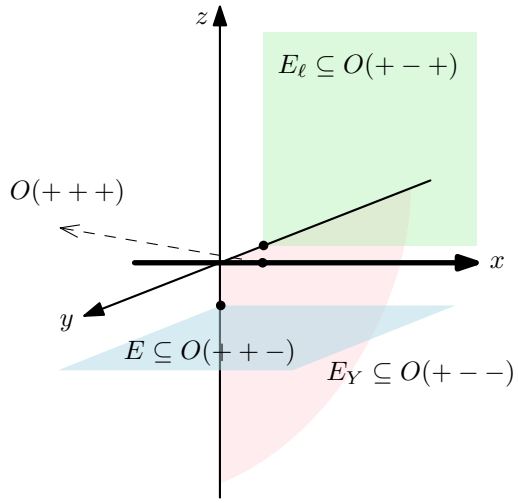

Figure 7.26: The construction is simultaneously realizable, because the tetrahedra of E_ℓ are contained in the octant $O(+-+)$, the tetrahedra of E are contained in the octant $O(++-)$, the tetrahedra of E_Y are contained in the octant $O(+--)$, and the tetrahedra of the multiplication and addition gadgets are contained in the octant $O(+++)$.

Therefore, we have proved Theorem 47. ■

This finishes our discussion of the computational complexity of area-universality. We have proved that several related problems are $\forall\exists\mathbb{R}$-complete. For further interesting candidates of $\forall\exists\mathbb{R}$-complete problems, we refer to our paper [Dobbins et al., 2018].

8 | Future Direction – Air Pressure

In this chapter, we present a promising idea for proving area-universality. The air pressure method is inspired by the physical principle of pressure compensation and has been successfully used to show area-universality of rectangular layouts [Felsner, 2014]. Starting with some drawing of a plane graph, the idea is to theoretically pump air in the faces such that faces with too little area have high pressure and faces with too much area have low pressure. Then the air pressure exerts forces on the vertices. If a vertex moves in the direction of its force the drawing *improves*. Ideally, in every non-realizing drawing, there exists a non-balanced vertex which can be moved in the direction of its force. By iteratively moving vertices to better positions, we wish to arrive at a realizing drawing.

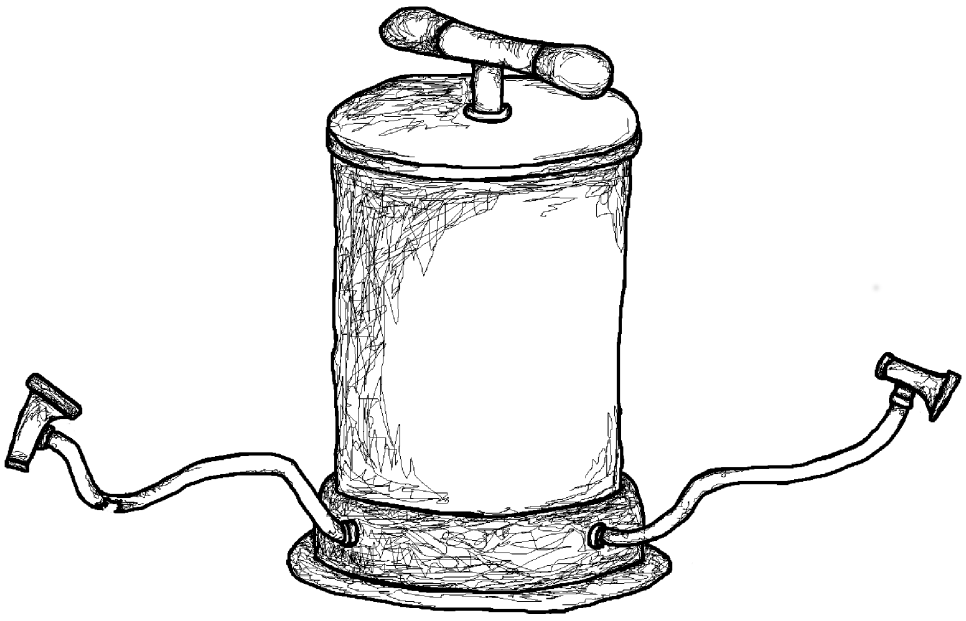

Figure 8.1: An air pump which may be used to pump air the faces of the a plane graph.

8.1 Air Pressure Method

In this chapter, we restrict to drawings that are not degenerate, i.e. planar, and therefore consider a plane graph G with an area assignment $\mathcal{A}\colon F' \to \mathbb{R}_{>0}$. The *pressure* $\mathfrak{p}_f(D)$ of an inner face f of G in a fixed drawing D is defined as the ratio of the prescribed area and the area in D, i.e.,

$$\mathfrak{p}_f(D) := \frac{\mathcal{A}(f)}{\text{AREA}(f, D)}.$$

The area of f is realized in D if and only if its pressure is 1. Since the drawing is planar, the area of each face is positive. The pressure $\mathfrak{p}_f(D)$ of face f exerts a force on an incident vertex v as follows: Let v_1 and v_2 denote the two neighbors of v on f such that v_1, v, v_2 appear in counter clockwise orientation on the boundary of f. Figure 8.2 depicts this situation. Let $s(v, f)$ denote the vector connecting its neighbors from v_2 to v_1, i.e., we

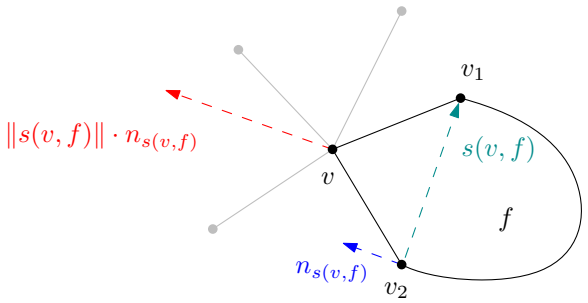

Figure 8.2: Illustration of how the pressure of a face exerts a force on an incident vertex.

define $s(v, f) := v_1 - v_2$. The force of f on v is proportional to the pressure of f and the length of $s(v, f)$. Its direction is the normal of $s(v, f)$. Denoting the normal of a vector s by n_s, the total *force* $\mathfrak{f}_v(D)$ acting on v in the drawing D is described by

$$\mathfrak{f}_v(D) := \sum_{f : v \in f} \mathfrak{p}_f(D) \cdot \|s(v, f)\| \cdot n_{s(v,f)}.$$

We say a vertex is *in balance* (of forces) in D if its force vanishes, i.e., has length 0. Otherwise a vertex is *unbalanced*.

Observation 8.1. *Vertex v is in balance if and only if*

$$\sum_{f : v \in f} \mathfrak{p}_f(D) \cdot s(v, f) = \vec{0}.$$

To show that the drawing improves when a vertex is moved in the direction of its force vector, we introduce the entropy function. The *entropy of a face* f of G in D is defined as $E_f(D) := -\mathcal{A}(f) \cdot \log(\mathfrak{p}_f(D))$. The *entropy function* $E\colon \mathcal{D} \to \mathbb{R}$ assigns to each drawing $D \in \mathcal{D}$ of G the sum of face entropies:

$$E(D) := \sum_f E_f(D) = \sum_f -\mathcal{A}(f) \cdot \log(\mathfrak{p}_f(D)).$$

It follows from the definition that

Observation 8.2. *The entropy function is smooth.*

Indeed, moving a vertex v in direction of its force $\mathfrak{f}_v$ increases the entropy. This is easy to understand given the following interplay of the entropy and the forces.

▶ **Proposition 8.3.** *The vector field of forces* $\mathfrak{v}\colon \mathcal{D} \to \mathbb{R}^{2(n-3)}, \mathfrak{v}(D) = (\mathfrak{f}_v(D))_v$ *is a gradient vector field with the entropy function* $E\colon \mathcal{D} \to \mathbb{R}$ *as its potential.*

Proof. Let v be a vertex with coordinates (v_x, v_y). We show that up to scaling, the force of v is the gradient of E restricted to two coordinates. In particular, it holds that

$$\frac{1}{2}\mathfrak{f}_v = \frac{\partial E}{\partial v_x}\begin{pmatrix}1\\0\end{pmatrix} + \frac{\partial E}{\partial v_y}\begin{pmatrix}0\\1\end{pmatrix}.$$

Since only vertex v moves, we interpret $E(\cdot)$, $\mathfrak{p}(\cdot)$, and $\textsc{area}(\cdot)$ as functions of (v_x, v_y). The area of a face f incident to v can be expressed with respect to the position v_0 of v in D:

$$\textsc{area}(f, v) = \textsc{area}(f, v_0) + \frac{1}{2} \cdot ||s(v,f)|| \cdot \left\langle n_{s(v,f)}, \begin{pmatrix}v_x\\v_y\end{pmatrix} - v_0 \right\rangle$$

For the partial derivative, it therefore holds that

$$\frac{\partial \textsc{area}\,(f,v)}{\partial v_x} = \frac{1}{2} \cdot ||s(v,f)|| \cdot \left\langle n_{s(v,f)}, \begin{pmatrix}1\\0\end{pmatrix} \right\rangle$$

By some straight-forward manipulations, we obtain

$$\frac{\partial E(v)}{\partial v_x} = \sum_{f\colon v\in f} \frac{\partial}{\partial v_x}\Big(- \mathcal{A}(f) \cdot \log(\mathfrak{p}_f(v))\Big) = \sum_{f\colon v\in f} \mathfrak{p}_f(v) \cdot \frac{\partial \textsc{area}}{\partial v_x}\,(f,v) = \frac{1}{2}\left\langle \mathfrak{f}_v, \begin{pmatrix}1\\0\end{pmatrix}\right\rangle.$$

Analogously, it holds that $\partial E/\partial v_y = 1/2\langle \mathfrak{f}_v, (0,1)\rangle$ This yields the claim. ◀

A further useful fact is that the entropy is always non-positive and vanishes only in realizing drawings. This property has already been used before.

▶ **Lemma 8.4** ([Felsner, 2014], Lemma 6)**.** *The entropy* $E(D)$ *is non-positive for all* $D \in \mathcal{D}$ *and* $E(D) = 0$ *if and only if* D *is a realizing drawing.*

The idea of the air pressure method is to find realizing drawings with the following gradient descent procedure:

> Algorithmic Idea
>
> While D not realizing
> - find a vertex v with $\mathfrak{f}_v \neq 0$,
> - move vertex v along $\mathfrak{f}_v$ by preserving planarity.

Clearly for this algorithm to work, the following property is essential: If a drawing is not realizing, then

(i) there exists a vertex v with $\mathfrak{f}_v \neq 0$ such that
(ii) vertex v can be moved along the trajectory of its force $\mathfrak{f}_v$ preserving planarity.

In fact, property (i) can be guaranteed for cubic graphs and property (ii) can be guaranteed for triangulations. Unfortunately, we do not know of a graph class where we can prove both properties simultaneously. While there is no hope that (i) holds for triangulations, we are still positive that there is some way to show property (ii) for cubic graphs.

Due to the fact that the above algorithm would stop, we call a non-realizing drawing where all vertices are in a balance of forces a *deadlock*. We call a vertex v *movable* in D if it can be moved along the trajectory of $\mathfrak{f}_v$ (for a little bit) such that the redrawing is still a planar straight-line drawing. We continue to sketch the above properties for the mentioned graphs classes.

8.1.1 Vertices are Movable in Triangulations

Throughout this subsection, we consider a plane triangulation T with an area assignment $\mathcal{A}\colon F' \to \mathbb{R}_{>0}$. For the following properties, it turns out that the positivity of the area assignment is crucial.

▶ **Lemma 8.5.** *Every vertex v in T is movable; even to a balanced position.*

Proof. If $\mathfrak{f}_v = 0$, the statement is vacuous. So we assume that $\mathfrak{f}_v \neq 0$. Let $\mathcal{P}$ denote the set of all points in the plane such that D remains crossing-free when v is moved to this point. In Figure 8.3, the gray region illustrates the set $\mathcal{P}$. We want to show that $\mathfrak{f}_v$ points in a direction contained in $\mathcal{P}$. It is easy to see that $\mathcal{P}$ is the intersection of half spaces:

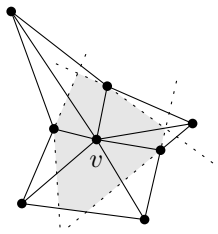

Figure 8.3: Illustration of Lemma 8.5.

For each incident triangle t of v, consider the line ℓ_t supporting the unique triangle edge which is not incident to v. Then v must lie in the half space defined by ℓ_t containing v. Moreover, approaching any point on the boundary of $\mathcal{P}$, some triangle t has infinitesimal area, resulting in unbounded pressure. Consequently, close to the boundary of $\mathcal{P}$, the force $\mathfrak{f}_v$ points inwards. Thus, v is movable.

In order to show the existence of a balanced position, the idea is to follow $\mathfrak{f}_v$ as long as possible. Recall that, by Proposition 8.3, the force $\mathfrak{f}_v(p)$ is a gradient vectorfield on $\mathcal{P}$ with the entropy $E(D_p)$ as its potential. By the *extreme value theorem* (Weierstraß), the continuous function $E(D_p)$ attains its maximum on the non-empty compact set $\mathcal{P}$. Due to the direction of the force vectors, no boundary point of $\mathcal{P}$ is a maximum. Consequently, the maximum is attained at an inner point p. Therefore, the gradient in p vanishes and it holds that $\mathfrak{f}_v(p) = 0$. ◀

The statement of Lemma 8.5 can be strengthened as follows. The proof is presented in Section 8.1.3.

▶ **Lemma 8.6.** *Every vertex v in T can be moved to a balanced position; this position is unique when all other vertices are kept at their position.*

In the following, we consider a sequence $(D_i)_i$ of drawings of a plane triangulation T where D_{i+1} is obtained from D_i by moving an unbalanced vertex v into the balanced position. We call a rule for selecting an unbalanced vertex v *attentive* if it fulfills the following property: If v is unbalanced in D_i, then there is a $j > i$ such that v is balanced in D_j.

▶ **Lemma 8.7.** *Let T be a plane triangulation with an area assignment $\mathcal{A}\colon F' \to \mathbb{R}_{>0}$ and let D_0 be a drawing of T where the outer face has area ΣA. Let $(D_i)_{i\in\mathbb{N}}$ be a sequence of drawings of T, where D_{i+1} is obtained from D_i by moving an unbalanced inner vertex v into a balanced position. If the selection rule of the vertices is attentive, then there is a subsequence $(D'_i)_{i\in\mathbb{N}}$ of drawings with limit $D' := \lim_{i\to\infty} D'_i$ which is either an $\mathcal{A}$-realizing drawing or a deadlock.*

A proof of this lemma is presented in Section 8.1.3. It implies that the following algorithm approaches realizing drawings or deadlocks.

> Air Pressure Algorithm 1
>
> While there exists an unbalanced vertex,
> - pick an unbalanced vertex v with an attentive selecting rule and
> - move v into its balanced position.

Hence, we obtain the following fact:

■ **Corollary 50.** *Let T be a plane triangulation with an area assignment $\mathcal{A}\colon F' \to \mathbb{R}_{>0}$. Then, the* Air Pressure Algorithm 1 *yields a drawing that is arbitrarily close to a realizing straight-line drawing or a deadlock.*

Unfortunately, there exist deadlocks even if realizing drawings exist. Figure 8.4 depicts two distinct equiareal drawings of the plane octahedron graph and a deadlock an equiareal area assignment. Intuitively, the algorithm is torn between the two realizing drawings.

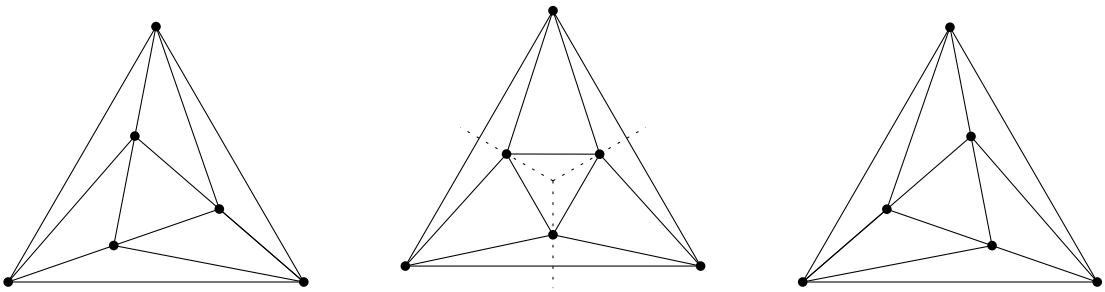

(a) An equiareal drawing. (b) A deadlock. (c) An equiareal drawing.

Figure 8.4: Two equiareal drawings of the octahedron graph in (a) and (c) and a deadlock drawing *between* these to realizing drawings in (b).

▶ **Proposition 8.8.** *Triangulations may have deadlocks – even if a realizing drawing exists.*

Proof. We consider the area assignment of the octahedron graph where all face areas are assigned to 1. We claim that there exists a rotational symmetric deadlock situation where all inner vertices lie on the bisectors as illustrated in Figure 8.4(b). Consider the neighborhood of an inner vertex in such a symmetric drawing. We denote the incident faces of v by f_i for $i \in [4]$ as depicted in Figure 8.5 where f_i has pressure $\mathfrak{p}_i$ and $s_i := s(v, f_i)$. Note that the 4-cycle formed by the neighbors of v has two parallel sides.

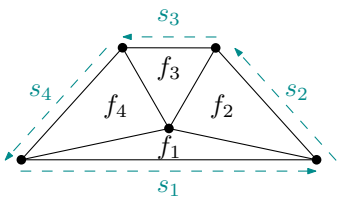

Figure 8.5: Computing the direction of the force vectors.

Thus, for some $\alpha > 0$ it holds that $-\alpha \cdot s_1 = s_3$ and $s_2 + s_4 = (1-\alpha) \cdot s_1$. By symmetry, the faces f_2 and f_4 have the same pressure. Therefore, the sum of the (rotated) forces equals

$$\sum \mathfrak{p}_i \cdot s_i = (\mathfrak{p}_1 + (1-\alpha) \cdot \mathfrak{p}_2 - \alpha \cdot \mathfrak{p}_3) \cdot s_1.$$

Consequently, the force has direction $\pm n_{s_1}$ and thus points along the bisector. Moving all three vertices simultaneously in the direction of their force, the length of their force vectors continuously decreases and we end in a deadlock. ◀

8.1.2 Plane Cubic Graphs have no Deadlock

In this section, we show that plane cubic graphs are free of deadlocks. To do so, we study vertices in balanced positions. Throughout this subsection, we consider a plane cubic graph G with an area assignment $\mathcal{A}\colon F' \to \mathbb{R}_{>0}$. For a vertex v, we denote its three incident faces by f_i with $i \in [3]$ and define $s_i := s(v, f_i)$ as well as $\mathfrak{p}_i$ as the pressure of f_i.

▶ **Lemma 8.9.** *In a plane cubic graph G, vertex v is in balance if and only if one of the following conditions hold*

a) the pressures of its incident faces are identical, i.e., $\mathfrak{p}_1 = \mathfrak{p}_2 = \mathfrak{p}_3$, or

b) the three neighbors of v are collinear and the pressure $\mathfrak{p}_3$ in the face with reflex angle is the weighted average of pressures $\mathfrak{p}_1$ and $\mathfrak{p}_2$, i.e., $\mathfrak{p}_3\|s_3\| = \mathfrak{p}_1\|s_1\| + \mathfrak{p}_2\|s_2\|$.

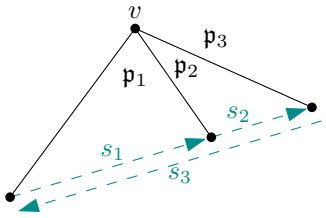

Figure 8.6: Illustration of property (b) in Lemma 8.9: Vertex v is in balance if its neighbors are collinear and the pressure $\mathfrak{p}_3$ is the weighted average of $\mathfrak{p}_1$ and $\mathfrak{p}_2$.

Proof. It is easy to check that conditions (a) and (b) imply a balance of forces with the following two facts. Firstly, it holds that $\sum_i s_i = \vec{0}$ and secondly, by Observation 8.1, a vertex v is in balance if and only if $\sum_i \mathfrak{p}_i \cdot s_i = 0$.

For the reverse direction we assume without loss of generality that s_3 is a longest segment and distinguish two cases: If s_1 and s_2 are linearly independent, they form a basis of the plane. Hence, given a pressure $\mathfrak{p}_3$, there are unique coefficients $\mathfrak{p}_1, \mathfrak{p}_2$ for s_1, s_2 such that $\mathfrak{p}_1 s_1 + \mathfrak{p}_2 s_2 = -\mathfrak{p}_3 s_3$. Since $\sum_i s_i = \vec{0}$ it holds that $\mathfrak{p}_1 = \mathfrak{p}_2 = \mathfrak{p}_3$. This is a trivial balance of forces and thus condition (a).

If s_1, s_2 are linearly dependent then, by their vanishing sum, all three segments are pairwise linearly dependent. This implies collinearity of the three neighbors of v. Since v is in balance it holds that $-\mathfrak{p}_3 s_3 = \mathfrak{p}_1 s_1 + \mathfrak{p}_2 s_2$. In particular, the length of the left and right vector coincide, that is $\| - \mathfrak{p}_3 s_3\| = \|\mathfrak{p}_1 s_1 + \mathfrak{p}_2 s_2\|$. Due to the collinearity and the fact that s_3 is the longest segment, it holds that $\|\mathfrak{p}_1 s_1 + \mathfrak{p}_2 s_2\| = \mathfrak{p}_1\|s_1\| + \mathfrak{p}_2\|s_2\|$. This directly implies condition (b). ◀

With this characterization, we obtain the following lemma.

▶ **Lemma 8.10.** *In a drawing D of a plane cubic graph, every vertex is in balance in D if and only if D is realizing, i.e., there is no deadlock.*

Proof. Assume, for a contradiction, that all vertices are in balance but there exists a face area that is not realized. Consequently, not all pressures are equal. Consider the union of all faces of minimal pressure; we call this region R. Observe that a vertex v on the boundary ∂R of R with an edge strictly inside R is unbalanced: Due to their equal pressure, the faces inside R behave as one face when we are computing the force vectors. Therefore, the vertex v corresponds to a vertex of degree 2, where the two segments connecting its neighbors are scaled by different pressures. Consequently, v is unbalanced. Thus, no edge of G lies strictly within R. Since G is cubic, this implies that R is a collection of disjoint faces. We set R to one of these faces and distinguish two cases:

In case 1, R is not convex. Then we consider a vertex v which has a reflex angle in R. By assumption, v is balanced and, by Lemma 8.9, the pressure of R is the weighted average of the other two neighboring faces of v. However, this is a contradiction to the fact that the pressure of R is minimal.

In case 2, R is convex. Then we consider the induced subgraph of the vertices on ∂R and their neighbors. For all vertices v on ∂R, its neighbors are collinear by Lemma 8.9. Due to planarity, collinearity, and convexity of R, the induced subgraph resembles a windmill as displayed in Figure 8.7. Moreover, the pressure of the face of v with the reflex angle is the weighted average of the other two faces of v. Since R is convex, the reflex angle lies

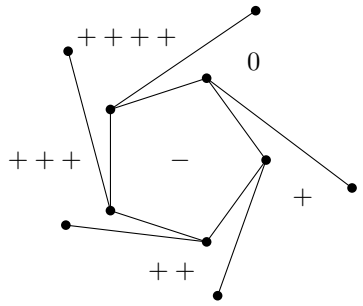

Figure 8.7: In case 2, the neighborhood of R resembles a windmill.

outside R. Consequently, the pressure increases circularly around R, which implies that all pressures are equal. However, this means that R has the same pressure – a contradiction to the fact that R is an isolated face of minimal pressure. ◀

8.1.3 More Details

In this section, we present the pending proofs of this chapter.

▶ **Lemma 8.6.** *Every vertex v in T can be moved to a balanced position; this position is unique when all other vertices are kept at their position.*

Proof. In light of Lemma 8.5, it remains to show that the balanced position is unique. Let D_p denote the modified drawing of D where v is moved to position $p \in \mathcal{P}$. Assume, for a contradiction, that there exist two distinct positions $p, q \in \mathcal{P}$ such that $\mathfrak{f}_v(D_p) = \mathfrak{f}_v(D_q) = 0$. By convexity of $\mathcal{P}$, the segment connecting p and q is contained in $\mathcal{P}$. For $t \in [0, 1]$, p_t denotes the position $p + td$ where $d := (q - p)$. Let $\mathfrak{f}_v(t)$ denote the force vector of v in

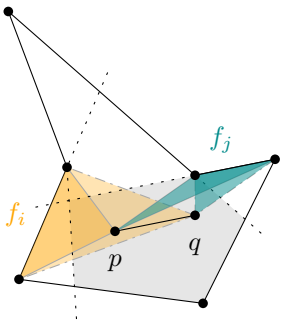

Figure 8.8: Moving v from p to q, there exists a triangle which continuously shrinks or grows. In the illustrated case, the area of f_i grows, while the area of f_j remains constant.

the drawing D_t where v is at position p_t. We consider $g(t) := \langle f_v(t), d \rangle$, the force of v in direction d by moving v from p to q. Let n_i be the normal of the segment connecting the neighbors of v in face f_i. We set $c_i := \langle n_i, d \rangle$. Since T is a triangulation, there exist an i such that $c_i \neq 0$. Note the following relationships:

$$c_i > 0 \iff \textsc{area}(f_i, D_t) \text{ is strictly increasing} \iff p_i(D_t) \text{ is strictly decreasing}$$

$$c_i < 0 \iff \textsc{area}(f_i, D_t) \text{ is strictly decreasing} \iff p_i(D_t) \text{ is strictly increasing}$$

Consequently, for all i it holds that $c_i \cdot p_i(t)$ is a decreasing function in t and there exists an i such that $c_i \cdot p_i(t)$ is strictly decreasing. Therefore, $g(t)$ is strictly decreasing:

$$g(t) = \langle f_v(t), d \rangle = \sum_i p_i(t) \cdot \|s(v, f)\| \cdot \langle n_i, d \rangle = \sum_i c_i \cdot p_i(t) \cdot \|s(v, f)\|$$

By assumption it holds that $\mathfrak{f}_v(0) = f_v(1) = 0$ and thus $g(0) = g(1) = 0$; a contradiction to strict monotonicity unless $p = q$. ◀

In order to find the balanced position, it suffices to optimize in two directions. For $i \in [2]$, let e_i be a standard basis vector and $g_i(t) = \langle f_v(t), e_i \rangle$. We seek t with $g_i(t) = 0$ for all i. If $g_1(t) = g_2(t) = 0$, then $\mathfrak{f}_v(t) = 0$.

Now, we prove the following lemma.

▶ **Lemma 8.7.** *Let T be a plane triangulation with an area assignment $\mathcal{A}\colon F' \to \mathbb{R}_{>0}$ and let D_0 be a drawing of T where the outer face has area ΣA. Let $(D_i)_{i\in\mathbb{N}}$ be a sequence of drawings of T, where D_{i+1} is obtained from D_i by moving an unbalanced inner vertex v into a balanced position. If the selection rule of the vertices is attentive, then there is a subsequence $(D'_i)_{i\in\mathbb{N}}$ of drawings with limit $D' := \lim_{i\to\infty} D'_i$ which is either an $\mathcal{A}$-realizing drawing or a deadlock.*

Proof. As before, we encode a drawing D_i of T by its vertex placement. Since the outer vertices coincide in all drawings and form a fixed triangle $\triangle$ of area $\Sigma\mathcal{A}$. By Lemma 2.12, the set of vertex placements $\mathcal{D}|_{f_o\to\triangle}$ where the outer face f_o is fixed to $\triangle$ is bounded. Clearly, the subset of non-degenerate vertex placements, denoted by $\tilde{\mathcal{D}}|_{f_o\to\triangle}$, is also bounded. Hence, by Bolzano-Weierstrass, there exists a converging subsequence $(D'_i)_{i\in\mathbb{N}}$ with limit D'. We denote the corresponding entropy sequence by $(e_i)_{i\in\mathbb{N}}$.

First, we show that D' is not degenerate. This follows from the facts that the entropy sequence is monotonically increasing and that the entropy of a face tends to infinity as the area goes to 0. In particular, we show that there exists a constant $c > 0$ such that for each face f in every drawing D'_i it holds that $\textsc{area}(D'_i, f) > c$. This implies that $\textsc{area}(D', f) \geq c$ for all f and guarantees that D' is not degenerate.

Consider an arbitrary but fixed drawing D'_i. By construction, the entropy is increasing and hence, $e_0 \leq e_i$. For each face f, we get

$$-E_f(D'_i) \leq e_i - e_0 - E_f(D'_i) = \sum_{\tilde{f}\in F'-f} E_{\tilde{f}}(D'_i) - e_0$$

Naturally, every face area is upper bounded by the area of $\triangle$, namely $\Sigma\mathcal{A}$. Consequently, for every drawing D in $\tilde{\mathcal{D}}|_{f_o\to\triangle}$ and all faces f, it holds that $\textsc{area}(f, D) \leq \Sigma\mathcal{A}$. Hence,

$$C_{f,1} := \sum_{\tilde{f}\in F-f} \mathcal{A}(\tilde{f}) \cdot \log\Big(\frac{\mathcal{A}(\tilde{f})}{\Sigma\mathcal{A}}\Big) \leq \sum_{\tilde{f}\in F-f} \mathcal{A}(\tilde{f}) \cdot \log\Big(\frac{\mathcal{A}(\tilde{f})}{\textsc{area}(\tilde{f}, D'_i)}\Big) = -\sum_{\tilde{f}\in F-f} E_{\tilde{f}}(D'_i).$$

This gives $-E_f(D'_i) \leq -C_{f,1} - e_0$. Using the definition of the entropy and solving for $\textsc{area}(f, D'_i)$ yields

$$\textsc{area}(f, D'_i) \geq C_{f,2} := \mathcal{A}(f) \cdot \exp\left(\frac{e_0 + C_{f,1}}{\mathcal{A}(f)}\right) > 0$$

Setting $c := \min_{f\in F} C_{f,2}$, we obtain a positive lower bound on the area of all faces.

The entropy sequence $(e_i)_{i\in\mathbb{N}}$ is strictly increasing by Proposition 8.3 and, by Lemma 8.4, bounded from above by zero. Hence, $(e_i)_{i\in\mathbb{N}}$ converges to some real constant $e < 0$. By continuity of the entropy, cf. Observation 8.2, we obtain that

$$E(D') = E(\lim_{i\to\infty} D'_i) = \lim_{i\to\infty} E(D'_i) = \lim_{i\to\infty} e_i = e.$$

If $e = 0$, then Lemma 8.4 guarantees that D' is realizing drawing. It remains to show that if D' is not an $\mathcal{A}$-realizing drawing, then it is a deadlock. Therefore, we assume that $e < 0$ and that there exist a vertex v with $\mathfrak{f}_v(D') \neq 0$. By Lemma 8.6, v is movable to a balanced position. Let ϵ denote the increase in entropy by shifting v in D' to the balanced position p and D_p the resulting drawing, i.e., $\epsilon := E(D_p) - E(D')$. We show the following property:

*** Claim 8.11.** *There exist an $N \in \mathbb{N}$ such that for all $i > N$, vertex v is unbalanced in D'_i and the entropy increases by at least $\frac{\epsilon}{2}$ when v is moved in D'_i to a balanced position.*

For notational convenience, we denote the vertex placements of drawings D, D_i, D' by z, z_i, z', respectively. For moving v in D by d, we also write $z + d \cdot \chi_v$. Let $B_r(D)$ denote the open ball of radius r around the vertex placement z of D. Since $\tilde{\mathcal{D}}|_{f_o \to \triangle}$ is open, there exists $r > 0$ such that $B_r(D_p) \subset \tilde{\mathcal{D}}|_{f_o \to \triangle}$. By continuity of E, there exists $\delta > 0$ such that for all $D \in \tilde{\mathcal{D}}|_{f_o \to \triangle}$ it holds that

$$\|z' - z\| < \delta \implies |E(D') - E(D)| < \frac{\epsilon}{4} \quad \text{and} \tag{8.1}$$

$$\|z_p - z\| < \delta \implies |E(D_p) - E(D)| < \frac{\epsilon}{4}. \tag{8.2}$$

Since $(D'_i)_{i \in \mathbb{N}}$ converges to D', there exist $N \in \mathbb{N}$ such that for all $i > N$ it holds that $\|z' - z'_i\| < \min\{r, \delta\}$. Thus, we consider a drawing D'_i with $i > N$. Let D^*_i denote the drawing where v is moved to the balanced position in D'_i. To show that $E(D^*_i) - E(D'_i) \geq \frac{\epsilon}{2}$, we consider an intermediate drawing where v is first moved by d. For the drawing $D_{i,p}$ with vertex placement $z_{i,p} := (z'_i + d \cdot \chi_v)$, it holds that

$$\|z_{i,p} - z_p\| = \|(z'_i + d \cdot \chi_v) - (z' + d \cdot \chi_v)\| = \|z'_i - z'\| < \min\{r, \delta\}.$$

Thus, by the triangle inequality and properties (8.1) and (8.2), we get the following fact:

$$\begin{aligned} \epsilon = E(D_p) - E(D') &\leq |E(D_p) - E(D_{i,p})| + |E(D_{i,p}) - E(D'_i)| + |E(D'_i) - E(D')| \\ &\leq \frac{\epsilon}{4} + |E(D_{i,p}) - E(D'_i)| + \frac{\epsilon}{4}. \end{aligned}$$

Since the balanced position is a unique optimal position for v moved in D'_i, it holds that $E(D^*_i) \geq E(D_{i,p})$. Moreover, $\|z_{i,p} - z_p\| < \min\{r, \delta\}$ implies that $E(D_{i,p}) > E(D')$; otherwise $E(D_p) - E(D_{i,p}) = E(D_p) - E(D') + E(D') - E(D_{i,p}) = \varepsilon + |E(D') - E(D_{i,p})| \geq \varepsilon$, a contradiction since $E(D_p)$ and $E(D_{i,p})$ differ by at most $\frac{\varepsilon}{4}$ by (8.1). It follows that $E(D_{i,p}) > E(D') > E(D'_i)$ and the claim is shown by the following chain of inequalities:

$$E(D^*_i) - E(D'_i) \geq E(D_{i,p}) - E(D'_i) = |E(D_{i,p}) - E(D'_i)| \geq \frac{\epsilon}{2}.$$

Since e is the limit of the sequence $(e_i)_{i \in \mathbb{N}}$, there exists an $M \in \mathbb{N}$ such that for all $i > M$ it holds that $e_i > e - \frac{\epsilon}{2}$. If vertex v was selected in iteration $i > \max\{M, N\}$ then $e_{i+1} \geq e_i + \frac{\epsilon}{2} > e$. This is a contradiction since e is the limit of an increasing sequence. Consequently, for all $i > \max\{M, N\}$, vertex v is unbalanced and not selected. This is a contradiction to the attentive selecting rule. Hence, every vertex in D' is balanced and D' is an $\mathcal{A}$-realizing drawing or a deadlock. ◀

9 | Open Problems and Conjectures

We conclude by stating interesting ways to continue the study of plane graphs and faces areas. We present several research directions together with our favorite open problems. The directions fall into the following categories: area-universal graph classes, equiareal graph classes, computational complexity, and optimal bend drawings. For each open question, we recall relevant related results. Afterwards, we identify relations between the problems.

Area-universal graph classes Our favorite open problem concerns the area-universality of plane bipartite graphs. We conjecture that the answer to the following question is positive.

Open Problem 1: Are plane bipartite graphs area-universal?

In Chapter 4, we introduced first tools to tackle this conjecture and proved that a minimal counter example has at least 14 vertices. In Section 6.1, we showed that even for 3-connected quadrangulations we cannot hope for convex realizing drawings (Theorem 38). However, it might be true that quadrangulations are strongly area-universal.

As partial results, we know the area-universality of 2-degenerate quadrangulations (Proposition 2.6), of grid graphs (Proposition 4.3), as well as the area-universality of angle graphs of triangulations with a subdivision number of at most 1 (Theorem 18).

Moreover, angle graphs of wheels have some very nice properties, namely they are convex area-universal and strongly area-universal as proved in Theorems 23 and 37.

Some indication that the subdivision number of quadrangulations with m edges is smaller than for plane graphs with m edges is given by the fact that the small subdivision number is bounded by $m/2$ (Theorem 31); whereas our upper bound for general plane graphs is m (Theorem 26). However, we do not expect any of these bounds to be close to the truth.

As a promising tool to prove area-universality, we introduced the air pressure method in Chapter 8. Thus, we pose the following open problem.

Open Problem 2: Can the air pressure method be used to prove area-universality of interesting graph classes? More specifically, do non-realizing drawings of plane cubic graphs always have a non-balanced movable vertex?

Equiareal graph classes Equiareal drawings may be visually very appealing as discussed in Section 6.2. Unfortunately, as Ringel [Ringel, 1990] showed, not every plane graph is equiareal. Since his example was a triangulation, any equiareal graph class does not allow for separating triangles. It is thus natural to restrict the search to 4-connected graphs. While we presented many 4-connected triangulations that are not area-universal, we do not know of any that are not equiareal. Therefore, we ask:

Open Problem 3: Is every 4-connected triangulation equiareal?

Recall that Sabariego and Stump [Sabariego and Stump, 2006] tackled this question by investigating small examples by computer search. They found a triangulation for which their heuristic did not find a close to equiareal drawing. However, in Proposition 6.5, we showed that this triangulation is indeed area-universal.

Moreover, we have seen in Proposition 6.4, equiareality is a property of plane graphs rather than planar graphs. Thus, it is not enough to test only one embedding of every planar graph. Theorem 40 asserts that a plane graph, which can be obtained from an area-universal graph by disjoint diamond additions, is equiareal. With this result, we proved that a smallest counter example has at least 11 vertices (Corollary 42). Moreover, Theorem 40 implies that every double stacking graph is equiareal (Corollary 41). Thus for every n, there exist an equiareal 4-connected triangulation on n vertices.

More generally, it would be interesting to know whether for 4-connected triangulations, there exist constant factor approximate equiareal drawings. In other words, does there exist a constant c such that every 4-connected triangulation has a drawing where the ratio between the largest and smallest face area does not exceed c. If the answer to Open Problem 3 is positive, then $c = 1$. Recall that there is no hope for constant factor approximate drawings of plane graphs in general as discussed in Section 3.1.1.

Computational Complexity The complexity class $\forall\exists\mathbb{R}$ is a natural generalization of $\exists\mathbb{R}$, a complexity class capturing the computational complexity of many interesting geometric problems. It lies somewhere between NP and PSPACE:

$$\text{NP} \subseteq \exists\mathbb{R} \subseteq \forall\exists\mathbb{R} \subseteq \text{PSPACE}.$$

As discussed in Chapter 7, we conjecture that the computational complexity of deciding whether a plane graph is area-universal is $\forall\exists\mathbb{R}$-complete.

Open Problem 4: What is the computational complexity of deciding whether a plane graph is area-universal?

We have already seen that the containment is very straight forward (Proposition 7.1). So the open problem of the conjecture is to show the $\forall\exists\mathbb{R}$-hardness. Recall that we proved several variants of area-universality to be hard for $\exists\mathbb{R}$ or $\forall\exists\mathbb{R}$. In particular, we showed that the 3-dimensional analogue of deciding if volume assignment of a simplicial complex is realizable is $\exists\mathbb{R}$-complete Proposition 7.2. We have introduced restricted but hard variants of ETR and UETR which might be helpful to prove the conjecture or hardness of other problems.

Area-universality may turn out to be the first natural geometric problem which is complete for this class. This would give the complexity class $\forall\exists\mathbb{R}$ some relevance. For further natural candidates of $\forall\exists\mathbb{R}$-complete problems we refer to [Dobbins et al., 2018].

Optimal Bend Drawings We showed that the 1-subdivision of every plane graph is area-universal (Theorem 26). Consequently, one bend per edge always suffices to realize any given area assignment for every plane graph. However, studying particular graphs yields the impression that the number of necessary bends may be a lot smaller. In Chapter 5, we introduced the *bend number* $b(G)$ and *subdivision number* $s(G)$ of a plane graph G as possible notions for *optimal bend drawings*.

Recall that, by Proposition 5.3, for every plane graph G holds that $b(G) \leq s(G)$. However, we do have not a single instance where the bend and subdivision number of a graph differ. This suggests the following questions.

Open Problem 5 a: Do the bend number and subdivision number fall apart? Is the subdivision number bounded by a function of the bend number?

We also considered the bend and subdivision number of a graph class $\mathcal{G}$ which are defined as

$$b(\mathcal{G}) := \max_{G \in \mathcal{G}} b(G) \quad \text{and} \quad s(\mathcal{G}) := \max_{G \in \mathcal{G}} s(G).$$

For the class $\mathcal{G}_m$ of plane graphs with m edges, Corollary 29 shows that $s(\mathcal{G}_m) \in \Theta(m)$.

Open Problem 5 b: What is the bend and subdivision number of the class $\mathcal{G}_m$ of plane graphs with m edges? What is the correct constant c such that $s(\mathcal{G}_m) = c \cdot m$?

Corollary 29 shows that c lies between $1/12$ and 1. Clearly, narrowing the gap between the upper and lower bound is also of interest.

Now we show that the above problems are not totally independent.

9.1 Relationship of Open Problem 1 and Open Problem 5 b

If we settle the conjecture of plane bipartite graphs, then this has interesting consequences for the subdivision number of the class of plane triangulations.

▶ **Proposition 9.1.** *If plane bipartite graphs are area-universal, then for every plane triangulation $T = (V, E)$ it holds that $s(T) \leq 1/3|E|$.*

Proof. Let T be a plane triangulation on n vertices. Then T has $2n - 4$ faces. The dual graph T^* of T is a bridgeless cubic graph and hence, has a perfect matching M^* of size $n-2$ by Petersen's theorem. Deleting the dual edges M of M^* in T yields a quadrangulation $Q := T - M$. If plane bipartite graphs are area-universal, then there exists a realizing drawing for Q for every area assignment. By Proposition 2.4, we insert the edges of M with at most one bend. Therefore at most $n - 2$ of the $3(n - 2)$ edges of T have a bend. ◀

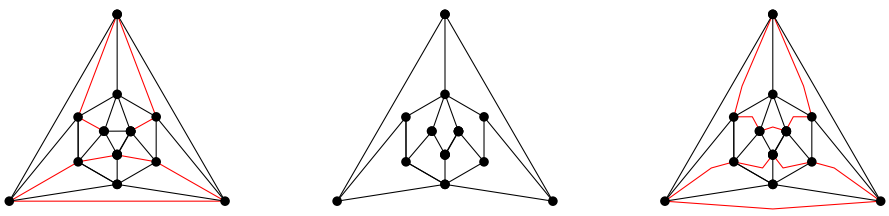

Figure 9.1: Illustration of Proposition 9.1 for the icosahedron graph.

9.2 Relationship of Open Problem 1 and Open Problem 3

Now we comment on the connection of the first and third open problem. Indeed, a positive answer to the third problem dominates a positive answer to the first problem due to the following fact.

▶ **Proposition 9.2.** *If every 4-connected triangulation is equiareal, then every plane bipartite graph is area-universal.*

Proof. Firstly, we show that every integral area assignment of a quadrangulation is realizable. Secondly, we argue that indeed every area assignment is realizable. Then, the claim for general plane bipartite graphs follows from Lemma 2.2.

Let Q be a plane quadrangulation and $\mathcal{A}$ an integral area assignment. Let f be a face with $\mathcal{A}(f) =: k$. We partition f into $4k$ triangles with the following procedure. First, we partition f into k quadrangles with the operation depicted in Figure 9.2(a) and obtain the quadrangulation Q'. Then, we partition every face into four by inserting a vertex into every face f of Q' and connecting it to all vertices of f. Figure 9.2(b) illustrates the second step.

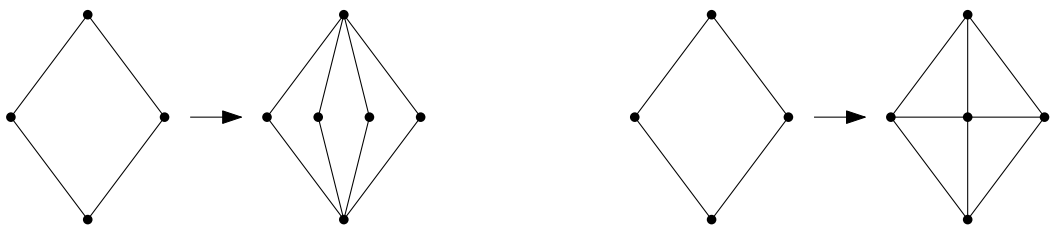

(a) Step 1 (b) Step 2

Figure 9.2: The two steps to enhance a quadrangulation to a 4-connected triangulation.

We claim that the resulting graph T contains no separating triangle. Let v be a vertex inserted during the second step. Clearly, each triangle incident to vertex v is facial. Moreover, since Q' is triangle free, every triangle in T is incident to at least one vertex inserted during the second step. Consequently, there exists no separating triangle and thus T is a 4-connected triangulation.

If every 4-connected triangulation is equiareal, then there exists a drawing of T where every face has area $1/4$. Since every face of Q corresponds to $4k$ faces in G, deleting the edges and vertices introduced in step 1 and 2 yields a $\mathcal{A}$-realizing drawing of Q.

It remains to consider an area assignment $\mathcal{A}$ which is not integral. Since the rational numbers are dense in the set of real numbers, we may consider a sequence $(\mathcal{A}_i)_i$ of rational area assignments converging to $\mathcal{A}$. By scaling and Lemma 2.1, each $\mathcal{A}_i$ is realizable. Moreover, we may consider realizing drawings D_i where the outer vertices of T_i coincide. Thus, by Bolzano-Weierstrass, the sequence $(D_i)_i$ contains a converging subsequence with limit D. By definition of $(\mathcal{A}_i)_i$ and $(D_i)_i$, D is a $\mathcal{A}$-realizing. ◀

Bibliography

[Abel et al., 2016] Abel, Z., Demaine, E. D., Demaine, M. L., Eisenstat, S., Lynch, J., and Schardl, T. B. (2016). Who Needs Crossings? Hardness of Plane Graph Rigidity. In *32nd International Symposium on Computational Geometry (SoCG 2016)*, volume 51 of *LIPIcs*, pages 3:1–3:15.

[Abrahamsen et al., 2018] Abrahamsen, M., Adamaszek, A., and Miltzow, T. (2018). The art gallery problem is $\exists\mathbb{R}$-complete. In *Proceedings of the 50th Annual ACM SIGACT Symposium on Theory of Computing (STOC 2018)*, pages 65–73.

[Alam et al., 2012] Alam, M. J., Biedl, T. C., Felsner, S., Kaufmann, M., and Kobourov, S. G. (2012). Proportional contact representations of planar graphs. *Journal of Graph Algorithms and Applications*, 16(3), pages 701–728.

[Alam et al., 2013] Alam, M. J., Biedl, T. C., Felsner, S., Kaufmann, M., Kobourov, S. G., and Ueckerdt, T. (2013). Computing cartograms with optimal complexity. *Discrete & Computational Geometry*, 50(3), pages 784–810.

[Angelini et al., 2016] Angelini, P., Lozzo, G. D., Battista, G. D., Donato, V. D., Kindermann, P., Rote, G., and Rutter, I. (2016). Windrose planarity: Embedding graphs with direction-constrained edges. In *Proceedings of the Twenty-Seventh Annual ACM-SIAM Symposium on Discrete Algorithms (SODA 2016)*, pages 985–996.

[Arnborg et al., 1987] Arnborg, S., Corneil, D. G., and Proskurowski, A. (1987). Complexity of finding embeddings in ak-tree. *SIAM Journal on Algebraic Discrete Methods*, 8(2), pages 277–284.

[Arora and Barak, 2009] Arora, S. and Barak, B. (2009). *Computational Complexity: A Modern Approach*. Cambridge University Press, Cambridge; New York.

[Bager, 1957] Bager, A. (1957). Lösung der Aufgabe 260. *Elemente der Mathematik*, 12, page 43.

[Basu et al., 2006] Basu, S., Pollack, R., and Roy, M.-F. (2006). *Algorithms in Real Algebraic Geometry*. Springer-Verlag, Berlin; Heidelberg.

[Bernáthová, 2009] Bernáthová, A. (2009). Kreslení grafů s podmínkami na velikosti stěn. `https://is.cuni.cz/webapps/zzp/detail/63479/20281489/`. Bachelor thesis, Charles University Prague.

[Biedl and Velázquez, 2011] Biedl, T. C. and Velázquez, L. E. R. (2011). Orthogonal cartograms with few corners per face. In *Algorithms and Data Structures Symposium (WADS 2011)*, pages 98–109.

[Biedl and Velázquez, 2013] Biedl, T. C. and Velázquez, L. E. R. (2013). Drawing planar 3-trees with given face areas. *Computational Geometry*, 46(3), pages 276–285.

[Blum et al., 1998] Blum, L., Cucker, F., Shub, M., and Smale, S. (1998). *Complexity and Real Computation*. Springer & Business Media, New York, NY.

[Bodlaender, 1988] Bodlaender, H. L. (1988). *Planar graphs with bounded treewidth*, volume 88. Technical Report RUU-CS-88-14, Department of Computer Science, Utrecht University.

[Cook, 1971] Cook, S. A. (1971). The complexity of theorem-proving procedures. In *Proceedings of the Third Annual ACM Symposium on Theory of Computing (STOC 1971)*, pages 151–158.

[de Berg et al., 2009] de Berg, M., Mumford, E., and Speckmann, B. (2009). On rectilinear duals for vertex-weighted plane graphs. *Discrete Mathematics*, 309(7), pages 1794–1812.

[de Fraysseix et al., 1991] de Fraysseix, H., Ossona de Mendez, P., and Pach, J. (1991). Representation of planar graphs by segments. *Intuitive Geometry*, 63, pages 109–117.

[de Fraysseix et al., 1994] de Fraysseix, H., Ossona de Mendez, P., and Rosenstiehl, P. (1994). On triangle contact graphs. *Combinatorics, Probability and Computing*, 3, pages 233–246.

[Debrunner, 1956] Debrunner, H. (1956). Aufgabe 260. *Elemente der Mathematik*, 11, page 20.

[Dirac, 1952] Dirac, G. A. (1952). A property of 4-chromatic graphs and some remarks on critical graphs. *Journal of the London Mathematical Society*, 1(1), pages 85–92.

[Dobbins et al., 2018] Dobbins, M. G., Kleist, L., Miltzow, T., and Rzążewski, P. (2018). Is area universality $\forall\exists\mathbb{R}$-complete? In *Graph-Theoretic Concepts in Computer Science (WG 2018)*, volume 11159 of *LNCS*, pages 164–175. Springer.

[Eppstein et al., 2012] Eppstein, D., Mumford, E., Speckmann, B., and Verbeek, K. (2012). Area-universal and constrained rectangular layouts. *SIAM Journal on Computing*, 41(3), pages 537–564.

[Evans et al., 2017] Evans, W., Felsner, S., Kaufmann, M., Kobourov, S. G., Mondal, D., Nishat, R. I., and Verbeek, K. (2017). Table cartogram. *Computational Geometry*, 68, pages 174 – 185. Special Issue in Memory of Ferran Hurtado.

[Evans et al., 2018] Evans, W., Felsner, S., Kleist, L., and Kobourov, S. G. (2018+). On area-universal quadrangulations. *In preparation*.

[Fáry, 1948] Fáry, I. (1948). On straight line representations of planar graphs. *Acta Scientiarum Mathematicarum*, 11, pages 229–233.

[Felsner, 2014] Felsner, S. (2014). Exploiting air-pressure to map floorplans on point sets. *Journal of Graph Algorithms and Applications*, 18(2), pages 233–252.

[Gutner, 1996] Gutner, S. (1996). The complexity of planar graph choosability. *Discrete Mathematics*, 159(1), pages 119 – 130.

[Haack and Wiechel, 1903] Haack, H. and Wiechel, H. (1903). *Kartogramm zur Reichstagswahl: zwei Wahlkarten des Deutschen Reiches in alter und neuer Darstellung mit politisch-statistischen Begleitworten und kartographischen Erläuterungen.* Justus Perthes. cited in Kretschmer, 1986, page 397.

[Harborth, 1994] Harborth, H. (1994). Match sticks in the plane. In *The Lighter Side of Mathematics. Proceedings of the Eugne Strens Memorial Conference on Recreational Mathematics and Its History*, MAA spectrum, pages 281–288.

[Hartman et al., 1991] Hartman, I. B.-A., Newman, I., and Ziv, R. (1991). On grid intersection graphs. *Discrete Mathematics*, 87(1), pages 41–52.

[Heinrich, 2018] Heinrich, H. (2018). Ansätze zur Entscheidung von Flächenuniversalität. `www.math.tu-berlin.de/~felsner/Diplomarbeiten/heinrich.pdf`. Master thesis, Technische Universität Berlin.

[Igamberdiev et al., 2017] Igamberdiev, A., Meulemans, W., and Schulz, A. (2017). Drawing planar cubic 3-connected graphs with few segments: Algorithms & experiments. *Journal of Graph Algorithms and Applications*, 21(4), pages 561–588.

[Kawaguchi and Nagamochi, 2007] Kawaguchi, A. and Nagamochi, H. (2007). Orthogonal drawings for plane graphs with specified face areas. In *Theory and Applications of Model of Computation (TAMC 2007)*, pages 584–594.

[Kleist, 2016] Kleist, L. (2016). Drawing planar graphs with prescribed face areas. In Heggernes, P., editor, *Graph-Theoretic Concepts in Computer Science (WG 2016)*, volume 9941 of *LNCS*, pages 158–170. Springer.

[Kleist, 2018a] Kleist, L. (2018a). Drawing planar graphs with prescribed face areas. *Journal of Computational Geometry (JoCG)*, 9(1), pages 290–311.

[Kleist, 2018b] Kleist, L. (2018b). On the area-universality of triangulations. In Biedl, T. and Kerren, A., editors, *Graph Drawing and Network Visualization (GD 2018)*, volume 11282 of *LNCS*, pages 333–346. Springer.

[Kurz and Pinchasi, 2011] Kurz, S. and Pinchasi, R. (2011). Regular matchstick graphs. *The American Mathematical Monthly*, 118(3), pages 264–267.

[Levi, 1926] Levi, F. (1926). Die Teilung der projektiven Ebene durch Gerade oder Pseudogerade. *Berichte über die Verhandlungen der Sächsischen Akademie der Wissenschaften zu Leipzig, Mathematisch-Physische Klasse*, 78, pages 256–267.

[Levin, 1973] Levin, L. A. (1973). Universal enumeration problems. *Problemy Peredači Informacii*, 9(3), pages 115–116.

[Matoušek, 2014] Matoušek, J. (2014). Intersection graphs of segments and $\exists\mathbb{R}$. *arXiv preprint arXiv:1406.2636.*

[Meister, 1769] Meister, A. L. F. (1769). *Generalia de genesi figurarum planarum et inde pendentibus earum affectionibus.*

[Mnëv, 1988] Mnëv, N. E. (1988). The universality theorems on the classification problem of configuration varieties and convex polytopes varieties. In *Topology and geometry: Rohlin Seminar*, volume 1346 of *LNM*, pages 527–543. Springer.

[Nusrat and Kobourov, 2016] Nusrat, S. and Kobourov, S. (2016). The state of the art in cartograms. In *Computer Graphics Forum*, volume 35, pages 619–642. Wiley Online Library.

[Renegar, 1992] Renegar, J. (1992). On the computational complexity and geometry of the first-order theory of the reals. Part I: Introduction. Preliminaries. The geometry of semi-algebraic sets. The decision problem for the existential theory of the reals. *Journal of Symbolic Computation*, 13(3), pages 255–299.

[Richter-Gebert, 2011] Richter-Gebert, J. (2011). *Perspectives on projective geometry: a guided tour through real and complex geometry*. Springer, New York.

[Ringel, 1990] Ringel, G. (1990). Equiareal graphs. In Bodendiek, R., editor, *Contemporary Methods in Graph Theory, in honour of Prof. Dr. K. Wagner*, pages 503–505. BI Wissenschaftsverlag Mannheim.

[Rotman, 2015] Rotman, J. J. (2015). *Advanced modern algebra Part 1*, volume 165 of *Graduate studies in mathematics*. American Mathematical Society, Providence, Rhode Island, 3^{rd} edition.

[Sabariego and Stump, 2006] Sabariego, P. and Stump, C. (2006). On equiareal triangulations. `http://homepage.univie.ac.at/christian.stump/ChristianStumpOnEquiarealTriangulations.pdf`. Student project report.

[Schaefer and Štefankovič, 2017] Schaefer, M. and Štefankovič, D. (2017). Fixed points, nash equilibria, and the existential theory of the reals. *Theory of Computing Systems*, 60(2), pages 172–193.

[Scheucher, 2017] Scheucher, M. (2017). On area-universal graphs: How to win a mug. `http://page.math.tu-berlin.de/~scheuch/supplemental/winMug.pdf`. unpublished.

[Stein, 1951] Stein, S. K. (1951). Convex maps. *Proceedings of the American Mathematical Society*, 2(3), pages 464–464.

[Stoepel, 2010] Stoepel, C. (2010). Population cartogram of germany. `https://commons.wikimedia.org/wiki/File:Germany-population-cartogram.png`. Licensed under "CC BY-SA 3.0", `https://creativecommons.org/licenses/by-sa/3.0/deed.de`, accessed on 2018-02-25.

[Szekeres, 1967] Szekeres, E. (1967). Einfache Beweise zweier Dreieckssätze. *Elemente der Mathematik*, 22, pages 17–18.

[Thomassen, 1992] Thomassen, C. (1992). Plane cubic graphs with prescribed face areas. *Combinatorics, Probability & Computing*, 1(4), pages 371–381.

[Tobler, 2004] Tobler, W. (2004). Thirty five years of computer cartograms. *Annals of the Association of American Geographers*, 94, pages 58–73.

[Tsai and West, 2011] Tsai, M.-T. and West, D. B. (2011). A new proof of 3-colorability of Eulerian triangulations. *Ars Mathematica Contemporanea*, 4(1), pages 73–77.

[Tutte, 1960] Tutte, W. T. (1960). Convex representations of graphs. *Proceedings of the London Mathematical Society*, 10(1), pages 304–320.

[Tutte, 1963] Tutte, W. T. (1963). How to draw a graph. *Proceedings of the London Mathematical Society*, 3(1), pages 743–767.

[Wagner, 1936] Wagner, K. (1936). Bemerkungen zum Vierfarbenproblem. *Jahresbericht der Deutschen Mathematiker-Vereinigung*, 46, pages 26–32.

[Wald and Colbourn, 1983] Wald, J. A. and Colbourn, C. J. (1983). Steiner trees, partial 2–trees, and minimum ifi networks. *Networks*, 13(2), pages 159–167.

[West, 2001] West, D. B. (2001). *Introduction to graph theory.* Prentice Hall, Upper Saddle River, NJ, 2^{nd} edition.

[Whitney, 1933] Whitney, H. (1933). 2-isomorphic graphs. *American Journal of Mathematics*, 55(1), pages 245–254.

[Wimer et al., 1988] Wimer, S., Koren, I., and Cederbaum, I. (1988). Floorplans, planar graphs, and layouts. *IEEE Transactions on Circuits and Systems*, 35, pages 267–278.